A.Y. 2020/2021

Biostimulants in horticulture: evaluation of their mode of action on crops using a platform for high-throughput automated phenotyping

Supervisor: Prof. Youssef Rouphael Co-Supervisor: Dr Klára Panzarová

PhD Candidate: Mirella Sorrentino

Ph.D in Sustainable Agricultural and Forestry Systems and Food Security

XXXIII Cycle

DIPARTIMENTO DI AGRARIA

Index

Index **1**

Publications **4**

List of figures **5**

Abstract **14**

Introduction **16**

1. Overview and context 16

2. Biostimulants 17

2.1 Categories of biostimulants 18

2.2 Biostimulants and phenotyping 23

3. High-throughput automated plant phenotyping 27

3.1 History of plant phenotyping 27

3.2 Sensors 28

3.3 Integration of phenomics with metabolomics 35

3.4 Future of plant phenotyping 36

4. Abiotic stresses 38

4.1 Drought stress 38

4.2 Salinity stress 40

Aim of the thesis 42

Results 45

1. Chapter 1 45

Seed – Emergence assay in coated wheat seeds 45

1.1 Introduction 45

1.2 Materials and methods 47

1.3 Results 52

1.4 Discussion 63

1.5 Conclusions 65

2. Chapter 2 66

Seedlings – In vitro Arabidopsis assay 66

3. Chapter 3 106

Mature crops – In-planta lettuce and tomato trials 106

3.1 Drought stress 106

4.1 Salinity stress..... 190

4.1.1 Lettuce and tomato..... 190

Overall conclusions 239

Literature cited.....242

Appendix 284

List of publications..... 284

Conferences..... 285

Poster presentations..... 285

Oral presentations..... 286

Courses and seminars..... 286

Publications

1. Paul K, **Sorrentino M**, Lucini L, Rouphael Y, Cardarelli M, Bonini P, Reynaud H, Canaguier R, Trtílek M, Panzarová K and Colla G (2019) Understanding the Biostimulant Action of Vegetal-Derived Protein Hydrolysates by High-Throughput Plant Phenotyping and Metabolomics: A Case Study on Tomato. *Front. Plant Sci. 10:47. doi: 10.3389/fpls.2019.00047*
2. Paul K, **Sorrentino M**, Lucini L, Rouphael Y, Cardarelli M, Bonini P, Miras Moreno MB, Reynaud H, Canaguier R, Trtílek M, Panzarová K and Colla G (2019) A Combined Phenotypic and Metabolomic Approach for Elucidating the Biostimulant Action of aPlant-Derived Protein Hydrolysate on Tomato Grown Under Limited Water Availability. *Front. Plant Sci. 10:493. doi: 10.3389/fpls.2019.00493*
3. **Sorrentino M**, Colla G, Rouphael Y, Panzarová K and Trtílek M. (2020). Lettuce reaction to drought stress: automated high-throughput phenotyping of plant growth and photosynthetic performance. *Acta Horticulturae, (1268), 133–142. doi:10.17660/actahortic.2020.1268.17*
4. **Sorrentino M**, De Diego N, Ugena L, Spíchal L, Lucini L, Miras-Moreno B, Zhang L, Rouphael Y, Colla G and Panzarová K (2021) Seed Priming with Protein Hydrolysates Improves Arabidopsis Growth and Stress Tolerance to Abiotic Stresses. *Front. Plant Sci. 12:626301. doi: 10.3389/fpls.2021.626301*
5. **Sorrentino M**, Panzarová K, Spyroglou I, Spíchal L, Buffagni V, Ganugi P, Rouphael Y, Colla G, Lucini L and De Diego N. Integration of phenomics and metabolomics datasets reveals different mode of action of biostimulants based on protein hydrolysates in lettuce and tomato under salinity. *Accepted in Front. Plant Sci.*

List of figures

Introduction

Figure 1| Categories of biostimulants 18

Figure 2|Protein hydrolysates 21

Figure 3| Biostimulants and phenotyping 25

Figure 4| Plant Biostimulant Characterization Index 26

Figure 5| Cameras used in plant phenotyping and their wavelengths 29

Figure 6|Photosystem II and usage of light 30

Figure 7| From seeds to crops 43

Results - Chapter 1

Figure 1|Seeds preparation. 48

Figure 2| Experimental setup 49

Figure 3| Empirical emergence curves 53

Figure 4| Empirical emergence curves 54

Figure 5| Final seedlings heights 56

Figure 6|Final fresh weights. **58**

List of figures

Figure 7| Final dry weights ***59***

Figure 8| Characterization of the plant biostimulants ***60***

Results - Chapter 2

Figure 1| Scheme of experimental protocol *75*

Figure 2| Total nitrogen and total carbon *77*

Figure 3| Top view RGB pictures. *80*

Figure 4| Characterization of the 11 plant biostimulants. *82*

Figure 5|Hierarchical cluster analysis *90*

Figure 6| Products of biosynthesis in the rosettes' tissues *91*

Supplementary Figure S1| Growth of the plants in control conditions following the priming with the set of protein hydrolysates. *98*

Supplementary Figure S2| Growth of the plants in moderate salt stress conditions following the priming with the set of protein hydrolysates. *99*

Supplementary Figure S3| Growth of the plants in severe salt stress conditions following the priming with the set of protein hydrolysates. *100*

Supplementary Figure S4| Maximum quantum yield of PSII photochemistry in the dark-adapted state (Fv/Fm) of the Arabidopsis seedlings. *101*

Supplementary Figure S5| OPLS-DA C vs D *102*

List of figures

Results - Chapter 3.1.1

Figure 1| RGB images and ChlF images *111*

Figure 2| Growth performance of lettuce plants. *111*

Figure 3| Photosynthetic performance of the lettuce plants *113*

Results - Chapter 3.1.2

Figure 1| Schematic overview of cultivation protocol and automated phenotyping protocol *123*

Figure 2| Color segmented side view Red Green Blue (RGB) images of tomato plants prior to and upon PHs application *125*

Figure 3| Photosynthetic performance of tomato plants visualized by kinetic chlorophyll fluorescence imaging in all protein hydrolysate treatments *127*

Figure 4| Spider plots of photosynthetic parameters deduced from kinetic chlorophyll fluorescence imaging on whole plant level in all treatments. *128*

Figure 5| Unsupervised hierarchical cluster analysis carried out from metabolomic profiles following application of selected protein hydrolysates *132*

Figure 6| Score plot of Orthogonal Projection to Latent Structures Discriminant Analysis (OPLS-DA) supervised modeling carried out on metabolomic profiles following application of selected protein hydrolysates *134*

Supplementary Figure 1| Schematic of the kinetic ChlF protocol in the PlantScreenTM Modular System 1343

Supplementary Figure 2| Schematic of top and side view RGB image processing. *134*

List of figures

Supplementary Figure 3| Variation in shoot colors of tomato plants..... 134

Results - Chapter 3.1.3

Figure 1| Non-invasive image-based phenotypical analysis of PHs treated and control tomato plants grown under water limiting conditions by using PlantScreen™ Modular System. *..... 165*

Figure 2| Growth performance of PHs treated and control tomato plants *..... 166*

Figure 3| Photosynthetic performance of the tomato plants treated or untreated with protein hydrolysate *..... 167*

Figure 4| Unsupervised hierarchical cluster analysis *..... 170*

Figure 5| Score plot of Orthogonal Projection to Latent Structures Discriminant Analysis (OPLS-DA) *. 174*

Supplementary Figure 1| Schematic overview of plant handling and phenotyping protocol.. 1340

Supplementary Figure 2| Destructive biomass quantification and correlation with digital biomass..... 134

Supplementary Figure 3| Variation in shoot colors of tomato plants prior to and following the biostimulant treatment..... 134

Supplementary Figure 4| Photosynthetic performance of the tomato plants..... 1343

Supplementary Figure 5| Leaf temperature quantification and estimation of transpiration use efficiency (TUE) in tomato plants prior to and following PH treatment... 134

Supplementary Figure 6| Chemical Similarity Enrichment Analysis (ChemRICH)... 134

List of figures

Results - Chapter 3.2.1

Figure 1|Scheme of plant cultivation and phenotyping protocol. *216*

Figure 2| Salinity response in tomato and lettuce plants *217*

Figure 3| Characterization of the biostimulants effect on performance of tomato and lettuce plants grown in control and salinity conditions..... *218*

Figure 4| Cluster Dendrograms for all phenotypical data *219*

Figure 5| Metabolomic analysis of lettuce plants *220*

Figure 6| Metabolomic analysis of tomato plants..... *221*

Figure 7| Metabolites in lettuce plants..... *222*

Figure 8| Metabolic processes (A), secondary metabolism (B) and (C) hormone biosynthesis impaired by treatments in tomato plants compared to control samples. *223*

Supplementary Figure 1| Morphological and physiological parameters of lettuce plants in control and stress conditions... ..... *223*

Supplementary Figure 2| Morphological and physiological parameters of tomato plants under control and stress conditions... ..... *224*

Supplementary Figure 3| Morphological and physiological parameters of lettuce plants in control conditions: PHs treated and untreated lettuce plants... ..... *225*

Supplementary Figure 4| Morphological and physiological parameters of lettuce plants in salt stress conditions: PHs treated and untreated lettuce plants... ..... *226*

List of figures

Supplementary Figure 5| Morphological and physiological parameters of tomato plants in salt stress conditions: PHs treated and untreated lettuce plants... ..... *227*

Supplementary Figure 6| Relative Growth Rate and final biomass of lettuce plants treated with PHs... ..... *228*

Supplementary Figure 7| Relative Growth Rate and final biomass of tomato plants treated with PHs……. *229*

Supplementary Figure 8| Temperature of the leaves for lettuce and tomato plants under control and salt stress conditions... ..... *230*

Supplementary Figure 9| Metabolomic analysis for the best (H) and worst (B) performing biostimulants.... ..... *231*

Supplementary Figure 10| Score plot of metabolomics profiles..... *232*

Supplementary Figure 11| Identified metabolites in control conditions..... *233*

Supplementary Figure 12| Identified metabolites in NaCl conditions..... *234*

Supplementary Figure 13| Graphical output of co-Inertia analysis (CIA)..... *235*

List of tables

Results - Chapter 1

Table 1| *List of biostimulants used for seeds coating.* *47*

Table 2|*PBC Index traits.* *51*

Table 3| *Emergence parameters.* *55*

Table 4| *PBC index* *62*

Results - Chapter 2

Table 1|*Plant Biostimulant Characterization (PBC) index.* *85*

Results - Chapter 3.1.1

Table 1| *Values of projected top view area* *112*

Results - Chapter 3.1.2

Table 1| *Discriminant metabolites* *140*

Supplementary Table S1 | Projected shoot area (PSA) of the tomato plants extracted from multiple side view RGB 146

Supplementary Table S2 | Projected shoot area (PSA) of the tomato plants extracted from top view RGB . 146

Supplementary Table S3 | Width of the tomato plants 147

List of tables

Supplementary Table S4 | Height of the tomato plants 148

Supplementary Table S5 | Digital Biomass of the tomato plants..... 148

Supplementary Table S6 | Variation in shoot colours of tomato plants 149

Supplementary Table S6 | Photosynthetic performance of tomato plants 150

Results - Chapter 3.1.3

Table 1| *Metabolites discriminating biostimulant-treated tomato plants (foliar and drench application) from control* *176*

Supplementary Table S1 | Projected shoot area (PSA) of the tomato plants from multiple side view RGB images *186*

Supplementary Table S2 | Projected shoot area (PSA) of the tomato plants from top view RGB images..... *186*

Supplementary Table S3 | Digital Biomass of the tomato plants..... *187*

Supplementary Table S4 | Width of the tomato plants..... *187*

Supplementary Table S5 | Height of the tomato plants *188*

Supplementary Table S6 | Variation in shoot colours of the tomato plants *189*

Results - Chapter 3.2

Table 1| *Classification of the 7 PHs with PBC index..* *215*

Results - Chapter 3.2

Supplementary Tables *236*

Abstract

In the last decades, with the constant increase in world population, the fast reduction of fertile arable land and the deteriorating environmental conditions, optimization of agriculture has become a priority. The main focus is on increasing the final yield and protecting the crops from unfavourable growing conditions in a sustainable way. A possible solution to this problem is represented by biostimulants, bioactive substances of diverse origins. A very large number of new biostimulants enter the market every year. However, a thorough knowledge of the mode of action of the substances in different crops and in different environmental conditions is still lacking. Traditional testing methods are time-consuming, expensive and, in most cases, destructive. Therefore, in the last years high-throughput automated phenotyping platforms started to be considered an interesting alternative to traditional characterization assays, drawing the attention of biostimulant producers. Different cameras and sensors can be implemented into high-throughput phenotyping platforms, allowing to screen the effects of different substances on a large number of morpho-physiological plant traits in a fast, efficient, cost-effective and non-destructive manner.

In our work, we developed a precise methodology to test the effects of a large set of protein hydrolysates on multiple plant species (wheat, Arabidopsis, lettuce and tomato) subjected to abiotic stresses (drought and salinity) at all phenological phases, from seed up to the crop maturity. A large number of morpho-physiological traits of the plants were analysed throughout their life cycle, before and after the application of the PHs substances.

The original set of PHs has been subjected to an initial *in vitro* screening on Arabidopsis plantlets; the substances were applied as seed priming in three different concentrations. The best-performing PHs in control and salt stress conditions have then been used for trials *in planta,* where they were applied as foliar spray. With the use of a Plant Biostimulant Characterization Index (PBC), we were able to categorize the substances into functional classes according to their mode of action, classifying them as Growth Promoters and /or Stress Alleviators. Leaves of the plants treated with the best- and worst-performing substances were collected and subjected to untargeted metabolomic analysis to elucidate the biochemical pathways activated by the PHs applications.

Abstract

It was clear that the effects of the biostimulants on plants can vary depending on the mode and time of application, the growing conditions, the dose and the plant species they are applied to; therefore, before putting a new biostimulant on the market, it is essential to select the target crop species that could benefit from the treatment. High-throughput automated phenotyping platforms can be an extremely useful tool to speed up the testing process and precisely investigate the effects of the same substance on multiple morpho-physiological traits.

Introduction

1. Overview and context

Contemporary crop production is facing major challenges to feed 7 billion people while maintaining high productivity and quality standards, without overexploiting natural resources such as water and soil. Furthermore, alterations in weather patterns due to changes in climate are impacting crop productivity globally. Biostimulants have been proven to be beneficial to crops' fitness, improving the final yield and the resistance to adverse environmental conditions. However, the effectiveness of biostimulants can vary, according to the crops they are applied to, the dose and the time of application. It is therefore important to test the mode of action of potential new substances in different conditions, concentrations and crops, before starting the commercialization of the products. High-throughput automated phenotyping techniques can be extremely helpful in the validation phase; hence, the development of reliable, reproducible pipeline for the investigation of the mode of action of a substance is of fundamental importance.

In this thesis, I am going to present:

- A comprehensive literature review about the three main topics of my work: biostimulants, high-throughput automated phenotyping and abiotic stresses. – Chapters 2- Biostimulants, 0 - High-throughput automated plant phenotyping and 4 – Abiotic stresses.

- The studies characterising the mode of action of several biostimulants on different plant species (Arabidopsis, wheat, lettuce and tomato), applied at different phenological stages (seeds, seedlings and adult crops), both in control and stress conditions. Through the calculation of a Plant Biostimulant Characterization Index (PBC), the substances are classified as Growth Promoters, Stress Alleviators or Growth Inhibitors.

- The development of robust protocols for the application of different abiotic stresses on selected plant species.

- The characterisation of morpho-physiological traits related to stress application and PHs administration in different plant species that were detected by high-throughput automated phenotyping techniques.

- The results of metabolomic analysis of the plant tissues, performed in order to understand the molecular mechanisms triggered by the abiotic stresses and the biostimulants application.

- The realization of a statistical analysis pipeline for the integration of complex omics data, with the purpose of identifying the relevant plant traits affected by the biostimulant treatments.

2. Biostimulants

The first mention of the term "biostimulant" can be found in the "Ground Maintenance" web journal (http://grounds-mag.com) in 1997, where Zhang and Schmidt from the Department of Crop and Soil Environmental Sciences of the Virginia Polytechnic Institute and State University defined them as 'materials that, in minute quantities, promote plant growth'. It was already clear at the time that crop plant production methods based only on improving agricultural technology (e.g., tillage, re-cultivation, fertilization, irrigation, etc.) are limited due to the inability to effectively use the biological potential of the cultivated varieties (Posmyk and Szafrańska, 2016). Zhang and Schmidt explained the biostimulator action by hormonal effects and, secondly, by protection against abiotic stress by antioxidants. In the scientific literature, the word biostimulant was first defined by Kauffman et al. (2007), with modifications from the previous definition: 'biostimulants are materials, other than fertilisers, that promote plant growth when applied in low quantities.' Kauffman and co-workers also attempt to summarize what biostimulants are, by introducing a classification: 'Biostimulants are available in a variety of formulations and with varying ingredients but are generally classified into three major groups on the basis of their source and content. These groups include humic substances (HS), hormone containing products (HCP), and amino acid containing

products (AACP). HCPs, such as seaweed extracts, contain identifiable amounts of active plant growth substances such as auxins, cytokinins, or their derivatives'. The word biostimulant was increasingly used by the scientific literature over the following years, expanding the range of substances and of modes of actions (Calvo et al., 2014; du Jardin, 2012). In fact, 'biostimulant' appears as a versatile descriptor of any substance beneficial to plants without being nutrients, pesticides, or soil improvers. The 'European Biostimulants Industry Council' (EBIC) in 2012 provided a complete description of biostimulants as products "containing substance(s) and/or micro-organisms whose function when applied to plants or the rhizosphere is to stimulate natural processes to enhance/benefit nutrient uptake, nutrient efficiency, tolerance to abiotic stress, and crop quality."

2.1 Categories of biostimulants

Even though biostimulants can be categorized by source, this is not entirely correct as very substantial differences can exist between products that have the same origin (Yakhin et al., 2017). However, to simplify the introduction to biostimulants, we are going to categorize them according to their origin (**Figure 1**).

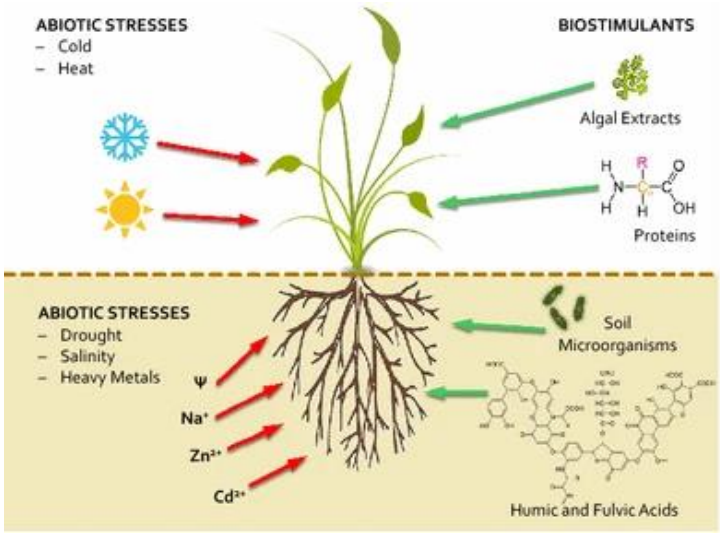

Figure 1| Categories of biostimulants. *Main categories of plant biostimulants and abiotic stressors they have proven effective against (from Van Oosten et al., 2017).*

2.1.1 Humic and fulvic acids

Humic substances (HS) are natural constituents of the soil organic matter, resulting from the decomposition of plant, animal and microbial residues, but also from the metabolic activity of soil microbes using these substrates. HS are categorized according to their molecular weights and solubility into humins, humic acids and fulvic acids (du Jardin, 2015). Regarding the sources of HS, they are extracted from naturally humified organic matter (i.e., from peat or volcanic soils), from composts and vermi-composts, or from mineral deposits (leonardite, an oxidation form of lignite) (du Jardin, 2015). Humic substances have been recognized for long as essential contributors to soil fertility, acting on physical, physico-chemical, chemical and biological properties of the soil.

2.1.2 Seaweed extracts

Seaweeds are applied to plants as extracts and as purified compounds, which include the polysaccharides laminarin, alginates and carrageenans and their breakdown products. Other constituents contributing to the plant growth promotion include micro- and macronutrients, sterols, N- containing compounds like betaines, and hormones (Craigie, 2011; Khan et al., 2009). Seaweeds can be applied on soils, in hydroponic solutions or as foliar treatments. In soils, their polysaccharides contribute to gel formation, water retention and soil aeration. Positive effects via the soil microflora are also described. Anti-stress effects are also reported and both protective compounds within the seaweed extracts, like antioxidants, and regulators of endogenous stress-responsive genes could be involved (Calvo et al., 2014).

2.1.3 Inorganic compounds

Chemical elements that promote plant growth but are not required by all plants are called beneficial elements (Pilon-Smits et al., 2009). The five main beneficial elements are Al, Co, Na, Se and Si, present in soils and in plants as different inorganic salts. These beneficial functions can be constitutive, like the strengthening of cell walls by silica deposits or expressed in defined environmental conditions, like pathogen attack for selenium and osmotic stress for sodium (du Jardin,

2015). Many effects of beneficial elements are reported by the scientific literature, which promote plant growth, the quality of plant products and tolerance to abiotic stress.

2.1.4 Beneficial fungi

Fungi interact with plant roots in different ways, from mutualistic symbioses to parasitism (Behie and Bidochka, 2014). Among the different forms of physical interactions and fungi taxa involved, the Arbuscule-Forming Mycorrhiza (AMF) are a widespread type of endomycorrhiza associated with crop and horticultural plants, where fungal hyphae penetrate root cortical cells and form branched structures called arbuscules (Bonfante and Genre, 2010; Behie and Bidochka, 2014). Other fungal endophytes, like *Trichoderma* spp. (Ascomycota) are able to live at least part of their life cycle away from the plant, to colonize roots and to transfer nutrients to their hosts (Behie and Bidochka, 2014).

2.1.5 Beneficial bacteria

With regard to the agricultural uses of biostimulants, two main types of bacteria should be considered: (i) mutualistic endosymbionts of the type Rhizobium and (ii) mutualistic, rhizospheric PGPRs (‘plant growth-promoting rhizobacteria’). PGPRs are multifunctional and influence all aspects of plant life: nutrition and growth, morphogenesis and development, response to biotic and abiotic stress, interactions with other organisms in the agroecosystems (du Jardin, 2015).

2.1.6 Protein hydrolysates and other N-containing compounds

Protein hydrolysates (PHs) are mainly produced by chemical and/or enzymatic hydrolysis of proteins contained in agro-industrial by-products from animal (i.e., leather, viscera, feathers, blood) or plant origin (i.e., vegetable by-products) (Maini, 2006; Schiavon et al., 2008; du Jardin, 2012). PHs have been identified to improve the performance of several horticultural crops, including increased shoot, and root biomass and productivity (Kunicki et al., 2010; Lisiecka et al., 2011; Paradikovic et al., 2011; Colla et al., 2014; Ertani et al., 2014). Application of PHs to plant leaves and roots has been shown to increase Fe and N metabolism, nutrient uptake, and water and nutrient use efficiencies for

both macro and microelements (Cerdán et al., 2009; Ertani et al., 2009; Halpern et al., 2015). PHs could also interfere with the phytohormone balance of the plant, thereby influencing plant development due to the presence of bioactive peptides and precursors of phytohormone biosynthesis, such as tryptophan (Colla et al., 2014). Moreover, many scientific papers reported that the application of plant-derived PHs elicited auxin- and gibberellin-like activities and thus promoted crop performances (Schiavon et al., 2008; Ertani et al., 2009; Matsumiya and Kubo, 2011; Colla et al., 2014). In addition, PH application has been also shown to avoid or reduce losses in production caused by unfavourable soil conditions and environmental stresses. These include thermal stress, salinity, drought, alkalinity, and nutrient deficiency (Botta, 2013; Cerdán et al., 2013; Ertani et al., 2013; Colla et al., 2014; Petrozza et al., 2014; Lucini et al., 2015; Visconti et al., 2015) **(Figure 2).** Overall, the effects of PHs are dependent on species/cultivar, environmental conditions, phenological stages, time and mode of applications (foliar vs. root) and leaf permeability to the biostimulant (Kauffman et al., 2007; Kunicki et al., 2010; Ertani et al., 2014).

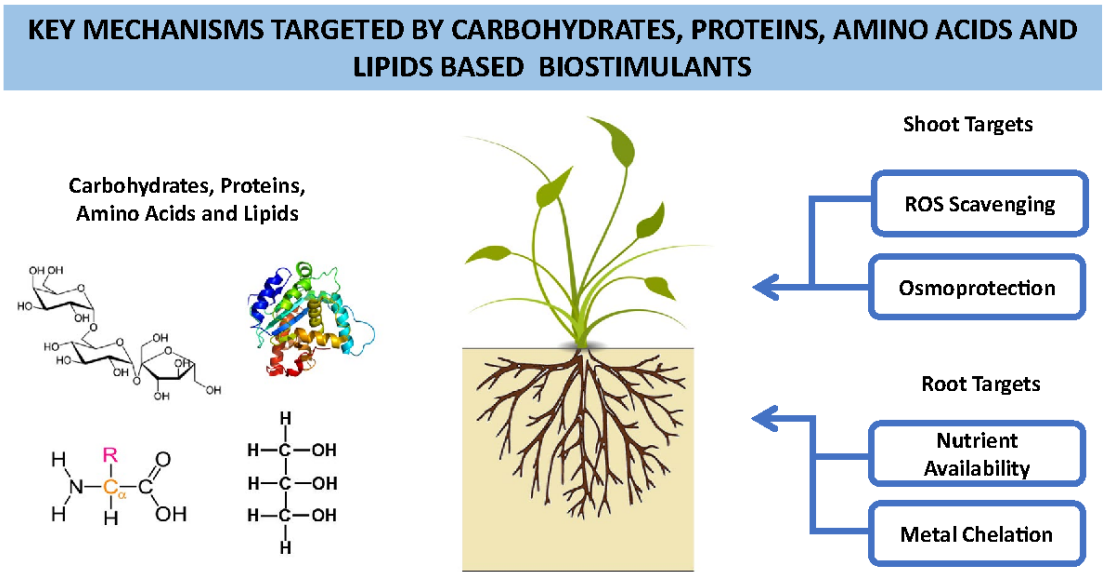

Figure 2\|Protein hydrolysates. *Main key mechanisms targeted by carbohydrate-, protein-, amino acid-, and lipid-based biostimulants (from Van Oosten et al., 2017).*

Protein/peptides and free amino acid contents in PHs widely differ, according to the source of proteins. Besides amino acids and peptides, PHs contain other compounds that can contribute to the biostimulant action. These compounds include fats, carbohydrates, phenols, mineral elements, phytohormones and other organic compounds (e.g., polyamines) (Colla et al., 2015a). Moreover, plant-based PHs contain soluble carbohydrates and phenols, which play an important role in energy metabolism and oxidative stress defences. In contrast, animal-derived PHs lack carbohydrates, phenols and phytohormones. Mineral content is also affected by protein source, usually being higher in the products from plant-derived PHs (Colla et al., 2015a).

2.1.6.1 Effects of protein hydrolysates on plant metabolism and physiology

Amino acids and small peptides are absorbed by both roots and leaves and then translocated into the plant, as demonstrated by Watson and Fowden (1975), Soldal and Nissen (1978) and Matsumiya and Kubo (2011). Following root/foliar uptake, amino acids and peptides are transported from cell to cell and over long distances through the plant vascular system (xylem and phloem) to support plant metabolism and development. Amino acids represent in most plants the principal transport form for organic N, and they can be used directly for protein synthesis and other essential N compounds (Rentsch et al., 2007). Protein hydrolysates have also been shown to be effective in improving the enzymes involved in N and C metabolism (Ertani et al., 2013). Applications of PHs have been shown to promote the vegetative growth and macro- and micronutrient uptake in several horticultural crops, resulting in increased crop productivity (Halpern et al., 2015).

2.1.6.2 Protein hydrolysates and abiotic stress tolerance

The application of PHs and specific amino acids can induce plant defence responses and increase plant tolerance to a variety of abiotic stresses (Chen and Murata, 2008; Kauffman et al., 2007; Apone et al., 2010; Calvo et al., 2014). Several studies (Kauffman et al., 2007; Apone et al., 2010; Ertani et al., 2013) reported the positive effects exerted by PHs and amino acids in inducing secondary plant metabolism and increasing plant defence responses and tolerance to stresses, including salinity, drought and temperature and oxidative conditions. In a metabolomics study, Lucini et al. (2015) observed an increase of several secondary metabolites (e.g., terpenes, glucosinolates) after

application of a commercial plant-derived PH (Trainer®, commercialized by ItalPollina S.p.A., Rivoli Veronese, Italy) on lettuce plants grown under saline conditions. These secondary metabolites were involved in improving salinity tolerance of lettuce by modulating the signalling that activates defence pathways.

The biostimulants effectiveness to counteract the adverse conditions depends on several factors, such as timing of application and the concentration of the substance used. Incorrect application timing and concentration rates, along with variability of the stress exposure, are the primary reasons for poor efficacies of the biostimulants (Fleming et al., 2019). Thus, the identification of the right time of biostimulant application is as important as the determination of the exact dose, in order to avoid waste of product, high production costs, and unexpected results (Bulgari et al., 2019).

2.2 Biostimulants and phenotyping

Considering all the above, it is easy to predict that biostimulants will have a huge importance in the future of agriculture. The biostimulants market was estimated to account for $2.6 billion in 2019 and is projected to reach $4.9 billion by 2025 at a Compound Annual Growth Rate (CAGR) of 11.24% during the forecast period. The primary drivers of this growth are:

- the strong market demand for high-value crops across the globe;

- the increasing need to support crop growth due to abiotic stress, arising from changing climatic conditions;

- technological advancements by the key agricultural players in the world – such as India, Indonesia, Pakistan, Turkey, China, Brazil, Nigeria - that have led to high demand for biostimulant products (Biostimulants Market, 2020).

However, as stated before, the major limiting step in process of implementation and the commercialization of new biostimulants are the limited resources for effective prediction of plant

specific responses to given biostimulant and therefore the challenge remains in unpredictable response of a crop to the specific substance. In fact, the mode of action of PHs has been proven to be dependent not only on the species the biostimulants are applied to, but also on the dose, the time and mode of application, and also the environmental conditions (Kauffman et al., 2007; Kunicki et al., 2010; Ertani et al., 2014). Therefore, it is crucial to go through an in-depth testing of the product, before thorough validation and initiation of the commercialization process.

In the last 5 years, high-throughput automated phenotyping techniques have gained a massive popularity in the biostimulant field, as means to unravel the mode of action of biostimulants in a fast and precise way. The first publication referring to keywords "biostimulants" and "phenotyping" are used together is a review from Arioli and co-workers (2015). In this review, they focus on the use of seaweed extracts in Australian agriculture, pointing out that phenotyping is an extremely promising technique to investigate optimal application rates and timing of application of biostimulants on plants. However, with the term "phenotyping" they refer only to the use of time-lapse photography to follow the development of root and shoot biomass after the application of the biostimulants. Two years later, in 2017, Burrell and co-workers developed the 'Microphenotron' platform, once again to unravel the effects of several biostimulant compounds on the root and shoot development of Arabidopsis plantlets. In their review from 2018, Rouphael and co-workers pointed out that the application of high-throughput automated technology in the biostimulant field has been extremely limited, referring only to a work from Petrozza et al. (2014), where tomato plants subjected to drought stress and treated with a commercial biostimulant were monitored using visible light (RGB), fluorescence, and near infra-red (NIR) cameras. The following 2 years have seen a steady rise in the number of peer-reviewed papers (**Figure 3)** focusing on high-throughput automated phenotyping technology to investigate the effects of biostimulants on different crops – tomato (Danzi et al., 2019; Mutale-joan et al., 2020), pepper (Dalal et al., 2019), soybean (Briglia et al., 2019), wheat (Danzi et al., 2019; Ben-Jabeur et al., 2020) and maize (Akhtar et al., 2020) – with a main emphasis on the alleviation of the effects of abiotic stresses on the final yield.

The main aim of this doctoral work is to add a valuable contribute to the field of PHs functional characterisation in plants, shedding light on the enormous potential of high-throughput automated phenotyping technology in the biostimulants field.

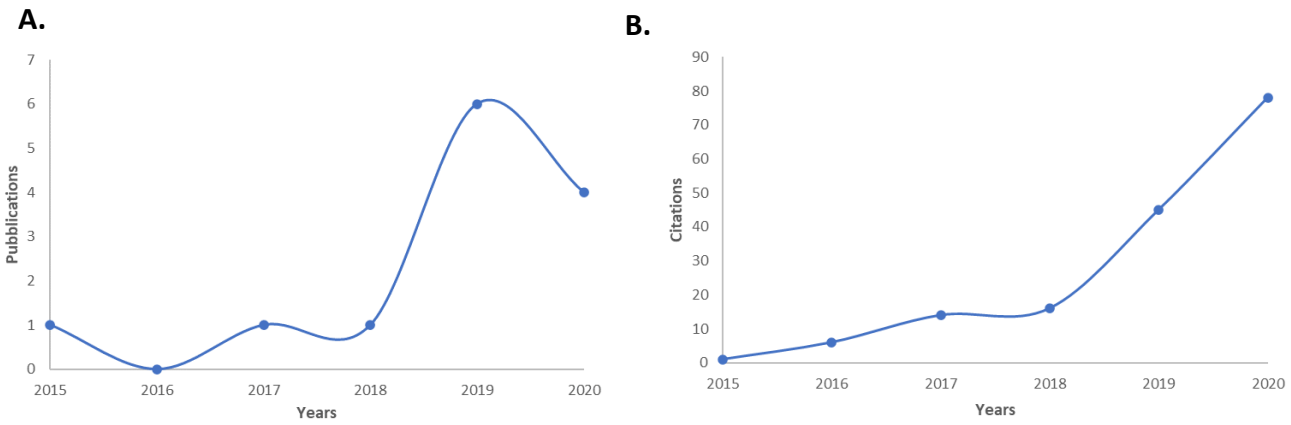

Figure 3| Biostimulants and phenotyping. *Number of publications per year of publishing (A) and number of citations for the publications (B) having both "phenotyping" and "biostimulants" as keywords, for the last 5 years (from Web of Science, 2021).*

2.2.1 Plant Biostimulant Characterization (PBC) Index.

To estimate the mode of action of the PHs in a clear-cut way, in our work we used the Plant Biostimulant Characterization (PBC) index, developed by Ugena and co-workers (2018). The aim of the PBC index is to unambiguously evaluate the mode of action of a specific substance, allowing to investigate the outcome on multiple parameters at once and to compare the effects of different doses in diverse growing conditions. To obtain the PBC index, it is necessary to calculate the log2 of the ratio between treated and untreated plants for the chosen morpho-physiological parameters and for each concentration of the compounds and growth conditions (control or stress). The sum of the obtained values corresponds to a single numeric value that could categorize the compounds in a

straight-forward way (**Figure 4**): if positive, the effect of the substance is biostimulant-like; if negative, the effect is inhibiting.

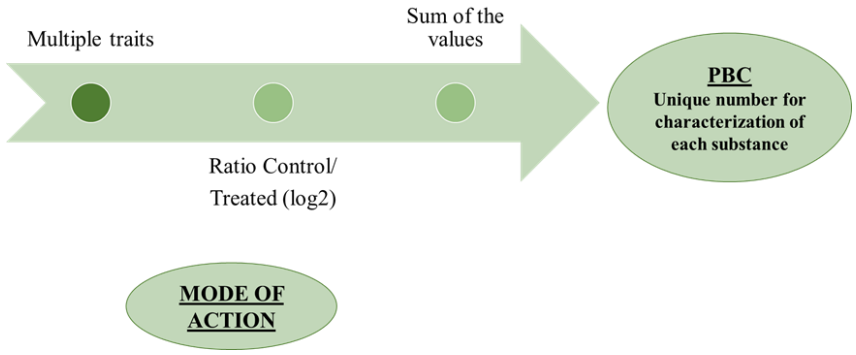

Figure 4| Plant Biostimulant Characterization Index. *Scheme that illustrates the steps for calculating the PBC Index of a substance.*

3. High-throughput automated plant phenotyping

3.1 History of plant phenotyping

In 2020, the International Plant Phenotyping Network (IPPN) has defined plant phenotyping as "the comprehensive assessment of complex plant traits such as growth, development, tolerance, resistance, architecture, physiology, ecology, yield, and the basic measurement of individual quantitative parameters that form the basis for more complex traits." Plant phenotyping investigates the combined effect of the genotype and the environment on the plant phenotype, that is, the complex of all its quantitative and qualitative observable traits (biomass, root morphology, leaves and fruits characteristics, yield-related traits). The term "phenotype" was coined by the Danish plant scientist Wilhelm Johannsen (1857-1927), that performed experiments on the heritability of seed size in beans (Walter et al., 2015). Johannsen also stated that natural history has always been based on the observation of the phenotypes, long before this term was even invented. The observation of plant phenotype can be traced back to the first farmers that, around 12000 years ago, were already selecting the wild crops to domesticate according to their observable features (such as the increase in both seed size and number) (Vergauwen and De Smet, 2017), with no knowledge of the underlying genetic components that contributed to these qualities. However, the term 'phenotyping' begun to be used only in the 1960s. At the time, the measurement of morpho-physiological traits on plants was conducted with manual, time-consuming and often destructive methods.

The first semi-automated and non-destructive instrument for the measurement of plant's growth was most probably the auxanometer, developed by the German botanist and plant physiologist Julius von Sachs (1832-1897), with the objective of measuring the growth of plants during short periods (Beach, 1914). In the following years Von Sachs' assistant, Wilhelm Pfeffer (1845-1920), described a new method for the use of photography to study plant movements and growth (Pfeffer, 1907), developing the first method for an image-based, non-destructive method of plant phenotyping. In the wake of this idea, during the 1980s and 1990s several sensors and computer vision tools have been developed and became fundamental for quantifying plant traits with increasing accuracy. Image and time-lapse analysis have been used for growth analysis of in-vitro plants (Motooka et al., 1991; Smith and

Spomer, 1987) or for the measurement of elongation and movements of roots and shoots (Care et al., 1998; Gordon et al., 1992).

In the last years, further steps toward precision and automatization in measurement have been made, with the development of high-throughput phenotyping platforms. These platforms use robotics, precise environmental control and imaging technologies to assess plant growth and performance (Li et al., 2014). Different cameras and sensors can be implemented into high-throughput phenotyping platforms, with the objective of investigating plants' phenotyping through the interaction between light and plants such as reflected photons, absorbed photons, or transmitted photons. A broad range of imaging cameras covering different portions of the electromagnetic spectrum is available to assay non-invasively a discrete number of plant traits.

3.2 Sensors

Plant phenotyping based on spectral reflection information relies on the properties of the light reflected, absorbed or transmitted by the tissues of the plant. The canopy spectral signature is described by the ratio of the intensity of reflected light to that of the illuminated light for each wavelength in visible (400–750 nm), near-infrared (750–1200 nm) and shortwave infrared (1200–2400 nm) spectral regions. The way healthy plants interact with electromagnetic radiation is different from that of suffering or unhealthy plants; therefore, the measurement of the light reemitted or absorbed by plants in different wavelengths provides valuable information on plants' properties, especially those that cannot be observed by naked eye (Li et al., 2014).

Different sensors have been developed to measure the interaction of plant tissue with light at different wavelengths, in controlled or semi-controlled environment (e.g., growth chambers, greenhouses) or field conditions. Our trials were exclusively performed in growth chambers and greenhouses; therefore, in this section we are not discussing the use of imaging sensors in field phenotyping (**Figure 5**).

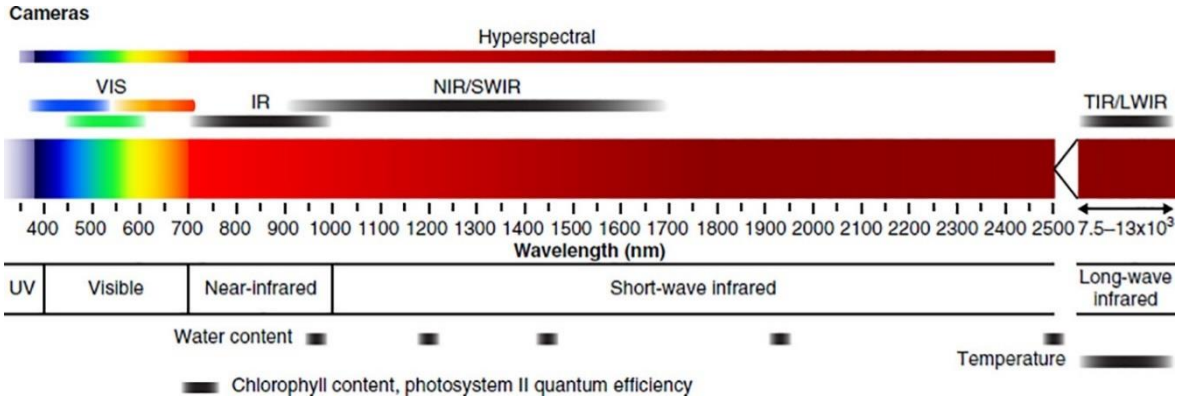

Figure 5| Cameras used in plant phenotyping and their wavelengths. *Principal sensors used in plant phenotyping and the light wavelengths they are able to measure (from Kolhar and Jagtap, 2021).*

3.2.1 RGB cameras

The visible band cameras (400-700 nm) are commonly defined as RGB (Red, Green and Blue) cameras, since the raw data of an image is typically presented in spatial matrices of intensity values corresponding to photon fluxes in the red (~600 nm), green (~550 nm), and blue (~450 nm) spectral bands of visible light. In RGB images, plant leaves appear green because green light (500–560 nm) is less efficiently absorbed by chlorophylls a and b than red or blue light, and therefore green light has a higher probability to become diffusely reflected from cell walls than red or blue light (Virtanen et al., 2020). RGB image data is most commonly used to measure plant size and biomass, but also colour, shape and leaf movements (Pandey et al., 2017). In fact, image-processing algorithms are used to identify pixels that are plant-derived, and the identified object is used for measuring morphological (shape, structure), geometric (length, area), and color properties of each plant (Fahlgren et al., 2015). Repeated RGB imaging throughout the plant life cycle can provide information about the growth rate of the plant and can be used to estimate the sum of stress response mechanisms. RGB imaging has been used to monitor plant responses to salinity (Awlia et al., 2016; Atieno et al., 2017; De Diego et al., 2017), drought (Berger et al., 2010; Neilson et al., 2015; Fisher et al., 2016), cold (Humplík et al., 2015a), heat (Gao et al., 2020; Abdelhakim et al., 2021), nutrient deficiency (Zhao et al., 2005; Naik et al., 2017) and a series of other abiotic stresses.

3.2.2 Chlorophyll fluorescence imaging

Chlorophyll fluorescence is a non-invasive measurement of photosystem II (PSII) activity. Because of the high sensitivity of PSII to environmental conditions and biotic and abiotic stresses and increased availability of the suitable technological solutions, the measurement of chlorophyll fluorescence has become more and more common. Chlorophyll fluorescence is based on the principle that the light absorbed by plants has to either be used up completely or dissipated, to avoid oxidative damages to the tissues. This process is called energy "quenching" (Ruban, 2016). In quenching, light adsorbed can be either used to perform photosynthesis (**photochemical quenching**), dissipated as heat (**non-photochemical quenching**) or re-emitted as light in the red wavebands (**chlorophyll fluorescence or chlorophyll quenching**) (**Figure 6**). These three processes occur in competition; hence, the measurement of the light re-emitted in longer wavebands can provide information about the amount of light used for photosynthesis (Baker, 2008).

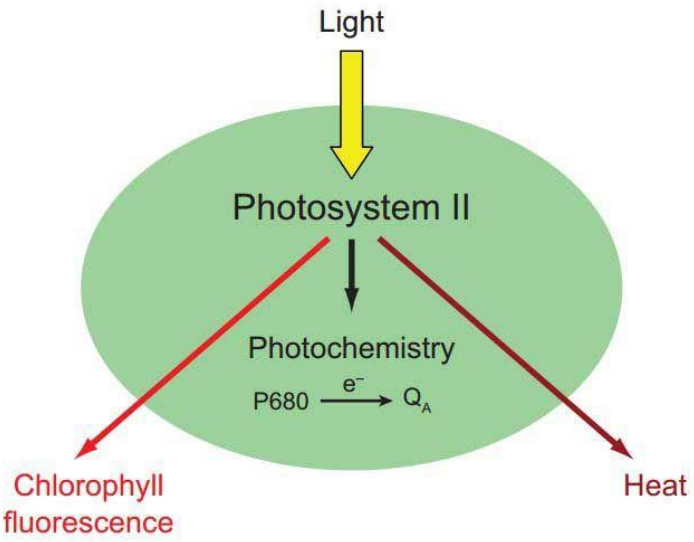

Figure 6\|Photosystem II and usage of light. *Simple model of the three possible fates of light energy absorbed by photosystem II (PSII) (from Baker, 2008).*

Cameras for the detection of chlorophyll fluorescence in high-throughput automated phenotyping platform belong mostly to the category of the Pulse Amplitude Modulated (PAM) Fluorometers. With this instrument, an initial light pulse, of an intensity too low to induce photosynthesis but high

enough to elicit a minimum value for chlorophyll fluorescence (F_0) is followed by a series of rapid pulses of very high intensity saturating light that overwhelm the acceptor pools, resulting in a rapid increase in fluorescence due to a lag phase before CO_2 fixation process occurs; this event leads to sequential quenching of fluorescence by activation of quenching mechanism (photochemical and non-photochemical) (Ritchie, 2008). In healthy and non-stressed dark-adapted plants there is no NPQ; therefore, the maximal possible value for fluorescence, F_m, is recorded. The difference between F_0 and F_m is the variable fluorescence, F_v. F_v/F_m quantifies the maximum quantum yield of PSII. For unstressed leaves, the value of F_v/F_m is highly consistent, with values of ~0.83 (Murchie and Lawson, 2013).

A leaf in continuous actinic light has a fluorescence level termed F', which rises to the maximal fluorescence level, Fm', when the leaf is exposed to a brief saturating light pulse. The difference between Fm' and F' is designated Fq' (Baker, 2008). Measurements of Fq'/Fm' (also defined as φPSII in literature) provide a rapid method to determine the PSII operating efficiency under different light conditions. Another important fluorescence parameter is represented by Fv'/Fm' (where Fv' corresponds to F0'-Fm'), that estimates the maximum quantum yield of PSII photochemistry that can be achieved in the light-adapted leaf (Baker, 2008). While Fv'/Fm' can be used to evaluate the contribution of changes in non-photochemical quenching to changes in PSII operating efficiency, levels of nonphotochemical quenching are often assessed by the parameter NPQ. NPQ is calculated from (Fm/Fm') − 1 and since it compares non-photochemical quenching from a dark-adapted leaf at F_m to that at F_m' for the leaf exposed to actinic light, it can only be measured for dark-adapted samples (Baker, 2008).

The modulated measuring systems proved to be reliable enough to have been used without undergoing any substantial changes for a relatively long period of time (Schreiber et al., 1986). Then, the application of Charge-Coupled Device (CCD) cameras to chlorophyll fluorescence, that combined the kinetic capability of the PAM Fluorometer with high-resolution imaging of the plants (Nedbal, 2000), has allowed to record the photosynthetic activity of a leaf, allowing the study of heterogeneity on leaf lamina and the screening of a large numbers of samples (Guidi and Degl'Innocenti, 2011). The FluorCam devices, developed by PSI in 1996, represent the first commercially available fluorescence imaging systems and it was firstly described by Nedbal and co-

workers in 2000. FluorCam work with weak modulated measuring light in combination with saturating light flashes and actinic light (light that drives photosynthetic electron transport) according to the PAM-principle and thereby enable the separation of photochemical and non-photochemical fluorescence quenching processes (Tschiersch et al., 2017).

Imaging-based devices for chlorophyll fluorescence measurement were successfully used to monitor the effects on photosynthetic efficiency of abiotic stresses, such as high light (Barczak-Brzyzek et al., 2017; Serôdio et al., 2017), drought (Yao et al., 2018; Marchetti et al., 2019; Abdelhakim et al., 2021), salinity (Awlia et al., 2016; Adhikari et al., 2019), high or low light intensity (Shin et al., 2021; Novák et al., 2021) and sub-optimal temperatures (Abdelhakim et al., 2021; Novák et al., 2021).

3.2.3 Thermal imaging

IR thermography 'visualises' surface temperature distribution of an object by focusing the longwave radiation (~8–14 mm wavelength range) emitted by the object onto a temperature sensitive detector (Sirault et al., 2009). The detection of thermal infrared emissions by plants has long been used for studies on crops' surface temperature, as indicator of water or nutrients stress and stomatal conductance (Jones, 2004; Jones et al., 2009; Maes and Steppe, 2012); in fact, a major determinant of leaf temperature is the rate of evaporation or transpiration from the leaf. The cooling effect of transpiration arises because a substantial amount of energy is required to convert liquid water to water vapour, and this energy is then taken away from the leaf in the evaporating water and, thus, cools it (Jones et al., 2009). Stomatal closure is known to be a sensitive response to soil water deficit, occurring even in the absence of any change in plant water status, as a result of root signalling (Davies et al., 2000). However, the traditional methods of measuring stomatal conductance (using porometers or infra-red gas analysers) are time-consuming, labour-intensive, and only give point measurements (Grant et al., 2007). Thermal imaging systems, on the other hand, allow rapid and non-invasive collection of data, integrated over the area of individual leaves or entire canopies. They may reveal spatial heterogeneity within or between leaves, and can be used repeatedly on the same leaves to monitor responses over time, without affecting the natural behaviour of the leaves. The increase in

temperature is an early symptom of stress on crops, and its measurement has been used to detect the effects of heat (Janka et al., 2013; Abdelhakim et al., 2021), salinity (Sirault et al., 2009; Siddiqui et al., 2014) and drought (Grant et al., 2007; Munns et al., 2010; Martynenko et al., 2016; Lee et al., 2019) on different plant species.

3.2.4 HyperSpectral Imaging

The term "hyperspectral imaging" was first mentioned by Goetz et al. (1985) in a work focusing on remote sensing (i.e., the observation of a target by a device without physical contact). The real story of hyperspectral imaging applied to plants began in 1987, when Alexander Goetz and his colleagues of the NASA's Jet Propulsion Laboratory (JPL), developed their hyperspectral Airborne Visible/Infrared Imaging Spectrometer, AVIRIS. AVIRIS was the first imaging spectrometer to measure the solar reflected spectrum from 400 nm to 2500 nm with 10 nm intervals (Green, 1998). Because of that first device and the similar ones that followed, a common definition of hyperspectral imaging is the simultaneous acquisition of spatial images in many spectrally contiguous bands measured from a remotely operated platform (Schaepman, 2007). The combined nature of imaging and spectroscopy in a hyperspectral imaging enabled this system to simultaneously provide physical and geometrical features of the product (i.e., shape, size, appearance, and colour) as well as the chemical composition of the object through spectral analysis (Elmasry et al., 2012). A spectral image (that can be hyperspectral, multispectral or ultraspectral) is a stack of images of the same object, each at a different spectral narrowband. The difference between these classes is the number of bands and the form of the spectrum obtained. The numbers of spectral bands in case of multispectral imaging systems are very few (normally less than 10 bands), while hundreds of contiguous and regularly spaced bands are the main feature of hyperspectral images (Elmasry et al., 2012). Therefore, multispectral imaging systems do not provide a real spectrum in every image pixel; meanwhile each pixel in the hyperspectral image has a full spectrum (Ariana and Lu, 2008).

Usually, not all the wavelengths that compose the spectrum are informative in plant science. Useful spectral regions have been identified, such as the transition from red to near-infrared, the peak of green reflectance, and the water absorption bands around 970 nm, 1600 nm and 2100 nm (Fiorani et

al., 2012). These spectral features can be used to quantify vegetation indices that usually relate the reflected intensity of a reference band to that of spectral bands responding to specific characteristics of plants or canopies. Two of the most commonly used indices are the normalized difference vegetation index (**NDVI**) comparing the red and the near infrared reflectance (closely related to leaf chlorophyll content) and the photochemical reflectance index (**PRI**) that correlates with the functional status of non-photochemical energy protection (Fiorani et al., 2012). Spectral indices proved to be an excellent instrument for detection of abiotic stresses on crops, such as low nitrogen availability (Zhao et al., 2005) and salinity (Lara et al., 2016; El-Hendawy et al., 2017; Sytar et al., 2017), as well as for the estimation of nitrogen content (Thorp et al., 2017; Ye et al., 2019; Banerjee et al., 2020).

3.2.5 Integrative phenotyping

The three main traits of a plant phenotyping system, as described by Dhont and co-workers in their review from 2013, are:

1. **throughput:** number of individuals that can be analysed for specific trait/s in a certain span of time. In this case, the adjective "high-throughput" refers to platforms that can image hundreds of plants per day;
2. **resolution**: it can be either spatial, referring to the level of organization of the subject chosen for the analysis – from a single cell to an entire plant population – or temporal, referring to the time intervals at which the measurements are repeated, and for how long;
3. **dimensionality**: it refers to the diversity of phenotypic traits measured at different spatial and temporal resolutions and in different categories, such as plant structure, physiology, and performance (Großkinsky et al., 2015).

Dimensionality is especially interesting when working with complex high-throughput automated phenotyping platforms. In fact, the users can choose between a single imaging method or an integrative approach, signifying simultaneous use of some or all the sensors available in the system (Kolhar and Jagtap, 2021). The use of single sensors enables the measurements of simple traits but,

from a technical point of view, shows limitations in the determination accuracy of more complex traits (Busemeyer et al., 2013).

While traditional phenotyping mostly focused on yield and yield-related traits, plant scientists are now focusing on adaptive and evolutionary traits of crops to external stressors (Pratap et al., 2019). Therefore, fusing multiple data (e.g., colour data, morphological data, spectral data and so on) provided by several sensors will provide a more complex response to the question addressed by the researchers regarding plant growth, development, responses to environment, as well as selection of appropriate genotypes in molecular breeding strategies (Humplík et al., 2015b). The combinate use of multiple sensors offers opportunities to identify spectral markers associated with early signs of plant physiological responses (Mochida et al., 2018). For this reason, many studies have already combined spectral data obtained from different imaging sensors. RGB imaging combined with kinetic chlorophyll fluorescence imaging was used on Arabidopsis plantlets under salt stress (Awlia et al., 2016) and on barley subjected to drought (Marchetti et al., 2019). The further integration of thermal imaging has recently helped researchers investigate the effects of heat stress on crops (Gao et al., 2020; Abdelhakim et al., 2021). Integrated phenotyping techniques were also used to study the effects of biostimulants in terms of early detection of plant physiological stresses (Petrozza et al., 2014). The use of multiple sensors can also be used for more complex applications: for example, Shi and co-workers (2020) have developed an algorithm that uses thermal imaging in combination with RGB imaging for monitoring fruit surface temperature to manage apple sunburn.

The integration of the information provided by the aforementioned imaging sensors allows a more in-depth analysis of plant structural characteristics, but also requires high-speed computers (Omari et al., 2020) and generates a huge quantity of multi-dimensional phenotypic data (Li et al., 2020).

3.3 Integration of phenomics with metabolomics

Metabolomics is defined as the comprehensive study of metabolites, small molecules (≤1500 Da in size) which participate in different cellular events in a biological system (Yang et al., 2021). Metabolomics is particularly important in plant systems, because plants produce more metabolites

than either animals or microbes. The secondary metabolites produced by plants are helpful in responses to environmental stress. Thus, metabolomics is a promising area in stress-physiology, focusing on plant response to numerous abiotic stresses in relation to their metabolite changes (Brunetti et al., 2013) and providing a comprehensive understanding of the biochemical status of an organism, e.g., to inform on the processes involved in disease progression or environmental adaptation (Hamany Djande et al., 2020). It is therefore clear why, in the late years, there is growing interest in combining phenomics data with other "-omics" data, such as metabolomics (Yang et al., 2021). However, one current challenge is integrating additional technologies to provide a multi-omics approach to study biological mechanisms and their response to environmental stresses for important agronomic traits (Moreira et al., 2020); in fact, the bigger the amount of data, the more challenging the statistical analysis and the interpretation of the results. For phenotyping projects that engage several hundred samples, it can be useful to use more oriented analysis. Preliminary metabolomics work might indicate which substances are the main contributors to the phenotype of interest and lead to a focused analysis that is more productive and cost effective for phenotyping than previous methods (Sytar et al., 2018). In general, the term 'metabolomics' covers two basic approaches. First, the non-targeted approach, which aims to determine as many compounds in the sample as possible. This approach may lead to discoveries of new active molecules, but it is slower and more expensive than the second approach. The second, targeted, approach aims at research for practical applications, such as food or pharmaceutical needs, targeting a single, or relatively narrow, well-defined group of compounds (e.g., amino acids, phenolics) (Verpoorte et al. 2005). Depending on the target metabolites, several possible non-invasive techniques may be used in the early stages of metabolomics research.

3.4 Future of plant phenotyping

Integrative phenotyping, either if it means to integrate data from different sensors or from different "-omics" technologies, generate a huge amount of data. Therefore, according to the experts, the future progress in image-based plant phenotyping will require a combined effort in image processing for feature extraction and machine learning for data analysis (Ubbens and Stavness, 2017). In fact, the application of computer vision and pattern recognition technologies to plant phenotyping can reduce

the work intensity of the scientists. Machine learning methods are already used for simple image-based tasks, such as object detection and localization or image classification (LeCun et al., 2015). However, more complex tasks such as leaf/fruit counting, injury ratings, disease detection and age estimation add a higher level of abstraction which requires a more complicated image processing pipeline; furthermore, at the present time the image-based phenotyping tools are often also only applicable for processing pictures of individual plants taken under highly controlled conditions. In response to the limited flexibility of classical image processing pipelines for complex phenotyping tasks, machine learning techniques are expected to take a prominent role in the future of image-based phenotyping (Tsaftaris et al., 2016). Algorithms based on deep learning, an emerging subfield of machine learning, often show more accurate performance compared with traditional approaches to computer vision-based tasks, including plant identification (Mochida et al., 2018). Furthermore, deep learning simplifies the process of extracting phenotypic features and improves plant phenotyping applications greatly. However, at the present time these technologies show several limitations, such as the availability of high-quality image to train the algorithm, and the robustness of said algorithms, that do not generalize well due to the large differences in colour, shape, size and other characteristics between different detection objects (Li et al., 2020). The future research in the field is therefore aimed at collecting better and more diverse material for the training of more complex and robust algorithms.

4. Abiotic stresses

Agriculture is one of the most climate-dependent socio-economic sectors, since most of the agriculture productivity and quality are directly dependent on different climatic factors (McArthur, 2016). In fact, around 60–70% of the global yield losses in agriculture are estimated to be attributable to abiotic stresses (Yakhin et al., 2017). In agriculture, an abiotic stress is defined as environmental conditions that reduce growth and yield of a crop below optimum level (Cramer et al., 2011). Plant responses to abiotic stresses can be elastic (reversible) and plastic (irreversible) (Skirycz and Inze, 2010). In addition, the level and duration of stress (acute vs chronic) can have a significant effect on the complexity of the response (Tattersall et al., 2007). The most severe abiotic stresses, namely the ones that cause most of the damages to the main crops, are related to water scarcity and high salinity content of irrigation waters (Vernieri et al., 2006).

4.1 Drought stress

Water deficiency, assumed to be soil and/or atmospheric water deficit, is a severe environmental stress, and has a negative impact on crop yields worldwide (Pennisi, 2008). Due to the increasing water needs required by agriculture, pollution of natural water resources, and climate change scenarios, for the next few years, issues related to water scarcity and reduction of irrigation water availability could became preponderant (Ferrara et al., 2011). The severity of drought is unpredictable as it depends on many factors such as occurrence and distribution of rainfall, evaporative demands and moisture storing capacity of soils (Wery et al., 1994). Water deficit is a multidimensional stress affecting plants at various levels of their organization (Yordanov et al., 2000). Thus, the effects of stress are often manifested at morpho-physiological, biochemical and molecular level (Aimar et al., 2011).

Stomatal closure, together with leaf growth inhibition, are among the earliest responses to drought, protecting the plants from extensive water loss, which might result in cell dehydration and death

(Chaves et al., 2003). It is clear that stomata close progressively as drought progresses, followed by a parallel decline in net photosynthesis. Drought stress affects photosynthesis also through damages to the photosynthetic apparatus and reduction in the activities of Calvin cycle enzymes, which are important causes of reduced crop yield (Monakhova and Chernyadèv, 2002). However, there are various morphological, biochemical and physiological mechanisms that plants can use to maintain growth in conditions of low water supply (Berger et al., 2010). Classically, plant resistance to drought has been divided into escape, avoidance and tolerance strategies (Levitt, 1972; Turner, 1986). Plants that escape drought exhibit a high degree of developmental plasticity, being able to complete their life cycle before physiological water deficits occur (Chaves et al., 2003). While natural selection has favoured mechanisms for adaptation and survival, breeding activity has directed selection towards increasing the economic yield of cultivated species. Minimizing the 'yield gap' and increasing yield stability under different stress conditions are of strategic importance in guaranteeing food for the future (Khan et al, 2015).

In our work, we have analysed the responses to drought stress of lettuce and tomato.

Lettuce (*Lactuca sativa* L.) is a leaf-edible vegetable that shows extreme sensitivity to drought due to shallow root system (Knepper and Mou, 2015) and high-water content (95 to 97%). Apart from the reduction of cell elongation, interruption of the water flow may also lead to changes in root morphology, such as decrease in specific root length and surface area, with a consequent reduction in nutrient uptake capacity. Due to drought stress, final biomass and final yield of lettuce could be seriously reduced. Most commercial tomato (*Lycopersicum esculentum* Mill.) cultivars are drought sensitive at all stages of plant development, with seed germination and early seedling growth being the most sensitive stages (Foolad et al., 2003). The amount of water required daily for tomato in different growing systems varies from 0.89 to 2.31 m^3/plant/day (Tiwari, 2003).

Losses in agricultural yield due to water stress probably exceed the losses inflicted by all other causes combined. Therefore, at present, with the aim of improving agricultural yield within the earth's limited resources, it is necessary to make the plants robust enough to give a high yield when growing in stressed or sub-optimal environments (Sánchez-Rodríguez, 2010).

4.2 Salinity stress

Salinity is a soil condition characterized by a high concentration of soluble salts. Soils are classified as saline when the ECe is 4 dS/m or more (USDA-ARS. 2008), a value that significantly reduces the yield of most crops. Because NaCl is the most soluble and widespread salt, it is not surprising that all plants have evolved mechanisms to regulate its accumulation and to select against it in favour of other nutrients commonly present in low concentrations, such as K^+ and NO_3^- (Munns, 2005). Agricultural productivity is severely affected by soil salinity because salt levels that are harmful to plant growth affect large terrestrial areas of the world (Yamaguchi and Blumwald, 2008). It was estimated that about 20% (45 million ha) of irrigated land, producing one-third of the world's food, is salt-affected (Shrivastava and Kumar, 2015). Soil salinity affects an estimated 1 million hectares in the European Union, mainly in the Mediterranean countries, and is a major cause of desertification (Machado and Serralheiro, 2017). Low rainfall, high evaporation, poor water management and the indiscriminate use of huge quantities of chemical fertilizers have also exacerbated growing concentrations of salts in the rhizosphere (Mahajan and Tuteja, 2005). It has been estimated that more than 50% of the arable land would be salinized by the year 2050 (Jamil et al., 2011).

Most of the vegetable crops are glycophytes and, therefore, highly susceptible to soil salinity (Shannon and Grieve, 1999). Moreover, the salinity response of crops throughout their growth cycle may change in relation to several interacting variables, such as the plant developmental stage, the salt concentration and the time of exposure (Munns, 2002). The general effect of salinity is to reduce the growth rate (Shannon and Grieve, 1999). Soil salinity stresses plants in two ways: high concentrations of salts in the soil make it harder for roots to extract water (**osmotic effect**), and high concentrations of salts within the plant can be toxic (**ionic effect**). In the first, osmotic phase, which starts immediately after the salt concentration around the roots increases to a threshold level, the rate of shoot growth falls significantly. In the second, ionic phase, toxic concentrations of salts take time to accumulate inside plants before they affect plant function (Munns and Tester, 2008). The most readily measurable plant response to salinity is a decrease in stomatal aperture. Stomatal responses are undoubtedly induced by the osmotic effect of the salt outside the roots (Fricke et al., 2004). A decrease in maximum quantum yield of PSII and an increase in non-photochemical quenching have

been recorded in a number of species subjected to salinity stress, such as barley and maize (Kalaji and Rutkowska, 2004).

Plants differ greatly in their tolerance of salinity. While some have relative resistance, others are sensitive to even low levels of salinity (Afzal et al., 2005). Lettuce is a leafy vegetable considered as "moderately sensitive" to the effects of salinity, with tolerance differing significantly between varieties (Maas, 1990). The production is proven to decline by approximately 13% by each unit of increase in salinity threshold, which is 1.3 dS m^{-1} (Maas, 1986). On the other hand, a moderate salinity stress is proved to improve the fruit quality of tomato by increasing the level of total soluble solids, including sugars, organic acids, and amino acids in fruits (Krauss et al., 2006; Saito et al., 2008), but to also reduce the final fruit yield (Saito and Matsukura, 2015). However, it was found that short-term (<21 days) salinity stress during any of the growth stages did not affect tomato growth, and during the vegetative stage did not affect yield. Salinity stress during the flowering and fruiting stages caused a reduction in tomato yield, which was due to a reduction in the number of fruits produced, rather than the fruit size (Zhang et al., 2016).

Aim of the thesis

This doctoral work was performed in the frame of the European Union's Horizon 2020 research and innovation program "Solar Energy to Biomass (Se2B) - Optimisation of light energy conversion in plants and microalgae", funded by the Marie Skłodowska-Curie grant agreement No 675006 and in frame of the PRIN project no. 2017FYBLPP "Use of Protein-HydrOlysates as BiOstimulants of vegetable cropS: elucidating their mode of action and optimizing their effectiveness through a multidisciplinary approach – PHOBOS", funded by the Italian Ministry of Education, Universities and Research.

The main aim of the work was to develop and validate an effective and reproducible protocol to characterize the mode of action of biostimulants of diverse origins on crops by using high-throughput automated plant phenotyping and to validate this evaluation through metabolomic analysis. The experimental work was conducted mainly in the Research Centre of Photon Systems Instruments (PSI, Drasov, Czechia) using different automated phenotyping platforms developed by PSI itself and partially in the Centre of the Region Haná for Biotechnological and Agricultural Research (Czech Advanced Technology and Research Institute, Olomouc, Czechia) in the group of Dr. Lukáš Spíchal. Metabolomic analysis have been conducted in the Department for Sustainable Food Process (DiSTAS, Catholic University of the Sacred Heart, Piacenza, Italy) by the group of Prof. Luigi Lucini.

The main goal of this work was to test the activity of a set of biostimulants on different plant species (wheat, Arabidopsis, lettuce and tomato), applying the biostimulants in different doses by using different methods of application and primarily quantitatively evaluating their mode of action throughout the entire life cycle of the plants. The presented approach can be divided into three phases, referring to the developmental stage of the plant at which the biostimulants were applied and the mode of action was assessed (**Figure 7**):

Aim of the thesis

1. **Seed stage referring to** germination assay on wheat seeds; seeds coated with different biostimulants in 2 doses were cultivated in control conditions and subjected to salt stress – **Results, Chapter 1**;

2. **Seedling stage referring to** *in-vitro* assay on Arabidopsis plantlets; plantlets originated by seeds primed with 11 different biostimulants in 4 doses were cultivated in control conditions and subjected to salt stress – **Results, Chapter 2**;

3. **Mature crops stage referring to** assays on plants of lettuce and tomato at vegetative phase, either sprayed or watered with solutions of 11 biostimulants in 1 dose and subjected to drought or salt stress – **Results, Chapter 3.**

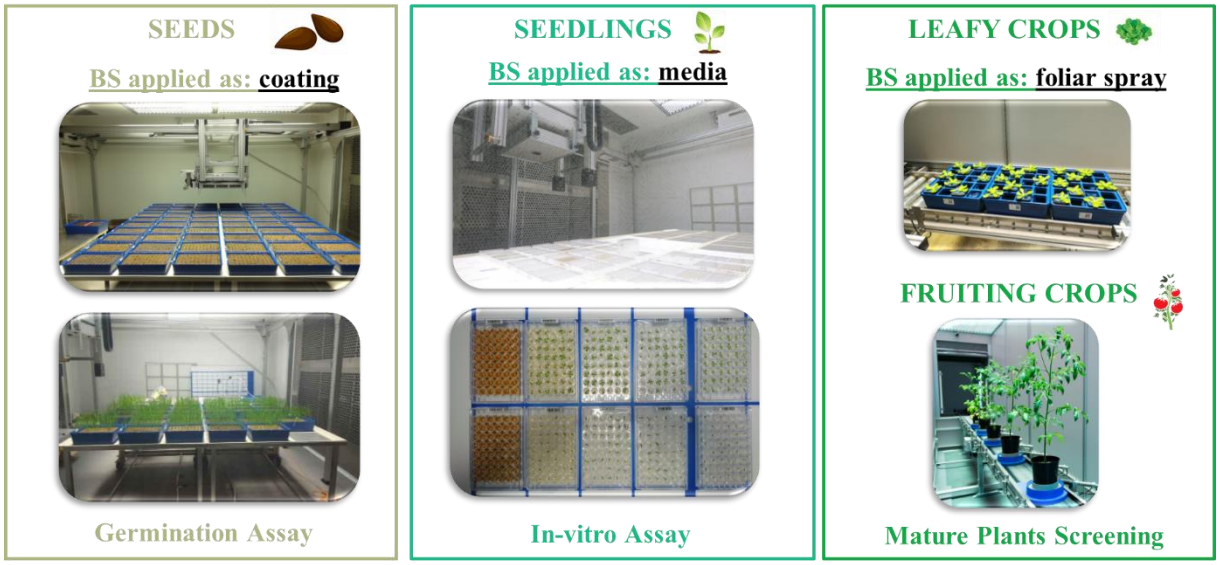

Figure 7| From seeds to crops. *The three different stages of the doctoral work: observation of the biostimulants effects on seeds, seedlings and mature crops.*

Using an array of image-based sensors implemented in the PlantScreen™ phenotyping platform of PSI Research Centre, different morpho-physiological traits were analysed in the given assay stage, crop and condition. The values of the treated plants were then compared to the controls, to quantitatively evaluate the response of the plants to different abiotic stresses and the relative variations in mode of action of the different biostimulants in the given environmental conditions.

The sum of each normalized trait in each concentration of the substance and growing condition (control and stress) was then used for the calculation of the Plant Biostimulant Characterization Index (PBC). Developed by Ugena and co-workers (2018), this index focuses on a straight-forward characterization of the mode of action of each substance. According to the PBC value we could effectively categorise the biostimulant substances as:

1. growth promoter;
2. growth inhibitor;
3. stress alleviator
4. growth promoter and stress alleviator.

The best performing compounds were further characterised by in-depth targeted and untargeted metabolomic analysis of the plants treated with the given substance, concentration and condition.

Finally, the complex sets of data obtained from the two omics approaches were integrated with the help of multivariate statistical analysis in order to extract the relevant information and identify the morpho-physiological traits that were influenced the most by the PHs applications, also highlighting the different responses of the two species.

Results

1. Chapter 1

Seed – Emergence assay in coated wheat seeds

1.1 Introduction

In annual plants life cycle, seedling emergence is the most fragile phase. Many environmental factors can influence emergence time, therefore impacting on plant survival and growth (Mercer et al., 2011). It is hence clear that this phase is particularly vulnerable to environmental stresses; one among them, soil salinity (Zhang et al., 2010). High osmotic pressure of the soil, caused by an elevate salt concentration in the soil solution, creates a condition similar to drought, in which water can hardly be extracted from the soil. This reduces the seeds capacity for imbibition, therefore delaying or hindering their germination. Furthermore, the absorption of excess Na^+ and Cl^- ions causes toxicity in the plantlets tissue, deterring the cells division and, therefore, the possibilities of successful establishment of the seedlings (Mwando et al., 2020).

To increase the germination rate, even in adverse environmental conditions, it is essential to improve the seeds quality. One of the most common methods to increase seeds viability is seed coating, a technique proven to improve emergence and establishment of vegetables (Serena et al., 2012). Coating mixtures used on seeds may contain fungicides, fertilizers or biostimulants (Qiu et al., 2020). Commonly applied biostimulants include microbial inoculants, beneficial bacteria and fungi, nitrogen containing compounds, biopolymers, and plant extracts (Rouphael and Colla, 2018). If compared with the most common method of biostimulants application, foliar spray, seed coating provides an opportunity for reduced application rate per hectare, reducing the human labour and time needed for repeated foliar applications (Amirkhani et al., 2016). Furthermore, it allows to investigate

the effects of the biostimulants when they are applied in a very early phase, prior the emergence of the plantlet, and to evaluate their effect on a very delicate phenological stage.

However, manual scoring of seeds germination rate is time-consuming and laborious. To increase the scoring rate and make the process more effective and precise, Ugena and co-workers (data unpublished) used an automated plant phenotyping platform equipped with a RGB camera to develop a high-throughput bioassay that monitors seedling emergence under saline conditions by automated detection of the first appearance of a coleoptile (first green pixel). They further focused on different aspects of the emergence phase: final germination rate, time lag and emergence synchronicity, developing a multidimensional analysis of the emergence curves. They optimized their method using seeds primed with single stress-related molecules (spermine, spermidine and putrescine) applied at different concentration.

We have adjusted the methodology developed by Ugena et al. for the screening of a population of seeds coated with complex biostimulant compounds. The biostimulants used were carefully selected protein hydrolysates of plant origin (soybean or pea), algae extracts (*Ascophyllum nodosum)* and extracts from beneficial fungi (mycorrhizal fungi and *Trichoderma atroviride*). The coated seeds were cultivated for 12 days in controlled environmental conditions after being watered either with plain water or a 150 mM NaCl solution. The seeds were scored twice a day using PlantScreen™ XYZ System, a RGB camera mounted on robotic arms that moves on the Cartesian axes. The RGB images were then analysed to monitor the emergence and the early growth of the plantlets. Using this very simple and rapid scoring approach, in the frame of two weeks we could classify the substances as Germination Promotors or Stress Alleviators, according to their effects on the emergence of the coated seeds. We were able to identify one of the newly-developed biostimulant as the best performing substance, both in control and in salt stress conditions. In our work, we show that our multidimensional analysis of the emergence curves provides useful information related to the response of the wheat population to the coating with 6 different biostimulants, over a range of concentrations, in control and salt stress conditions.

1.2 Materials and methods

6 biostimulants of different origins, provided by Hello Nature Inc. (former Italpollina), were applied as film coating on seeds of *Triticum aestivum* cv Bandera. The 6 products, diluted in water at different concentrations, were sprayed on the seeds using 2 L of solution per 100 kg of seeds. The description and the concentrations of the substances used for the coating are listed in **Table 1**.

Table 1| List of biostimulants used for seeds coating. *The substances are listed according to the letter code used in the trial. Origin and concentration of each substance are included.*

Code	***Composition***	***Concentrations***	***Description***
C	Mycorrhizal fungi and *Trichoderma atroviride*	80 g/100 kg of seeds	Commercial product (***Coveron*** ®)
		160 g/100 kg of seeds	
T	Soybean extract	80 ml/100 kg of seeds	Commercial product (***Trainer*** ®)
		320 ml/100 kg of seeds	
B	Pea seeds extract	80 ml/100 kg of seeds	Experimental product
		320 ml/100 kg of seeds	
TA	Soybean extract + *Ascophyllum nodosum*	80 ml/100 kg of seeds	Experimental product
		320 ml/100 kg of seeds	
A	*Ascophyllum nodosum*	80 ml/100 kg of seeds	Experimental product
		320 ml/100 kg of seeds	
H	Protein hydrolysate from legumes + plant extract	320 ml/100 kg of seeds	Commercial product (***Heptamin®)***

300 seeds coated with each substance in given dose were distributed between two square Petri dishes containing water-soaked filter paper and stratified in the dark at 4°C for 16 hours. Afterwards, 26 nursery trays TEKU IP 3050/160 T provided with 110 holes, each one filled in with soil (Substrate 2, Klassmann Deilmann, Geeste, Germany), were cut to fit into hydroponic inserts for standard PlantScreen™ measuring trays Figure **1**).

After the sowing of the seeds, one per hole, each tray was watered from the bottom up to its full field capacity, either with tap water or with a saline solution (150 mM NaCl). Afterwards, all trays were given 1 L of tap water every third day until the end of the experiment.

Figure 1\Seeds preparation. *On top: stratified coated seeds on wet filter paper: On bottom: nursery tray with 110 holes filled with Klassman 2 substrate, in which the seeds were then sown.*

1.3.1 Phenotyping protocol and growing conditions

One hour after the first watering, the trays were moved into the OloPhen platform that uses PlantScreen™ XYZ System (Photon Systems Instruments, Drasov, Czech Republic), installed in a growth chamber with a controlled environment and cool-white LED lights. The environmental conditions were 22◦C/20◦C in a 16/8 h light/dark cycle, an irradiance of 120 µmol photons of PAR m^{-2} s^{-1} and a relative humidity of 60%.

Figure 2| Experimental setup. *Image of the phenotyping trays containing the seeds, randomized on the growing table in the OloPhen platform (courtesy of Nuria De Diego).*

The PlantScreen™ XYZ system consists of a robotically driven arm holding an RGB camera that moves on the Cartesian axes and a growing table with a total area of approximately 7 m^2, where the trays were positioned in fixed places. The XYZ robotic arm was automatically moved above the growing table to take RGB images of the single trays from the top (**Figure 2**). Starting from the first measure, RGB pictures were taken every second hour over the twelve days of the experiment.

1.3.2 Destructive measurements

After the last RGB imaging, we measured the heights at the collar of 15 random plants per tray. After that, all the plants were cut at the collar level and weighted, put into paper bags and placed in the dryer at 105°C for 3 days. The dry weights were then measured.

1.3.3 Data analysis

The RGB pictures were automatically stored in PlantScreen XYZ database, exported by PlantScreen Data Analyzer software and analysed using an in-house software routine implemented in MatLab R2015, that subtracted the background in order to evaluate only the green pixels belonging to the plants' surface. For each seed, the time of emergence (i.e., the moment of the coleoptile appearance)

was recorded. The seeds were considered germinated when the first green pixel was detected in the RGB image. Some seedlings may have not emerged at all until the end of the experiment.

1.3.4 Evaluation of the germination curves and derived parameters

Data about seeds germination differ from other types of biological data. For example, in a population of seeds, some of them remain non-germinated when the experiment ends, and there is no way to know when these seeds would have germinated if the experiment had continued indefinitely (Ugena et al., unpublished). Therefore, instead of the more broadly used logistic curve, we used the Gompertz curve, that is one of the most frequently used sigmoid models fitted to growth data (Tjørve and Tjørve, 2017). Paine et al., in their work from 2012, claim that the Gompertz model fits better than linear growth models in the case of plants communities, since it assumes a final asymptotic phase due to the resource-limited growth of populations. In the Gompertz model, RGR declines exponentially over time; this means that convex part of the emergence curve (around the time of emergence of the fastest seeds) tends to proceed faster than the concave part of the emergence curve (around the time of emergence of the slowest seeds). This curve is non-symmetrical and it can be generalized to allow non-zero initial masses and variation in the inflection point, and it is therefore particularly suitable to survival analysis such as germination trials.

Our Gompertz curve corresponds to the equation:

$$y(t) = A \exp(-x(t)) \quad (1)$$

and it consists of an initial exponential phase, an approximately linear phase (which contains the inflection point), and a finally asymptotic phase, in which the curve approaches a constant (the final number of seeds emerged).

Three main traits can be extrapolated from the Gompertz curves:

1. the **emergence rate** in the last day of measurement, corresponding to A in the equation (1) – it is obtained dividing the number of actually germinated seeds in a tray by the total number of seeds in the tray;

2. the **time lag**, the amount of time occurring between the germination of half of the control seeds and half of the treated seeds, corresponding to t in the equation (1) – it is estimated by subtracting the time when 55 untreated seedlings had emerged under control conditions (0) from the time the treated seedlings emerged;

3. the **speed** or **synchronicity of emergence**, represented by the coefficient k in the equation (1) – it corresponds to the slope of the Gompertz curve.

1.3.5 Plant Biostimulant Characterization (PBC) Index

For the calculation of the PBC index, we considered the three parameters extracted from the emergence curve: the **Emergence Rate**, the **Speed** and the **Time Lag** (**Table 2**).

***Table 2|PBC Index traits**. List of the parameters extracted from the emergence curve and used for the calculation of the Plant Biostimulant Characterization Index.*

Parameter	Unit	Definition
Emergence rate	%	Percentage of seeds germinated per each tray in the last day of phenotyping.
Time lag	days	Time elapsed between the germination of 55 control seeds and 55 coated seeds.
Speed or synchronicity of emergence	arbitrary unit	Slope of the emergence curve.

To obtain the PBC index, we first calculated the log2 of the ratio between coated and uncoated seeds for the first two parameters (emergence rate and speed) for both concentrations of the compound and growth conditions (control or salt stress). For the time lag, the difference was estimated by

subtracting the time when 55 uncoated seeds had germinated under control conditions (designated as 0) from the time the coated seeds under control or salt stress conditions emerged.

1.3.6 Statistical analysis

One-way analysis of variance (ANOVA) with post hoc Tukey's Honest Significant Difference (HSD) test ($p < 0.05$) was used for statistical differences in phenotyping data, using the MVApp application (mmjulkowska/MVApp: MVApp.pre- release_v2.0; Julkowska et al., 2019).

1.3 Results

1.4.1 Coating of seeds with diverse biostimulants differently modulate emergence parameters under salinity stress conditions

Emergence of the seeds was scored twice a day using PlantScreen™ XYZ System by a RGB camera. Plant objects were segmented using the image processing pipeline and sum of the plants for given treatment was used to develop empirical emergence curves characterising cumulative number of seeds germinated over time. A Gompertz curve was created per each treatment and dose of biostimulants, for seeds growing in control (**Figure 3**) and salt stress conditions (**Figure 4**). In each graph, lower and higher dose of each substance are compared to the untreated control.

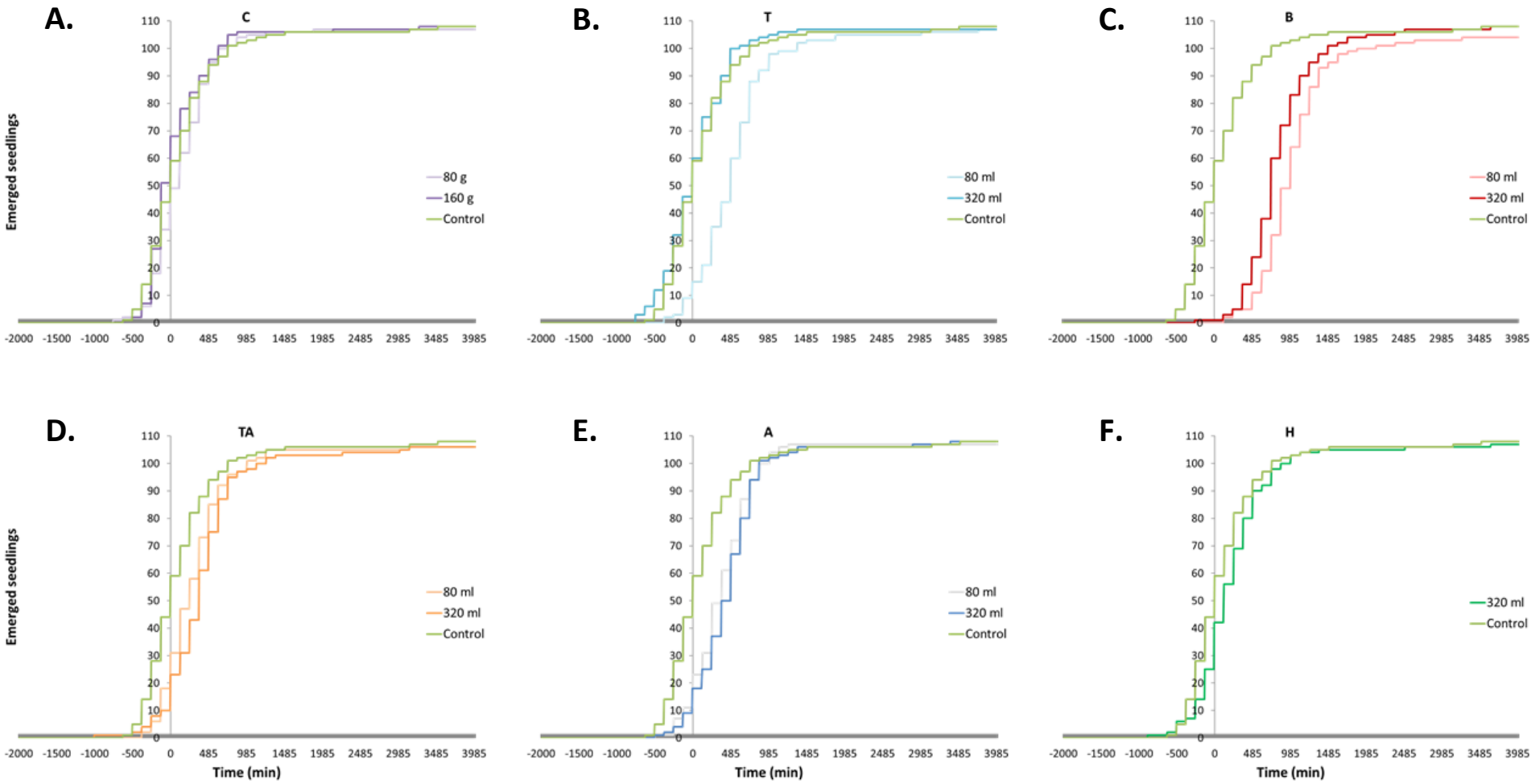

Figure 3| Empirical emergence curves. *Cumulative number of seeds germinated over time in control conditions. A.) Comparison between uncoated seeds and seeds coated with the substance C in the concentrations 80 g/100 kg and 160 g/100 kg. B) T in the concentrations 80 ml/100 kg and 320 ml/100 kg, C) B in the concentrations 80 ml/100 kg and 320 ml/100 kg (C.), TA in the concentrations 80 ml/100 kg and 320 ml/100 kg (D.), A in the concentrations 80 ml/100 kg and 320 ml/100 kg (E.) and H in the concentration 320 ml/100 kg (F.) Time 0 corresponds to the moment when half of the control seeds were germinated.*

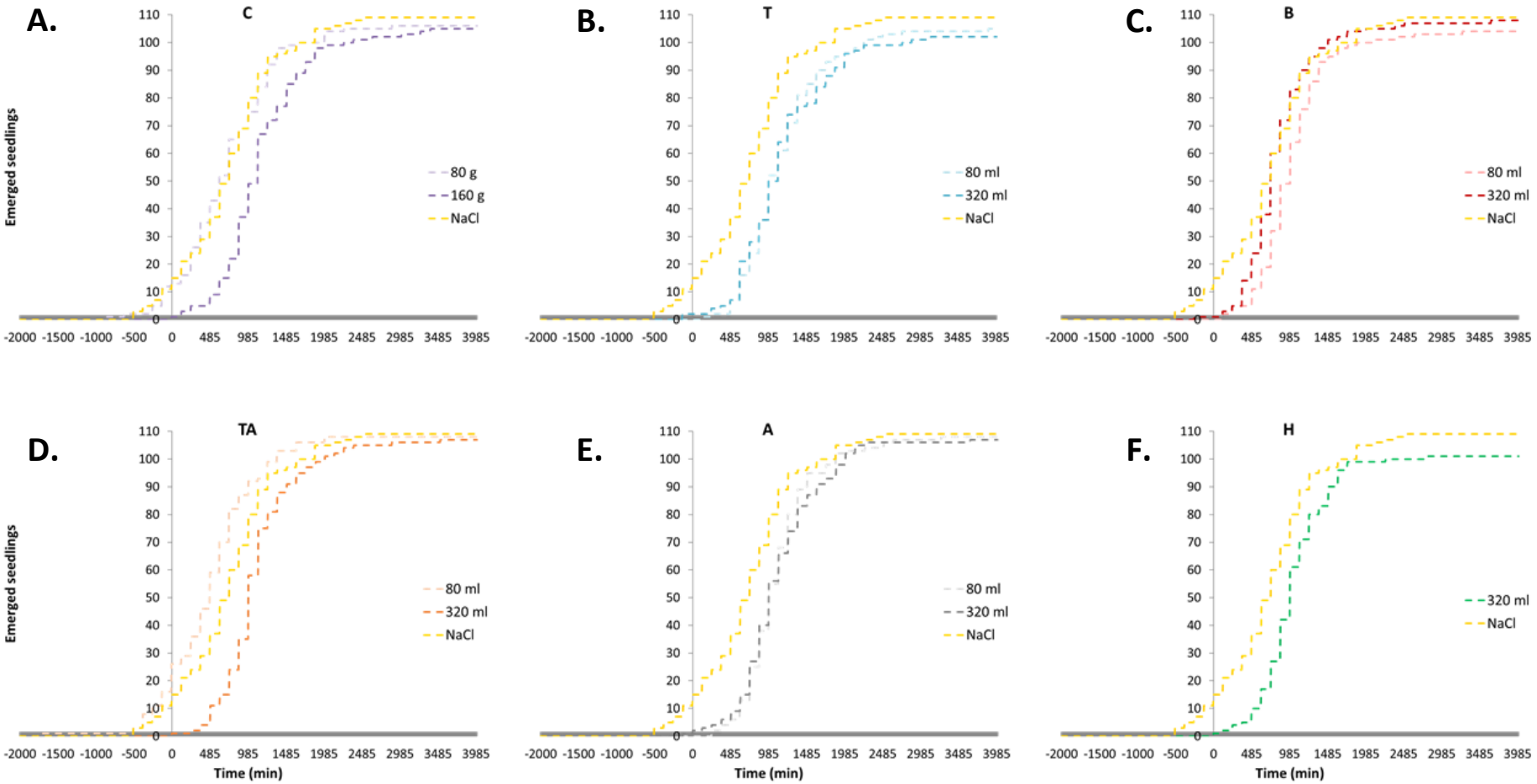

Figure 4| Empirical emergence curves. *Cumulative number of seeds germinated over time in salt stress conditions. A.) Comparison between uncoated seeds and seeds coated with the substance C in the concentrations 80 g/100 kg and 160 g/100 k, B) T in the concentrations 80 ml/100 kg and 320 ml/100 kg, C) B in the concentrations 80 ml/100 kg and 320 ml/100 kg (C.), TA in the concentrations 80 ml/100 kg and 320 ml/100 kg (D.), A in the concentrations 80 ml/100 kg and 320 ml/100 kg (E.) and H in the concentration 320 ml/100 kg (F.) Time 0 corresponds to the moment when half of the control seeds were germinated.*

From each emergence curve, corresponding to a different biostimulant substance, dose of application and growing condition, we were able to extract three descriptive traits: **Emergence rate**, **Speed** and **Time lag** (**Table 3**).

Table 3| Emergence parameters. *Table showing the three main parameters extrapolated from the germination curves: final emergence rate in the last day of measurement, time lag and speed or synchronicity of emergence. In blue, the values that were improved by the seeds coating; in red, parameters that were negatively affected by the coating.*

Substances	*Concentrations*	*Emergence rate*		*Speed*		*Time lag*	
		Control	*NaCl*	*Control*	*NaCl*	*Control*	*NaCl*
-	-	97.6	99.9	11	7	-	0.17
C	80 g/100 kg	97.3	96.7	12	7.3	0.02	0.16
	160 g/100 kg	98.1	95.2	13.1	9	0	0.29
T	80 g/100 kg	97	95.2	10.3	9	0.12	0.29
	320 g/100 kg	97.6	93.3	11.7	8.2	-0.01	0.28
B	80 g/100 kg	95.4	95.6	9.8	11.2	-0.02	0.26
	320 g/100 kg	94.3	97.8	14.7	11.6	-0.01	0.21
TA	80 g/100 kg	96.2	99.2	11.6	7.6	0.06	0.11
	320 g/100 kg	96	97	11.2	10.6	0.09	0.28
A	80 g/100 kg	97.6	98	11.4	10.7	0.09	0.29
	320 g/100 kg	98.4	97.5	11.3	9	0.11	0.28
H	320 g/100 kg	96.9	91.9	11	11.3	0.04	0.27

From the curves it is clear that, under control conditions, seeds coating did not yield significant improvements to the considered parameters, with very few exceptions. The final emergence rate was only slightly increased by the biostimulant **A** in its highest concentration (**Figure 3– E; Table 3**). The speed, i.e., synchronicity of germination, was increased by the biostimulant **B** in its highest concentration (320 ml/100 kg of seeds), while the time lag was generally unaffected. Only the biostimulant **B**, in its lowest concentration, had the effect of reducing the time lag (**Figure 3– C**), while the other substances had small or no effects.

In salt stress conditions, the effects of the biostimulants coating were more evident. Final emergence rate was not an informative parameter, since in the uncoated seeds was close to 100%, while always slightly lower for the coated seeds (**Figure 4**; **Table 3**), reaching a minimum of 91.2% in the seeds coated with the biostimulant **H** (**Figure 4 - F**). On the other hand, all the coated seeds showed a higher synchronicity of germination when compared with the uncoated seeds, in which the value was reduced of the 36% if compared to the uncoated seeds growing in optimal conditions. Even in this

case, the biostimulant **B** in its highest concentration (320 ml/100 kg of seeds) had positive effect on the synchronized germination.

The last parameter, time lag, which defines the amount of time occurring between the germination of half of the control seeds and half of the treated seeds, was significantly reduced only by the compound **TA** in its lowest concentration (**Figure 4– D**), if compared to the uncoated control in the same growing conditions. All the other compounds and doses delayed the emergence of the seeds if compared to the untreated controls. The time lag values were especially increased by T and A, and the highest concentration of C (**Figure 4; Table 3**).

1.4.2 Final weights and heights of the seedlings are not influenced by the seed coating

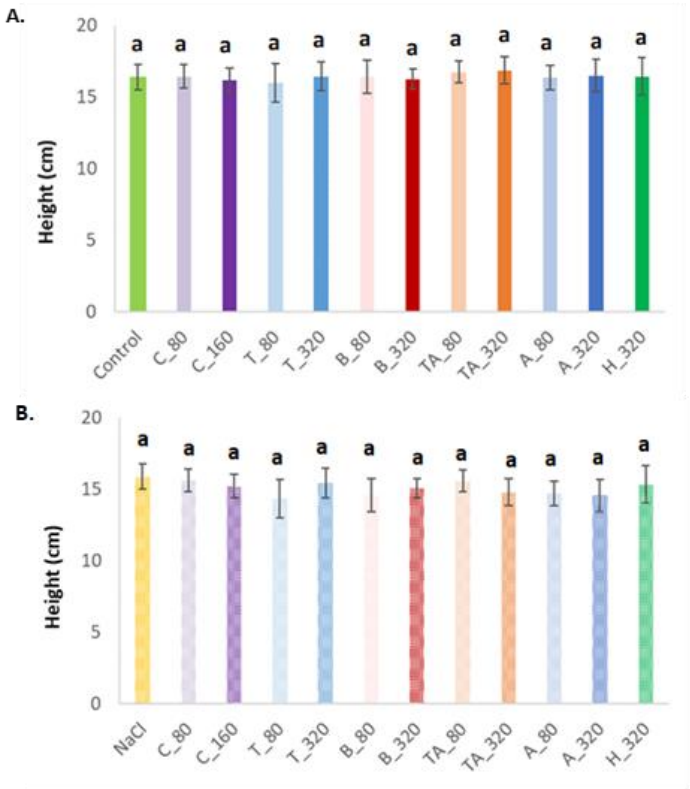

***Figure 5| Final seedlings heights**. Final heights at the collar of 15 random seedlings per each combination of biostimulant and concentration, of the seedlings growing in control (A.) and salt stress conditions (B.). The values represent the average of 15 repetition per treatment, error bars represent standard deviation.*

After the last RGB measurements of the seedlings, we manually scored the heights of 15 random plantlets per each tray. As shown in **Figure 5**, we could not detect any significant differences and seedlings height did not prove to be an informative trait. In salt stress conditions, the heights of the uncoated seedlings were 3% lower than those of the plants in control conditions. The coating did not cause any difference in height, neither in control nor in salt stress conditions (**Figure 5**).

After measuring the heights, all the emerged plantlets were cut at the collar and the weight of the total biomass was recorded for each growing condition, biostimulant and concentration used for seed coating. Since the number of germinated seeds was not the same in each tray, the total weight in itself was not a reliable parameter. Therefore, we calculated the approximate weight of a single plantlet, dividing the total weight of plantlets harvested for given treatment by the number of emerged seedlings per tray. In control conditions, the fresh weight of the emerged seedlings was not significantly influenced by most of the seed coatings. The substance **C**, in its lowest concentration, slightly increased the final weight (+4.6%) if compared to the uncoated seeds in the same growing conditions, but the difference was not significant. On the other end, the weight of the plantlets treated with the substance **T** in the 80 ml/100 kg dose was significantly lower (-11%) (**Figure 6-A**).

In salt stress conditions, the coated seeds had lower final weights if compared to the uncoated control. The more relevant reduction in fresh weight was recorded for the treatment **TA** in the low concentration (-20%) (**Figure 6-B**).

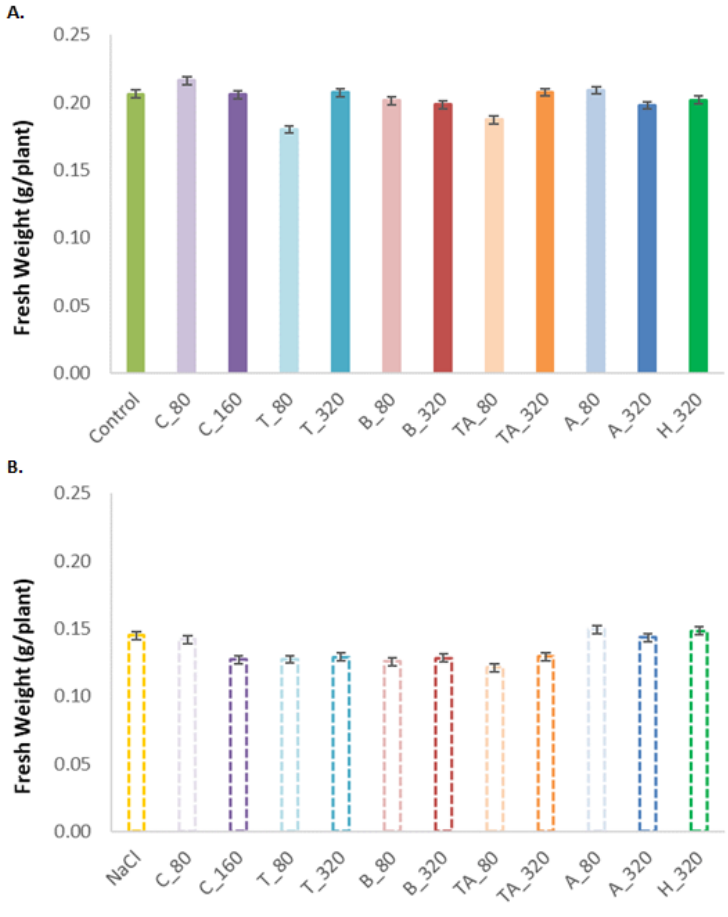

Figure 6|Final fresh weights. *Fresh weights of the final vegetal biomass per each combination of biostimulant and concentration, of the seedlings growing in control (A.) and salt stress conditions (B.). The values are obtained dividing the total fresh weight of each tray by the number of germinated seeds. Error bars represent standard error.*

No significant differences between treatments could be spotted in the dry weight. In general, the values were slightly lower for the coated seeds. The final dry weight was especially reduced by the substance **T** in its lowest concentration (-14%) in control conditions, and by the compound **C** (160 ml/100kg) in salt stress conditions (-11%) (**Figure 7-A, B**).

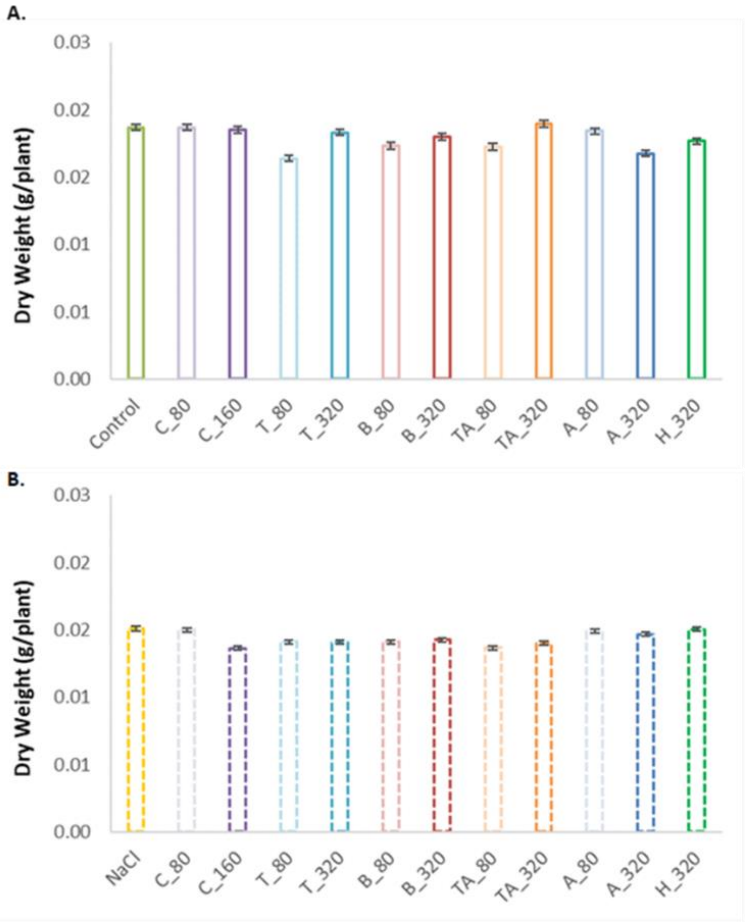

Figure 7| Final dry weights. *Dry weights of the final vegetal biomass per each combination of biostimulant and concentration, of the seedlings growing in control (A.) and salt stress conditions (B.). The values are obtained dividing the total fresh weight of each tray by the number of germinated seeds. Error bars represent standard error.*

1.4.3 Characterization of different compounds by using the Plant Biostimulant Characterization Index

For a better visualization of the calculated values, the log2 values obtained per each of the three parameters (emergence rate, speed and time lag), for each compound, concentration of the compound

and growth conditions (control or salt stress) were represented in a parallel coordinate plot (**Figure 8**).

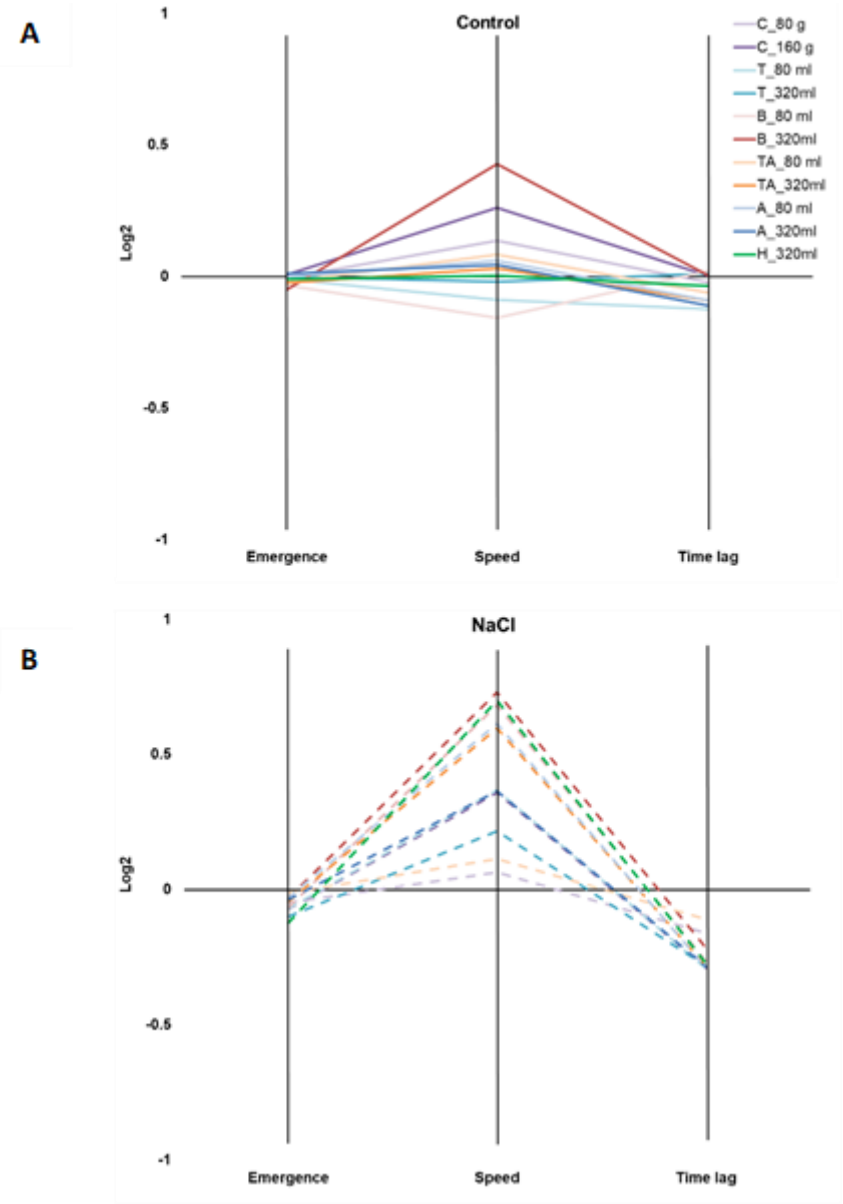

***Figure 8| Characterization of the plant biostimulants**. Parallel coordinate plots of the 3 main traits (final emergence rate, speed or synchronicity of emergence and time lag) of the wheat seeds coated with the 6 different biostimulants in control (A) and salt stress conditions (B).*

By means of this visualisation, we could confirm that in control conditions the **final emergence rate** was not a very informative trait, because there was almost no difference between the coated and uncoated seeds, neither in control nor in salt stress conditions. On the contrary, the **speed of emergence** was greatly increased by the coating with most of the substances, especially ***B*** (320 ml/100 kg) in both growing conditions, while the lower concentration of the same compound has reduced the synchronicity of germination in control conditions. In salt stress conditions, coated seeds always showed a higher synchronicity of germination, if compared to the uncoated one (**Figure 8 A-B**).

The last parameter, **time lag**, was in general not positively influenced by the seed coating, The coating with the biostimulant **B** in its higher concentration slightly accelerated the seedlings emergence in control conditions, while all the other substances caused a delay in germination if compared to the untreated seeds (**Figure 8 A**). In salt stress conditions, all the seedlings coming from coated seeds emerged later than the untreated controls (**Figure 8 B**).

The three parameters (final emergence rate, speed of emergence, time lag) obtained per each combination of biostimulant, concentration and growing condition were then summed up to calculate the PBC index, ending with a single numeric value that could categorize the compounds in a straight-forward way. The value obtained could be negative (red) or positive (blue), providing information regarding the effects of the substance on the seedlings' emergence compared to the respective controls (uncoated seeds in control or salt stress conditions). The value of the PBC index helped us to categorize the compounds, according to their mode of action, into substances that promoted emergence [positive values (blue) in coated seeds germinated in control conditions], substances that had alleviating effect in stress conditions referred to as stress alleviator [positive values (blue) in coated seeds germinated in salt stress conditions], or both acting as stress alleviator and growth improver [positive values in coated seeds both in control and stress conditions].

Table 4| PBC index. *Table showing the PBC index of each substance, in each concentration and growing condition. Highlighted in blue, the positive values for substances who improved the growing performances of the coated seeds if compared to the controls; highlighted in red, negative values corresponding to substances who worsened the seeds' performances. The darker the colour, the further the value from the uncoated control (corresponding to 0).*

Substance	Concentration	Control	NaCl
C	80 g/100 kg	0.18	-0.23
	160 g/100 kg	0.27	-0.26
T	80 g/100 kg	**-0.4**	0.29
	320 g/100 kg	0	**-0.43**
B	80 g/100 kg	-0.23	0.08
	320 g/100 kg	**0.29**	0.28
TA	80 g/100 kg	-0.15	-0.28
	320 g/100 kg	-0.09	0.07
A	80 g/100 kg	-0.01	**0.31**
	320 g/100 kg	-0.1	-0.01
H	320 g/100 kg	-0.07	0.22

*Our data clearly suggest that **B** substance (the pea seeds extract) in the dose 320 g/100 kg was the best performing biostimulant, clearly improving the vitality of the seeds both in control and salt stress conditions (*

Table 4). Other substances proved to be beneficial as well, but their effect was dependent on the concentration used and on the growth conditions. For example, as the values of the PBC index clearly show, **C** was acting as a germination inducer in control conditions, especially in its higher concentration (160 g/100 kg), but it did not have any beneficial effects in salt stress conditions. Instead, in saline environment **A** and **T** in their lowest concentrations increased the fitness of the seedlings. Interestingly, in our experimental conditions the commercial compound T proved to be the substance with most growth inhibiting effects in control conditions, especially in high dose. In saline conditions, a contrasting response was detected with stress alleviating response in lower dose of the biostimulant and growth inhibiting response in higher dose of biostimulant.

1.4 Discussion

The coating with plant-derived (Rady et al., 2018) or microbial-based biostimulants (Ma et al., 2018) has long been proved as treatment increasing the seeds germination and early establishment of seedlings in adverse environmental conditions (Campobenedetto et al., 2020). Nevertheless, in most of the studies biostimulants are applied primarily as foliar spray on fully-developed plants, while very little in-depth research has been conducted on the mode of action of biostimulants used for seed treatments (Amirkhani et al., 2016). The few works available on this matter mainly focus on the germination rate and final biomass and was measured with manual methods at a single timepoint (Wilson et al., 2018; Amirkhani et al., 2019; Qiu et al., 2020). In our work, we used the method developed by Ugena and co-workers (unpublished) – previously used to evaluate the seed priming effects of specific polyamines - to test the mode of action of complex compounds applied as seeds coating by screening the growth performance of the plants in high throughput by automated phenotyping platform. Compared to more traditional approaches, our model allowed to follow the germination of the seeds for a longer period of time, taking in account the germination of delayed seeds and the synchronicity of seeds germination, that could be easily missed when performing manual, one-time point observations. With the use of a simple RGB camera, we were able to obtain high-precision information related to the seed's germination and the early establishment of the seedlings, developing a fast and highly-reproducible protocol that requires little human work and that could be easily adapted to different crops, coating substances and growing conditions.

The cumulative number of germinated seeds over time was displayed using a Gompertz curve, that better fits to the empirical emergence curve if compared to the traditional exponential models. From the Gompertz curve, we could extract three traits related to the germination: final emergence rate, time lag (defined as Time elapsed between the germination 50% of the control seeds and 50% of the coated seeds) and emergence synchronicity. Finally, the PBC index was used to summarize the effects of the substances on the three parameters at the same time. By using the PBC index we were able to classify the substances as growth improvers, inhibitors, stress alleviators or both. Finally, we characterized the biostimulant B as the best performing substance in both optimal and sub-optimal growing conditions. The biostimulant B was a pea seeds extract, an experimental substance tested for the biostimulant properties for the first time in our trial. Pea seeds, like other legumes, are

extremely rich in flavonoids (Troszyńska et al., 2001), secondary metabolites with low molecular weight, involved in plant physiological functions, often demonstrating protective effects against biotic and abiotic stresses (Shah and Smith, 2020) including salinity stress in tobacco (Chen et al., 2019). Flavonoids, in fact, have important roles in the resistance to oxidative damage caused by ROS during plant growth and abiotic stresses (Agati et al., 2012). Furthermore, there is evidence that flavonoids play a role in interrupting seed dormancy and promoting germination, also in optimal growing conditions (Shirley, 1998).

While the pea seeds extract was the only substance that improved both the germination of the seeds and their resistance to stress, other compounds were also beneficial to the seeds, but only in one of the two growing conditions. In control conditions, the germination was improved by the substance C in both concentrations. C corresponded to the commercial product Coveron®, a mixture of spores of arbuscular mycorrhizal fungi and of *Trichoderma atroviridae*. In a previous study, the coating of wheat seeds with Coveron® significantly reduced the mean emergence time by 33.3%, if compared to the uncoated controls, while the final germination rate was not affected (Colla et al., 2015b). These observations are coherent with what we experienced in our work.

In salt stress conditions, the highest PBC index was recorded for the biostimulant A, referring to isolate of an endophytic fungus, *Trichoderma atroviridae*. Biopriming of seeds with *Trichoderma* was previously shown to improve seed performance in many crops (Howell, 2003). More specifically, Trichoderma species are known to release a variety of compounds that induce resistance responses to biotic and abiotic stresses (Kumar et al., 2016); for example, they are able to produce indole-3-acetic acid (IAA) under salt stress, enhancing salt tolerance of seeds (Oljira et al., 2020).

In our trial we also include the commercial compound Trainer® (the biostimulant T) as an internal control. Many studies demonstrated that the application of Trainer® to crops (lettuce, corn, tomato) increased marketable yield, biomass accumulation, N uptake, N, P and chlorophyll content and root development (Colla et al., 2013; Colla et al., 2014; Ertani et al., 2013; Lucini et al., 2015). However, in our study the coating of the seeds with Trainer® did not improve germination or early development

of the seedlings in control conditions. On the other hand, Trainer® increased the tolerance to salinity of the seedlings when supplied in its lower concentration (80 g/100 kg;

Table 4). This is coherent with the observations made by Ertani and co-workers on corn in 2013.

1.5 Conclusions

In summary, our study presents a simple high-throughput method for rapid and effective testing of biostimulants of multiple origins as seeds coating under different growing conditions. The results proved that this pipeline could be very useful in comparing the effects of multiple substances at different concentrations, reducing the time and the human work usually needed for the traditional germination assays. Furthermore, we show that use of the Gompertz model provides information on many aspects of the emergence phase that are extremely important when screening a big population of seeds. The method can be easily reproduced allowing to test the performances of many biostimulants coating on different crop species, growing under a variety of abiotic stresses.

2. Chapter 2

Seedlings – In vitro Arabidopsis assay

ORIGINAL RESEARCH article
Front. Plant Sci., 08 June 2021 | https://doi.org/10.3389/fpls.2021.626301

Seed Priming With Protein Hydrolysates Improves Arabidopsis Growth and Stress Tolerance to Abiotic Stresses

Mirella Sorrentino[1,2†], Nuria De Diego[3†], Lydia Ugena[4], Lukáš Spíchal[3], Luigi Lucini[5], Begoña Miras-Moreno[5], Leilei Zhang[5], Youssef Rouphael[2], Giuseppe Colla[6*] and Klára Panzarová[1*]

[1]PSI (Photon Systems Instruments), spol. s r.o., Drásov, Czechia
[2]Department of Agricultural Sciences, University of Naples Federico II, Naples, Italy
[3]Centre of Region Haná for Biotechnological and Agricultural Research, Czech Advanced Technology and Research Institute, Olomouc, Czechia
[4]Department of Chemical Biology and Genetics, Centre of the Region Haná for Biotechnological and Agricultural Research, Faculty of Science, Palacký University Olomouc, Olomouc, Czechia
[5]Department for Sustainable Food Process - DiSTAS, Università Cattolica del Sacro Cuore, Piacenza, Italy
[6]Department of Agriculture and Forest Sciences, University of Tuscia, Viterbo, Italy

Seed Priming with Protein Hydrolysates Improves Arabidopsis Growth and Stress Tolerance to Abiotic Stresses

Mirella Sorrentino[1,2a], Nuria de Diego[3a], Lydia Ugena[3], Lukáš Spíchal[3], Luigi Lucini[4], Begoña Miras-Moreno[4], Leilei Zhang[4], Youssef Rouphael[2], Giuseppe Colla[5*] and Klára Panzarová[1*]

[1]*PSI (Photon Systems Instruments), spol. S.r.o., Drasov, Czech Republic*

[2]*Department of Agricultural Sciences, University of Naples Federico II, via Università 100, 80055 Portici (NA), Italy*

[3]*Department of Chemical Biology and Genetics, Centre of the Region Haná for Biotechnological and Agricultural Research, Faculty of Science, Palacký University, Olomouc, Czechia*

[4]*Department for sustainable food process - DiSTAS, Università Cattolica del Sacro Cuore, via Emilia Parmense 84, 29122 Piacenza, Italy*

[5]*Department of Agriculture and Forest Sciences, University of Tuscia, via San Camillo De Lellis snc, 01100 Viterbo, Italy*

[a] These authors contributed equally.

ABSTRACT

The use of plant biostimulants contributes to more sustainable and environmentally friendly farming techniques and offers a sustainable alternative to mitigate the adverse effects of stress. Protein hydrolysate-based biostimulants have been described to promote plant growth and reduce the negative effect of abiotic stresses in different crops. However, limited information is available about their mechanism of action, how plants perceive their application, and which metabolic pathways are activating. Here we used a multi-trait high-throughput screening approach based on simple RGB imaging and combined with untargeted metabolomics to screen and unravel the mode of action/mechanism of protein hydrolysates in Arabidopsis plants grown in optimal and in salt-stress conditions (0, 75, or 150 mM NaCl). Eleven protein hydrolysates from different protein sources were used as priming agents in Arabidopsis seeds in three different concentrations (0.001, 0.01, or 0.1 µl ml^{-1}). Growth and development-related traits as early seedling establishment, growth response under stress and photosynthetic performance of the plants were dynamically scored throughout and at the end of the growth period. To effectively classify the functional properties of the 11 products a Plant Biostimulant Characterization (PBC) index was used, which helped to characterize the activity of a protein hydrolysate based on its ability to promote plant growth and mitigate stress, and to categorize the products as plant growth promoters, growth inhibitors and/or stress alleviator. Out of 11 products, two were identified as highly effective growth regulators and stress alleviators because they showed a PBC index always above 0.51. Using the untargeted metabolomics approach, we showed that plants primed with these best performing biostimulants had reduced contents of stress-related molecules (such as flavonoids and terpenoids, and some degradation/conjugation compounds of phytohormones such as cytokinins, auxins, gibberellins, etc.), which alleviated the salt stress response-related growth inhibition.

Keywords: Protein hydrolysates; automated phenotyping; secondary metabolism; metabolomics; plant biostimulant characterization index; salinity; stress-related molecules.

INTRODUCTION

Nowadays, the actual yield from the main crops worldwide accounts for less than half of its potential because of the effects of abiotic stresses on plants (Bulgari et al., 2019). Among them, one of the most concerning condition is represented by salinity stress that decreases the quantity and quality of the final yield (Shahbaz and Ashraf, 2013; Yamaguchi and Blumwald, 2005), because most of the high-value agricultural crops are sensitive to salinity (Shannon and Grieve, 1999). Salinity stress generally occurs in those areas where the concentration of salt – most commonly sodium chloride (NaCl) - in the soil or in the groundwater is higher than the crop threshold sensitivity (Colla et al., 2010). This occurs especially in parts of the world where most of the agricultural areas are close to the sea, like in the Mediterranean basin (Viégas et al., 2001). Soil or water salinity can affect plants in different ways, from increasing the soil osmotic pressure to hindering the regular plant nutrition (Machado and Serralheiro, 2017). Plant biostimulants represent an eco-friendly and useful tool improving plant tolerance to abiotic adversities, like salinity (Colla et al., 2017a). According to the European Biostimulant Industry Council, in the EU alone, the economic value of biostimulants is estimated to be between 200 and 400 million euros. However, despite the high economic potential of these substances, few well-characterized products are commercially available. The main problem is represented by the limited knowledge about their mode of action, mainly because they are formulated from complex, diverse, and heterogeneous materials (Brown and Saa, 2015). For this reason, plant biostimulants are usually classified more according to the plant response they cause than by their composition. In fact, “plant biostimulants” is a hypernym used to describe very different substances such as seaweed extracts, humic and fulvic acids, animal and vegetal-based protein hydrolysates, rather than microorganisms like mycorrhizal fungi and rhizospheric bacteria (Colla and Rouphael, 2015; Carillo et al., 2020). Among all the existing plant biostimulants, protein hydrolysates (PHs) are recently gaining big popularity. They are mixtures of amino acids with oligo- to polypeptides derived from the partial hydrolysis of protein-rich sources either from plant or animal origin. The application of PHs goes from foliar spray or substrate drench to adult plants (Lucini et al., 2015; Sestili et al., 2018) to seed priming, which increases abiotic stress tolerance by reprograming the plant metabolism during the germination stages (Mahdavi, 2013; Sharma et al., 2014; Pichyangkura and

Chadchawan, 2015; Van Oosten et al., 2017). Many studies have proven the efficacy of PHs in improving the quantity and quality of the yield, especially under abiotic stress or limiting conditions (Ertani et al., 2009; Colla et al., 2015a; du Jardin, 2015). Indeed, they have been reported to exert multiple benefits in plants under sub-optimal conditions, including mitigation of oxidative imbalance, elicitation of osmolytes and modulation of secondary metabolism (Lucini et al., 2015). Therefore, PH-based biostimulant treatments modify plant metabolism and physiology for maximizing biomass yield under globally changing environmental conditions (Dudits et al., 2016).

In past years, significant advances were made in understanding the mode of action and in-depth characterization of biostimulants through combining omics-based methodological approaches (Rouphael et al., 2018b). It was clearly demonstrated that by combining multiple omics technologies, including the high-throughput phenotyping, new functional perspectives in the biostimulant field are emerging, allowing for the discovery, evaluation, and accelerated development of innovative biostimulants (Povero et al., 2016; Bulgari et al., 2017; Rouphael and Colla, 2018; Ugena et al., 2018; Briglia et al., 2019; Dalal et al., 2019; Paul et al., 2019b).

Precise and accurate assessment of the variation in plant morpho-physiological traits over time is crucial for unraveling and quantifying the biostimulant activity of different substances. Image-based automated plant phenotyping techniques increase both the speed and the accuracy of measurements (Rouphael et al., 2018b). Plant phenotyping platforms are automated systems normally operating in a fully-controlled growing chamber or in semi-controlled conditions such as greenhouses. Different sensors can be implemented into the plant phenotyping platform, allowing the user to monitor simultaneously multiple morpho-physiological plant traits in a non-destructive way. Additionally, the high number of variants and the possibility of repeated measurements from the same individuals in different phases of their growth enable the user to compare the plant development under different growth conditions and treatments, at the same time reducing costs and human labor, thus speeding up the process (Rouphael et al., 2018b). As demonstrated previously by Ugena et al. (2018), multi-trait high-throughput screening (MTHTS) based on the semi-automated analysis of Arabidopsis seedlings growth provides a powerful

tool for fast and large-scale discovery of new potential biostimulants, including characterization of their mode of action under optimal and stress conditions. The objective of the experiment was to use a multi-trait high-throughput screening approach based on simple RGB imaging and combined with untargeted metabolomics to screen and elucidate the mode of action/mechanisms of protein hydrolysates in Arabidopsis plants grown in optimal and in salt-stress conditions.

MATERIALS AND METHODS

Characterisation of the Protein Hydrolysates Tested

Eleven PHs were tested in the trial. Three of them were commercial products obtained by thermal-chemical hydrolysis of animal-derived proteins (Siapton® (I) commercialized by Sumitomo Chemical Italia S.r.l., Milano) or enzymatic hydrolysis of vegetal-derived proteins (Trainer® (D), and Vegamin® (H) commercialized by Hello Nature (former Italpollina S.p.A.,Rivoli Veronese, Italy). The other eight PHs were obtained from vegetal proteins by enzymatic hydrolysis as described previously (Colantoni et al., 2017; Ceccarelli et al., 2021). Plant biomass from *Fabacea*e (A, G, O), *Malvaceae* (C), *Brassicaceae* (F), *Solanaceae* (B), and *Graminaceae* (E, P) were used as protein sources for the other eight PHs. For chemical characterization, the total C and N were determined in triplicate through an elemental analyser (Elemental vario MAX CN, Langenselbold, Germany). Thereafter, the different PH were 2-folds diluted in methanol, filtered through a 0.2 membrane, and then the phytochemical profile characterized by mass spectrometry as reported by Senizza et al. (2020).

Plant Material and Growing Conditions

Arabidopsis thaliana (accession Col-0) seeds were sterilized and sown as described by De Diego et al. (2017) in Murashige-Skoog (MS) medium (Murashige and Skoog, 1962) (pH 5.7) using 0.6% Phytagel (Sigma–Aldrich, Germany) as a gelling agent. To investigate the effect of biostimulants on the growth of *Arabidopsis* plantlets, the eleven PHs were dissolved in demineralized water and added to the growing

media for seed priming at concentrations of 0.001, 0.01, or 0.1 µl ml^{-1}. The plates containing the different media and the seeds were maintained at 4 °C for 3 days and then transferred into a growth cabinet to maintain temperature and humidity setpoints (22 °C, 55% RH, 16/8 h light/dark photoperiod with an irradiance of 120 µmol photons of PAR m^{-2} s^{-1}).

Three days after germination, the seedlings were transferred into 48-well plates filled with 1× MS medium, either plain or enriched with NaCl for two salinity levels (75 and 150 mM NaCl) as described by Ugena et al. (2018). A total of 96 seedlings (two plates) per variant as biological replicates were used. The protocol schematized in **Figure 1** describes the experimental workflow.

High-throughput Automated Phenotyping

The plates were then transferred to the OloPhen platform (CRH Olomouc, Czechia). A generalized randomized block design was used for the random positioning of the plates in a cabinet equipped with the PlantScreen™XYZ system. The growth conditions were set to a regime of 22 °C /20 °C, 60% RH, and a 16/8 h light/dark cycle., while irradiance was set to 120 µmol photons of PAR m^{-2} s^{-1} (De Diego et al., 2017). Imaging was carried out twice per day (at 10:00 a.m. and 4 p.m.) for a period of 7 days (De Diego et al., 2017).

RGB imaging

RGB images from each plate were automatically stored in PNG format by PlantScreen™ XYZ (resolution 2500 × 2000 pixels) and analysed using an in-house software implemented in MatLab R2015 (De Diego et al., 2017). The total number of green pixels was used to assess the total green area for each well of the plate, further referred to as the projected shoot area. The daily pictures of the single 48-well plates were then used to monitor the increase in the rosette area throughout the whole period. The Relative Growth Rate was calculated using the following formula:

$$RGR = [\ln(\text{projected shoot area})t_i - \ln(\text{projected shoot area})t_{i-1}]/(t_i - t_{i-1})$$

where t is the time, expressed in days.

The value of the projected rosette area from the last day of imaging was lastly used for the calculation of the Coefficient of Variance, which provides information about the size homogeneity of the seedlings on the final day of the experiment for all the treatments at all the growth conditions tested.

For the salt stress variants, a fourth growth-related parameter was introduced: Survival Rate, representing the percentage of seedlings per plate still alive on the last day of phenotyping. A seedling was considered alive if at least 100 green pixels could be detected in the corresponding well (De Diego et al., 2017).

Chlorophyll Fluorescence Measurement

After the last RGB measurement (day 7, 10:00 a.m.), the plates were taken out of the OloPhen platform, and the perforated transparent foils were removed from each plate. Six plates at a time were randomly put onto a customized blue tray to perform kinetic chlorophyll fluorescence (ChlF) measurements of each plate, using FluorCam FC-800MF pulse amplitude modulated (PAM) chlorophyll fluorometer (Photon Systems Instruments, Drasov, Czechia) incorporated into a PlantScreen™ Conveyor System. After a 15 min dark-adaptation period in the adaptation tunnel, the trays were automatically transported by the conveyor belt to the ChlF imaging light-isolated cabinet. The changes of the photosynthesis-related parameters in Arabidopsis seedlings were measured at different photon irradiances using the light curve protocol (Henley, 1993; Rascher et al., 2000). The light curve protocol with four actinic light irradiances (cool-white actinic light at 95, 210, 320, 440 μmol $m^{-2}s^{-1}$) was used as described in Awlia et al. (2016) with a duration of 60 s, to quantify the photosynthetic efficiency. Fluorescence data were elaborated by the FluorCam7 Software (Photon Systems Instruments, Drasov, Czechia) as described by Tschiersch et al. (2017). Automation of plant masks for the single plantlets was difficult because of their small dimensions and the feeble or absent fluorescence emitted by dying or dead seedlings, especially in

severe salt stress conditions. Thus, plant masks were drawn manually, using the manual image segmentation in Fluorcam7, whereas background subtraction and calculations were performed automatically. The basic ChlF parameters were derived from fluorescence transient states (i.e., Fo, Fm, Fm', Ft, Fv, and Fp) and used to calculate plant photosynthetic performance parameters (Fv/Fm, Fv′/Fm′, NPQ and ΦPSII).

Untargeted Metabolomic Analysis

Arabidopsis rosettes were freeze-dried at harvest the material from controls and primed with the best-performing substances was then used for metabolomics as described by Senizza et al. (2020). In brief, samples (10 mg) were extracted in 2 ml of a methanol-water (80:20, v/v) mixture using ultrasounds (Fisher Scientific model FB120, Pittsburgh, PA, USA) at 80% amplitude. After that, the extracts were filtered through a 0.22 μm membrane and plant metabolites analysed by liquid chromatography quadrupole-time-of-flight mass spectrometry (UHPLC/QTOF) (Lucini et al., 2018). In summary, positive polarity and SCAN mode (100–1000 m/z range) at 30,000 FWHM were used. Chromatography used a water and methanol binary elution mixture (from 5% to 90% methanol, 35 min run time) flowing at 220 μl min^{-1} and an Agilent Zorbax Eclipse-plus column (75×2.1 mm i.d., 1.8 μm). The software Profinder B.07 (Agilent Technologies) was used for features deconvolution, alignments and the following annotations using accurate mass, isotope spacing and isotope ratio (Rouphael et al., 2016). The reference database was PlantCyc 9.6 (Plant Metabolic Network, http://www.plantcyc.org). The annotation process corresponded to Level 2 (putatively annotated compounds) of the COSMOS Metabolomics Standards Initiative (Salek et al., 2015). Compounds were finally filtered to only retain those present in 100% of replicates (N=4) within at least one treatment.

Results

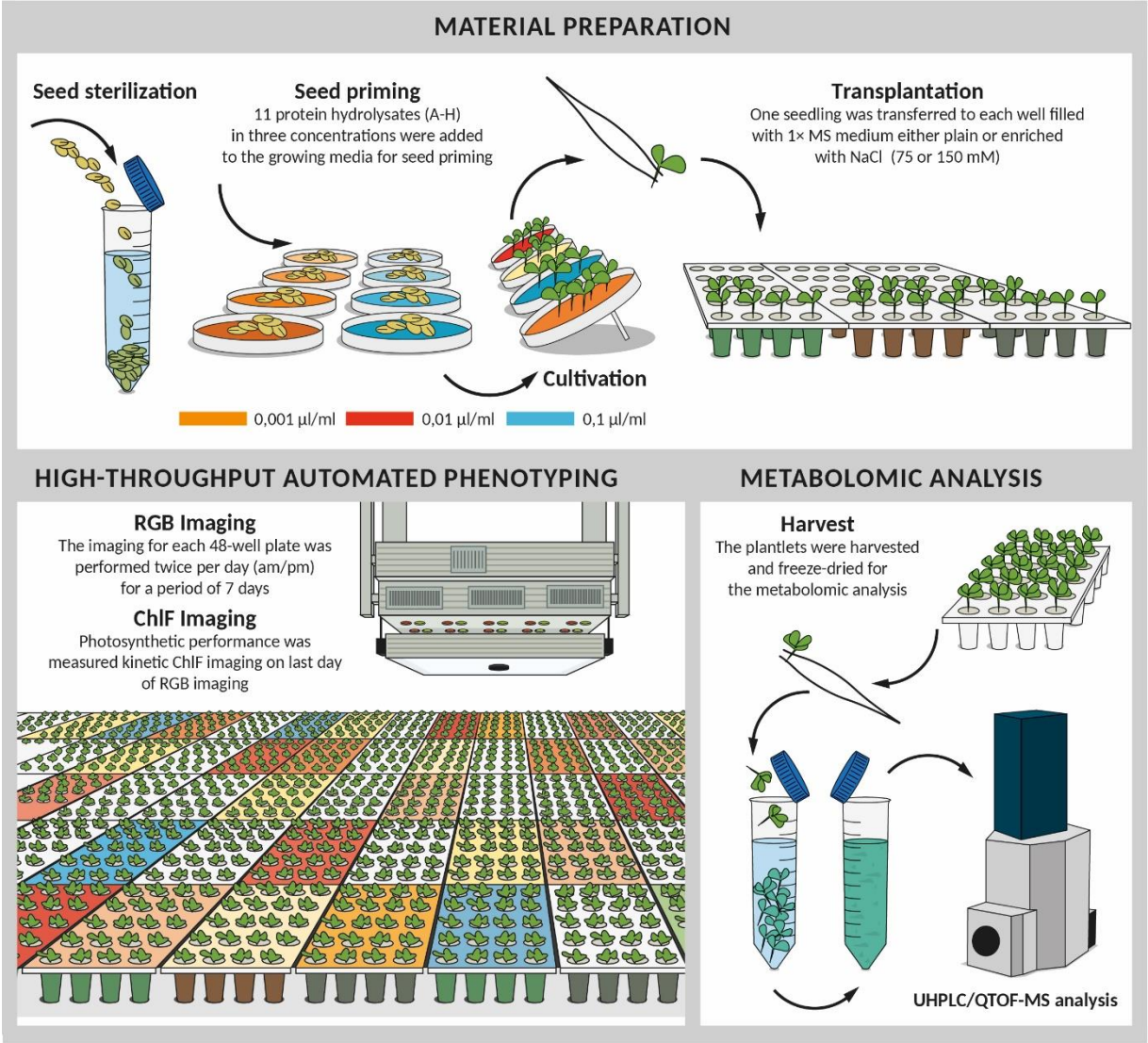

Figure 1| *Scheme of experimental protocol for high-throughput screening of biostimulant impact on Arabidopsis growth in control and salinity conditions. A) After sterilization seeds were germinated in 0.5× MS mixed with 11 different protein hydrolysates at three concentrations (0.001, 0.01 and 0.1 ml/ml). 4 days after cold stratification, seedlings of similar developmental stage were transplanted into 48-well plates with fresh MS medium either simple or supplemeted with NaCl (75 mM or 150 mM). B) Plates were placed for 7 days to the cultivation chamber with XYZ PlantScreenTM System used for daily (am and pm) automatic RGB imaging and growth analysis. At the end of the phenotyping period, the plates were used for the measurement of the chlorophyll fluorescence. C) Following the last measurement, the plantlets treated with the best-performing biostimulants including the controls were harvested, freeze-dried and used for subsequent metabolomic analysis.*

Data Analysis

One-way analysis of variance (ANOVA) with post hoc Tukey's Honest Significant Difference (HSD) test ($p < 0.05$) was used for statistical differences in phenotyping data, using the MVApp application (mmjulkowska/MVApp: MVApp.pre- release_v2.0; Julkowska et al., 2019). Correlation matrices and the significance were also performed in RStudio (Version 1.1.463 – © 2009–2018 RStudio, Inc.) using the packages *factoextra, FactoMineR* and *corrplot*.

Data from metabolomics were interpreted in Mass Profiler Professional B.12.06, (Agilent Technologies) as reported by Lucini et al (2018). Log2 transformation and normalization at the 75th percentile were carried out prior to naive elaboration through unsupervised hierarchical cluster analysis (HCA - Wards agglomerative algorithm of the Euclidean distances). Then, Volcano Plot analysis ($p<0.01$, fold-change >10; Bonferroni multiple testing correction) was used to identify differential metabolites in pairwise comparisons between treatments. These compounds were interpreted by the Omic Viewer Pathway Tool of PlantCyc (Stanford, CA, USA) to identify the pathways and metabolic classes elicited by the treatments (Caspi et al, 2013).

After that, OPLS-DA supervised analysis was performed in SIMCA 16 (Umetrics, Sweden) at default parameters. CV-ANOVA ($p< 0.01$) and permutation testing (n = 200) were used for model validation and to exclude overfitting, respectively. Fitness parameters were also calculated and Hotelling's T2 applied to exclude outliers. Subsequently, VIP analysis was used to objectively identify the most discriminant metabolites.

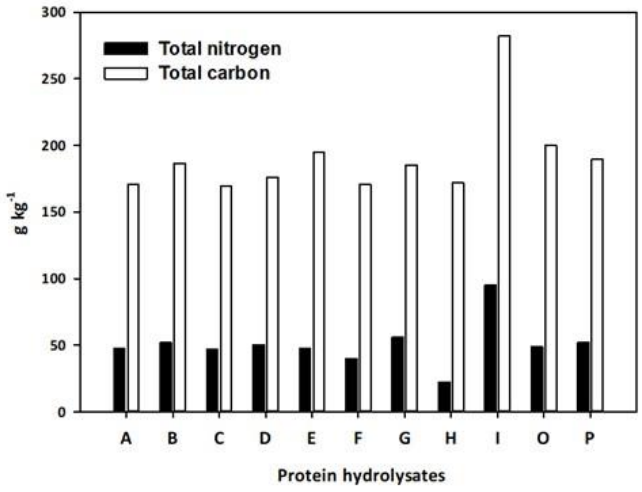

Figure 2| Total nitrogen and total carbon. *Total nitrogen and carbon content of the 11 protein hydrolysates selected for seed priming.*

RESULTS

Selection and Characterisation of the Protein Hydrolysates

Eleven PHs from different natural sources were selected and used for the study. Three of the PHs were previously characterised and are commercially available products (Trainer®, Vegamin® and Siapton®, here referred to as D, H and I, respectively). The other eight PHs were obtained by enzymatic hydrolysis of plant-derived proteins and were together with the three commercial products characterised by quantitative analysis of total nitrogen and carbon. Total nitrogen in the PHs ranged between 22.2 to 95.1 g per kg of product, while total carbon content varied between 170.5 to 281.9 g per kg of product (**Figure 2**). The highest value of nitrogen was found in I, while H had the lowest nitrogen content. Total carbon was also highest in I, while the biostimulant A exhibited the lowest carbon concentration value. The N and C content of PHs had a positive linear correlation (r = 0.884**). The untargeted analysis of the PHs revealed a broad chemical diversity that included amino acids and their derivatives, as well as other N-

containing compounds (mainly alkaloids), carbohydrates (mono- to oligosaccharides), and phenylpropanoids. Relatively less polar compounds such as fatty acids and phospholipids-related compounds, carotenoids and xanthophylls, steroids and terpenoids were also represented (**Supplementary Table S1**). A data reduction approach based on the fold-change-based heatmap clustering was used to hierarchically describe the similarity and the difference in the whole phytochemical profile across the different PH (**Supplementary Figure S1**). In detail, the unsupervised clustering highlighted two main clusters, one including PH A to D and another including the products E, F, G, O and P. The product H was distinct from these two macro-clusters, and the PH I was completely apart.

Multi-Trait High-Throughput Screening of Arabidopsis rosette growth for the characterization of the different PHs derived biostimulants

The Multi-Trait High-Throughput Screening (MTHTS) described by Ugena et al. (2018) was optimized for determining the mode of action of selected PHs that were here applied as priming agents (Figure 1). The seedlings from non-primed and primed seeds with different concentrations (0.001, 0.01, or 0.1 µl ml^{-1}) of PHs (**Supplementary Table S2**) were grown in control conditions and two intensities of salt-stress conditions. Six protein hydrolysates were evaluated in the first experimental round (A-F) and 5 in the second (G-P) round. 1st round counted 114 plates (5,472 seedlings) and the 2nd round consisted of 96 plates (4,608 plantlets), respectively. All plants were imaged by an RGB camera twice per day (at 10:00 a.m and 4 p.m.) for seven consecutive days.

Using the automated image analysis described by De Diego et al. (2017), we could quantify a variety of growth dynamics related traits such as rosette area and relative growth rate, together with homogeneity of the population (Weiner and Thomas, 1986; De Diego et al. 2017; Ugena et al., 2018).

First, we verified the reproducibility of the two rounds of the experiment, comparing the growth-related parameters of the control groups from the two rounds. Only a 2% difference between the final dimensions

of the control plants in the first and the second round was observed (Rosette size of 2362 and 2318 pixels, respectively). This result corroborated the very high level of reproducibility of the experimental protocol used in our platform as demonstrated De Diego et al. (2017). Further, we validated the screening assay with commercial product Trainer® (Hello Nature, Rivoli Veronese, Italy), here defined as substance D, that was previously characterised as growth improving substance (**Figure 3**) (Sestili et al., 2018).

Overall, our phenotyping data showed that the improved growth of the Arabidopsis seedlings primed with PHs was not only product-dependent but also dose-dependent under optimal growth conditions (**Figure 4A and Supplementary Table S2**). The priming with all tested concentrations of C and B proved to be especially beneficial to the plant's fitness, improving plant growth with better RGR under all growth condition, ending with a higher increase of the projected rosette area under control conditions (**Figure 4A, Supplementary Table S2, and Supplementary Figure S2**). In contrast, the impact on plant growth of the substances I and O was extremely dose-dependent (**Figure 4A, Supplementary Table S2 and Supplementary Figure S2)**. For example, when the plants were primed with I product and grown under optimal (control) conditions, the best response was observed in the highest concentration of the substance (0.1 µl ml^{-1}). In contrast, O product had the best effect when the lowest dose was used as a priming agent, while the highest concentration caused the opposite effect and resulted in the reduction of the final rosette area (**Figure 4A, Supplementary Table S2 and Supplementary Figure S2**). As expected, O is not the only substance that proved to be growth-inhibiting and/or toxic to the plants at a very high dose. The same detrimental effect was observed in groups primed with A, B, F, G and P. In summary, from our data, it is possible to identify the substances C and D (Trainer®) as the best growth promoters.

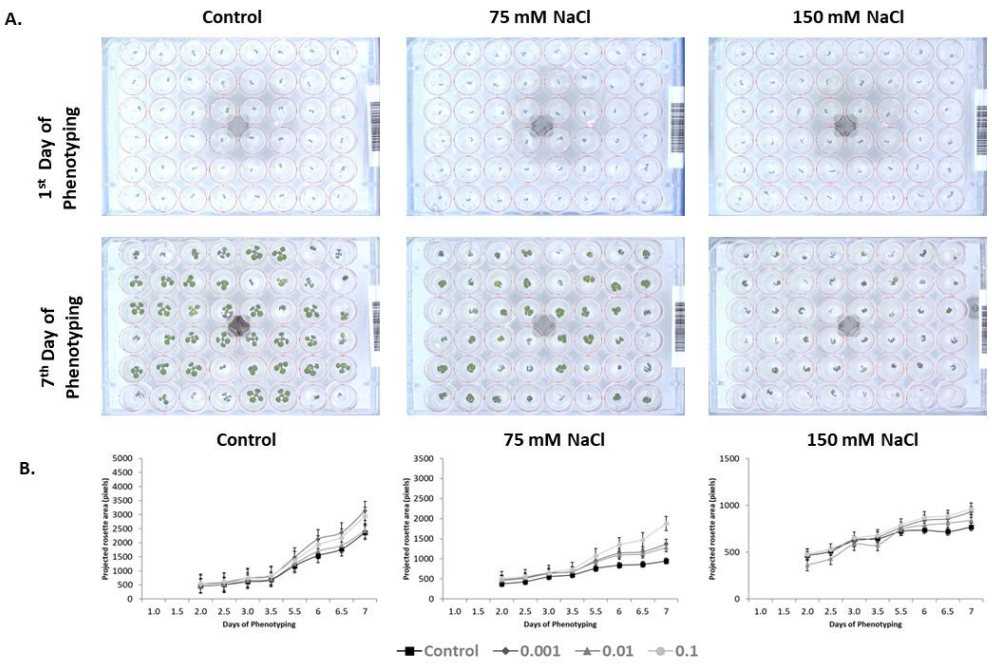

Figure 3 | *Top view RGB pictures of the 48-well plates and projected rosette area (pixels) of seedlings from seeds primed with D compound. RGB image of an individual 48-well plate at the first and the last day of the experiment, containing non-primed Arabidopsis seedlings or primed with the "D" product grown under control, moderate (75 mM NaCl) or severe (150 mM NaCl) salt stress conditions (A). Increase in projected rosette area (pixels) throughout the 7 days of the experiment for the same seedlings primed with D product (Trainer®) under control, moderate (75 mM NaCl) or severe (150 mM NaCl) salt stress conditions (B).*

Influence of the Protein Hydrolysates Applied as Seed Priming on Rosette Growth and Survival in Salt Stress Conditions

Thanks to the capacity of the OloPhen platform, we were able to evaluate the effect of our substances under two levels of salt stress: moderate (75 mM NaCl) and severe (150 mM NaCl). The two NaCl concentrations were selected based on the work from De Diego et al. (2017). As a main result, we observed that for the seedlings primed with PHs, independently of the origin of the substances used for the priming, the stress-induced growth inhibition was usually alleviated so in many cases bigger Arabidopsis rosettes and RGR were observed. However, the effects of the PHs on the seedlings were extremely dose-dependent and dependent on the severity of the salt stress applied.

Results

At 75 mM NaCl, only 3 of the 11 substances (C, D and O) significantly increased the final projected rosette area compared to the non-primed seedlings (**Figure 4B, Supplementary Table S2 and Supplementary Figure S3**). The beneficial effect of C, D and O was significant over all concentrations tested, resulting in dose-independent stress alleviating action. Interestingly, C's improving effect was more noticeable in the lowest concentration (0.001 μl ml^{-1}), whereas for D in the highest concentration (0.1 μl ml^{-1}). This result suggested that these two products varied in the mode of action for mitigating the negative effects of salt stress. Similarly, only the seed priming with any of the concentrations of C or D (Trainer®) improved the RGR values showing that only 2 of the PHs used (C and D) behaved as stress alleviators (**Figure 4B, Supplementary Table S2 and Supplementary Figure S3**), with higher values for 0.001 μl ml^{-1} in C and 0.1 μl ml^{-1}in D. Interestingly, E and I (Siapton®) had an inhibiting effect on RGR, reducing this parameter in all three concentrations.

For the salt stress variants, a third growth-related parameter was introduced; the survival rate (%) was calculated on the last day of the experiment. The survival rate of the seedlings was not seriously compromised in moderate salt stress conditions (~100%) (**Figure 4B and Supplementary Table S2**).

At 150 mM NaCl, no substance caused an increase in the final area (**Figure 4C, Supplementary Figure S4 and Supplementary Table S2**). However, the RGR was improved by the seed priming with D and P substances. D acted as a stress alleviator in all concentrations, especially with 0.01 μl ml^{-1} dose, whereas P substance only improved the RGR when the highest concentration (0.1 μl ml^{-1}) was used. Contrarily, E and F inhibited the growth of the seedlings in all concentrations. Severe salt stress also reduced the survival rate of the seedlings, with values around 95% for unprimed plants. The seed priming with B, C, D and O maintained higher survival rates but the effect was present in a dose-dependent manner (**Supplementary Table S2**); the most effective concentration for C and D (Trainer®) was 0.001 μl ml^{-1}, while for B and O was 0.1 μl ml^{-1}. Remarkably, the seeds priming with E and F at all concentrations had a reduced survival rate.

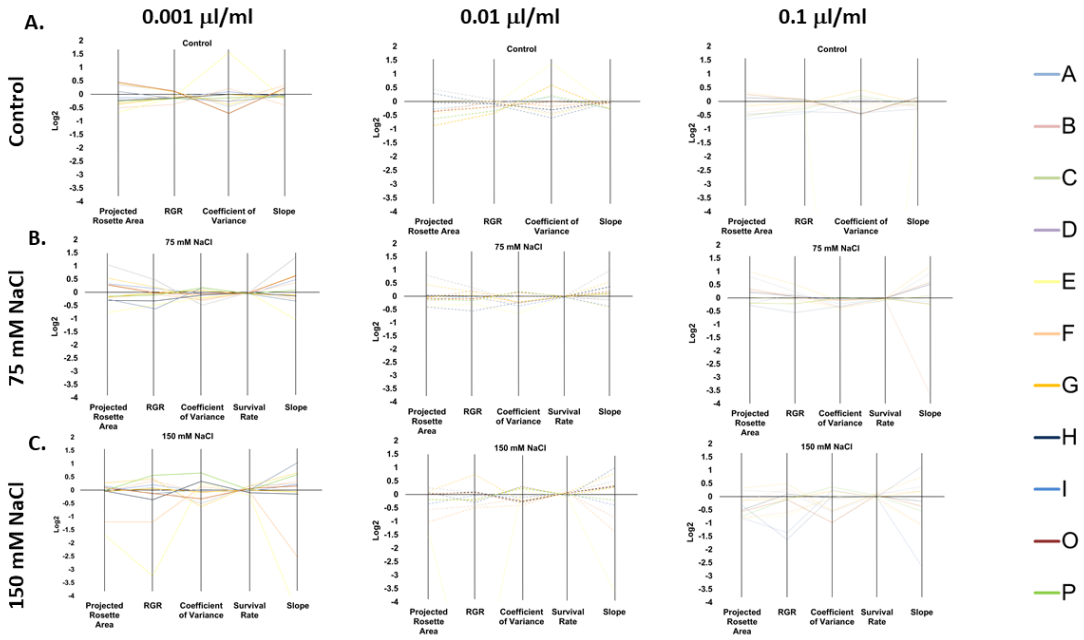

Figure 4| Characterization of the 11 plant biostimulants*. Parallel coordinate plot of the traits (Projected Rosette Area, Relative Growth Rate, Coefficient of Variance, Survival Rate and Slope of the Growth Curve) obtained from the Multi-trait HTS of Arabidopsis seeds primed with the PHs at three concentrations (0.001, 0.01 and 0.1 ml/ml) and grown in control (A) under moderate (75 mM NaCl) (B) or severe (150 mM NaCl) (C) salt stress conditions.*

Influence of Seed Priming with Protein Hydrolysates on Seedlings Homogeneity

Despite the two selection steps for the plant material (seed size and seedling size at the transfer moment), some variability between seedlings is always present. However, the level of variability in the population can be modified by the growth conditions and/or priming agents (De Diego et al. 2017; Ugena et al. 2018).

For that, we evaluated the effects of the priming with the different PHs on the plant-to-plant variability. The coefficient of variation (CV = standard deviation/mean) was used as a standard measurement of relative variation (Weiner and Thomas, 1986) and calculated on the last day of phenotyping, before the harvest. In control conditions, O was the only substance that improved the homogeneity of the seedlings,

except when it was applied at the highest concentration. In conditions of moderate salt stress, the CV was reduced by C in the 0.001 µl ml^{-1} concentration and by E in the 0.01 µl ml^{-1}concentration compared with their respective control. In severe stress conditions, the highest variability occurred, probably because most of the seedlings stopped growing in the early phase of the experiment (**Figure 4C and Supplementary Table S2**). In this case, the substances B (in the 0.1 µl ml^{-1}concentration), D (0.001 µl ml^{-1}), H (0.01 µl ml^{-1}) and O (0.1 µl ml^{-1}) improved the uniformity of the plantlets significantly (**Figure 4C and Supplementary Table S2**).

Evaluation and Classification of the Substances through the Plant Biostimulant Characterization Index

In order to uniquely classify the 11 PHs according to their effect on seedlings as growth promoters and/or stress alleviators, we used the Plant Biostimulant Characterization (PBC) index developed by Ugena et al. (2018). This index considers the five parameters previously mentioned: Projected Rosette Area on the last day of measuring, Relative Growth Rate throughout the entire period of the experiment, coefficient of variance in the final day of the experiment, the slope of the growth curve, and the final survival rate for the variants grown under salt stress conditions. The log2 of the ratio between primed and unprimed seedlings was calculated for each of the five parameters, the concentration of the PHs (0.001, 0.01 or 0.1 µl ml^{-1}) and growth conditions [optimal (control), moderate salt stress (75 mM NaCl) or severe salt stress (150 mM NaCl)], values that concur with those represented in the parallel plot **(Figure 4).** As example, for the A substance at 0.001 µl ml^{-1} applied to the plants growing in moderate salt stress conditions (75 mM NaCl), the log2 of the analysed traits were: for final area [log2 (1184.25/ 947) = 0.3225], for RGR [log2 (0.20/0.18) = 0.1448], for CV [-log2 (53.5665071/ 55.38435406) = -0.0481, as it is a negative trait], for survival [log2 (95.83/100) = -0.0614] and for slope [log2 (149.1805556/106.3796296) = 0.4878]. The five values obtained were then summed up to calculate the PBC index, ending with a single numeric value that could categorize the compounds in a straight-forward way. The value obtained for the single compound, concentration and growth condition could be negative (red) or positive (blue), telling us if this specific combination was beneficial in terms of plant

performance in the given conditions compared to the respective control variant (from non-primed seeds) **(Table 1)**. Additionally, the obtained values allowed us to divide the compounds into three groups; **plant growth promotor** [only positive values (blue) in primed seedlings grown under control conditions], **stress alleviator** [only positive values (blue) in primed seedlings grown under stress conditions], or **both** [positive values in primed seedlings under control and stress conditions].

Overall, our data clearly suggest that C and D (Trainer®) were the best biostimulants in all their concentrations and growth conditions, acting both as plant growth promotors and salt stress alleviators. C was especially effective as stress alleviator in the 75 mM NaCl-enriched media, with a PBC value 208% (for 0.001 µl ml^{-1}), 129% (for 0.01 µl ml^{-1}) and 335% (for 0.1 µl ml^{-1}) higher than the non-primed seedlings. On the contrary, D (Trainer®) had a better stress-alleviating effect on the plants growing in 150 mM NaCl- enriched media, with a PBC value 108% (for 0.001 µl ml^{-1}), 276% (for 0.01 µl ml^{-1}) and 221% (for 0.1 µl ml^{-1}) higher than the non-primed variant.

Some of the remaining substances proved to be effective as well, although in a concentration and growth condition-dependent manner. For example, as the PBC index shows (**Table 1A**), the substance O can be classified as a growth promotor when applied at the two lower concentrations. At the same time, the highest dose was even detrimental to the plantlets' development in control conditions. The substance B, however, can be classified as a stress alleviator but when used in high doses it was inhibiting the growth when plants were grown in 75 mM NaCl-enriched media (**Table 1B**). E and F were the worst performing substances, inhibiting the growth of the seedlings in all concentrations and growing conditions and especially under 150 mM NaCl salinity conditions (**Table 1C**).

Results

***Table 1|Plant Biostimulant Characterization (PBC) index**. The PBC index (related to each control) calculated as the sum of the log2 of the ratio between control and primed seedlings for the five main traits extracted from the RGB images (Parallel plot, Figure 2) measured under control (A), moderate (B) and severe salt stress conditions (C). Red colour and blue colour mean worse and better performance than the non-primed variants, respectively.*

A.

Control

	0.001 µl/ml	0.01 µl/ml	0.1 µl/ml
A	-0.46	-0.77	-1.22
B	-1.50	-0.28	-1.06
C	1.09	1.03	0.51
D	1.03	0.53	0.70
E	-0.99	-0.83	0.08
F	0.26	-0.58	-0.17
G	-0.68	-0.33	-2.01
H	-0.40	0.83	0.19
I	0.15	-0.69	0.76
O	1.51	0.89	-0.61
P	-0.37	-1.15	-1.45

B.

75 mM NaCl

	0.001 µl/ml	0.01 µl/ml	0.1 µl/ml
A	0.94	0.04	-0.01
B	0.99	0.48	-3.01
C	3.34	2.35	2.21
D	1.58	1.15	2.81
E	-2.09	-0.48	0.43
F	-0.26	-0.11	0.13
G	-0.44	0.34	-0.67
H	-0.68	0.38	0.83
I	-1.47	-1.14	-0.76
O	0.93	-0.15	1.03
P	-0.39	-0.34	-0.43

C.

150 mM NaCl

	0.001 µl/ml	0.01 µl/ml	0.1 µl/ml
A	0.40	-0.65	-5.09
B	0.76	-1.66	0.97
C	0.94	1.22	1.44
D	2.14	1.98	2.26
E	-10.11	-13.50	-2.78
F	-5.16	-2.35	-2.44
G	0.01	-0.41	-0.23
H	-0.98	0.70	-0.52
I	1.04	0.39	-0.84
O	0.52	0.77	0.03
P	0.49	-0.83	-1.72

Influence of Protein Hydrolysates on Photosynthetic Performance

To verify the effect of the priming on the photosynthetic performance of the seedlings, a range of ChlF parameters was measured using the PAM method and light curve quenching kinetics on the last day of the experiment, after the RGB imaging for all the plates was completed. A set of fluorescence parameters reflecting the photosynthetic function of PSII were calculated (**Supplementary Table S3**). The maximum quantum yield of photosystem II in dark-adapted (F_v/F_m) was used to characterise photosynthetic performance of the control and stressed seedlings (**Supplementary Figure S5**). F_v/F_m was shown to be a robust indicator of plant stress (Rousseau et al., 2013; Wang et al., 2016; Wu et al., 2018) and especially of salt stress (Lucini et al., 2015; Simko et al., 2016; Adhikari et al., 2019). In our experiment, the value of F_v/F_m was significantly reduced in the plants grown in the 150 mM NaCl-enriched media, but not under moderate salt stress (**Supplementary Figure S5**). Overall, the seedling's photosynthetic efficiency belonging to the moderate stress group was not severely compromised (**Supplementary Figure S5 and Supplementary Table S3**). Only the seedlings primed with 0.01 µl ml^{-1} and the 0.1 µl ml^{-1} H, or with a 0.1 µl ml^{-1} solution of A and O improved the F_v/F_m under moderate stress conditions. The seed priming with the highest concentration of the substance F was even able to increase the value F_v/F_m higher than the values observed in the non-primed seeds grown under optimal conditions in control conditions (**Supplementary Figure S5 and Supplementary Table S3**). Contrarily, B at the 0.001 ml^{-1} concentration negatively affected the photosynthetic performances of the seedlings in moderate stress conditions, reducing the F_v/F_m values to those observed in the plants grown under severe salt stress (150 mM NaCl) (**Supplementary Figure S5 and Table S3**).

Finally, to understand how the fluorescence parameters conditioned plant growth under the three different growth conditions studied, we performed three different correlation matrices using the phenotyping data per well plate (a total of 70 plates per growth condition) **(Figure 5)**. As a result, there was not a clear correlation between the growth parameters (rosette size and RGR) with the fluorescence parameters under control and moderate salt stress conditions **(Figure 5A and B)**. However, under severe stress conditions the RGR was positively correlated with higher Fv'/Fm' (*$p < 0.05$) and negatively with

NPQ (*$p < 0.05$) (Figure 5C), showing that under severe salt stress a higher photosynthetic efficiency related with the RGR and hence, the plant growth and final rosette size.

Metabolomics insights into the Mode of Action of Selected Protein Hydrolysates

Once the best performing substances were identified according to the PBC index (C and D), we carried out a non-targeted metabolomic analysis based on UHPLC-ESI/QTOF-MS. The priming seedlings from these treatments, together with their respective controls were collected at the end of the phenotyping experiment. The metabolic analysis also included the three studied growth conditions [optimal growth conditions (control), and moderate (75 mM NaCl) or severe (150 mM NaCl) salt stress], in which seedlings from non-primed or primed seeds with the substance C (*Malvaceae*-derived PH) or D (Trainer®) were compared. The lowest concentration (0.001µl/l) was selected for the analysis of Arabidopsis seedlings grown under control and moderate stress conditions for two main reasons; this concentration presented the highest PCB index values in both substances (Table 1) and because the use of lower concentration has economic benefits. However, under severe salt stress the highest concentration 0.1µl/l of D and C was analysed because it showed the best performance in the phenotyping data (**Table 1**). The whole list of metabolites annotated, together with individual abundances and composite mass spectra, is provided as supplementary material (**Supplementary Table S4**).

The unsupervised hierarchical clustering indicated different metabolic profiles when comparing non-primed or primed seedlings, as thereafter confirmed by the supervised OPLS-DA modelling (**Figure 6**). The clustering built from the fold-change based heatmap (**Figure 6A**) highlighted two main clusters: a first including the seedlings primed with the D substance under the three tested growth conditions, and a second cluster with the non-primed seedlings and those primed with the C substance. This last cluster was also divided into two subclusters that separated the non-primed seeds from the primed ones with substance C, independent of the growing conditions. These results indicated that the main clustering factor was the type of priming agent used.

To corroborate these results, we performed an OPLS-DA supervised multivariate analysis, in which the two substances were independently compared to the non-primed seeds (controls) under the three tested growth conditions (**Figure 6B and C**). In both analyses, the results provided a score plot in agreement with hierarchical clustering, showing that the priming agent is the principal factor separating the samples followed by the growth conditions (**Figure 6B and C**). The investigation of the most discriminant compounds in both OPLS-DA models (*i.e.,* variables of importance in projection—VIP analysis) was then carried out. The **Supplementary Table S5** includes two columns (one for the substance C and another for the substance D) reporting the discriminant metabolites identified (VIP score >1.3). Overall, from the comparison between non-primed seeds and the seeds primed with the C or D substance (Sheets-VIPs markers C or VIPs markets D) 97 and 127 compounds were identified, respectively. Due to this different metabolic profiling between the plants from seeds primed with C or D substance, we also carried out an additional OPLS-DA and identified the most discriminant compounds that differed between these two treatments. As an outcome, a total of 253 compounds were identified (**Supplementary Table S6**), confirming that C and D substances affected in different ways the seeds and hence the plant growth. For example, only the D-primed seedlings increased compounds such as *β*-solanine, guaiacol or plant hormones-related compounds such as gibberellin 34, the brassinosteroids 6-deoxo-24-epicathasterone and campest-5-en-3-one, the sugar maltose or some flavones such as baicalin and 7-hydroxyflavone, among others (**Supplementary Table S6)**. However, C but not D increased certain sesquiterpenoids such as curcuquinone or the main precursor for the synthesis of the aromatic amino acids, shikimate, relevant pathway controlling plant growth and development (Tzin and Galili, 2010), or the metabolite *meso*-diaminopimelate, substrate for the synthesis of L-lysine (Crowther et al. 2019) (**Supplementary Table S5**).

To go further with the study of the mode of action, we inferred the biochemical processes that these two substances are activating in the *Arabidopsis* seedlings to modulate plant growth and promote stress alleviation. To this aim, the discriminating compounds were compared in each growth condition by Volcano Plot analysis (**Figure 7** and **Supplementary Table S7**). First of all, the different compounds were grouped in functional classes; synthesis of amino acids, nucleotides, carbohydrates, fatty acids or

lipids, hormones, cofactor synthesis with the metabolites related to secondary metabolism being the most represented in all the growth conditions, especially in the case of Trainer ® (D) (**Figure 7**). Secondly, the compounds that differ the most (opposite behaviour as in one up accumulated and in another one without changes or down accumulated) between the two PHs were identified (**Supplementary Table S6**). As an example, when the plants primed with D substance were grown under moderate salt stress (75 mM NaCl), secondary metabolites such as flavonoids and terpenes decreased.

A similar profile was observed when plants were grown under severe salt stress conditions (150 mM NaCl) (**Figure 7C**). However, in this case many derivate forms of plant hormones such as benzyladenine-7-glucoside, 16,17-dihydro-16α-17-dihydroxy gibberellin 12 and methylgibberellin 4, the IAA-derivate 4-(indol-3-yl)butanoyl-β-D-glucose or the brassinosteroid castasterone were highly reduced in the seedlings primed with D substance but not with C, compared to the plants coming from non-primed seeds. Altogether, it is clear that being both PH products, including when they are from the same type of botanical material but not the same family, their application to the plants affect different metabolic thways, including the phytohormone balance, that finally condition the plant response to the environment in which is grown.

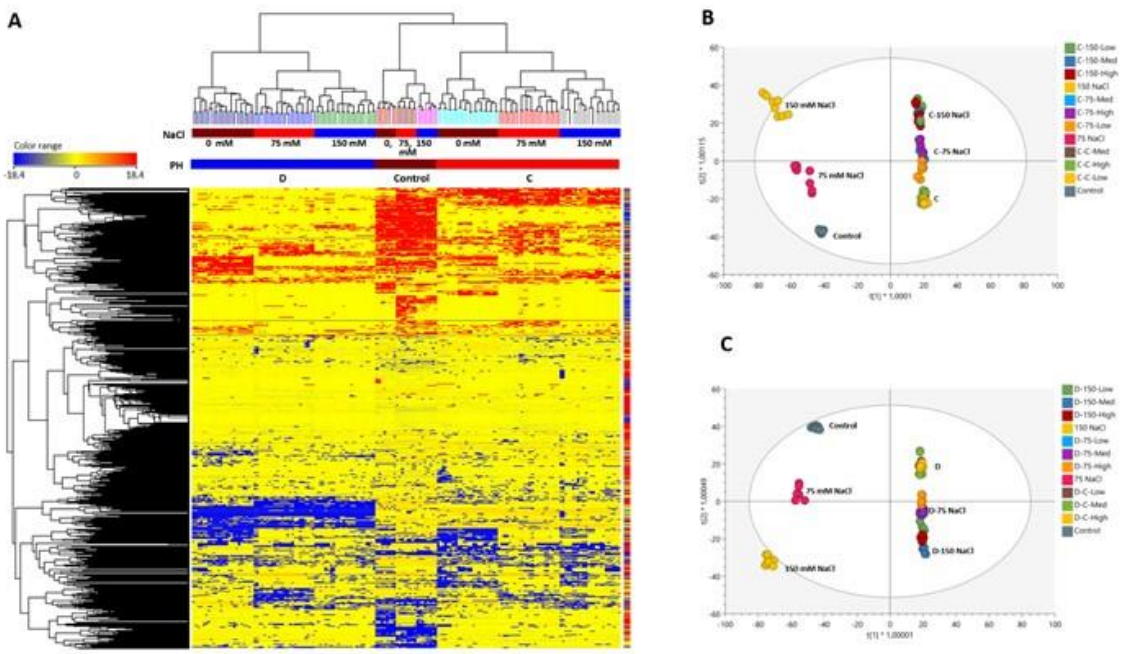

Figure 5|*Hierarchical cluster analysis (A); OPLS-DA of the two best performing protein hydrolysates, C (B) and D (C).*

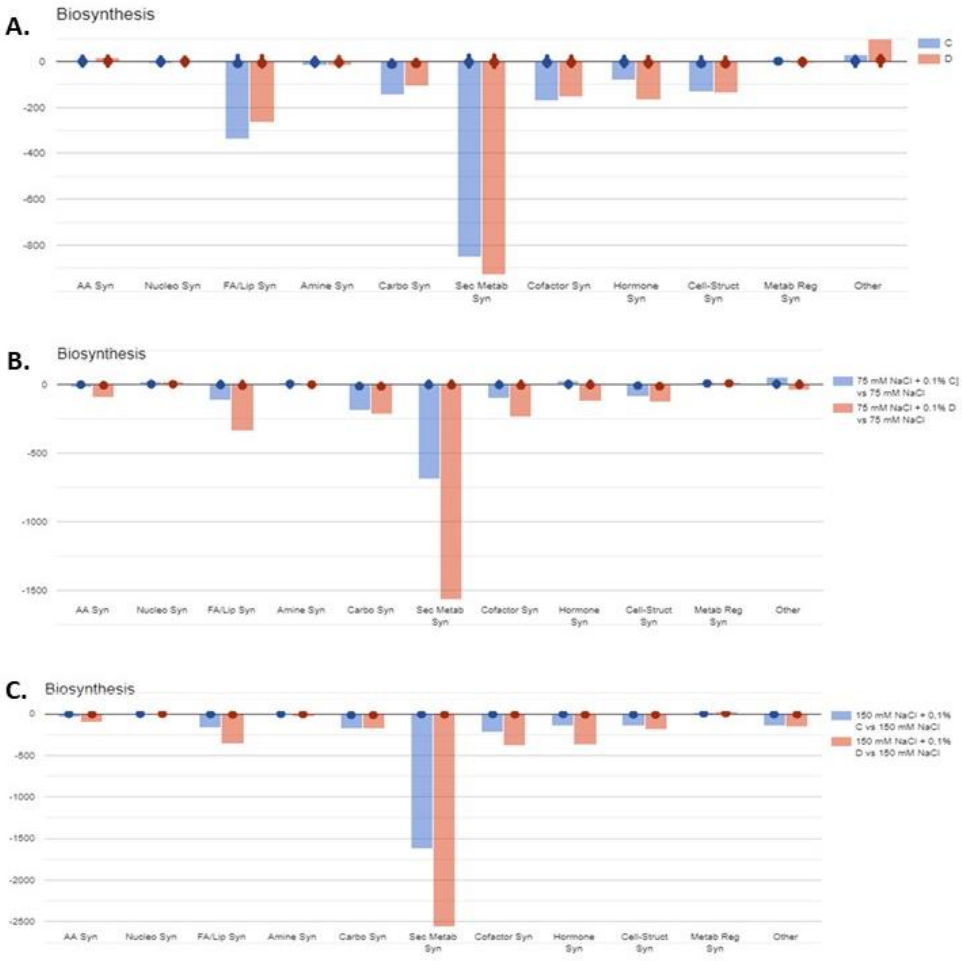

Figure 6| *Products of biosynthesis in the rosettes' tissues: plants treated with the lowest concentration of both PHs and unprimed control (A); plants treated with the highest concentration of C and D in the 75 mM NaCl-enriched media and unprimed control (B); plants treated with the highest concentration of C and D in the 150 mM NaCl-enriched media and unprimed control (C).*

DISCUSSION

Sustainable approaches able to promote plant growth and enhance crop productivity represent a priority in modern agriculture (Xu and Geelen, 2018). Protein hydrolysates, as natural products mainly deriving from agricultural waste and able to reduce dependency on chemical fertilizers, are therefore of great

interest. However, due to the diverse origins of the biostimulants, their manufacturers require fast and efficient tools for identifying and characterizing new functional biostimulants and to identify their mode of action (Ugena et al., 2018). In the last years, platforms for high-throughput automated phenotyping have been frequently used for fast and highly reproducible screenings of the effects of potential biostimulants on growth-related traits of plants, both in control and stress conditions (Rahaman et al., 2015; De Diego et al., 2017; Ugena et al., 2018; Paul et al., 2019a; Paul et al., 2019b). However, most platforms are limited in their capacity of measuring a large number of individuals (or variants) at the same time. In contrast, the comparison between plants primed with different doses of biostimulants and growing in diverse stress severities is fundamental to prove the effectiveness of the substances as biostimulants and elucidate their mode of action. The biostimulant activity of a product, in fact, is strongly dependent on the severity of the stress applied to the plant (Bulgari et al., 2019) as well as on the time of exposure; therefore, the beneficial effects of a substance can vary with the concentration and time of exposure of the plants to the stress (Colla et al., 2010). Transferring to *in-vitro* conditions using a model plant such as *Arabidopsis* allows increasing the number of treatments and replicates (De Diego et al., 2017). Starting from these premises, we followed the same protocol described by Ugena et al. (2018). The effects of potential biostimulant substances were tested on *Arabidopsis* seedlings grown under optimal conditions and salt stress in two different intensities (75 mM and 150 mM NaCl). However, instead of using single compounds such as polyamines, we tested the effects of 11 complex products based on protein hydrolysates from different natural origins, applied in three different concentrations (0.001, 0.01 and 0.1 µl ml^{-1}) as seed priming agents. Priming induces preliminary germination (Jisha et al., 2012; Paparella et al., 2015), enhances synchronized germination, promotes plant growth (Bryksová et al. 2020) and can elicit resilience to stressors (Conrath, 2011; Paparella et al., 2015). Priming can improve seed performance, ensure higher uniformity among the seeds, result in faster and better. Priming finds application particularly in vegetables like carrot, onion, celery, lettuce, endive, pepper and tomato (Paparella et al., 2015). This is why in our study the seed priming with PHs-based substances was used instead of mixing them into the media, so the amount of the substances used for the priming is highly reduced saving product and costs, and of course reducing the potential toxicity of the high dosages. As corroboration, we could see that the seed priming with the high dosages of some PHs-

based substances inhibited plant growth (**Table 1** and **Figure 4**) but did not kill the plants as happened in previous studies in which the substances were applied to the growth media (data not shown).

Simple RGB daily pictures were able to provide us with plenty of information related to the plants' growth and fitness using the MTHTS approach: starting from the mere dimensions of the plants, we could calculate the slope of the growth curve, the RGR, the Coefficient of Variance and the Survival Rate in salt stress conditions. Exactly as described by Ugena et al. (2018), the phenotyping traits were used to calculate the Plant Biostimulant Characterization (PBC) index, which ended with a single number making easier the characterization of each biostimulant according to their mode of action: growth promotor/inhibitor and/or stress alleviator. Thus, the PBC index showed that the effects of the substances on plants was not only dependent of the PH substance tested but also dose dependent. For most of the substances, the highest concentration (0.1 µl ml^{-1}) was not beneficial or reduced plant growth (**Table 1** and **Figure 4**). It is known that PHs contain carbohydrates, amino acids, and lipids that may improve crop fitness, acting as plant growth regulators (growth promoters) in the absence of any external stress, due to the presence of bioactive peptides (Colla et al., 2014, 2015a) with a range of phytohormone-like activities (Ito et al., 2006; Kondo et al., 2006). PHs may as well increase plant tolerance to abiotic stresses (Van Oosten et al, 2017) because certain amino acids affect the ion fluxes across membranes, most having a positive effect on reducing NaCl-induced potassium efflux (Cuin and Shabala, 2007). However, when PHs based substances are applied to the plants at high dosages an excess of free amino acids or phenols can have the opposite effect and induce growth retardation (Cerdán et al., 2009; Muscolo et al., 2013; Ertani et al., 2018), explaining the inhibitory effect observed in some of the variants. Only the substances C and D improved plant growth under control and stress conditions, including when they were applied in high concentration, with better results in the case of D, our positive control. In this regard, Trainer® has been demonstrated to improve the growth of many crop species and to mitigate the deleterious effects of salt stress (Colla et al., 2014; Lucini et al., 2015; Rouphael et al., 2017b; Di Mola et al., 2019a; Luziatelli et al., 2019; Paul et al., 2019a). Altogether, we showed that the MTHTS of Arabidopsis rosette growth is an advantageous and fast approach to test new biostimulants under a wide range of concentrations and growth conditions. Besides, our results are comparable with those obtained

in other interesting plant species including crops with agronomical interest, confirming the biological translation of the results obtained in Arabidopsis to them. The PHs-derived biostimulants C and D have in common the plant origin but differ in the plant family from which they are produced (*Malvaceae* and *Fabaceae*, respectively).

At the end of the experiment, chlorophyll fluorescence measurement of all the plants have also been performed and the light curve protocol (Henley, 1993; Rascher et al., 2000) was used as it was proven to be especially effective in providing detailed information on plant adaptation to adverse conditions (Brestic and Zivcak, 2013; Awlia et al., 2016). As a result, we observed that the maximum quantum yield of PSII photochemistry in the dark-adapted state (F_v/F_m) was reduced in salt stress conditions, especially in the 150 mM NaCl-enriched media. This is coherent with previous works (Baker and Rosenqvist, 2004; Awlia et al., 2016), where F_v/F_m proved to be a robust parameter, being affected only under severe stress. Additionally, the seed priming with some PHs based substances at certain concentrations also improved the F_v/F_m under optimal and salt stress conditions (**Supplementary Figure S5** and **Supplementary Table S3**). This is in agreement with previous experiments, in which the use of plant-derived PHs promoted photosynthetic efficiency and increased the accumulation of photosynthetic pigments (Yakhin et al., 2017). However, this effect was not very remarkable in the case of the best performing PH (D). A possible explanation is that this product did not influence the light phase of the photosynthesis (fluorescence parameters) but could increase the dark phase of the photosynthesis and hence, the efficiency of the plant, as has been described previously in PHs treated lettuce (Xu and Mou, 2017)

Another explanation for this result can relate to the broad metabolic reprogramming induced by PHs. For example, the seedlings primed with D substance accumulated higher levels of maltose compared to the controls. Maltose is a soluble sugar and the major starch-degrading product (Thalmann and Santelia, 2017). Starch degradation (a common plant stress response) is the main mechanism D- primed plants used, resulting in accumulating certain soluble sugars, especially maltose (**Supplementary Table S5**). As corroboration of the beneficial maltose accumulation, its exogenous application in wheat plants improved plant growth, yield and some biochemical components when grown under drought conditions

(Ibrahim and Abdellatif, 2016). The Arabidopsis seedlings primed with D substance also displayed lower levels of flavonoids and terpenoids. These compounds are mainly accumulated in plants under stress condition resulting in reactive oxygen species (ROS) production (D'Amelia et al. 2018; Sharma et al. 2019a). Altogether, we suggest that the reduced presence of flavonoids and terpenoids pointed to the D-primed seedlings as healthier plants with lower levels of ROS that allow the plants to grow better. Finally, recent studies have shown strong crosstalk between flavonoids and some plant growth regulators such auxins and cytokinins, controlling biological processes such as nodulation in *Medicago truncatula* and, hence, plant growth (Ng et al. 2015). In this regard, the D-treated plants showed a clear reduction in many products of degradation or conjugation (mainly related to inactivation) of cytokinins, auxins and brassinosteroids. Thus, they could maintain the levels of the active phytohormone forms to preserve the general homeostasis of the plants. In this regard, both the activation and inactivation of cytokinin degradation genes have been mentioned to give plant stress tolerance (Vojta et al. 2016; Prerostova et al., 2018). In Arabidopsis, for example, the inducible 35S: CKX plants were approximately half those of WT plants under well-watered conditions, their rosette growth rates were actually more sensitive to soil drying, and they recovered more slowly after re-watering (Prerostova et al., 2018). These results are in accordance with the better growth of the D-treated Arabidopsis seedlings and the reduced benzyladenine-7-glucoside levels. Finally, these seedlings also accumulated brassinosteroid precursors such as 6-deoxo-24-epicathasterone and campest-5-en-3-one and reduced the formation of castasterone. Brassinosteroids (BRs) are a category of plant steroid hormones having multiple roles in plant growth, development, and stress responses (Ahammed et al., 2020). In fact, the accumulation of castasterone has been related to plant stress response and detoxification under metal and pesticide stress (Sharma et al., 2019b; Ahammed et al., 2020). Interestingly, brassinosteroids have been reported to modulate plant growth and stress management, including under saline conditions (Vidya Vardhini, 2017). This suggests a lower level of castasterone indicated that the plants experienced new homeostasis in which the effect or toxicity induced by salt stress is reduced. Our findings indicate that this modulation of brassinosteroids might be the consequence of an improved resilience towards salinity induced by the biostimulants in our plants.

CONCLUSIONS

The present study presented a complex pipe-plan to select and understand the mechanism of action of 11 PHs-substances used as priming agents. The results demonstrated that the high-throughput phenotyping approach, such as MTHTS of Arabidopsis rosette, is a valuable tool to compare a high number of biostimulants at different concentrations in plants grown under different conditions (with and without stress). This approach has proven to be able to accelerate the selection of the best performing substances in a highly effective manner. Besides, the obtained results corroborated the biological translation from Arabidopsis to other crops with agronomical interest. Additionally, the combination of the phenomics with untargeted metabolic analysis revealed that the priming with the best-performing substance modifies the plant homeostasis thus promoting growth and allowing a higher survival by reducing the oxidative damages induced by the stress and by regulating the crosstalk between different plant hormones. Finally, this approach can help to accelerate the selection and characterization of new biostimulants that make the plants more efficient and more resistant to stress. Further studies will be performed using model crops to go further in the understanding of the mode of action of PHs based biostimulants.

AUTHORS CONTRIBUTIONS

YR, LL and GC prepared and selected the protein hydrolysates. MS, NDD, LS and KP designed the phenotyping experiments. MS and LU performed the phenotyping experiments. MS and NDD performed the image processing, and image-based data analysis. LL, BM-M and LZ carried out the untargeted metabolomics. LL, BM-M and NDD analysed the metabolomic results. All authors discussed the results and contributed to writing the manuscript.

FUNDING

This work was supported by European Union's Horizon 2020 Research and Innovation Program under the Marie Skłodowska- Curie grant agreement no. 675006, by Italian Ministry of Education, University and Research (MiUR) under the PRIN 'PHOBOS' (no. 2017FYBLPP), by the project "Plants as a tool

for sustainable global development" (registration number: CZ.02.1.01/0.0/0.0/16_019 /0000827) within the program Research, Development and Education (OP RDE) and by European Regional Development Fund-Project "SINGING PLANT" (No. CZ.02.1.01/0.0/0.0/16_026/0008446) with a financial contribution from the Ministry of Education, Youths and Sports of the Czech Republic through the National Programme for Sustainability II funds.

ACKNOWLEDGEMENTS

We thank Hello Nature Company (Rivoli Veronese, Italy) for helping in the development of tested protein hydrolysates. We also thank Jana Nosková from the Centre of the Region Haná (Olomouc, Czechia) for her help with the preparation of the plant material and the implementation of the experiment. This work is a result of a postdoctoral contract for the training and improvement abroad of research staff (Begoña Miras-Moreno; 21252/PD/19) financed by the Consejería de Empleo, Universidades, Empresa y Medio Ambiente of the CARM, through the Fundación Séneca-Agencia de Ciencia y Tecnología de la Región de Murcia (Spain).

Supplementary Figures

Supplementary Figure S1| Growth of the plants in control conditions following the priming with the set of protein hydrolysates. Projected rosette area (pixels) of Arabidopsis seedlings primed with the 11 protein hydrolysates (A-P) at three concentrations (0.001, 0.01 and 0.1 ml/ml) and grown for 7 days in 48-well plates under control conditions. Rosette area was extracted from RGB images acquired twice a day (am and pm) over the period of 1 week. Values represent the average of the 96 biological replicates per treatment, error bars represent standard error.

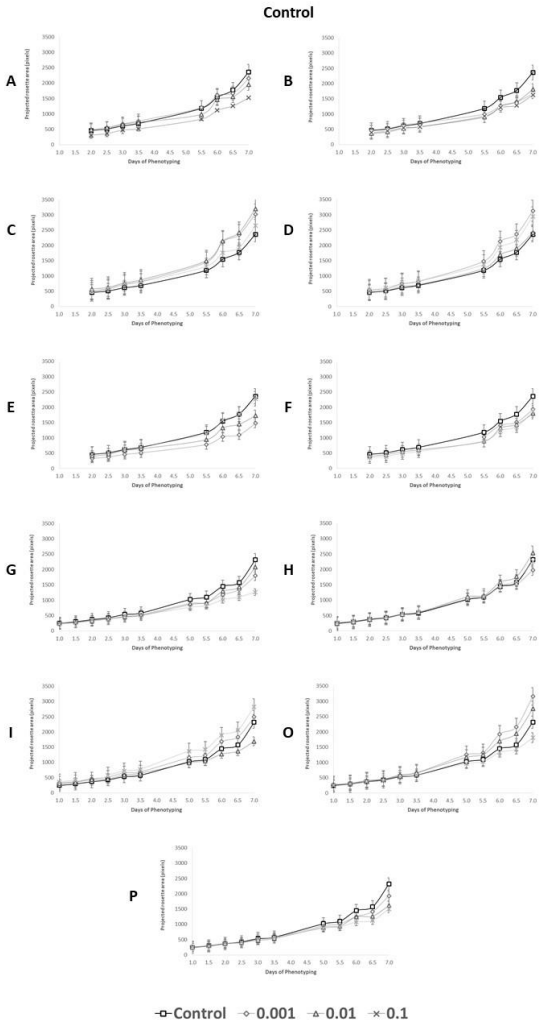

Supplementary Figure S2| Growth of the plants in moderate salt stress conditions following the priming with the set of protein hydrolysates. Projected rosette area (pixels) of Arabidopsis seedlings primed with the 11 protein hydrolysates (A-P) at three concentrations (0.001, 0.01 and 0.1 ml/ml) and grown for 7 days in 48-well plates under moderate (75 mM NaCl) salt stress conditions. Rosette area was extracted from RGB images acquired twice a day (am and pm) over the period of 1 week. Values represent the average of the 96 biological replicates per treatment, error bars represent standard error.

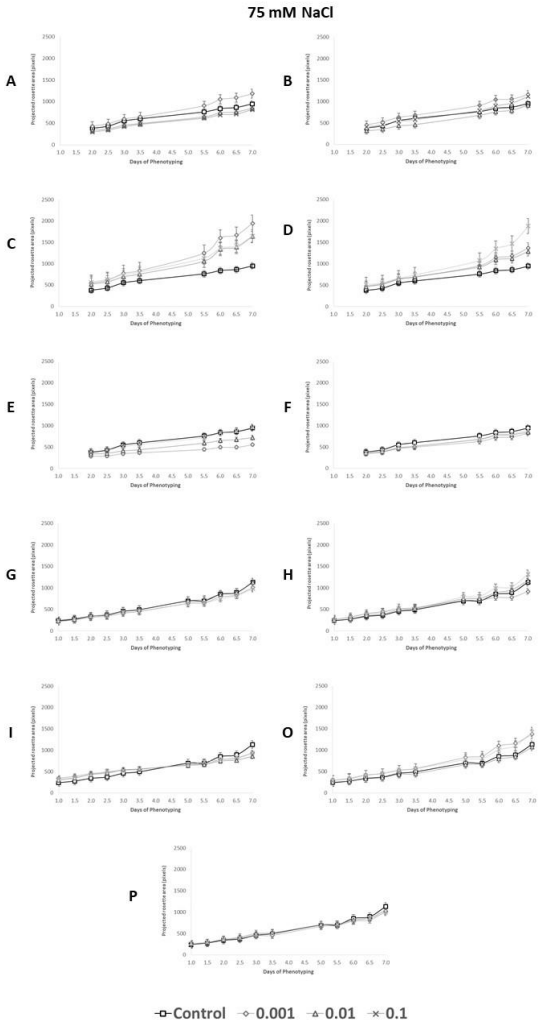

Supplementary Figure S3| Growth of the plants in severe salt stress conditions following the priming with the set of protein hydrolysates. Projected rosette area (pixels) of Arabidopsis seedlings primed with the 11 protein hydrolysates (A-P) at three concentrations (0.001, 0.01 and 0.1 ml/ml) and grown for 7 days in 48-well plates under severe (150 mM NaCl) salt stress conditions. Rosette area was extracted from RGB images acquired twice a day (am and pm) over the period of 1 week. Values represent the average of the 96 biological replicates per treatment, error bars represent standard error.

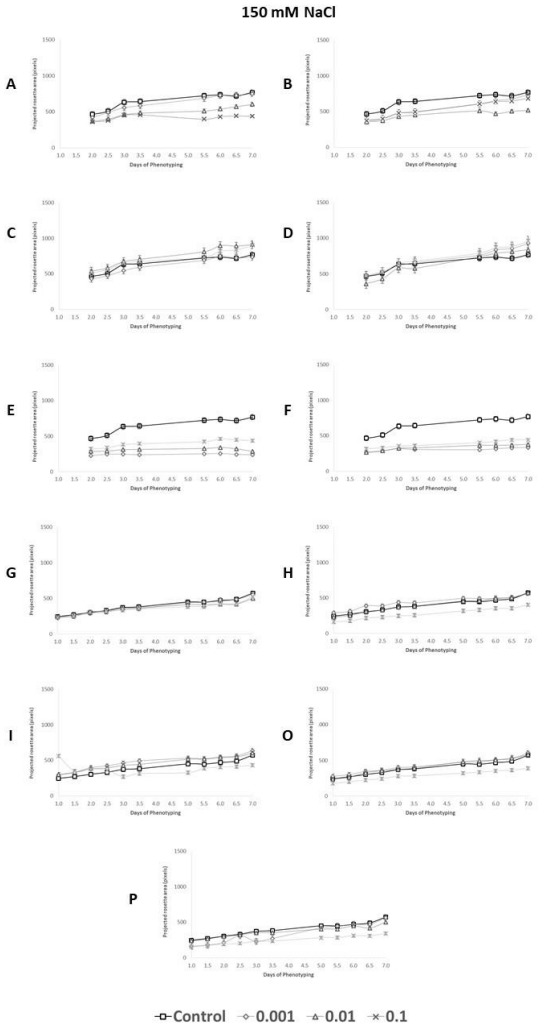

Supplementary Figure S4| Maximum quantum yield of PSII photochemistry in the dark-adapted state (F_v/F_m) of the Arabidopsis seedlings. Graphs show the maximum quantum yield of the plantlets after 7 days of in control, moderate (75 mM NaCl), and severe (150 mM NaCl) salt stress conditions. Seedlings were primed with the 11 protein hydrolysates at three concentrations (0.001, 0.01 and 0.1 ml/ml). Values represent the average of the 96 biological replicates per treatment, error bars represent standard error. Different letters are used to indicate the significant differences between the accessions and conditions as tested with one-way ANOVA with post hoc Tukey's test ($p < 0.05$).

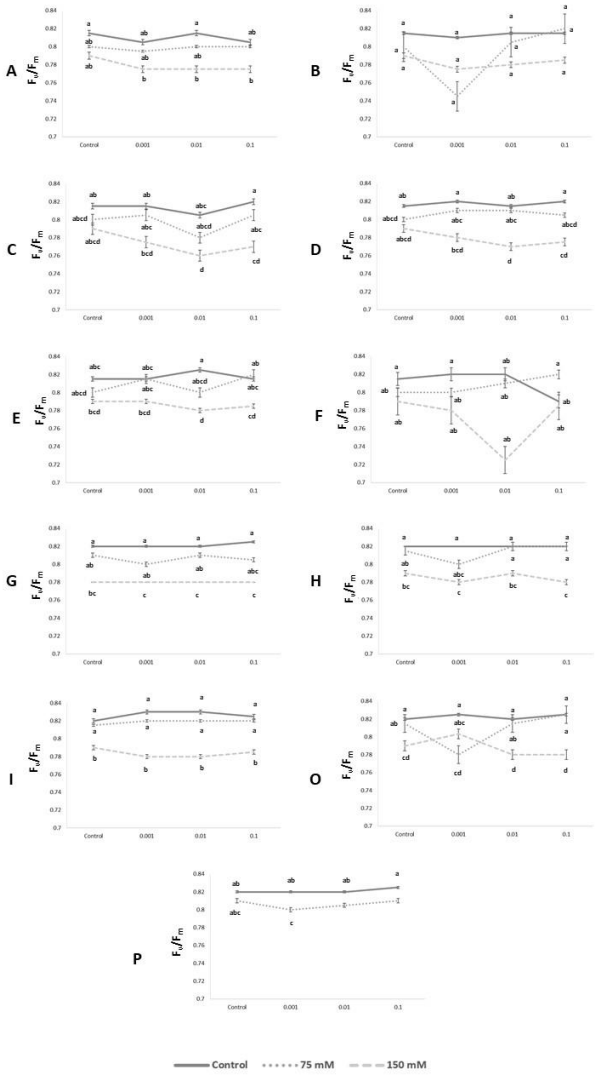

Supplementary Figure S5| OPLS-DA C vs D (including all the concentrations).

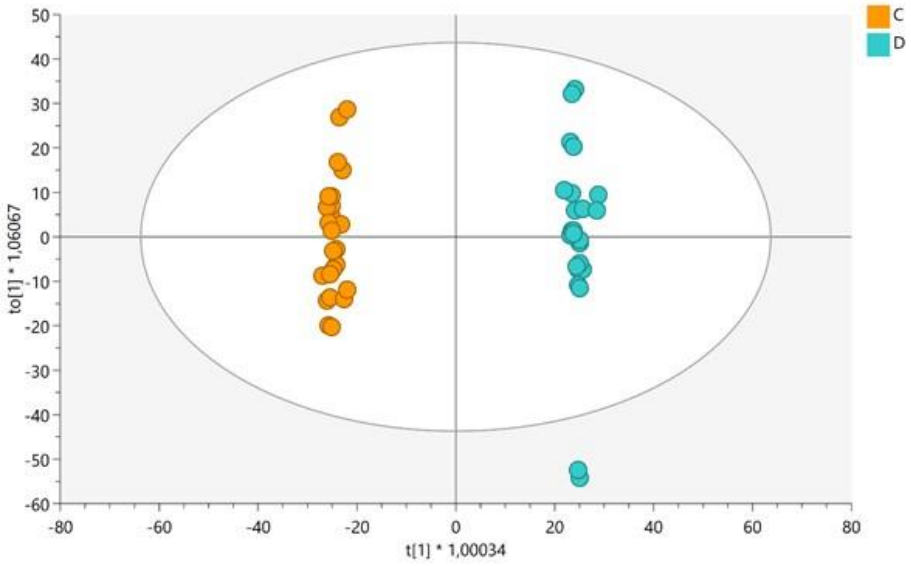

Supplementary Table S1 | List and characterisation of the protein hydrolysate compounds selected for seed priming.

Category		PlantScreen system Used	Definition	Abbreviation
1	Morphological (Measured or Calculated)	PlantScreen XYZ System	Projected Shoot Area in the last day of phenotyping.	Final area (pxl)
2			Relative growth rate (increase in area between 2 time points).	RGR (pxl pxl^{-1} day^{-1})
3			Coefficient of Variance (area variability) in the last day of phenotyping.	CV (%)
4			Final Survival Rate in salt stress conditions.	Survival (%)
5			Slope of the growth curve.	Slope
6	Chlorophyll fluorescence parameters (Measured)	PlantScreen Conveyor System	Maximum PSII quantum yield in dark-adapted state.	F_v/F_m
7			Maximum quantum yield of PSII in the light-adapted state.	F_v'/F_m'
8			PSII operating efficiency.	ΦPSII
9			Steady-state non-photochemical quenching.	NPQ

Supplementary Table S2| Growth-related parameters extracted from the RGB images. Values for the Slope of the growth curve, projected rosette area (pixels) in the last day of measurement, RGR (pixel pixel^{-1} day^{-1}) for the entire period of the experiment and survival rate (%) estimated at the last day of the trial. The values displayed correspond to Arabidopsis seedlings from non-primed seeds or primed with 11 different PHs at 3 concentrations (0.001, 0.01 and 0.1 ml/ml) grown under control (A), moderate (B) and severe salt stress conditions (C).

	75 mM NaCl																			
	No Biostimulant					0.001 mM					0.01 mM					0.1 mM				
	Final Area (pxl)	RGR (pxl pxl^{-1} day^{-1})	CV (%)	Survival (%)	Slope	Final Area (pxl)	RGR (pxl pxl^{-1} day^{-1})	CV (%)	Survival (%)	Slope	Final Area (pxl)	RGR (pxl pxl^{-1} day^{-1})	CV (%)	Survival (%)	Slope	Final Area (pxl)	RGR (pxl pxl^{-1} day^{-1})	CV (%)	Survival (%)	Slope
A						1292 *def*	0.21 *abcd*	54 *a*	96 *b*	136.89	899 *hij*	0.18 *cde*	43 *a*	97 *ab*	97.57	863 *ijk*	0.20 *bcde*	47 *a*	98 *ab*	96.00
B						1235 *defg*	0.19 *bcde*	45 *a*	99 *ab*	136.89	978 *ghij*	0.21 *bcde*	46 *a*	99 *ab*	113.64	1149 *fghi*	0.20 *bcde*	43 *a*	100 *a*	130.64
C	1181 *efgh*	0.18 *bcde*	55 *a*	100 *a*	106.38	2014 *a*	0.25 *a*	39 *a*	100 *a*	269.07	1754 *abc*	0.22 *abc*	46 *a*	99 *ab*	210.68	1870 *a*	0.21 *ab*	44 *a*	100 *a*	204.72
D						1513 *bcd*	0.21 *abcd*	48 *a*	99 *ab*	167.22	1471 *cde*	0.20 *abcd*	55 *a*	100 *a*	155.13	1822 *ab*	0.26 *a*	51 *a*	99 *ab*	245.57
E						570 *k*	0.13 *f*	48 *a*	99 *ab*	51.54	760 *jk*	0.15 *ef*	36 *a*	100 *a*	78.10	1017 *fghij*	0.18 *cde*	41 *a*	98 *ab*	109.03
F						883 *hij*	0.17 *cde*	46 *a*	100 *a*	89.32	914 *hij*	0.17 *de*	46 *a*	100 *a*	96.86	1015 *fghij*	0.18 *cde*	44 *a*	100 *a*	101.03
G						1038 *abcd*	0.25 *ab*	56 *a*	96 *a*	101.32	1242 *abcd*	0.27 *a*	46 *a*	100 *a*	115.99	1063 *cd*	0.22 *abc*	52 *a*	98 *a*	91.88
H						1023 *cd*	0.21 *bcd*	49 *a*	99 *a*	98.58	1343 *abc*	0.26 *a*	53 *a*	99 *a*	140.22	1457 *ab*	0.27 *a*	51 *a*	99 *a*	155.36
I	1242 *abcd*	0.26 *ab*	53 *a*	100 *a*	108.87	1092 *cd*	0.17 *d*	60 *a*	96 *a*	86.72	936 *d*	0.18 *cd*	45 *a*	98 *a*	83.34	1119 *cd*	0.18 *d*	43 *a*	99 *a*	92.85
O						1528 *a*	0.25 *ab*	51 *a*	99 *a*	168.63	1302 *abc*	0.24 *ab*	59 *a*	100 *a*	124.04	1528 *a*	0.26 *a*	50 *a*	100 *a*	162.95
P						1144 *bcd*	0.24 *ab*	60 *a*	97 *a*	115.67	1177 *abcd*	0.23 *abc*	60 *a*	99 *a*	119.17	1106 *cd*	0.22 *ab*	54 *a*	95 *a*	115.63
	Control																			
	No Biostimulant					0.001 mM					0.01 mM					0.1 mM				
	Final Area (pxl)	RGR (pxl pxl^{-1} day^{-1})	CV (%)	Survival (%)	Slope	Final Area (pxl)	RGR (pxl pxl^{-1} day^{-1})	CV (%)	Survival (%)	Slope	Final Area (pxl)	RGR (pxl pxl^{-1} day^{-1})	CV (%)	Survival (%)	Slope	Final Area (pxl)	RGR (pxl pxl^{-1} day^{-1})	CV (%)	Survival (%)	Slope
A						2205 *cdef*	0.28 *bcde*	52 *a*		0.29	1972 *defg*	0.25 *de*	54 *a*		0.26	1626 *gh*	0.31 *abc*	52 *a*		0.30
B						1742 *fgh*	0.23 *e*	56 *a*		0.24	1771 *fgh*	0.29 *abcd*	43 *a*		0.30	1676 *gh*	0.26 *cde*	52 *a*		0.27
C	2312 *cde*	0.32 *ab*	48 *a*	100 *a*	0.32	2872 *ab*	0.34 *a*	35 *a*	100 *a*	0.35	3000 *a*	0.32 *ab*	36 *a*	100 *a*	0.34	2662 *abc*	0.31 *ab*	37 *a*	100 *a*	0.30
D						3009 *a*	0.33 *ab*	37 *a*		0.35	2398 *bcd*	0.32 *ab*	35 *a*		0.32	2888 *ab*	0.32 *ab*	39 *a*		0.32
E						1477 *h*	0.28 *bcde*	49 *a*		0.28	1847 *efgh*	0.28 *bcde*	49 *a*		0.28	2180 *cdef*	0.29 *abcd*	41 *a*		0.30
F						1885 *efgh*	0.29 *abcd*	40 *a*		0.39	1807 *fgh*	0.28 *bcde*	46 *a*		0.29	1875 *efgh*	0.31 *ab*	43 *a*		0.32
G						1795 *defg*	0.31 *cdef*	57 *abc*		0.31	2028 *cdef*	0.33 *abcde*	54 *abc*		0.31	1468 *g*	0.28 *ef*	72 *a*		0.28
H						2042 *efghijk*	0.31 *cdef*	54 *abc*		0.33	2350 *bc*	0.34 *ab*	39 *bc*		0.37	2298 *cdef*	0.35 *abcd*	44 *bc*		0.33
I	2245 *bcde*	0.34 *ab*	54 *abc*	100 *a*	0.34	2384 *bc*	0.37 *ab*	45 *bc*	100 *a*	0.32	1801 *defg*	0.33 *abcde*	40 *bc*	100 *a*	0.28	2691 *ab*	0.19 *g*	42 *bc*	100 *a*	0.33
O						2954 *a*	0.38 *a*	33 *c*		0.39	2635 *ab*	0.36 *abc*	39 *bc*		0.37	1956 *cdefg*	0.31 *cdef*	54 *abc*		0.32
P						1903 *cdefg*	0.31 *cdef*	49 *abc*		0.32	1766 *efg*	0.30 *def*	62 *ab*		0.30	1580 *fg*	0.26 *f*	63 *ab*		0.28
	150 mM NaCl																			
	No Biostimulant					0.001 mM					0.01 mM					0.1 mM				
	Final Area (pxl)	RGR (pxl pxl^{-1} day^{-1})	CV (%)	Survival (%)	Slope	Final Area (pxl)	RGR (pxl pxl^{-1} day^{-1})	CV (%)	Survival (%)	Slope	Final Area (pxl)	RGR (pxl pxl^{-1} day^{-1})	CV (%)	Survival (%)	Slope	Final Area (pxl)	RGR (pxl pxl^{-1} day^{-1})	CV (%)	Survival (%)	Slope
A						745 *bcd*	0.11 *abc*	66 *abc*	90 *abcd*	60.94	559 *defg*	0.08 *abcde*	63 *abc*	93 *abcd*	29.12	486 *fgh*	0.11 *abcd*	80 *a*	82 *abcd*	60.65
B						672 *cdef*	0.08 *abcde*	64 *abc*	93 *abcd*	73.81	533 *efgh*	0.06 *bcde*	62 *abc*	93 *abcd*	68.29	672 *cdef*	0.11 *abc*	47 *c*	95 *abc*	8.38
C	815 *abc*	0.08 *abcde*	68 *abc*	88 *abcd*	52.25	718 *bcde*	0.09 *abcde*	48 *c*	98 *ab*	61.72	881 *ab*	0.06 *bcde*	54 *bc*	93 *abcd*	73.81	854 *abc*	0.10 *abcde*	46 *c*	93 *abcd*	68.29
D						897 *ab*	0.12 *ab*	44 *c*	98 *ab*	82.58	841 *abc*	0.14 *a*	57 *abc*	93 *abc*	89.54	983 *a*	0.14 *a*	46 *c*	97 *ab*	87.98
E						277 *i*	0.03 *e*	82 *a*	76 *d*	2.03	353 *hi*	0.03 *e*	76 *ab*	80 *cd*	4.28	456 *ghi*	0.05 *cde*	69 *abc*	80 *cd*	24.38
F						369 *ghi*	0.04 *de*	74 *ab*	89 *bcd*	8.91	409 *ghi*	0.09 *abcde*	51 *bc*	94 *abc*	20.20	439 *ghi*	0.05 *cde*	64 *abc*	90 *abcd*	24.81
G						547 *a*	0.14 *ab*	40 *ab*	88 *b*	49.45	503 *a*	0.12 *bcd*	51 *ab*	98 *a*	38.94	502 *fghij*	0.12 *bcd*	49 *ab*	95 *ab*	32.88
H						534 *a*	0.09 *cd*	53 *ab*	88 *b*	37.94	564 *a*	0.15 *ab*	35 *ab*	98 *a*	51.51	568 *defgh*	0.14 *ab*	41 *ab*	95 *ab*	37.22
I	556 *a*	0.13 *abc*	42 *efghi*	94 *ab*	46.49	587 *a*	0.11 *bcd*	43 *ab*	96 *ab*	46.54	535 *a*	0.09 *d*	52 *ab*	90 *ab*	44.91	577 *defgh*	0.10 *bcd*	52 *ab*	93 *ab*	46.49
O						580 *a*	0.12 *bcd*	33 *ab*	98 *a*	46.99	580 *a*	0.14 *ab*	35 *ab*	98 *a*	52.99	646 *cdefg*	0.14 *ab*	21 *ab*	99 *a*	32.70
P						573 *a*	0.17 *a*	67 *a*	94 *ab*	63.55	501 *a*	0.12 *bcd*	49 *ab*	93 *ab*	36.31	500 *fghij*	0.12 *bcd*	36 *ab*	96 *ab*	28.86

Results

Supplementary Table S3| Fluorescence related parameters. Values of the maximum quantum yield of PSII photochemistry in the dark-adapted state (F_v/F_m), the maximum quantum efficiency in light-adapted state (F'_v/F'_m), the steady-state non-photochemical quenching (NPQ) and the steady-state operating efficiency of PSII in the light (**ΦPSII**) in the last day of the trial of the experiment. The values displayed correspond to plantlets treated with all the 11 PHs, in the 3 concentrations (0.001, 0.01 and 0.1 ml/ml), in control (A), moderate (B) and severe salt stress conditions (C).

Control

	No Biostimulant				***0.001 mM***				***0.01 mM***				***0.1 mM***			
	F_v/F_m	F'_v/F'_m	ΦPSII	NPQ	F_v/F_m	F'_v/F'_m	ΦPSII	NPQ	F_v/F_m	F'_v/F'_m	ΦPSII	NPQ	F_v/F_m	F'_v/F'_m	ΦPSII	NPQ
A	0.82 *a*	0.76 *a*	0.52 *a*	0.42 *a*	0.81 *a*	0.76 *a*	0.53 *a*	0.37 *a*	0.82 *a*	0.77 *a*	0.53 *a*	0.37 *a*	0.81 *a*	0.76 *a*	0.56 *a*	0.29 *a*
B					0.81 *a*	0.77 *a*	0.52 *a*	0.3 *a*	0.82 *a*	0.76 *a*	0.53 *a*	0.38 *a*	0.82 *a*	0.77 *a*	0.51 *a*	0.4 *a*
C					0.82 *a*	0.77 *a*	0.51 *a*	0.37 *a*	0.81 *a*	0.73 *a*	0.49 *a*	0.53 *a*	0.82 *a*	0.76 *a*	0.51 *a*	0.43 *a*
D					0.82 *a*	0.78 *a*	0.54 *a*	0.31 *a*	0.82 *a*	0.78 *a*	0.56 *a*	0.31 *a*	0.82 *a*	0.77 *a*	0.51 *a*	0.34 *a*
E					0.82 *a*	0.77 *a*	0.53 *a*	0.38 *a*	0.83 *a*	0.77 *a*	0.51 *a*	0.40 *a*	0.82 *a*	0.75 *a*	0.5 *a*	0.46 *a*
F					0.82 *a*	0.76 *a*	0.52 *a*	0.43 *a*	0.82 *a*	0.76 *a*	0.52 *a*	0.42 *a*	0.79 *a*	0.77 *a*	0.57 *a*	0.35 *a*
G	0.82 *a*	0.77 *a*	0.51 *a*	0.39 *a*	0.82 *a*	0.78 *a*	0.52 *a*	0.37 *a*	0.82 *a*	0.78 *a*	0.51 *a*	0.34 *a*	0.83 *a*	0.77 *a*	0.51 *a*	0.42 *a*
H					0.82 *a*	0.77 *a*	0.51 *a*	0.36 *a*	0.82 *a*	0.78 *a*	0.52 *a*	0.32 *a*	0.82 *a*	0.76 *a*	0.50 *a*	0.40 *a*
I					0.83 *a*	0.79 *a*	0.52 *a*	0.39 *a*	0.83 *a*	0.79 *a*	0.52 *a*	0.30 *a*	0.83 *a*	0.79 *a*	0.52 *a*	0.30 *a*
O					0.83 *a*	0.78 *a*	0.51 *a*	0.38 *a*	0.82 *a*	0.77 *a*	0.51 *a*	0.48 *a*	0.83 *a*	0.77 *a*	0.51 *a*	0.45 *a*
P					0.82 *a*	0.77 *a*	0.51 *a*	0.35 *a*	0.82 *a*	0.78 *a*	0.51 *a*	0.33 *a*	0.83 *a*	0.77 *a*	0.51 *a*	0.42 *a*

75 mM NaCl

	No Biostimulant				***0.001 mM***				***0.01 mM***				***0.1 mM***			
	F_v/F_m	F'_v/F'_m	ΦPSII	NPQ	F_v/F_m	F'_v/F'_m	ΦPSII	NPQ	F_v/F_m	F'_v/F'_m	ΦPSII	NPQ	F_v/F_m	F'_v/F'_m	ΦPSII	NPQ
A	0.8 *ab*	0.74 *a*	0.54 *a*	0.39 *a*	0.80 *ab*	0.74 *a*	0.53 *a*	0.38 *a*	0.80 *ab*	0.74 *a*	0.50 *a*	0.43 *a*	0.8 *ab*	0.74 *a*	0.52 *a*	0.46 *a*
B					0.75 *b*	0.72 *a*	0.48 *a*	0.51 *a*	0.81 *ab*	0.74 *a*	0.52 *a*	0.48 *a*	0.82 *a*	0.75 *a*	0.48 *a*	0.60 *a*
C					0.81 *ab*	0.74 *a*	0.50 *a*	0.47 *a*	0.78 *ab*	0.73 *a*	0.50 *a*	0.41 *a*	0.81 *ab*	0.74 *a*	0.47 *a*	0.44 *a*
D					0.81 *ab*	0.74 *a*	0.51 *a*	0.48 *a*	0.81 *ab*	0.74 *a*	0.51 *a*	0.51 *a*	0.81 *ab*	0.73 *a*	0.50 *a*	0.52 *a*
E					0.82 *a*	0.74 *a*	0.49 *a*	0.54 *a*	0.80 *ab*	0.74 *a*	0.49 *a*	0.42 *a*	0.82 *a*	0.75 *a*	0.50 *a*	0.52 *a*
F					0.80 *ab*	0.75 *a*	0.53 *a*	0.41 *a*	0.81 *ab*	0.75 *a*	0.52 *a*	0.43 *a*	0.82 *a*	0.76 *a*	0.48 *a*	0.51 *a*
G	0.82 *a*	0.77 *a*	0.51 *a*	0.42 *a*	0.81 *a*	0.75 *a*	0.49 *a*	0.45 *a*	0.81 *a*	0.75 *a*	0.49 *a*	0.49 *a*	0.81 *a*	0.76 *a*	0.51 *a*	0.36 *a*
H					0.80 *ab*	0.76 *a*	0.51 *a*	0.31 *a*	0.82 *a*	0.74 *a*	0.47 *a*	0.67 *a*	0.82 *a*	0.76 *a*	0.50 *a*	0.42 *a*
I					0.82 *a*	0.76 *a*	0.52 *a*	0.41 *a*	0.82 *a*	0.77 *a*	0.51 *a*	0.41 *a*	0.82 *a*	0.76 *a*	0.50 *a*	0.51 *a*
O					0.81 *a*	0.72 *a*	0.52 *a*	0.36 *a*	0.82 *a*	0.77 *a*	0.52 *a*	0.33 *a*	0.83 *a*	0.75 *a*	0.49 *a*	0.59 *a*
P					0.80 *ab*	0.75 *a*	0.49 *a*	0.38 *a*	0.81 *a*	0.74 *a*	0.49 *a*	0.42 *a*	0.81 *a*	0.73 *a*	0.48 *a*	0.54 *a*

150 mM NaCl

	No Biostimulant				***0.001 mM***				***0.01 mM***				***0.1 mM***			
	F_v/F_m	F'_v/F'_m	ΦPSII	NPQ	F_v/F_m	F'_v/F'_m	ΦPSII	NPQ	F_v/F_m	F'_v/F'_m	ΦPSII	NPQ	F_v/F_m	F'_v/F'_m	ΦPSII	NPQ
A	0.79 *a*	0.72 *a*	0.50 *a*	0.48 *a*	0.78 *a*	0.72 *a*	0.54 *a*	0.39 *a*	0.78 *a*	0.7 *a*	0.51 *a*	0.49 *a*	0.78 *a*	0.70 *a*	0.48 *a*	0.55 *a*
B					0.78 *a*	0.70 *a*	0.49 *a*	0.56 *a*	0.78 *a*	0.71 *a*	0.50 *a*	0.52 *a*	0.79 *a*	0.71 *a*	0.50 *a*	0.48 *a*
C					0.78 *a*	0.72 *a*	0.49 *a*	0.39 *a*	0.76 *a*	0.69 *a*	0.50 *a*	0.42 *a*	0.77 *a*	0.72 *a*	0.49 *a*	0.32 *a*
D					0.78 *a*	0.72 *a*	0.52 *a*	0.41 *a*	0.77 *a*	0.71 *a*	0.55 *a*	0.42 *a*	0.78 *a*	0.71 *a*	0.49 *a*	0.46 *a*
E					0.79 *a*	0.73 *a*	0.50 *a*	0.35 *a*	0.78 *a*	0.71 *a*	0.49 *a*	0.49 *a*	0.79 *a*	0.71 *a*	0.50 *a*	0.55 *a*
F					0.78 *a*	0.72 *a*	0.51 *a*	0.43 *a*	0.73 *a*	0.71 *a*	0.50 *a*	0.45 *a*	0.79 *a*	0.71 *a*	0.51 *a*	0.55 *a*
G	0.79 *b*	0.74 *a*	0.54 *a*	0.32 *a*	0.78 *b*	0.72 *a*	0.50 *a*	0.40 *a*	0.78 *b*	0.72 *a*	0.51 *a*	0.40 *a*	0.78 *b*	0.71 *a*	0.50 *a*	0.41 *a*
H					0.78 *b*	0.73 *a*	0.52 *a*	0.37 *a*	0.79 *b*	0.73 *a*	0.52 *a*	0.35 *a*	0.78 *b*	0.72 *a*	0.50 *a*	0.42 *a*
I					0.78 *b*	0.74 *a*	0.53 *a*	0.27 *a*	0.78 *b*	0.73 *a*	0.51 *a*	0.36 *a*	0.79 *b*	0.74 *a*	0.53 *a*	0.46 *a*
O					0.81 *a*	0.75 *a*	0.51 *a*	0.40 *a*	0.78 *b*	0.72 *a*	0.50 *a*	0.37 *a*	0.78 *b*	0.73 *a*	0.52 *a*	0.34 *a*
P					-	-	-	-	-	-	-	-	-	-	-	-

3. Chapter 3

Mature crops – In-planta lettuce and tomato trials

The final part of our project focused on the evaluation of the mode of action of PH-based biostimulants on morpho-physiological traits of mature crops. We selected two species, lettuce – a leafy crop – and tomato – a fruit crop, extremely different in their growth patterns, commercial purpose and reaction to abiotic stresses.

Preliminary trials were performed on lettuce and tomato plants grown in control conditions and subjected to drought stress and salt stress, in order to create a protocol for the cultivation and the phenotyping of the two species in the given conditions.

In a second part of the work, selected cultivars of lettuce and tomato were subjected to salinity stress. 7 biostimulants out of the original 11, selected for their performances from the in-vitro assay (**Chapter 2**), were applied weekly as foliar spray. The mode of action of each of them was then evaluated by using the PBC index and by performing non-targeted metabolomic analysis on the harvested tissue.

3.1 Drought stress

3.1.1 Lettuce

Lettuce reaction to drought stress: automated high-throughput phenotyping of plant growth and photosynthetic performance

M. Sorrentino[1,2,a], G. Colla[3,b], Y. Rouphael[2], K. Panzarová[1,c] and M. Trtílek[1]

Published in **Acta Horticulturae**. 133–142 (2020)

Lettuce reaction to drought stress: automated high-throughput phenotyping of plant growth and photosynthetic performance

M. Sorrentino[1,3], G. Colla[2], Y. Rouphael[3], K. Panzarová[1], M. Trtílek[1]

[1]PSI (Photon System Instruments), spol. s r.o, Drasov, Czech Republic; [2]Department of Agriculture and Forest Sciences, University of Tuscia, via San Camillo De Lellis snc, 01100 Viterbo, Italy; [3]Department of Agricultural Sciences, University of Naples Federico II, 80055 Portici, Italy.

Keywords: *Lactuca sativa* L., Salanova, high-throughtput phenotyping, mild-drought stress

Abstract

The unavailability of fresh water is one of the main concerns for horticulture nowadays and it is supposed to get worse in the next future. Some crops are more vulnerable than others to drought stress such as leafy vegetables. It is therefore essential to identify and select varieties that can overcome this kind of abiotic stress with limited or no substantial reduction in final yield, and to do it in a fast and effective way. High throughput phenotyping combined with advances in genome sequences provide efficient and reproducible approaches that are facilitating the discovery of genes and varieties with improved plant performance under sub-optimal conditions. Drought resistance of two different Salanova® cultivars, Aquino (green butterhead) and Barlach (red butterhead), was tested, by using PlantScreenTM, a high-throughput non-invasive imaging platform developed at Photon Systems Instruments (PSI, Czech Republic). The two cultivars performed similarly in both control (70% soil water content) and mild drought stress conditions (40% soil water content). The results demonstrated that Aquino grew faster in control conditions at early growth phase, while in later phase it is the red Barlach that reached larger biomass. In drought conditions growth performance of both cultivars was rapidly compromised. However, Barlach cultivar grew better and had improved biomass in both control and mild-drought stress conditions in comparison with Aquino cultivar. Light curve protocol was used to address light use efficiency of the two cultivars. Interestingly, we observed a rapid decline in PS II operating efficiency

already three days upon mild drought stress initiation. Nevertheless, there was no obvious difference in the performances between the two cultivars. In conclusion, the results of quantitative analysis of plant growth and photosynthetic performance, allowed to set up a protocol for high-throughput image-based analysis of different morpho-physiological traits associated with the early phase of drought response.

INTRODUCTION

In nature, water is usually the most limiting factor for plant growth. A plant responds to a lack of water by halting growth and reducing photosynthesis and other plant processes in order to reduce water use (Khan et al., 2015). Lettuce is a leaf-edible vegetable that shows extreme sensitivity to drought due to shallow root system and high-water content. Furthermore, as a leafy green crop consisting of 95% to 97% water that depends on high soil water potential to maintain cell turgor for palatability, lettuce production could continue to face costly yield losses as water supplies continue to diminish. Lettuce is broadly grown also hydroponically (Barbosa et al., 2015); however, range of disadvantages are reported as e.g. high initial costs (Aires, 2018). Furthermore, organic greenhouse production in European Union, bans hydroponic production and allows organic cultivation only in soil (Gomiero, 2018). Improving lettuce tolerance to low water conditions in conventional soil cultivation is thus becoming a priority (Eriksen et al., 2016), since hydroponics is still not the ideal alternative. Breeders' efforts are focused on minimizing the gap between yield potential and yield under stress (Cattivelli et al., 2008) through the screening of new, more robust cultivars. Traditional plant phenotyping tools, which rely on manual measurement of selected traits from a small sample of plants, have very limited throughput and therefore prevent comprehensive analysis of traits within a single plant and across cultivars (Furbank and Tester, 2011). On the contrary, high-throughput integrative phenotyping facilities provide an opportunity to combine various methods of automated, simultaneous, non-destructive analyses of plant growth, morphology and physiology, providing a complex picture of the plant growth and vigour in one run, and repeatedly during the plant's life-span (Humplik et al., 2015). Automated phenotyping approaches provide tools for effective quantitative estimation of the genetic variability of yield, biomass accumulation and underlying processes in a variety of environmental scenarios (Tardieu et al., 2017). Here we used non-destructive imaged-based phenotyping technology to screen for mild-drought stress resistance of two different Salanova® cultivars, Aquino (green butterhead) and Barlach (red butterhead). We optimized the protocol to evaluate plant growth, color and photosynthetic traits by using PlantScreen^{TM}System, a high-throughput non-invasive imaging platform developed at Photon Systems Instruments (PSI, Czech Republic).

MATERIALS AND METHODS

Plant material, growth conditions and treatments

The trial was carried out in the PSI Research Center (Drasov, Czech Republic). The seeds of two cultivars of *Lactuca sativa* L. var. *capitata* (Salanova® Aquino and Barlach) were sown in 250 mL-pots filled in with Klassman 2 substrate. The seeds were cultivated in Walk-in FytoScope chamber (PSI, Czech Republic) at 23 °C Day and 19 °C night, 60% relative humidity and 12 h light-12 h dark regime (250 □mol m^{-2} s^{-1} white light, 5.5 □mol m^{-2} s^{-1} far-red light). Plants were watered every second day using the Weighing and Watering station of PlantScreen™ Compact System. The experiment was designed as a combination of two different watering regimes. 18 DAS (days after sowing), plants were divided into control plants (70% of soil water content (control, C)) and mild-drought stressed plants (40% of soil water content (drought, D)). Plants were arranged in blocks in a randomized design with 14 plants per each cultivar and treatment.

High-throughput phenotyping

All the plants were automatically phenotyped every second day in PlantScreen™ Compact System (PSI, Czech Republic) for a period of 36 days, starting from the 11th day after sowing (DAS; referred to as 1st day of phenotyping (1 DoPh)) until 47 DAS (36 DoPh). Phenotyping protocol consisted of kinetic chlorophyll fluorescence (ChlF) imaging measurement for photosynthetic performance analysis and top view Red Green Blue (RGB) imaging for color, morphological and growth analysis, as described in Awlia et al. (2016). Plants were randomized in trays that were manually loaded into the PlantScreen™ Compact System. Trays on conveyor belts were transported within PlantScreen™ from dark/light acclimation chamber towards the individual light-isolated imaging cabinets and watering and weighing unit by a moving belt toward individual imaging and handling units. The phenotyping protocol was programmed to always start at the same time of the diurnal cycle. A single round of measuring consisted of an initial 15 min dark-adaptation period inside the acclimation chamber, followed by ChlF and RGB imaging, weighing and watering. Kinetic chlorophyll fluorescence (ChlF) measurements were acquired using an enhanced version of the FluorCam FC-800MF pulse amplitude modulated (PAM) chlorophyll fluorometer (PSI, Czech Republic) (Awlia et al., 2016). Photosynthetic performance in the plants was assessed by quantifying the rate of photosynthesis at different photon irradiances using the light curve protocol as described in Paul et al. (2019). Plant specific pixels and color were derived from RGB images and range of fluorescence parameters characterizing plant photosynthetic performance were calculated from the measured fluorescence transient states by ChlF imaging (Awlia et al., 2016). The PlantScreen™

Analyzer software (PSI, Czech Republic) was used to automatically process the raw data. At 32 DoPh (day of phenotyping), fresh and dry mass per plant were determined.

Statistical analysis

The statistical analysis of the experimental data was performed using one-way analysis of variance (ANOVA) with post hoc Tukey's Honest Significant Difference (HSD) test (P-value < 0.05), in an open-source online platform for multivariate analysis based on R, MVApp, which allows interactive data curation, in-depth data analysis and customized visualization.

Results and discussion

Visible RGB imaging to assess the effect of mild-drought stress on plant growth dynamics

Visible RGB digital color imaging was used for the assessment of range of visual traits as growth status and color properties (data not shown) in control plants and plants subjected to mild-drought stress (Fig.1A). As shown in figure 2 projected top area measured as number of plant specific pixels is rapidly reduced in both cultivars as consequence of mild-drought stress. Barlach and Aquino cultivars performed similarly in both control and stress conditions, however it seemed that Barlach (Fig.2B) is significantly more sensitive to mild-drought stress conditions as the growth reduced in stress variant earlier then in Aquino. However, at the end of the trial Barlach plants reached higher area values than Aquino ones and the trend was observed for both control and stress conditions (Table 1). The image-based data were in agreement with destructive plant biomass assessment by fresh and dry weight analysis showing reduction of 30-40% at the end of the experiment (data not shown). We further calculated plant water concentration (PWC) according to the equation of Gonzalez and Gonzalez-Vilar (2003) and could show that by end of the phenotyping PWC was significantly higher for Barlach than Aquino in both watering regimes (sub-Fig. 2B).

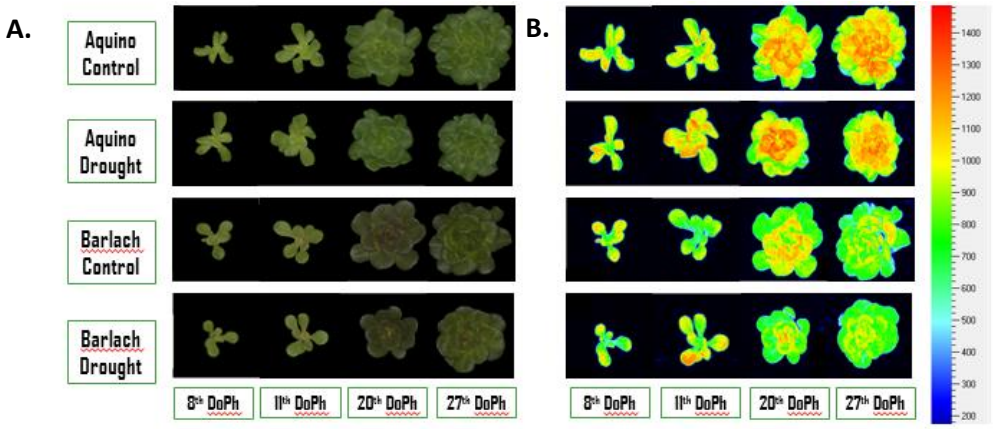

Figure 1| *RGB images and ChlF images for control and mild-drought stressed lettuce plants prior and upon the application of the two different watering regimes. A) Color segmented top view Red Green Blue (RGB) images. B) False-color images of maximum fluorescence values in dark-adapted state (Fm). DoPh refers to Day of Phenotyping.*

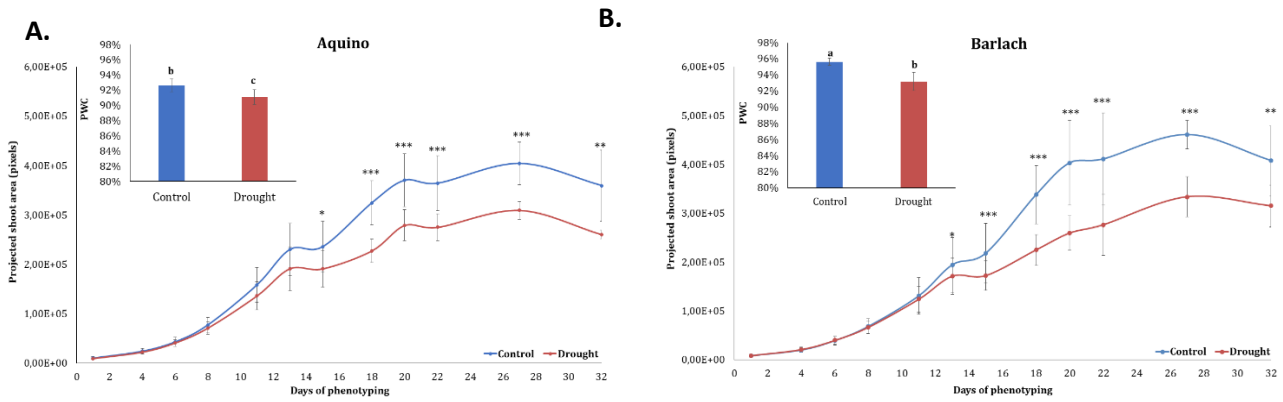

Figure 2| Growth performance of lettuce plants. *Projected top view area over time for Aquino (A) and Barlach (B) lettuce plants grown in control (blue) and mild-drought stress (red) conditions. The values represent average of 14 biological replicates per cultivar and treatment. Error bars represent standard deviation. Significant differences are indicated: * (P<0.05), ** (P<0.01), *** (P<0.001). In the sub-figures, plant water concentration of Aquino (A) and Barlach (B) lettuce plants grown in control (blue) and mild-drought stress (red) conditions. Significant differences (P<0.05) are indicated by different letters; groups that share a common letter do not have significantly different means.*

Table 1| *Values of projected top view area over time for 'Aquino' and 'Barlach' lettuce plants grown in control and mild-drought stress conditions.*

		Drought	8888.3 b
ANOVA			*
4	Aquino	Control	24508.2 a
		Drought	22556.1 b
	Barlach	Control	20117.8 b
		Drought	21378.5 b
ANOVA			*
6	Aquino	Control	43326.1 a
		Drought	41126.2 a
	Barlach	Control	39363.6 a
		Drought	40190.8 a
ANOVA			NS
8	Aquino	Control	77639.4 a
		Drought	71185.1 a
	Barlach	Control	68604.7 a
		Drought	67002.8 a
ANOVA			NS
11	Aquino	Control	158852.2 a
		Drought	136529.2 a
	Barlach	Control	131022.9 a
		Drought	124267.5 a
ANOVA			NS
13	Aquino	Control	230256.8 a
		Drought	191483.0 a
	Barlach	Control	194520.3 a
		Drought	171499.1 a
ANOVA			NS
15	Aquino	Control	235942.5 a
		Drought	191348.2 b
	Barlach	Control	218515.5 a
		Drought	172673.1 b
ANOVA			*
18	Aquino	Control	324799.3 a
		Drought	227698.8 b
	Barlach	Control	338226.2 a
		Drought	216788.4 b
ANOVA			***
20	Aquino	Control	383425.2 a
		Drought	279392.8 b
	Barlach	Control	403332.5 a
		Drought	259662.5 b
ANOVA			***
22	Aquino	Control	377240.2 a
		Drought	275469.9 b
	Barlach	Control	411128.8 a
		Drought	260879.1 b
ANOVA			***
27	Aquino	Control	398501.4 b
		Drought	309904.4 c
	Barlach	Control	461070.4 a
		Drought	324628.8 c
ANOVA			***
32	Aquino	Control	423253.3 a

High-throughput Phenotyping of Photosynthetic Performance in Lettuce Plants

Results

Chlorophyll fluorescence imaging is broadly used in plant biology as rapid non-invasive measurement of Photosystem II (PSII) activity. PSII activity is very sensitive to a wide range of stimuli, therefore chlorophyll fluorescence imaging is used as rapid indicator of plant photosynthetic performance in different developmental stages, and in response to environmental changes (Murchie and Lawson, 2013). To assess the physiological status of lettuce plants treated during the growth in control and mild-drought stress conditions, we used the automated chlorophyll fluorescence imaging setup as described in Awlia et al. (2016) and quantified the rate of photosynthesis at different photon irradiances using the light curve protocol (Henley, 1993; Rascher et al., 2000). As shown in figure 3 we observed rapid decline in PS II operating efficiency upon mild drought stress initiation that was occurring prior growth reduction. When we compared the photosynthetic performance of the two cultivars, we could not observe any significant differences. Nevertheless, it seemed that in Barlach (Fig.3B) reduction of PSII efficiency occurred earlier than in Aquino (Fig. 3A) that would correlate with was faster growth reduction in Barlach stressed plants detected by RGB imaging. This could probably be linked to the higher water content of Barlach as plants can endure drought conditions by avoiding tissue dehydration, while maintaining tissue water potential as high as possible, or by tolerating low tissue water potential (Chaves et al., 2003). Water loss is mainly minimized by closing stomata; however, stomata closure reduces CO_2 absorption and thus impact on photosynthesis and plant growth (Osakabe et al., 2014).

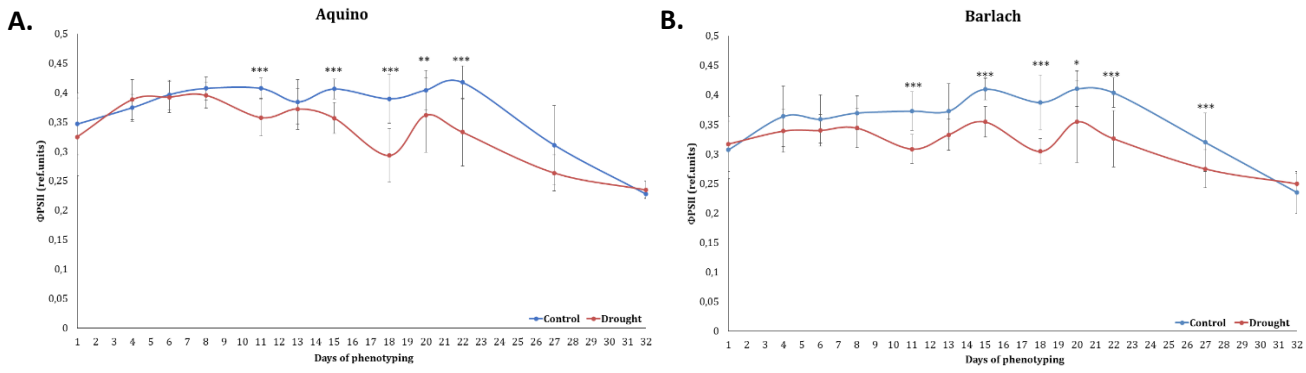

Figure 3| Photosynthetic performance of the lettuce plants. *Quantum yield of photosystem II (ΦPSII), defined as the ratio between the amount of light emitted and the amount used by the photosynthetic process, over time for Aquino (A) and Barlach (B) lettuce plants grown in control (blue) and mild-drought stress (red) conditions. The values represent average of 14 biological replicates per cultivar and treatment. Error bars represent standard deviation. Significant differences are indicated: * (P<0.05), ** (P<0.01), *** (P<0.001).*

CONCLUSIONS

In this study we show that dynamic monitoring of multiple quantitative traits by high-throughput phenotyping approach provides powerful tool for screening plant responses to mild-drought stress in two lettuce cultivars. Overall growth and photosynthetic performance were similar in both cultivars even if

at the later and final phase of the experiment Barlach cultivar grew better and had improved biomass in both control and mild-drought stress conditions. Red lettuce varieties have been characterized by a higher content of hydroxycinnamic acids, flavones, flavonols and anthocyanins compared to the green varieties of lettuce plants (Llorach et al., 2008) and it is well-known that polyphenolic compounds such as phenolic acids, flavonoids, proanthocyanidins and anthocyanins play an important role in reducing the detrimental effects of abiotic stress, such as drought and salinity (Hichem et al., 2009). Integrating thermal imaging into the pipeline together with quantification of water and transpiration use efficiency would be an important and interesting further step in more comprehensive characterization of plant performance in the limited water availability conditions.

Acknowledgements

This work was carried out at PPRC at Photon Systems Instruments (Czech Republic) and was supported by European Union's Horizon 2020 research and innovation program under the Marie Skłodowska-Curie grant agreement No 675006.

3.1. 2 Tomato part I – Control conditions

ORIGINAL RESEARCH article

Front. Plant Sci., 08 February 2019 | https://doi.org/10.3389/fpls.2019.00047

Understanding the Biostimulant Action of Vegetal-Derived Protein Hydrolysates by High-Throughput Plant Phenotyping and Metabolomics: A Case Study on Tomato

Kenny Paul[1†], Mirella Sorrentino[1†], Luigi Lucini[2], Youssef Rouphael[3], Mariateresa Cardarelli[4], Paolo Bonini[5], Hélène Reynaud[6], Renaud Canaguier[7], Martin Trtílek[1], Klára Panzarová[1*] and Giuseppe Colla[8,9*]

[1]Photon Systems Instruments (PSI, spol.sr.o.), Drásov, Czechia
[2]Department for Sustainable Food Process, Research Centre for Nutrigenomics and Proteomics, Università Cattolica del Sacro Cuore, Piacenza, Italy
[3]Department of Agricultural Sciences, University of Naples Federico II, Naples, Italy
[4]Centro di Ricerca Orticoltura e Florovivaismo, Consiglio per la Ricerca in Agricoltura e l'Analisi dell'Economia Agraria, Pontecagnano Faiano, Italy
[5]NGAlab, Tarragona, Spain
[6]Italpollina USA, Inc., Anderson, IN, United States
[7]Nixe, Valbonne, France
[8]Department of Agriculture and Forest Sciences, University of Tuscia, Viterbo, Italy
[9]Arcadia Srl, Rivoli Veronese, Italy

Understanding the Biostimulant Action of Vegetal-derived Protein Hydrolysates by High-throughput Plant Phenotyping and Metabolomics: A Case Study on Tomato

Kenny Paul[11], Mirella Sorrentino[11], Luigi Lucini[2], Youssef Rouphael[3], Mariateresa Cardarelli[4], Paolo Bonini[5], Hélène Reynaud[6], Renaud Canaguier[7], Martin Trtílek[1], Klára Panzarová[1]* and Giuseppe Colla[8,9]*

[1]Photon Systems Instruments (PSI, spol.sr.o.), Drásov, Czech Republic, [2]Department for Sustainable Food Process, Research Centre for Nutrigenomics and Proteomics, Università Cattolica del Sacro Cuore, Piacenza, Italy, [3]Department of Agricultural Sciences, University of Naples Federico II, 80055 Portici, Italy, [4]Consiglio per la Ricerca in Agricoltura e l'analisi dell'economia agraria, Centro di ricerca Orticoltura e Florovivaismo, Pontecagnano, Italy, [5]NGAlab, La Riera de Gaia, Tarragona, Spain, [6]Italpollina USA Inc., Anderson, IN 46016, United States, [7]Nixe, Les Espaces de Sophia, Valbonne, France, [8]Department of Agriculture and Forest Sciences University of Tuscia, 01100 Viterbo, Italy, [9]ARCADIA Srl, Rivoli Veronese, Italy

Abstract

Designing and developing new biostimulants is a crucial process which requires an accurate testing of the product effects on the morpho-physiological traits of plants and a deep understanding of the mechanism of action of selected products. Product screening approaches using omics technologies have been found to be more efficient and cost effective in finding new biostimulant substances. A screening protocol based on the use of high-throughput phenotyping platform for screening new vegetal-derived protein hydrolysates (PHs) for biostimulant activity followed by a metabolomic analysis to elucidate the mechanism of the most active PHs has been applied on tomato crop. Eight PHs (A-G, I) derived from enzymatic hydrolysis of seed proteins of *Leguminosae* and *Brassicaceae* species were foliarly sprayed twice during the trial. A non-ionic surfactant Triton X-100 at 0.1% was also added to the solutions before spraying. A control treatment foliarly sprayed with distilled water containing 0.1% Triton X-100 was also included. Untreated and PH-treated tomato plants were monitored regularly using high-throughput non-invasive imaging technologies. The phenotyping approach we used is based on automated

integrative analysis of photosynthetic performance, growth analysis, and color index analysis. The digital biomass of the plants sprayed with PH was generally increased. In particular, the relative growth rate and the growth performance were significantly improved by PHs A and I, respectively, compared to the untreated control plants. Kinetic chlorophyll fluorescence imaging did not allow to differentiate the photosynthetic performance of treated and untreated plants. Finally, MS-based untargeted metabolomics analysis was performed in order to characterize the functional mechanisms of selected PHs. The treatment modulated the multi-layer regulation process that involved the ethylene precursor and polyamines and affected the ROS-mediated signalling pathways. Although further investigation is needed to strengthen our findings, metabolomic data suggest that treated plants experienced a metabolic reprogramming following the application of the tested biostimulants. Nonetheless, our experimental data highlight the potential for combined use of high-throughput phenotyping and metabolomics to facilitate the screening of new substances with biostimulant properties and to provide a morpho-physiological and metabolomic gateway to the mechanisms underlying PHs action on plants.

Keywords: protein hydrolysates, integrative image-based high-throughput phenotyping, metabolomics, morpho-physiological traits, functional biostimulant characterization, ROS signalling.

INTRODUCTION

Over the past decade, interest in plant biostimulants (PBs) has been on the rise, compelled by the growing interest of researchers, private industry and farmers in integrating these products in the array of environmentally-friendly tools that secure improved crop productivity and yield stability under environmental stressor (Ertani et al., 2012, 2013; Haplern et al., 2015; Colla et al., 2017a; Yakhin et al., 2017; Rouphael et al., 2017a, b, 2018). Based on the new EU regulation, PBs are defined as '*CE marked products which stimulate plant physiological processes independently of their nutrient content by improving one or more of the following characteristics of the plant rhizosphere or phyllosphere: nutrient use efficiency, tolerance to abiotic stress, crop quality, availability of confined nutrients in the soil and rhizosphere, humification and degradation of organic compounds in the soil*' (European Commission, 2016). Protein hydrolysates (PHs) are an important category of PBs which are produced by chemical, enzymatic or by combining chemical and enzymatic hydrolysis of proteins from animal or plant source (Niculescu et al., 2009; Ertani et al., 2009, 2017; Calvo et al., 2014; Colla et al., 2015a, 2016, 2017a, b). Over the past ten years, plant-derived PHs produced through enzymatic hydrolysis have received huge interest from farmers due to their high agronomic value and the lack of limitation in their application on organically-produced crops (Colla et al., 2014; Nardi et al., 2016). PH-based biostimulants can be applied to plants through foliar application or soil/substrate drenching. PHs sprayed in foliar way reach mesophyll cells by absorption through cuticle, epidermal cells and stomata (Fernández and Eichert, 2009) while in drench application, the absorption occurs through root epidermal cells and gets redistributed through xylem (Subbarao et al., 2015). PHs can also be applied as seed treatments especially for field crops such as wheat, corn, and soybean (Rouphael et al., 2018a). PH application stimulates plant uptake of macro and micronutrients and helps in rapid plant growth and biomass accumulation, interfering with the carbon and nitrogen metabolic activities (Ertani et al., 2009, 2016; Colla et al., 2017a). PHs can also improve crop tolerance to abiotic stresses such as drought, salinity, and thermal stress (Ertani et al., 2013; Colla et al., 2017a). Therefore, improving metabolic and physiological traits by PH-based biostimulant treatments provides novel strategies for maximizing biomass yield (Dudits et al., 2016). Development of highly effective PH-based biostimulants requires an accurate evaluation of the effects of candidate products on morpho-physiological traits of selected crops during different developmental stages and environmental conditions. As conventional screening methods are time consuming, destructive (e.g., fresh and dry weight estimation), labour intensive and expensive, high-throughput plant phenotyping procedures were recently proposed as effective and high-precision tools for product screening in order to increase the probability of finding new bioactive substances in a more

cost- and time-effective manner (Povero et al., 2016; Ugena et al., 2018; Rouphael et al., 2018b). 'Phenomics' as a technological tool considers systematic management of complex traits in genome (G) × environment (E) interactions (Houle et al., 2010). Plant phenotyping systems are fully-automated robotic systems usually installed in a controlled environment or in semi-controlled greenhouse conditions. The phenotyping platforms are designed to ensure not only non-invasive monitoring of plants in throughput of few up to several hundreds of plants, but also provide means for automated cultivation and handling of the plants such as automated watering/weighing or nutrient delivery units (Fahlgren et al., 2015; Großkinsky et al., 2015). High-throughput phenotyping systems, which can capture plant growth, morphology, colour and photosynthetic performance using RGB and chlorophyll fluorescence (ChlF) imaging tools, are highly promising and essential tools for dissecting physiological components in product screening and for dynamic quantitative analysis of plant growth and physiological performance (Rahaman et al., 2015; Awlia et al., 2016; Rouphael et al., 2018b). RGB imaging is used to estimate the true color of each pixel and by using image processing algorithms for identification of plant-derived pixels. For identified plant objects, morphological and geometrical features are quantified including colour properties (Rahaman et al., 2015). The pixel number-based assessment of plant volume or total leaf area correlates with fresh and dry weight of above ground plant biomass and can be thus used to evaluate green/fresh weight of the plants without cutting and measuring them (Feher- Juhasz et al., 2014; Fahlgren et al., 2015). Further image-based automated phenotyping permits time-series measurements that are necessary to follow the progression of growth performance and stress responses on individual plants.

Chlorophyll fluorescence is a popular technique in plant physiology used for rapid non-invasive measurement of photosystem II (PSII) activity. PSII activity is very sensitive to a range of biotic and abiotic factors and therefore the chlorophyll fluorescence technique is used as a rapid indicator of photosynthetic performance of plants in different developmental stages and/or in response to changing environment (Baker, 2008). The advantage of chlorophyll fluorescence measurements over other methods for monitoring stresses is that changes in chlorophyll fluorescence kinetic parameters often occur before other effects of stress are apparent (Murchie and Lawson, 2013). Chlorophyll fluorescence imagers integrated in high-throughput phenotyping platforms are becoming important tools for rapid screening for better photosynthetic performance and characterization of a plant´s ability to harvest light energy, which is directly related to plant biomass formation and plant architecture (Tschiersch et al., 2017).

Nonetheless, the comprehension of biochemical processes and physiological functions underlying the changes observed at phenotype level is of primary relevance to scientifically demonstrate and support the use of plant biostimulants, likely providing some clues on the best scenarios where these products can be used. It is expected that in the near future, provided that a regulatory framework will be implemented at least in the EU and USA, the information on mechanism/mode(s) of action will support biostimulants authorization and implementation. In this regard, metabolomics is being proposed as a close link between an organism's genotype and phenotype (Lamichhane et al., 2018), including plant-environment interactions (Feussner et al., 2015). In fact, recent advances in metabolomics, data treatment and multi-variate statistics offer the possibility to achieve a rather inclusive phytochemical profile in biological systems, including plants, thus opening new opportunities (Meier et al., 2017; Tsugawa, 2018). This makes metabolomics a promising tool to elucidate, among others, the mode of action rather than the physiological processes involved in plant response to biostimulants.

Taking this background into consideration, the aim of this study was to unravel the morphological, physiological and biochemical mechanisms of action for protein hydrolysate-based biostimulants on tomato plants at early stage of growth (*i.e.,* vegetative growth) by combining novel high-throughput plant phenotyping approach and metabolomics. Untreated and treated tomato plants were compared in terms of photosynthetic performance through kinetic chlorophyll fluorescence, and plant growth dynamics via RGB imaging by using high-throughput and non-invasive imaging technologies developed at Photon Systems Instruments (PSI, Czech Republic). Metabolomics analysis was performed to understand the mode of action of the best performing substances in improving plant growth. Evaluation of biostimulant activity at early growth stages of fruiting crops such as tomato can provide useful information for improving crop yield under field conditions. Crop traits like early vigour are associated with earliness of fruit maturity and high shoot biomass accumulation which have been often positively linked to increased yield of tomato crop (Kumar et al., 2015; Rouphael et al. 2017c). Finally, this study was also aimed to set up a methodology for screening plant biostimulants by combining an advanced phenotyping platform and metabolomic analysis.

MATERIALS AND METHODS

Plant Material and Growing Conditions

Seeds of tomato (*Solanum lycopersicum* L. - Hybrid F1 Chicco Rosso) were sown in trays with 100 ml size of pots containing freshly sieved soil (Substrate 2, Klasmann-Deilmann GmbH, Germany) watered to full soil-water holding capacity. Trays with seeds were stratified for 2 days at 4°C in the dark. Trays were then transferred to a climate-controlled chamber (FytoScope FS_WI, PSI, Drásov, Czech Republic) with cultivation conditions set at 16 h day/8 h night regime, temperature set at 22 °C day/20 °C night, relative humidity set at 60% and light intensity set at 250 µmol photons m^{-2} s^{-1} for cool-white LED and 5.5 µmol photons m^{-2} s^{-1} for far-red LED lighting (**Figure 1A**).

Plant Handling and Biostimulant Treatment

Prior initiation of automated phenotyping protocol, tomato plants were manually watered. Seven- and 14-day-old plants were watered to full saturation with fertilizers: 1.04 g L^{-1} calcium nitrate (15.5% N; 28% CaO), 0.04 g L^{-1} ammonium nitrate (34% N), 0.14 g L^{-1} monopotassium phosphate (52% P_2O_5, 34% K_2O), 0.18 g L^{-1} potassium sulfate (50% K_2O, 45%SO_3), 0.5 g L^{-1} magnesium sulfate (10%N, 16% MgO), and 0.5 ml L^{-1} FloraMicro (5% N, 1% K_2O, 5% Ca, 0.01% B, 0.001% Cu, 0.1% Fe, 0.05% Mn, 0.0008% Mo, 0.015% Zn).

Twenty-one-day-old plants reaching third true leaf stage were transplanted into 3 L pots filled with a mixture of Substrate 2 Klasmann soil and river sand in 3:1 ratio. Pots with soil mixture were prepared one day in advance of transplantation and were automatically watered in PlantScreen™ Modular System to ensure soil moisture reaching 60% container capacity. For optimizing container capacity, one set of soil pots was dried for 3 days at 80°C and another set was saturated with water and left to drain for 1 day before weighing 100% water holding capacity (Awlia et al., 2016). Following transplantation, plants were regularly watered to defined reference weight (60% container capacity) automatically in PlantScreen™ Modular System.

Plants were randomly distributed into nine groups with six biological replicates per group. Eight types of plant-derived protein hydrolysates (A-G, I) were provided by Italpollina Company (Rivoli Veronese, Italy). PHs were obtained by the advanced technology LISIVEG which is based on enzymatic hydrolysis of seed-derived proteins from different plant sources belonging to families of *Leguminosae* and *Brassicaceae*. Total nitrogen of each PH was as follow: 5.2% (A), 4.6% (B), 3.7% (C), 4.2% (D), 4.3% (E), 4.2% (F), 4.0% (G), 5% (I). PHs (A-G) were non-commercial products whereas I was a commercial biostimulant named 'Trainer®' derived from legume seeds. All PHs were foliarly sprayed in a water solution containing a non-ionic surfactant Triton X-100 at 0.1%. A control group sprayed with

distilled water containing 0.1% Triton X-100 was also included. Foliage sprays were performed twice: 5 DAT (days after transplantation) referred to as Treatment 1 (T1) and 12 DAT referred to as Treatment 2 (T2). For 24 hours prior to and post spraying, humidity in the cultivation chamber was kept at 85% relative humidity. For foliar spray treatments, 2 ml of given PH was diluted in 500 ml distilled water with 0.1% Triton X-100 and 60 ml of solution was applied by homogenous foliar spray over the entire plant surface per plant replica. Soil of each pot was covered with aluminum foil during and upon spraying and was removed prior to the next phenotypical analysis in PlantScreen™ Modular System (**Figure 1B**). Right after foliar spray treatment, plants were taken back to FytoScope FS-WI.

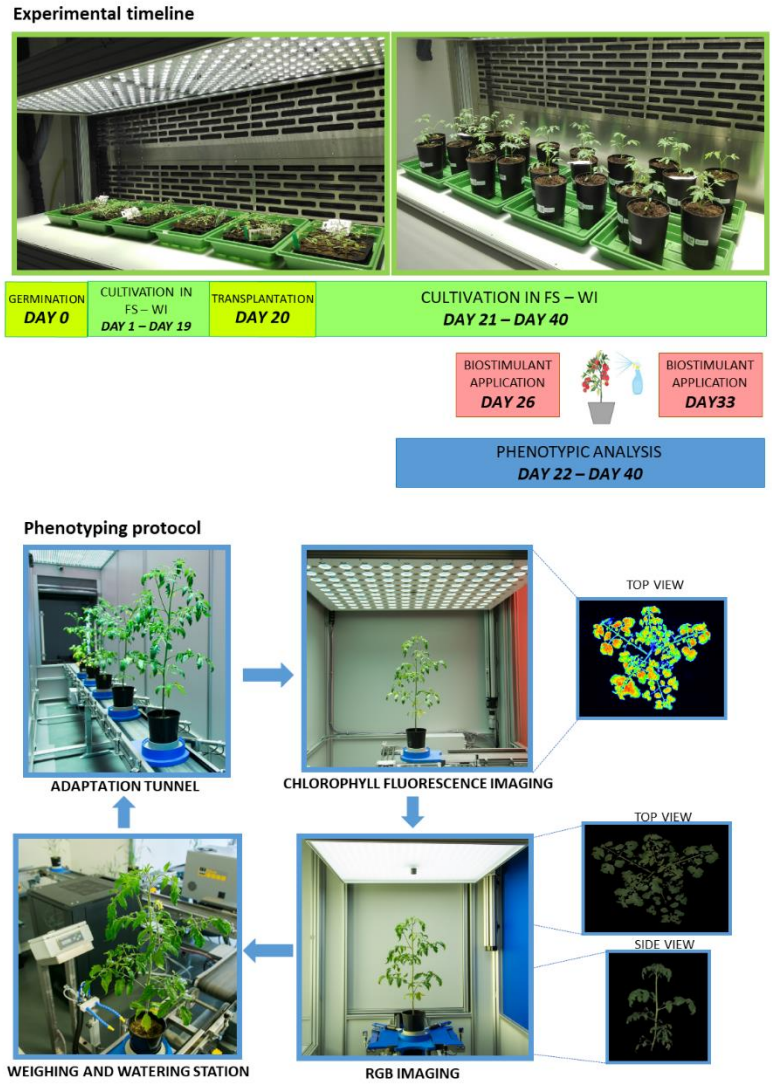

Figure 1| Schematic overview of cultivation protocol and automated phenotyping protocol. *A) Plants were cultivated for 20 days prior to transplantation in control conditions (FS-WI, PSI, Czech Republic) and were further kept in the same conditions for the next 19 days (DAT, days after transplantation). Eight types of protein hydrolysates (A-G, I) plus control treatment were applied twice to tomato plants by spraying 5 and 12 days after transplantation. Plant phenotypic measurements were performed during the experiment using PlantScreen™ Modular System installed in semi-controlled greenhouse environment conditions in PSI Research Center (PSI, Drásov, Czech Republic). B) Plant handling and automated phenotyping protocol. Tomato plants were transferred to PlantScreenTM Modular System and automated phenotyping protocol was initiated. Prior to and following the protein hydrolysates application, plants were regularly screened using the calibrated top and side view RGB camera and kinetic chlorophyll fluorescence camera for photosynthetic performance quantification. Plants were regularly watered and weighed using the automated watering and weighing station.*

Phenotyping Protocol and Imaging Sensors

Plant phenotypic measurements were performed using PlantScreen™ Modular System installed in semi-controlled greenhouse environment conditions in PSI Research Center (PSI, Drásov, Czech Republic). The platform was operated in a closed imaging loop that is within climatized environment with temperature ranging between 21-24 °C. The platform is equipped with four robotic-assisted imaging units, automatic height measuring light curtain unit, an acclimation tunnel, and a weighing and watering unit. Plants set in individual transportation disks were transported to the individual units by a moving belt toward individual imaging and handling units. Twenty-two-day-old plants were randomly distributed into six batches, each batch containing 11 plants. Plant imaging started 1 DAT (day 1 of phenotyping) and continued until 15 DAT (day 15 of phenotyping). Plants were imaged using the following protocol. Briefly, plants were manually transferred from the climate-controlled growth chamber to the manual loading station of the PlantScreen™ Modular System, transported to the acclimation tunnel through an automatic height measuring unit and dark adapted in an acclimation tunnel for 15 minutes prior to imaging. Successively, plants were automatically phenotyped for around 30 minutes per batch using kinetic chlorophyll fluorescence imaging measurement for photosynthetic performance analysis and top view and multiple angle side view Red Green Blue (RGB) imaging for morphological and growth analysis. Finally, plants were automatically transported to the watering and weighing unit for maintaining precise soil water holding capacity at 60%. After the end of the phenotyping protocol, plants were manually moved back to the climate-controlled growth chamber until the subsequent phenotyping day. Using the automatic timing function of PlantScreen™ Scheduler (PSI, Drásov, Czech Republic), the phenotyping protocol was programmed to always start at the same time of the diurnal cycle (after 3 hours of illumination in the climate-controlled growth chamber). Phenotyping protocol was recorded twice prior to biostimulant application in days 1 and 3 (pre-T measurements); three times post first biostimulant application in days 6, 8, 10 (post T1 application) and twice post second biostimulant application in days 13 and 15 (post T2 application). The acquired images were automatically processed using Plant Data Analyzer (PSI, Drásov, Czech Republic) and the raw data exported into CSV files were provided as input for further analysis.

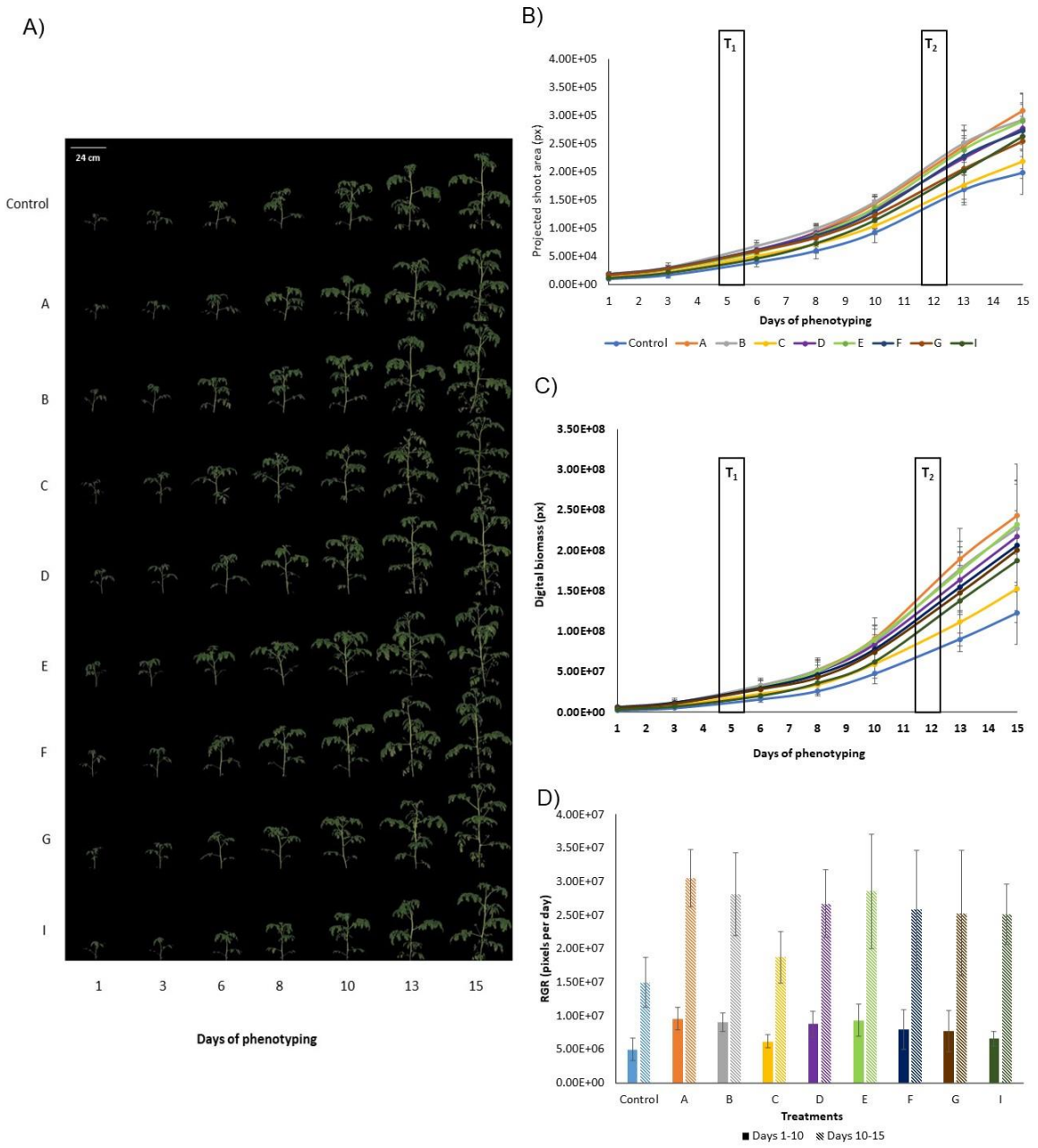

Figure 2| Color segmented side view Red Green Blue (RGB) images of tomato plants prior to and upon PHs application. *A) Side view (120°) RGB image of the tomato plants over the time of phenotyping period (D1-D15). B) Projected shoot area over time of phenotyping period. Values represent the average of six biological replicates per treatment. Error bars represent standard deviation. T1 and T2 correspond to days of protein hydrolysates application by foliar spraying. C) Digital biomass quantified over time of phenotyping period. Values represent the average of six biological replicates per treatment. Error bars represent standard deviation. T1 and T2 correspond to days of protein hydrolysates application by foliar spraying. D) Comparison of relative growth rate for the different treatments quantified over phenotyping period following the protein hydrolysate treatments (DAT 6-DAT 15). Values represent the average of six biological replicates per treatment. Error bars represent standard deviation.*

Kinetic Chlorophyll Fluorescence Imaging

Kinetic chlorophyll fluorescence (ChlF) measurements were acquired using an enhanced version of the FluorCam FC-800MF pulse amplitude modulated (PAM) chlorophyll fluorometer (PSI, Czech Republic) (Awlia et al., 2016) with an imaging area in top view position of 800 × 800 mm as described in Tschiersch et al. (2017). Photosynthetic performance in the plants was assessed by quantifying the rate of photosynthesis at different photon irradiances using the light curve protocol (Henley, 1993; Rascher et al., 2000) which was proven to provide detailed information on ChlF under stress, information on photosynthetic performance in many studies dealing with plants' stress and to quantify the rate of photosynthesis at different light irradiances (Digruber et al., 2018) (**Supplementary Figure 1**). Protocol described previously (Awlia et al., 2016) was optimized for the tomato plants from early to later developmental stage. Finally, three actinic light irradiances (Lss1- 170 µmol photons m^{-2} s^{-1}, Lss2 – 620 µmol photons m^{-2} s^{-1}, Lss3 - 1070 µmol photons m^{-2} s^{-1}) with a duration of 30 seconds in the light curve protocol were used to quantify the rate of photosynthesis.

A)

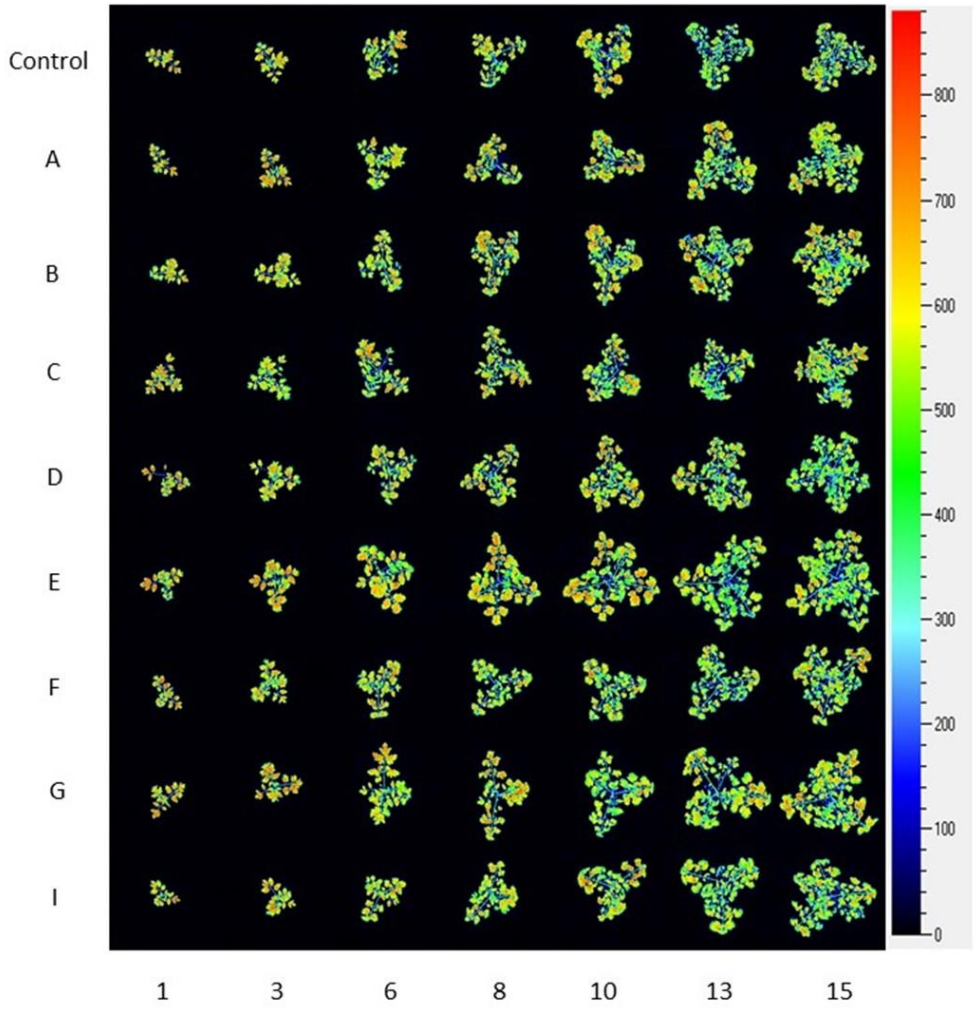

Figure 3| Photosynthetic performance of tomato plants visualized by kinetic chlorophyll fluorescence imaging in all protein hydrolysate treatments. *Representative images of chlorophyll fluorescence for tomato plants prior to and upon PHs treatment. False-color images of maximum fluorescence value (FM) for tomato plants over phenotyping period (days 1-15) are shown.*

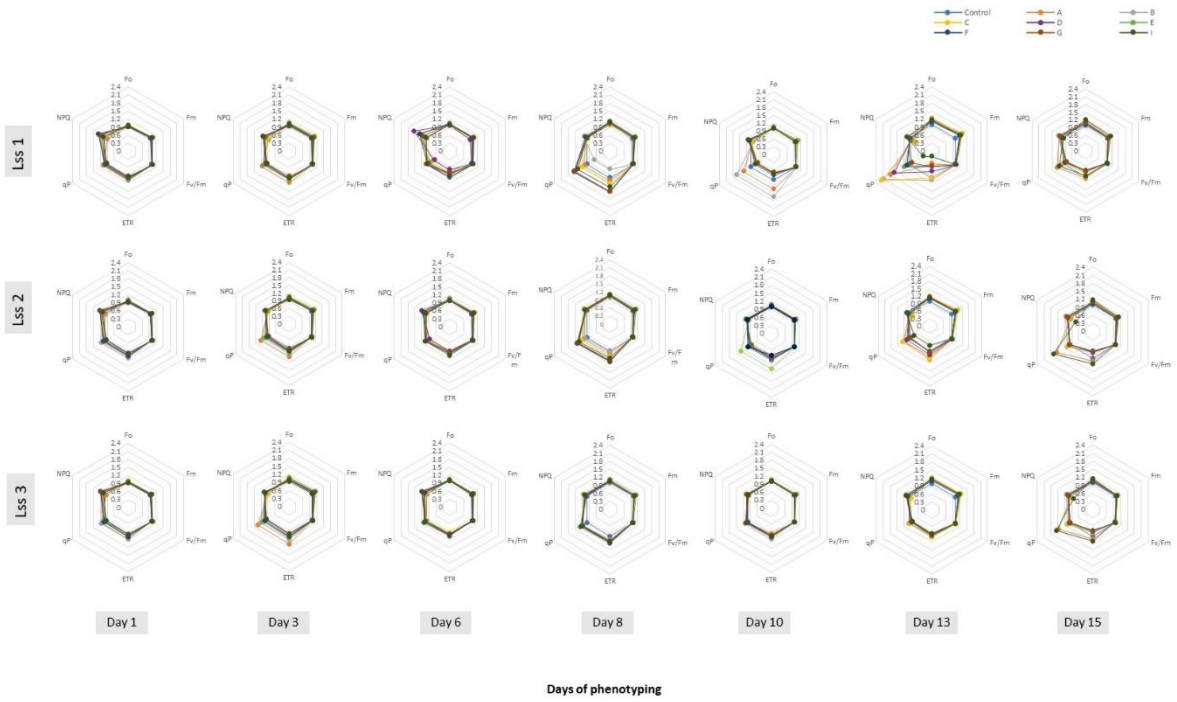

Figure 4| Spider plots of photosynthetic parameters deduced from kinetic chlorophyll fluorescence imaging on whole plant level in all treatments. *Minimal fluorescence in dark-adapted state (Fo), maximum fluorescence in dark-adapted state (Fm), maximum quantum yield of PSII photochemistry for the light-adapted state (Fv´/Fm´), the photochemical quenching coefficient that estimates the fraction of open PSII reaction centers (qP), steady-state non-photochemical quenching (NPQ) and electron transport rate (ETR) were measured using the light curve protocol for tomato plants prior to and upon PHs treatments. The data are shown for the protein hydrolysate treated plants after normalization to respective values obtained in the control treatment at various time points of phenotyping period. Data are mean of six independent plants per treatment. Lss1, Lss2 and Lss3 represent actinic photon irradiance measurements taken at 170, 620 and 1070 µmol photons m-2s-1, respectively.*

Visible RGB Imaging

To assess digital biomass of the plants, RGB imaging was done from top view (RGB2) and side view from multiple angles (RGB1) (**Supplementary Figure 2**). The RGB imaging unit implemented in PlantScreen^{TM} Modular System is a light isolated box equipped with a turning table with precise angle positioning, two RGB cameras (top and side) mounted on robotic arms and each supplemented with LED-based lighting source to ensure homogenous illumination of the imaged object. Imaged area in top view position is 800 × 800 mm, imaged area from side view is 1205 mm × 1005 mm (height × width). Here we acquired side view images from three different angles (0°, 120°, 240°) for side view RGB analysis. RGB images (resolution 2560 × 1920 pixels) of the plants were captured using the GigE uEye UI-5580SE-C - 5 Megapixels QSXGA Camera with 1/2" CMOS Sensor (IDS, Germany) from top and side view. For side view projections, line scan mode was used with a resolution –2560 × 2956 px/scan, 200 lines per second. Lighting conditions, plant positioning and camera settings were fixed throughout

the experiment. Raw RGB images were processed as described previously (Awlia et al., 2016) with some modifications for side view RGB image processing algorithms. Projected shoot area (PSA) for side view was calculated as average of plant specific pixels extracted from three side view images acquired from 0°, 120° and 240° angles. PSA extracted from top and side view projections was used to estimate shoot biomass. Briefly side view and top view RGB images of the plants were used for calculation of plant volume, using the formula from Klukas et al. (2014):

$$V = \sqrt{A_{s\,(average)}^2 \; x \; A_t^2}$$

where A_s and A_t are the projected areas from side-view (at different angles) and top-view images, respectively. Volume was termed as "digital biomass," as reported in a work from Rahaman et al. (2017). Digital biomass was used to calculate relative growth rate (RGR) between two timepoints T_1 and T_2 as follows:

$$RGR = (\ln W_2 - \ln W_1)/(T_2 - T_1)$$

In addition, height and width of the plants were calculated from the binary side view images. For shoot greenness evaluation, six hues of green were automatically generated using as input images all the original RGB images captured during the phenotyping period (DAT1 – DAT15). These six most representative hues were selected and used to estimate the variations in shoot colors and are shown in RGB color scale as a percentage of the shoot area (pixel counts).

Sample Harvest

Ninteen DAT (19th day of phenotyping) plant material was harvested. For metabolomic analysis of tomato plants treated with biostimulants A, B, I and control plants third and fourth fully expanded leaves from the top of each plant were harvested. The non-commercial biostimulants A and B were selected for the metabolomic analysis based on the higher morpho-physiological traits and were compared to the commercial biostimulant (I) as well as to the untreated control treatment. Final biomass of each plant was determined by measuring fresh weight and dry weight of remaining shoot in a ventilated oven at 65°C until constant weight.

Untargeted Metabolomics

Leaf samples (1.0 g) were extracted using an Ultra-Turrax (Ika T-25, Staufen, Germany), in 10 mL of 0.1% HCOOH in 80% aqueous methanol. The extracts were centrifuged (12000 × *g*), then filtered through a 0.22 µm cellulose membrane directly into amber vials for analysis. Thereafter, untargeted metabolomics were carried out through an UHPLC chromatographic system coupled to a hybrid quadrupole-time-of-flight mass spectrometer (UHPLC/QTOF-MS). The metabolomic platform included a 1290 ultra-high-performance liquid chromatograph, a G6550 iFunnel Q-TOF mass spectrometer and a JetStream Dual Electrospray ionization source (all from Agilent technologies, Santa Clara, CA, USA). The analysis was carried out as previously described (Rouphael et al., 2016). Briefly, chromatographic separation was achieved in reverse phase mode, using an Agilent Zorbax Eclipse-plus C18 column (100 × 2.1 mm, 1.8 µm) and a linear gradient (5% to 95% methanol in water, 34 min run time) foe elution, with a flow of 220 µL min^{-1} at 35°C. The mass spectrometric acquisition was done in positive polarity and extended linear dynamic range SCAN (100–1000 *m/z*).

Features deconvolution and post-acquisition processing were done in Agilent Profinder B.06. After mass and retention time alignment, compounds annotation was achieved using the 'find-by-formula' algorithm based on monoisotopic accurate mass, isotopes spacing and isotopes ratio, with a mass accuracy tolerance of < 5 ppm. The database PlantCyc 12.5 (Plant Metabolic Network, http://www.plantcyc.org; released April 2018) was used for annotation purposes. Based on the strategy adopted, identification was carried out according to Level 2 (putatively annotated compounds) of COSMOS Metabolomics Standards Initiative (http://cosmos-fp7.eu/msi).

A filter-by-frequency post-processing filter was applied to retain only those compounds that were present in 75% of replications within at least one treatment. The classification of differential compounds into biochemical classes was carried following PubChem (NCBI, https://pubchem.ncbi.nlm.nih.gov/) and PlantCyc information.

Data Management and Statistical Analysis

The data processing pipelines Plant Data Analyser (PSI, Drásov, Czech Republic) includes pre-processing, segmentation, feature extraction and post-processing. Values for projected shoot area were calculated from images taken in the visible light spectrum and correspond to volume estimation which were used as a proxy for the estimated biomass of the plants. Data were processed using MVApp application (mmjulkowska/MVApp: MVApp.pre-release_v2.0; Julkowska et al. unpublished). Using the

MVApp, outliers were identified with the interquartile range rule as plants whose volume had a value 1.5 times away from the mean. Those plants were removed from the data set. Statistical differences between treatments and time points were determined by one-way analysis of variance (ANOVA) with *post hoc* Tukey's Honest Significant Difference (HSD) test (P-value < 0.05) performed using appropriate scripts in MVApp tool. Data are displayed as mean ± standard deviation of the six independent plants per treatment.

Interpretation of metabolomic data was formerly carried out using Mass Profiler Professional B.12.06 as previously described (Salehi et al., 2018). Briefly, compound abundance was Log2 transformed and normalized at the 75th percentile and baselined against the median. Unsupervised hierarchical cluster analysis was formerly carried out using the fold-change based heatmap, setting similarity measure as 'Euclidean' and 'Wards' linkage rule. Thereafter, the dataset was exported in SIMCA 13 (Umetrics, Malmo, Sweden), UV-scaled and elaborated for Orthogonal Projections to Latent Structures Discriminant Analysis (OPLS-DA) modeling. This latter multivariate supervised statistic allowed separating variance into predictive and orthogonal (i.e., ascribable to technical and biological variation) components. Outliers were excluded using Hotelling's T2 and adopting 95% and 99% confidence limits, for suspect and strong outliers, respectively. Model cross validation was done through CV-ANOVA (p< 0.01) and permutation testing (N=300) was used to exclude overfitting. Model parameters (goodness-of-fit R^2Y and goodness-of-prediction Q^2Y) were also produced. Finally, Variable Importance in Projection (VIP) analysis was used to select the metabolites having the highest discrimination potential. A subsequent fold-change analysis was performed from VIPs to identify extent and direction of the changes in accumulation related to the biostimulants.

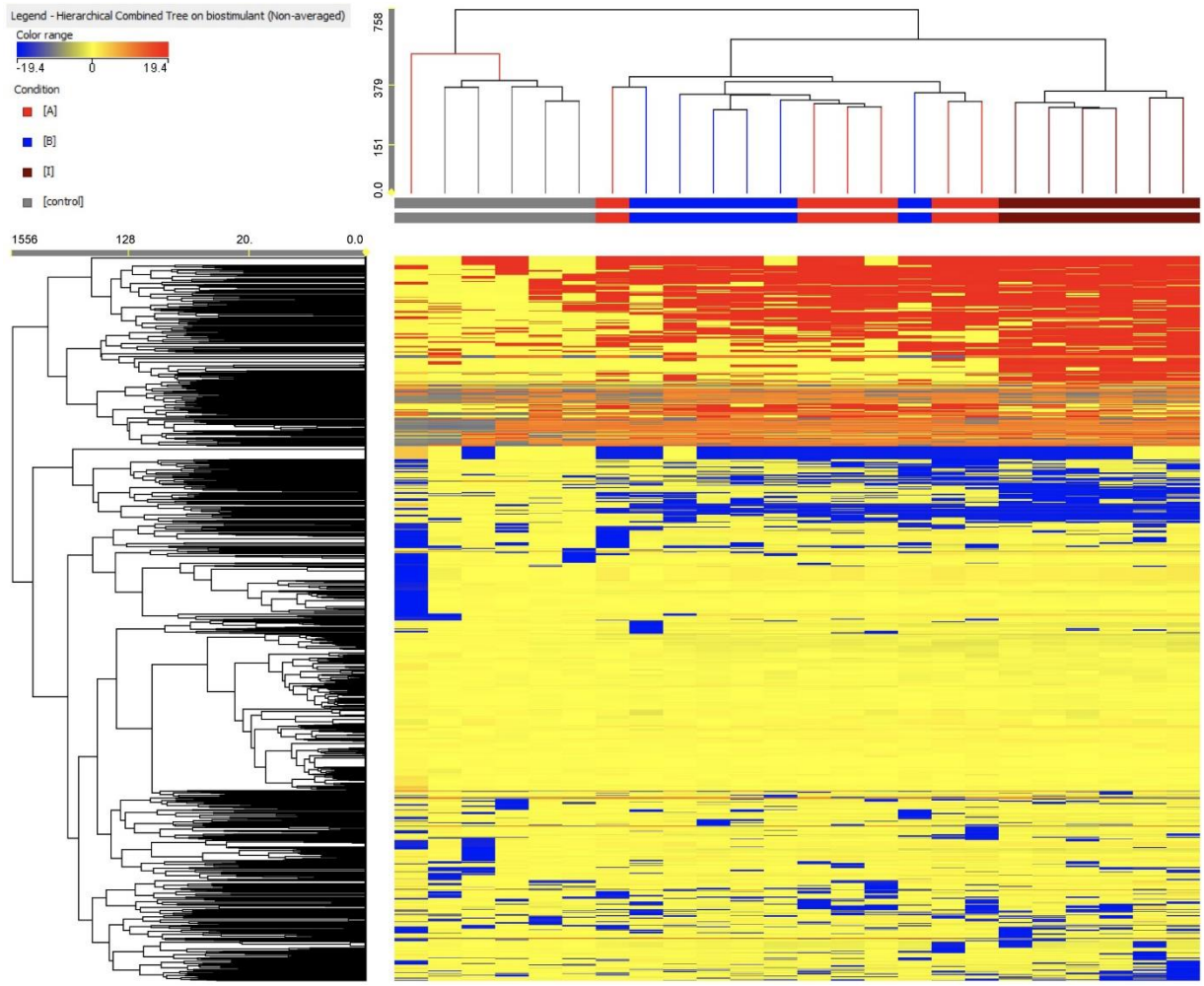

Figure 5| Unsupervised hierarchical cluster analysis carried out from metabolomic profiles following application of selected protein hydrolysates. *Dendrograms were produced on the basis of fold-change heat-maps using metabolites profile gained from UHPLC-ESI/QTOF untargeted metabolomic profiling. The Wards' linkage rule and Euclidean similarity were chosen to produce dendrograms.*

RESULTS AND DISCUSSION

High-Throughput Phenotyping of Tomato Plant Growth

Visible light Red Green Blue (RGB) digital imaging based on using cameras sensitive in visible spectral range (400 – 750 nm) allows non-invasive dynamic quantification of shoot biomass, measurement of a wide range of plant morphological parameters and analysis of shoot colour. Multiple angle side view images (**Figure 2, Supplementary Figure 2**) and simple image stacks acquired from top view were used to calculate plant volume that is an approximate of digital biomass of the plants throughout the cultivation

period. Regularly acquired multiple time points measurements were used to asses dynamic changes in plant morphology, colour and calculate growth rates.

In general, tomato plants treated with PHs showed better shoot biomass production in comparison with the untreated control plants (**Figure 2**). Top view projected shoot area was increased in tomato plants treated with PHs A and E post first foliar treatment (**Supplementary Table 1**). For A treatment this correlated with PSA extracted from multiple angle side view RGB images (**Supplementary Table 2**) with B treatment improving the PSA in period between the two foliar treatments. In terms of morphological features extracted from both top and side view images such as compactness, height and width of the plants, treatments A, B, D, E and F gave an increase of height and width of plants (**Supplementary Tables 3 and 4**). The digital biomass of the plants sprayed with PHs increased (**Figure 2C**), especially in the case of A treatment where the improved growth performance was significantly compared to untreated control plants from the eighth day of phenotyping, three days post first foliar spraying, respectively (**Supplementary Tables 5**). The same trend was recorded when the growth dynamics was considered by evaluating plant growth rates. We quantified relative growth rates from DAT6 – DAT15 representing growth performance of the plants following the two PH treatments that were applied on DAT5 and DAT12 (**Figure 2D**). For A, E and I treatment, growth rates were improved when compared to control plants, however the effect of A and E treatment could not be discriminated from the effects of the other PHs. Interestingly, the treatment I was identified as the one with highest growth rate among all PHs. Overall, among all treatments, the best growth performance trend in terms of biomass and growth rate was observed for tomato plants treated with treatment A, whereas tomato plants treated with PH named C were smaller with slower growth dynamics. This further correlated with analysis of dry and fresh weights of tomato shoots that were harvested following the end of the phenotyping period (r=0.87* and 0.85* for fresh and dry weight, respectively).

We further evaluated the variation in shoot green colours over the phenotyping period by using greenness hue abundance automatically computed from colour-segmented RGB images (**Supplementary Figure 3**). We calibrated the analysis algorithms by using RGB images from all treatments and all days of phenotyping as described previously in Awlia et al. (2016). Dynamic changes in green hues during the plant growth were observed, however no significant differences in the green hues were detected between the treatments (**Supplementary Table 6**).

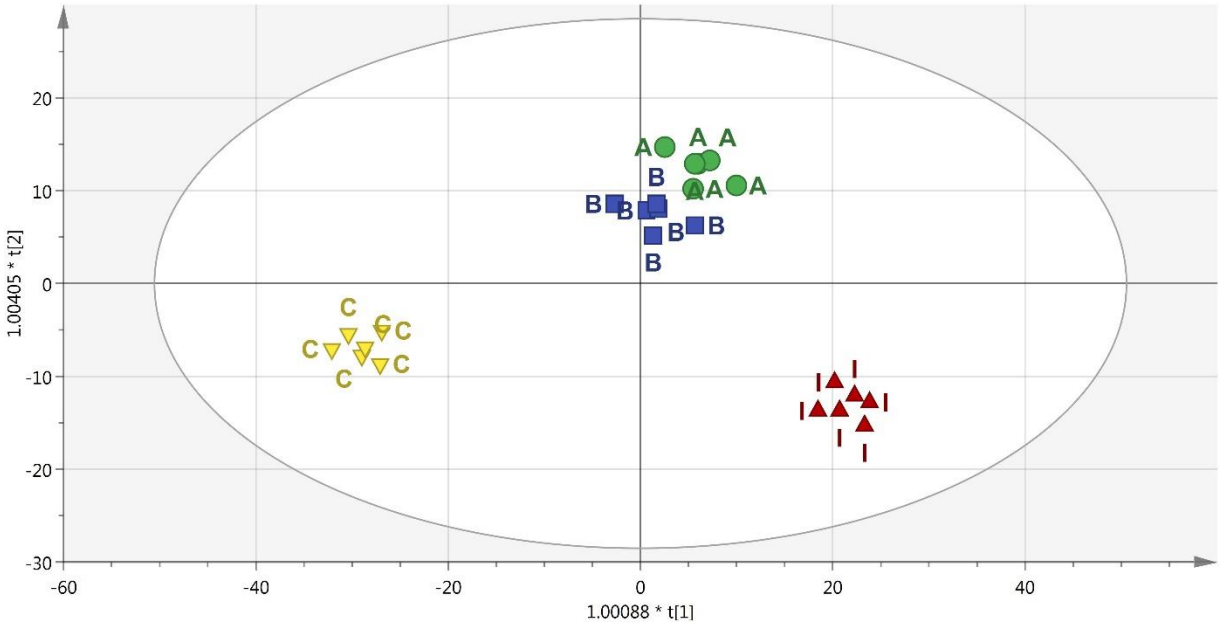

Figure 6| Score plot of Orthogonal Projection to Latent Structures Discriminant Analysis (OPLS-DA) supervised modeling carried out on metabolomic profiles following application of selected protein hydrolysates. *The variation between groups was separated into predictive and orthogonal components (i.e., that ascribable to technical and biological variation). The OPLS model was cross-validated using CV-ANOVA ($p < 0.01$) and permutation tested to exclude over fitting. Furthermore, the presence of outliers was investigated according to Hotelling's T2 method (i.e., the distance from the origin in the model) using 95% and 99% confidence limits for "suspect" and "strong" outliers, respectively. The pattern observed in the score plot was used to identify discriminant compounds based on Variable of Importance in projection (VIP) analysis.*

High-Throughput Phenotyping of Photosynthetic Performance in Tomato Plants

Chlorophyll fluorescence imaging has become one of the most powerful and popular tools in plant biology for rapid non-invasive measurement of Photosystem II (PSII) activity. Because PSII activity is very sensitive to a wide range of stimuli, chlorophyll fluorescence imaging can be used as rapid indicator of plant photosynthetic performance in different developmental stages, and in response to environmental changes (Murchie and Lawson, 2013).

To assess the physiological status of tomato plants treated with the biostimulants, we used the automated chlorophyll fluorescence imaging setup (**Figure 3, Supplementary Figure 1**) and quantified the rate of photosynthesis at different photon irradiances using the light curve protocol (Henley, 1993; Rascher et al., 2000). From the measured fluorescence transient states, the basic ChlF parameters were derived (i.e., F_o, F_m, F_t, F_v), which were used to calculate range of parameters characterizing plant photosynthetic performance (i.e., F_v'/F_m', NPQ, qP, ΦPSII) (for overview refer to Paul et al., 2011; Awlia et al., 2016; Tschiersch et al., 2017). In addition, ETR parameter was calculated which refers to

photosynthetic electron transport rate of photosystem II and indicates the efficiency of linear electron flow route in the photosynthetic machinery for producing energy rich molecules ATP and NADPH.

We selected six of the parameters to characterize dynamically photosynthetic function of PSII in the tomato plants prior to and post biostimulant treatment: the minimal level of fluorescence measured in dark-adapted state (F_o), the maximum level of fluorescence measured in dark-adapted state (F_m), the maximum quantum yield of PSII photochemistry in the light-adapted state (F_v'/F_m'), the photochemical quenching coefficient that estimates the fraction of open PSII reaction centers (qP), steady-state non-photochemical quenching (NPQ) and PS II operating efficiency (ΦPSII) used for calculation of electron transport rate (ETR). ETR is a process correlated to the quantum yield of the CO_2 assimilation mechanisms and to the overall photosynthetic capacity of the plants (Genty et al., 1989). As shown in **Figure 4**, the selected fluorescence parameters varied partially between the individual days following the PH treatment, however we could not observe any trend among the treatments. In addition, we were not able to detect any significant changes in the ChlF parameters assessed (**Supplementary Table 7**). This was the case for all treatments at any photon irradiances used.

Kinetic chlorophyll fluorescence imaging used for non-invasive quantitative analysis of PSII fluorescence emission is especially suited to monitor physiological traits via changes in photochemistry. In the field of automated high-throughput phenotyping, PAM Chl fluorescence imaging is still not widely used in the imaging sensor platforms, however a range of studies already demonstrated the broad potential of the technique to measure quantitatively physiological state of the plants and to diagnose the reactions of the plants to stress even before visible symptoms become apparent (Paul et al., 2011; Awlia et al., 2016; Tschiersch et al., 2017). Biostimulants have shown to increase photosynthetic efficiency, improve the efficiency of light utilization and dissipation of excitation energy in PSII antennae as well as an increase in photosynthetic pigments (Yahkin et al., 2017). The fact that in our case the application of the PHs did not result in improved photochemistry parameters, although the biomass of the biostimulant treated plants increased, might be associated with the beneficial action of PHs on stomatal conductance rather than on the PSII directly. This might improve net CO_2 assimilation rate and consequently biomass production. Another putative mechanism involved in the stimulation of plant growth and productivity of PH-treated tomato plants could be the occurrence of smaller and more responsive stomata that are proposed to be able to sustain higher photosynthetic activities (Rouphael et al., 2017d).

Metabolomics Analysis of Tomato Leaves for Understanding the Mode of Action of Selected PHs

A metabolomic approach was used, following phenotyping analysis, aimed to strengthen at the molecular level the effects of the PHs on morpho-physiological traits and plant growth. Indeed, the understanding of the mechanisms through which PHs act on a plant can effectively support their actual implementation into agricultural practices and possibly suggest specific contexts for their optimal and profitable use. With this aim, an untargeted UHPLC/QTOF-MS analysis was performed and multi variate statistics used to point out similarities/dissimilarities among metabolomic profiles of the PH-treated plants. The combination of a high-performance untargeted profiling, together with a rather comprehensive database (PlantCyc), resulted in a large dataset (overall, almost 1600 compounds annotated). A large chemical diversity was represented within the dataset, including compounds from a wide variety of biochemical classes and metabolic processes. The whole dataset, together with individual compounds' abundance and composite mass spectra, is provided in supplementary material (**Supplementary Table 8**).

As a first step of interpretation, a fold-change based hierarchical clustering was carried out (**Figure 5**). This unsupervised approach allowed producing two main clusters, one comprising all replications from the control and another including all PH-treated samples. In this latter, two further sub-clusters were evident, with products A and B being mixed together and with treatment I representing a separate sub-cluster. This unsupervised (i.e., naïve) classification of metabolomic profiles, based on individual fold-change values for each compound annotated, suggested that the PH treatments imposed a change in the plant metabolomic profile, and that treatments A and B induced a more comparable effect whereas treatment I had a more distinctive effect.

To better identify the specific responses induced in plants following the PH treatments, a supervised OPLS-DA multivariate modelling was carried out. This discriminant analysis approach allows discriminating among groups into score plot hyperspace, by separating predictive and orthogonal components (i.e., those components ascribable to technical and biological variation) of variance. Looking at the OPLS-DA score plot (**Figure 6**), the outcome of this supervised approach was in agreement with hierarchical clusters. Indeed, the control clustered in a separate region of score plot hyperspace, treatment with products A and B were separated but still closer to each other, and treatment I was confirmed to have the most distinctive profile. The model parameters of the OPLS-DA regression were excellent, being R^2Y and Q^2Y 0.94 and 0.63, respectively. The model was validated (CV-ANOVA P = 0.009) and

overfitting could be excluded through permutation testing (N = 100). Furthermore, the Hotelling's T2 showed that suspect and strong outliers could be excluded. Given the more than acceptable model parameters, the variable selection method called VIP (Variable Importance in Projection) was used to explain the differences observed. The most discriminating compounds (i.e., the markers possessing a VIP score > 1.4) were exported and subjected to fold-change analysis against the control, to identify the trends of regulation altered by the treatments. The discriminant compounds, together with their VIP score and fold-change values, were grouped into chemical classes and are provided in **Table 1**. Interestingly, few biochemical classes included the most of discriminant metabolites. In more detail, low molecular weight phenolic compounds, poly-hydroxy fatty acids, membrane lipids (glyco- and phospholipids), hydroxy-carotenoids and phytohormones (polyamines) were the most represented.

From an overall perspective, the metabolomic changes imposed by the PH treatment can be correlated to relatively few processes, all of them converging toward the ROS-related plant signalling network. Among plant growth regulators, 1-aminocyclopropane-1-carboxylate (ACC), i.e. the direct precursor of ethylene, was found up accumulated in treated plants. Considering that ethylene is not detectable by our metabolomic approach, the increase of ACC suggests and increase in ethylene itself. The effects of ethylene on growth and development have been found to vary, depending on other phytohormone profile, CO_2 and light (Small and Degenhardt, 2018). Although usually related to senescence and fruit ripening, ethylene has been reported to play many other regulations in plants, including flowering and overall plant growth, cell division and root initiation, as well as modulation of secondary metabolites light (Schaller, 2012; Small and Degenhardt, 2018). In fact, at relatively low concentration, ethylene has been reported to stimulate leaf growth (Dubois et al., 2018) and to promote yields (Habben et al., 2014). Scientific evidence suggests that such ethylene-dependent regulation of plant growth is related redox signalling pathways (Caviglia et al., 2018).

Notably, polyamine conjugates (namely sinapoyltyramine and triferuloyl spermidine, both up accumulated in treated plants) were additional plant growth regulators being induced by the treatments. Polyamines are preferentially detected in actively growing tissues and have been implicated in the control of cell division, embryogenesis, root formation, fruit development and ripening, and responses to biotic and abiotic stresses (Kumar et al., 1997; Gill and Tuteja, 2010; Agudelo-Romero et al., 2013; Rouphael et al., 2016). However, these metabolites are also reported to affect H_2O_2 signature under salt stress (Gémes et al., 2017) in a coordinate manner with ethylene (Hou et al., 2013).

Even though a clear trend could not be observed, a wide alteration of the profile of membrane lipids was observed in our experiments. Such modulation might be the consequence of the altered signature in signalling compounds and antioxidants. Nevertheless, it is important to consider that membrane lipids play an important role in secondary signalling cascades which control plant adaptation processes (Hou et al., 2016). The concurrent changes in antioxidant compounds such as phenolics and carotenoids, suggests a fine tuning of the ROS-mediated signalling in tomato following application of the biostimulants. Indeed, such secondary metabolites are well known to play a pivotal role in plant defence against oxidative stress (Shalaby and Horwitz, 2015; Lucini et al., 2018; Rouphael et al., 2018a). Such interplay between polyamines, ROS and ethylene was reported to alleviate the decrease of plant biomass under stress conditions (Gémes et al., 2017) and might have had a role also in our experiments. Consistently with our findings, it is interesting to note that such support to biomass accumulation was not related to photosynthetic efficiency (Gémes et al., 2017) and was linked to the accumulation of phenolic compounds (Gémes et al., 2016).

Unlike mammals, plants produce the most of ROS in chloroplast, under a controlled multi-level antioxidant-scavenging system that includes thiols, antioxidant enzymes and low molecular weight antioxidants to manage their accumulation and transmit oxidative signals. While the concept that deleterious and irreversible oxidation driven by ROS is embed in literature, the scientific consensus is now shifting towards the recognition of the positive roles of ROS as essential components of chloroplast-nucleus retrograde signalling pathways (Foyer et al., 2017, Foyer, 2018). Since H_2O_2 is relatively more stable than superoxide and singlet oxygen (both having short half-lives), this compound is believed the likely candidate to diffuse over any distances within the cell. Such redox signals interact with the phytohormone signalling network to regulate plant growth and defence processes (Foyer, 2018). This production of ROS is essential not only to convey communication regarding the redox pressure within the electron transport chain, but also to trigger short-term genetic responses (Foyer, 2018).

Within this redox-mediated multi-layer signalling process, carotenoids (together with glutathione and tocopherols) are among the most effective $^1O_2$ scavengers; in fact, alteration in carotenoid oxidized forms has been recorded in our experiments. Coherently, the down accumulation of pheophorbide *a*, *i.e.* a precursor of chlorophylls, is a known process plant uses to control ROS production in the photosynthetic organs, given the fact that the photoreduction of oxygen to the superoxide radical is related to a reduced electron transport in PSI (Ghandchi et al., 2016) Although the link between the application of our PHs and biostimulants activity tomato could not be fully elucidated, a general consensus towards ROS-phytohormone interplay can be postulated, based on the differential metabolites

identified by metabolomics. Such multi-level signalling might have played a role in determining the differences in growth observed through phenotyping.

CONCLUSIONS

The use of PBs in particular plant-derived protein hydrolysates (PHs) in agriculture has greatly increased in the last decade mostly due to their *multifaceted properties*. Highly efficient and effective PH-based biostimulant products can be obtained using the 'omics' sciences. A novel approach based on the use of high-throughput phenotyping technologies and metabolomics was successfully tested on tomato crop for identifying new PHs with biostimulant activity and for studying the PH effects on plants at the molecular level. Dynamic monitoring of plant performance by high-throughput phenotyping system has proven to be a powerful tool for substance screening on the basis of morpho-physiological traits quantification. The effects of PHs on tomato phenotype were more evident on digital biomass. Metabolomics followed by multivariate analysis allowed elucidating the metabolic signatures imposed by the specific PH treatments at the molecular level. PH treatments affected the metabolic profile of tomato leaves via the modulation of a complex signalling process that involved the direct precursor of ethylene and polyamine conjugates. The coordinated action of plant growth regulators together with antioxidant compounds such as carotenoids and phenolics, might have affected the ROS-mediated signalling pathways. Although further assays under defined conditions would strengthen our findings, the discriminant compounds pointed out by this approach suggest that treated plants might experience a metabolic reprogramming following the application of the tested biostimulants.

Table 1| *Discriminant metabolites as identified by Variables of Importance in Projection (VIP) analysis following OPLS-DA modelling on metabolomic profile of treated plants. Discriminant metabolites (VIP > 1.4) are provided together with individual scores, their standard error (SE) and metabolite fold-change (FC) Log values, as compared to control; missing values denote fold-change values < 1.5.*

		VIP score		[A] vs [control]		[B] vs [control]		I] vs [control]	
Class	**Metabolite**	**score**	**SE**	**Log FC**	**Regulation**	**Log FC**	**Regulation**	**Log FC**	**Regulation**
Phenolics	3.5-dihydroxyanisole	1.409	0.769						
	1.3.5-trimethoxybenzene	1.405	0.286	2.8	up	5.5	up	1.7	up
	4-hydroxybenzaldehyde	1.418	0.820						
	3.6.7.4'-tetramethylquercetagetin 3'-O-beta-D-glucoside	1.540	0.883						
	3-phenylpropanoate	1.457	0.308	0.3	up	5.5	up	1.7	up
	3-hydroxybenzaldehyde	1.418	0.820						
	gallocatechin	1.372	0.548	0.2	up	3.6	up	4.5	up
	leucocyanidin	1.372	0.548	0.2	up	3.6	up	4.5	up
	epigallocatechin	1.372	0.548	0.5	up	3.6	up	4.3	up
Glucosinolates	3-(7'-methylthio) heptylmalate	1.308	0.304	3.1	up	1.2	up	1.8	up
	2-(7'-methylthio) heptylmalate	1.308	0.304	3.7	up	1.2	up	1.8	up
Lipids	oleate	1.367	0.497	-29.4	down	0.2	up	3.9	up
	colneleate	1.515	0.219	-3.9	down	-4.0	down	2.0	up
	4-coumaryl alcohol	1.456	0.313	0.3	up	5.5	up	1.7	up
	germacra-1(10).4.11(13)-trien-12-ol	1.315	0.777	-8.7	down	-5.1	down	0.4	up
	dammarenediol II	1.428	0.899	6.2	up	6.2	up	6.0	up
	1-16:0-2-18:3-diacylglycerol-trimethylhomoserine	1.365	0.919	1.0	up	1.1	up	0.7	up
	1-16:0-2-18:2-digalactosyldiacylglycerol	1.394	1.122						
	sitosterol	1.317	1.095	-0.5	down	-1.1	down	-0.5	down
	(12Z.15Z)-9.10-epoxyoctadeca-12.15-dienoate	1.515	0.219	-3.9	down	-4.0	down	2.0	up
	An epoxy-octadeca-dienoate	1.515	0.219	-3.9	down	-4.0	down	2.0	up
	A dihydroxyoctadeca-dienoate	1.371	0.724	0.6	up	-0.4	down	1.5	up
	9.10-12.13-diepoxyoctadecanoate	1.316	0.617	11.6	up	1.2	up	6.9	up

	16-alpha-hydroxygypsogenate-28-beta-D-glucoside	1.319	0.684	0.6	up	8.8	up	1.5	up
	2-hydroxyhexadecanoate	1.413	0.883						
	2-*trans*-6-*trans*-farnesyl monophosphate	1.397	0.571	4.5	up	4.6	up	0.7	up
	geranyl monophosphate	1.376	0.378	3.2	up	3.1	up	1.6	up
	(9S)-HPODE / (13S)-HPODE	1.371	0.724	0.6	up	-0.4	down	1.5	up
	3--beta;-D-galactosyl-sn-glycerol	1.369	1.015						
	a 2-acyl-sn-glycero-3-phosphoethanolamine (n-C14:1)	1.357	0.447	3.1	up	9.4	up	1.9	up
	a 1-acyl-sn-glycero-3-phosphoglycerol (n-C14:1)	1.346	0.288	-0.4	down	-0.4	down	-1.8	down
	3.4-dihydroxy-5-iall-trans/i-hexaprenylbenzoate	1.323	0.679	-3.1	down	9.3	up	6.1	up
	4.4-dimethyl-5-alpha-cholest-7-en-3-beta-ol / 4.4-dimethyl-5-alpha-cholesta-8-en-3-beta-ol	1.317	1.095	-0.5	down	-1.1	down	-0.5	down
	1.2-dipalmitoyl-phosphatidylglycerol-phosphate	1.317	0.506	-9.4	down	-7.5	down	1.4	up
	(6E)-8-oxogeranial	1.315	0.666	-1.8	down	-1.8	down	-1.5	down
	(2E.6E)-farnesal	1.315	0.777	-8.7	down	-5.1	down	0.4	up
	4-alpha-carboxy-4-beta-methyl-5-alpha-cholesta-8-en-3-beta-ol	1.312	0.670						
Carotenoids	4-methylocta-2.4.6-trienedial	1.456	0.313	0.6	up	5.5	up	1.7	up
	5.6-epoxy-3-hydroxy-5.6-dihydro-12'-apo-beta;-caroten-12'-al	1.500	0.534	-0.28646278	down	-1.0	down	-1.3	down
	18'-hydroxy-chi; chi;-caroten-18-oate	1.304	0.646	-9.2	down	-1.5	down	-1.5	down
Hormones	1-aminocyclopropane-1-carboxylate	1.419	0.241	2.9	up	2.9	up	1.8	up
	salicylaldehyde	1.418	0.820						
Others	triferuloyl spermidine	1.503	0.350	0.6	up	2.8	up	1.7	up
	sinapoyltyramine	1.516	0.366	0.6	up	-0.4	down	1.8	up
	thiamin	1.450	0.539	4.6	up	4.5	up	0.4	up
	S-adenosyl 3-(methylthio) propylamine	1.431	0.440	-6.1	down	9.2	up	6.1	up
	methyl-1.4-benzoquinone	1.418	0.820						
	N-acetylneuraminate	1.384	0.363	-1.4	down	-1.5	down	-1.5	down
	menaquinol-8	1.367	0.491						

pyropheophorbide *a*	1.361	0.302	-1.1	down	-1.0	down	-1.2	down

Supplementary Figures

Suppl. Fig. 1| Schematic of the kinetic ChlF protocol in the PlantScreen™ Modular System. ChlF kinetics were captured with a PAM-based chlorophyll fluorometer. Images of the individual transient states were recorded. Corresponding frames were averaged for the measured parameters (F_o, F_m, F_m', F_t, and F_p) or calculated from the captured frames to compute the relative parameters such as F_v/F_m, ΦPSII, F_v'/F_m', NPQ and others. Automated ChlF image processing consisted of image segmentation by mask application, background subtraction and feature extraction. The signals from all pixels of each segment were averaged at each given time point. MF refers to the measuring flash, and yellow arrows indicate the saturation pulses that transiently saturated the electron transport chain. Lss1, Lss2 and Lss3 represent actinic photon irradiance measurements taken at 170, 620 and 1070 µmol photons m^{-2} s^{-1}, respectively.

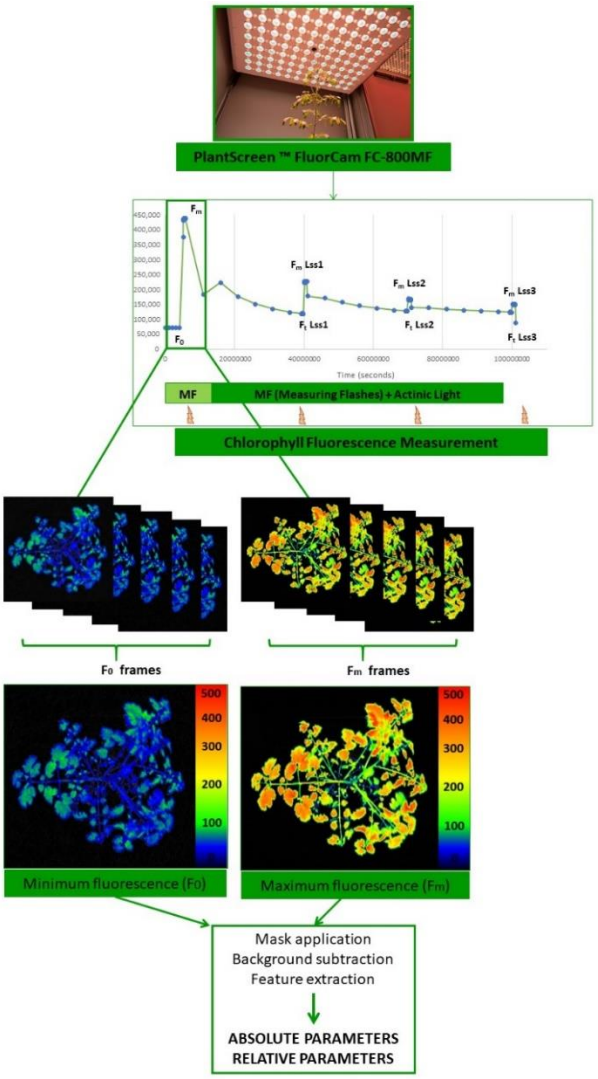

Suppl. Fig. 2. Schematic of top and side view RGB image processing. Original RGB images were automatically processed using the PlantScreen™Analyzer software to correct for barrel distortion caused by the fisheye lens, subtract the background and crop to isolate the plants within the imaged area, producing a binary (black and white) image. The binary images represent the plant surface (white) and background (black). Non-plant pixels, such as pots, were automatically removed to extract only plant pixels. Morphological analysis was conducted after separating the background from the plant shoot tissue. To evaluate color of plant shoot, RGB images were color-segmented to extract the green hues.

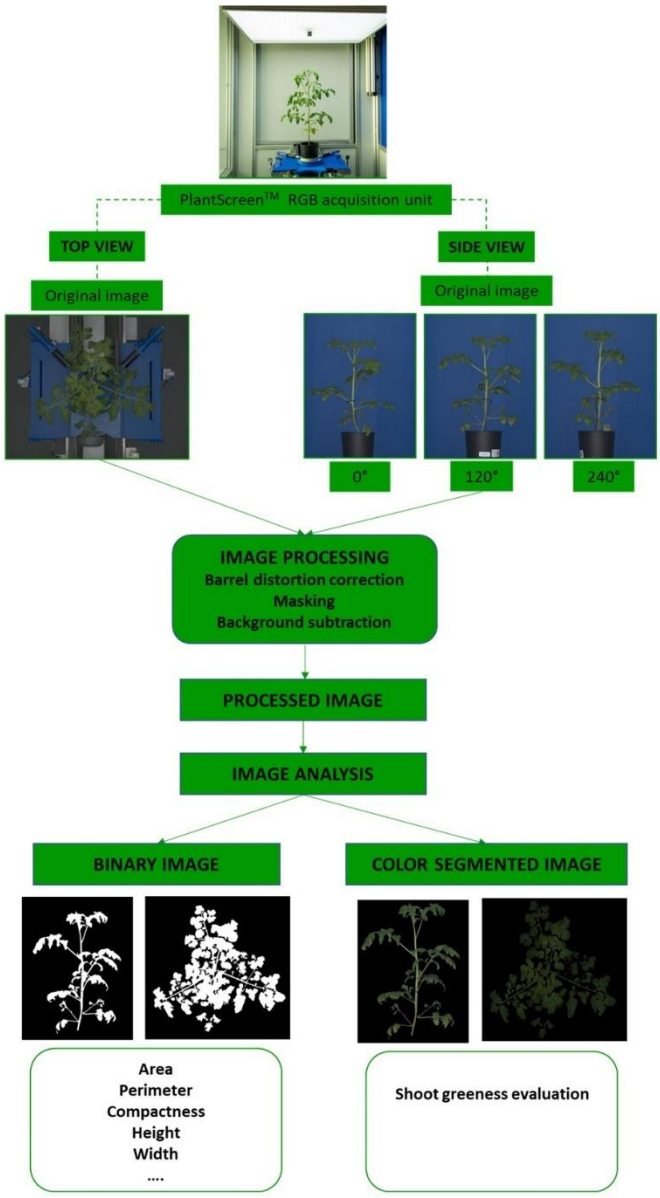

Suppl. Fig. 3. Variation in shoot colors of tomato plants. Dynamic relative changes in greenness hue abundance over the phenotyping period in control tomato plants and plants treated with protein hydrolysates (A-G, I). The six most representative color hues are shown in RGB color scale as percentage of the shoot area (pixel counts) of six biological replicates per treatment.

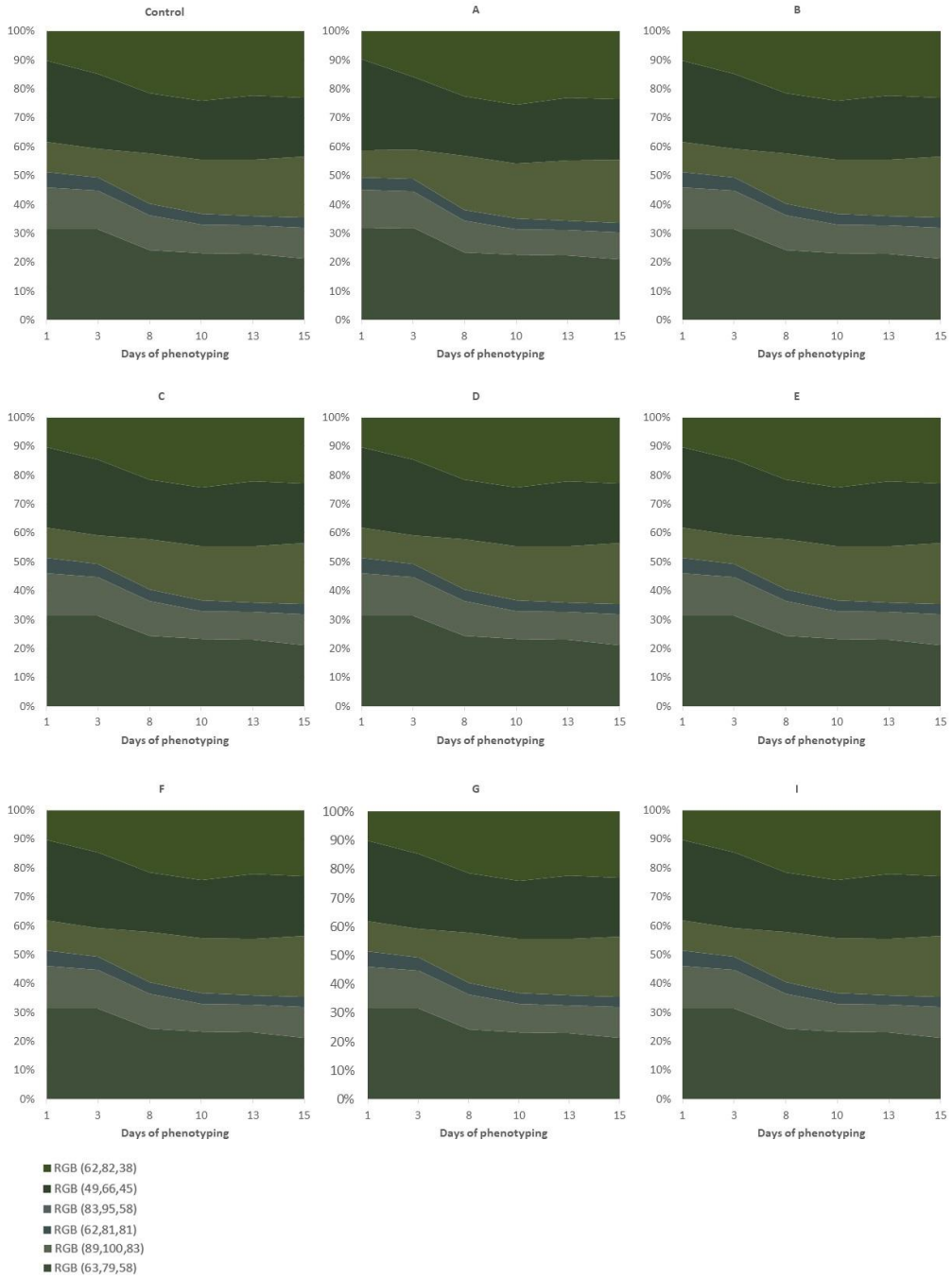

Suppl. Table 1 - Projected shoot area (PSA) of the tomato plants extracted from top view RGB images starting 3 days after the first PH application (day after transplanting, DAT = 8). Values are expressed as number of green pixels and represent the average of six biological replicates per treatment ± standard deviation. Within the same row and for the specified day different letters indicate significant difference according to one-way ANOVA post-hoc Tukey's test ($p<0.05$).

Treatment	DAT 8		DAT 10		DAT 13		DAT 15	
Control	185466 ± 35826	b	258193 ± 63543	b	284354 ± 64892	c	372389 ± 65568	b
A	308192 ± 66640	a	401201 ± 86993	ab	591422 ± 80799	a	623942 ± 103262	a
B	279199 ± 22870	ab	352267 ± 36509	ab	522508 ± 45840	ab	596301 ± 85018	ab
C	212243 ± 30323	ab	329613 ± 42744	ab	402183 ± 52599	bc	493099 ± 52191	ab
D	296033 ± 55898	ab	386651 ± 75258	ab	531811 ± 101546	ab	614138 ± 108998	a
E	318470 ± 66810	a	427899 ± 96048	a	529265 ± 108641	ab	633845 ± 140093	a
F	277338 ± 84209	ab	349063 ± 87243	ab	451202 ± 96820	abc	558543 ± 131051	ab
G	248847 ± 63712	ab	350400 ± 91132	ab	501446 ± 140366	ab	595604 ± 165820	ab
I	235300 ± 34032	ab	298350 ± 27153	ab	471633 ± 27146	abc	511575 ± 76212	ab

Suppl. Table 2 - Projected shoot area (PSA) of the tomato plants extracted from top view RGB images starting 3 days after the first PH application (day after transplanting, DAT = 8). Values are expressed as number of green pixels and represent the average of six biological replicates per treatment ± standard deviation. Within the same row and for the specified day different letters indicate significant difference according to one-way ANOVA post-hoc Tukey's test ($p<0.05$).

Treatment	DAT 8		DAT 10		DAT 13		DAT 15	
Control	59923 ± 13370	b	92541 ± 17482	b	168051 ± 26977	b	198508 ± 38446	b
A	94001 ± 11175	a	143824 ± 13861	a	245531 ± 28656	a	308341 ± 31873	a
B	100127 ± 7961	a	149679 ± 9030	a	254850 ± 13077	a	290212 ± 29779	ab
C	76815 ± 15976	ab	110956 ± 14366	ab	186505 ± 30943	ab	227891 ± 22048	ab
D	87448 ± 12726	ab	126782 ± 15202	ab	213147 ± 28892	ab	268372 ± 27609	ab
E	88806 ± 16064	ab	136145 ± 20241	ab	238890 ± 34472	ab	289130 ± 49503	ab
F	86740 ± 19461	ab	129395 ± 30760	ab	227561 ± 54753	ab	272347 ± 65978	ab
G	83272 ± 25856	ab	122908 ± 33987	ab	205683 ± 54293	ab	254734 ± 65385	ab
I	73733 ± 15831	ab	114782 ± 14845	ab	201741 ± 25541	ab	262794 ± 35375	ab

Suppl. Table 3 - Width of the tomato plants extracted from multiple side view RGB images starting 3 days after the first PH application (day after transplanting, DAT = 8). Values are expressed as number of green pixels and represent the average of six biological replicates per treatment ± standard deviation. Within the same row and for the specified day different letters indicate significant difference according to one-way ANOVA post-hoc Tukey's test ($p<0.05$).

Treatment	DAT 8		DAT 10		DAT 13		DAT 15	
Control	625 ± 74	c	695 ± 77	c	835 ± 95	c	952 ± 110	c
A	758 ± 102	a	840 ± 82	a	1045 ± 79	a	1097 ± 75	ab
B	754 ± 81	ab	854 ± 97	a	1051 ± 99	a	1104 ± 53	ab
C	651 ± 88	bc	742 ± 82	bc	909 ± 83	bc	1002 ± 82	bc
D	742 ± 88	ab	827 ± 110	a	1022 ± 86	a	1076 ± 77	ab
E	739 ± 115	ab	858 ± 126	a	997 ± 91	ab	1133 ± 100	a
F	736 ± 116	ab	828 ± 157	a	970 ± 131	ab	1072 ± 153	ab
G	686 ± 142	bc	787 ± 124	abc	974 ± 155	ab	1056 ± 135	abc
I	663 ± 93	bc	782 ± 88	abc	996 ± 87	ab	1067 ± 120	abc

Suppl. Table 4 - Height of the tomato plants extracted from multiple side view RGB images starting 3 days after the first PH application (day after transplanting, DAT = 8). Values are expressed as number of green pixels and represent the average of six biological replicates per treatment ± standard deviation. Within the same row and for the specified day different letters indicate significant difference according to one-way ANOVA post-hoc Tukey's test ($p<0.05$).

Treatment	DAT 8		DAT 10		DAT 13		DAT 15	
Control	546 ± 67	b	734 ± 163	bc	930 ± 110	d	1174 ± 186	c
A	668 ± 62	a	824 ± 60	ab	1123 ± 82	ab	1337 ± 95	ab
B	687 ± 38	a	868 ± 61	a	1178 ± 74	a	1376 ± 94	a
C	671 ± 78	a	809 ± 44	abc	1048 ± 83	bc	1274 ± 57	abc
D	718 ± 77	a	899 ± 80	a	1203 ± 135	a	1387 ± 118	a
E	670 ± 51	a	812 ± 61	ab	1121 ± 72	ab	1335 ± 69	ab
F	694 ± 100	a	857 ± 139	a	1117 ± 151	ab	13222 ± 134	ab
G	692 ± 96	a	838 ± 118	a	1103 ± 139	ab	1333 ± 156	ab
I	566 ± 55	b	705 ± 88	c	978 ± 52	cd	1229 ± 98	bc

Suppl. Table 5 - Digital biomass of tomato plants treated with different protein hydrolysates starting 3 days after the first PH application (day after transplanting, DAT = 8). Values are expressed as number of green pixels and represent the average of six biological replicates per treatment ± standard deviation. Within the same row and for the specified day different letters indicate significant difference in digital biomass, according to one-way ANOVA post-hoc Tukey's test ($p<0.05$).

Treatment	DAT 8		DAT 10		DAT 13		DAT 15	
Control	26219341 ± 8887016	b	47651702 ± 15809090	b	90417958 ± 25638354	b	122435561 ± 35815347	b
A	52264360 ± 10850713	a	90992135 ± 15856605	a	189586844 ± 35368971	a	243509393 ± 38332729	a
B	47904900 ± 5653942	ab	84638470 ± 12135054	a	141658655 ± 8446546	ab	212774506 ± 38839091	ab
C	33574660 ± 10094184	ab	59562525 ± 9510096	ab	111651986 ± 21820459	ab	153092758 ± 22195505	ab
D	50343526 ± 11684467	ab	84031217 ± 17622181	ab	164085417 ± 36705056	ab	217636972 ± 42325628	ab
E	50269320 ± 13269985	ab	89461571 ± 23301168	a	174201900 ± 40624119	ab	232126717 ± 68680821	a
F	48826198 ± 16971615	ab	81055632 ± 27571693	ab	164014105 ± 53660635	ab	218211048 ± 75060581	ab
G	42691685 ± 18852229	ab	74504589 ± 30119149	ab	148228609 ± 56845130	ab	200866573 ± 80737148	ab
I	38361957 ± 7396873	ab	66422847 ± 10361545	ab	144633820 ± 16579042	ab	198209362 ± 33876201	ab

Suppl. Table 6 - Variation in shoot colours of tomato plants treated with different protein hydrolysates at 15 days after transplanting. The values for 6 most representative colour hues are shown as percentage of the shoot area (pixel counts). Values represent the average of six biological replicates per treatment ± standard deviation. Within the same row and for the specified day different letters indicate significant difference according to one-way ANOVA post-hoc Tukey's test ($p<0.05$).

Treatment	RGB (63,79,58)		RGB (89,100,83)		RGB (83,95,58)		RGB (49,66,45)		RGB (62,81,81)		RGB (62,82,38)	
Control	23 ± 3	a	11 ± 1	a	21 ± 3	a	19 ± 4	a	4 ± 0.3	a	23 ± 3	a
A	21 ± 2	a	9 ± 1	a	22 ± 1	a	21 ± 1	a	3 ± 0.3	a	24 ± 2	a
B	22 ± 1	a	10 ± 1	a	21 ± 2	a	21 ± 2	a	4 ± 0.1	a	23 ± 1	a
C	21 ± 2	a	12 ± 1	a	22 ± 4	a	19 ± 4	a	3 ± 0.4	a	24 ± 2	a
D	20 ± 2	a	11 ± 3	a	20 ± 2	a	21 ± 3	a	4 ± 0.4	a	24 ± 2	a
E	20 ± 1	a	11 ± 2	a	22 ± 2	a	20 ± 3	a	4 ± 0.2	a	23 ± 1	a
F	22 ± 3	a	11 ± 2	a	21 ± 1	a	22 ± 3	a	4 ± 0.3	a	21 ± 3	a
G	20 ± 2	a	12 ± 2	a	21 ± 1	a	20 ± 4	a	3 ± 0.2	a	23 ± 2	a
I	23 ± 3	a	9 ± 1	a	20 ± 2	a	22 ± 3	a	3 ± 0.1	a	22 ± 3	a

Suppl. Table 7 - Photosynthetic performance of tomato plants at 15 days after transplanting. Photosynthetic parameters deduced from kinetic chlorophyll fluorescence imaging on whole plant level in all protein hydrolysate treatments. Minimal fluorescence in dark-adapted state (F_o), maximum fluorescence in dark-adapted state (F_m), maximum quantum yield of PSII photochemistry for the dark-adapted (F_v/F_m), the photochemical quenching coefficient that estimates the fraction of open PSII reaction centers (qP), steady-state non-photochemical quenching (NPQ) and electron transport rate (ETR) were measured using the light curve protocol for tomato plants prior and upon PHs application. Values represent the average of six biological replicates per treatment ± standard deviation. Within the same row and for the specified day different letters indicate significant difference according to one-way ANOVA post-hoc Tukey's test ($p<0.05$). Lss1, Lss2 and Lss3 represent actinic photon irradiance measurements taken at 170, 620 and 1070 µmol photons $m^{-2}s^{-1}$ PAR values respectively

Lss 1												
Treatment	F_0		F_m		F_v/F_m		qP		NPQ		ETR	
Control	67 ± 9	a	291 ± 27	a	0.77 ± 0.01	a	0.54 ± 0.16	a	0.60 ± 0.06	a	34 ± 9	a
A	73 ± 9	a	298 ± 30	a	0.76 ± 0.01	a	0.57 ± 0.14	a	0.71 ± 0.04	a	36 ± 8	a
B	67 ± 2	a	277 ± 7	a	0.76 ± 0.01	a	0.44 ± 0.19	a	0.72 ± 0.04	a	28 ± 12	a
C	68 ± 2	a	288 ± 18	a	0.76 ± 0.01	a	0.46 ± 0.18	a	0.66 ± 0.11	a	29 ± 12	a
D	68 ± 2	a	283 ± 5	a	0.76 ± 0.01	a	0.42 ± 0.17	a	0.71 ± 0.07	a	27 ± 11	a
E	68 ± 2	a	282 ± 13	a	0.76 ± 0.01	a	0.43 ± 0.17	a	0.70 ± 0.04	a	27 ± 11	a
F	66 ± 2	a	279 ± 9	a	0.76 ± 0.01	a	0.41 ± 0.05	a	0.67 ± 0.10	a	27 ± 11	a
G	69 ± 2	a	285 ± 8	a	0.76 ± 0.01	a	0.43 ± 0.18	a	0.70 ± 0.07	a	27 ± 11	a
I	76 ± 13	a	314 ± 35	a	0.76 ± 0.02	a	0.53 ± 0.31	a	0.60 ± 0.03	a	34 ± 10	a

Lss 2												
Treatment	F_0		F_m		F_v/F_m		qP		NPQ		ETR	
Control	61 ± 7	a	206 ± 10	a	0.70 ± 0.02	a	0.30 ± 0.16	a	1.10 ± 0.25	ab	55 ± 27	a
A	67 ± 7	a	214 ± 15	a	0.69 ± 0.02	a	0.33 ± 0.15	a	1.19 ± 0.30	ab	60 ± 25	a
B	62 ± 2	a	200 ± 3	a	0.69 ± 0.01	a	0.24 ± 0.09	a	1.42 ± 0.04	a	44 ± 16	a
C	63 ± 2	a	213 ± 12	a	0.70 ± 0.02	a	0.24 ± 0.09	a	1.25 ± 0.17	ab	45 ± 16	a
D	62 ± 2	a	205 ± 9	a	0.69 ± 0.01	a	0.23 ± 0.07	a	1.37 ± 0.08	a	42 ± 14	a
E	62 ± 2	a	207 ± 10	a	0.70 ± 0.01	a	0.22 ± 0.07	a	1.31 ± 0.08	ab	41 ± 13	a
F	61 ± 2	a	204 ± 14	a	0.70 ± 0.01	a	0.20 ± 0.07	a	1.29 ± 0.12	ab	40 ± 14	a
G	63 ± 2	a	206 ± 13	a	0.69 ± 0.01	a	0.23 ± 0.08	a	1.36 ± 0.09	a	42 ± 14	a
I	69 ± 11	a	221 ± 18	a	0.69 ± 0.03	a	0.37 ± 0.25	a	0.89 ± 0.35	b	66 ± 43	a

Lss 3												
Treatment	F_0		F_m		F_v/F_m		qP		NPQ		ETR	
Control	57 ± 6	a	168 ± 4	a	0.66 ± 0.03	a	0.23 ± 0.11	a	1.55 ± 0.23	ab	66 ± 27	a
A	63 ± 5	a	179 ±9	a	0.65 ± 0.02	a	0.25 ± 0.11	a	1.61 ± 0.29	ab	73 ± 26	a
B	58 ± 2	a	170 ± 1	a	0.65 ± 0.01	a	0.20 ± 0.06	a	1.87 ± 0.10	a	57 ± 16	a
C	60 ± 2	a	180 ± 12	a	0.67 ± 0.01	a	0.20 ± 0.05	a	1.66 ± 0.17	ab	57 ± 15	a
D	59 ± 2	a	172 ± 5	a	0.66 ± 0.01	a	0.19 ± 0.05	a	1.80 ± 0.06	a	55 ± 14	a
E	59 ± 2	a	175 ± 6	a	0.66 ± 0.01	a	0.18 ± 0.04	a	1.73 ± 0.07	ab	55 ± 12	a
F	57 ± 2	a	172 ± 9	a	0.66 ± 0.01	a	0.17 ± 0,05	a	1.71 ± 0.10	ab	52 ± 13	a
G	60 ± 1	a	174 ± 8	a	0.66 ± 0.01	a	0.19 ± 0.04	a	1.79 ± 0.05	ab	54 ± 13	a
I	63 ± 9	a	177 ± 11	a	0.64 ± 0.04	a	0.28 ± 0.17	a	1.35 ± 0.37	b	79 ± 44	a

3.1.3 Tomato II – Drought stress

ORIGINAL RESEARCH article
Front. Plant Sci., 03 May 2019 | https://doi.org/10.3389/fpls.2019.00493

A Combined Phenotypic and Metabolomic Approach for Elucidating the Biostimulant Action of a Plant-Derived Protein Hydrolysate on Tomato Grown Under Limited Water Availability

Kenny Paul[1†], Mirella Sorrentino[1†], Luigi Lucini[2], Youssef Rouphael[3], Mariateresa Cardarelli[4], Paolo Bonini[5], Maria Begoña Miras Moreno[2], Hélène Reynaud[6], Renaud Canaguier[7], Martin Trtílek[1], Klára Panzarová[1*] and Giuseppe Colla[8,9*]

[1]Photon Systems Instruments, spol. s.r.o., Drásov, Czechia
[2]Department for Sustainable Food Process, Research Centre for Nutrigenomics and Proteomics, Università Cattolica del Sacro Cuore, Piacenza, Italy
[3]Department of Agricultural Sciences, University of Naples Federico II, Portici, Italy
[4]Consiglio per la Ricerca in Agricoltura e l'Analisi dell'Economia Agraria, Centro di Ricerca Orticoltura e Florovivaismo, Pontecagnano Faiano, Italy
[5]NGAlab, Tarragona, Spain
[6]Italpollina USA, Inc., Anderson, IN, United States
[7]Nixe, Valbonne, France
[8]Department of Agriculture and Forest Sciences, Tuscia University, Viterbo, Italy
[9]Arcadia Srl, Rivoli Veronese, Italy

A Combined Phenotypic and Metabolomic Approach for Elucidating the Biostimulant Action of a Plant-derived Protein Hydrolysate on Tomato Grown under Limited Water Availability

Kenny Paul[ǂǂ], Mirella Sorrentino[ǂǂ], Luigi Lucini[2], Youssef Rouphael[3], Mariateresa Cardarelli[4], Paolo Bonini[5], Maria Begoña Miras Moreno[2], Hélène Reynaud[6], Renaud Canaguier[7], Martin Trtílek[1], Klára Panzarová[1]*, Giuseppe Colla[8]*

[1]Photon Systems Instruments (PSI, spol.sr.o.), Drásov, Czech Republic, [2]Department for Sustainable Food Process, Research Centre for Nutrigenomics and Proteomics, Università Cattolica del Sacro Cuore, Piacenza, Italy, [3]Department of Agricultural Sciences, University of Naples Federico II, Portici, Italy, [4]Consiglio per la Ricerca in Agricoltura e l'analisi dell'economia agraria, Centro di ricerca Orticoltura e Florovivaismo, Pontecagnano, Italy, [5]NGAlab, La Riera de Gaia, Tarragona, Spain, [6]Italpollina USA Inc., Anderson, IN 46016, United States, [7]Nixe, Les Espaces de Sophia, Valbonne, France, [8]Department of Agriculture and Forest Sciences, University of Tuscia, 01100 Viterbo, Italy

[ǂ] Authors of equal contribution to this work.

Abstract

Plant-derived protein hydrolysates (PHs) are an important category of biostimulants able to increase plant growth and crop yield especially under environmental stress conditions. PHs can be applied as foliar spray or soil drench. Foliar spray is generally applied to achieve a relatively short-term response whereas soil drench is used when a long-term effect is desired. The aim of the study was to elucidate the biostimulant action of PH application method (foliar spray or substrate drench) on morpho-physiological traits and metabolic profile of tomato grown under limited water availability. An untreated control was also included. A high-throughput image-based phenotyping (HTP) approach was used to non-destructively monitor the crop response under limited water availability (40% of container capacity) in controlled environment. Moreover, metabolic profile of leaves was determined at the end of the trial. Dry biomass of shoots at the end of the trial was significantly correlated with number of green pixels, (R^2= 0.90) projected shoot area, respectively. Both drench and foliar treatments had a positive impact on the digital biomass compared to control while photosynthetic performance of the plants we slightly influenced by treatments. Overall drench application under limited water availability more positively influenced biomass accumulation and metabolic profile than foliar application. Significantly higher transpiration use efficiency was observed with PH-drench applications indicating better stomatal conductance. The MS-based metabolomic analysis allowed identifying distinct biochemical signatures in PH-treated plants. Metabolomic changes involved a wide and organized range of biochemical processes that included, among others, phytohormones (notably a decrease in cytokinins and an accumulation of salicylates) and lipids (including membrane lipids, sterols and terpenes). From a general perspective, treated tomato plants exhibited an improved tolerance to ROS-mediated oxidative imbalance. Such capability to cope with oxidative stress might have resulted from a coordinated action of signaling compounds (salicylic acid and hydroxycinnamic amides), radical scavengers such as carotenoids and prenyl quinones, as well as a reduced biosynthesis of tetrapyrrole coproporphyrins.

Keywords: protein hydrolysates; high-throughput phenotyping; metabolomics; morpho-physiological traits; foliar spray; drench application.

INTRODUCTION

Competition among agriculture, industry and cities for limited water supplies is already constraining development efforts in many countries. As populations expand and economies grow, the competition for limited supplies will intensify and so will conflicts among water users. Agriculture is not only the world's largest water user in terms of volume, it is also a relatively low-value, low-efficiency and highly-subsidized water user (Rouphael et al., 2012).

These facts are forcing farmers to grow crops with diminishing water supplies. Limited water availability can affect morphological, physiological, biochemical and molecular processes in plants, resulting in growth depression and yield reduction (Liu et al., 2014; Kumar et al., 2017). Under these conditions, the application of plant biostimulants can help crops to use water more efficiently by changing the root to shoot ratio, the plant metabolism and hormonal balance (Ertani et al., 2012, 2016; Colla et al., 2017; Rouphael and Colla, 2018).

Protein hydrolysates (PHs) represent an important category of plant biostimulants that have been extensively used for improving crop yield and quality especially under abiotic stress conditions such as limited water, salinity and heavy metals (Ertani et al., 2009; Colla et al., 2015a; du Jardin et al., 2015). PHs could directly stimulate carbon and nitrogen metabolism and could indirectly enhance nutrient availability of substrates and increase nutrient uptake as well as nutrient-use efficiency in plants (Haplern et al., 2015; Colla et al., 2017b; Rouphael et al., 2017b). PHs can be applied by foliar spray or substrate drench affecting molecular and physiological crop response in a different way (Lucini et al., 2015; Sestili et al., 2018). In a recent study, substrate drench applications of a plant-derived PH were more effective to improve plant growth and total N uptake than foliar sprays in tomato (Sestili et al., 2018). In the same study, the application method (drench or foliar) of the plant-derived PH affected the expression of genes encoding ammonium and nitrate transporters differently as well as seven enzymes involved in N metabolism of tomato (Sestili et al., 2018).

A successful evaluation of biostimulant activity of PHs requires an accurate measurement of morpho-physiological traits of plants over time. Use of advanced image-based automated phenotyping platforms offers opportunities to both increase the speed at which these measurements are collected as well as the accuracy of measurements (Povero et al., 2016). Dynamic screening of plants can be done for multiple

morpho-physiological traits related to growth, yield, and performance throughout their development or onset, progression, and recovery from abiotic stress (Petrozza et al., 2014). Functional action and characterization of PHs in plants can be thus monitored with high precision and in high resolution in each phase of plant development and/or plant response to environmental conditions, depending on the target substance application or type of experimental layout (Rouphael et al., 2018a). Range of morpho-physiological traits can be monitored in a fully automated, high-resolution and high-sensitivity manner. A key descriptive parameter in plant physiology, except of root analysis, is the shoot growth of the plants and quantitative and qualitative dynamic assessment of growth performance by RGB imaging was used to characterize range of traits such as shoot biomass or yield (Li et al., 2014; Humplik et al., 2015). Non-invasive monitoring of plant photosynthetic activity is also critical for understanding the physiological and metabolic condition, as well as its susceptibility to various stress conditions (Gorbe and Calatayud, 2012; Petrozza et al., 2014; Paul et al., 2016). Pulse amplitude modulation based kinetic chlorophyll fluorescence imaging is a broadly applied technique used to understand the plant phenology in response to external stimuli or agents (Murchie and Lawson, 2013). In a high-throughput phenotyping set-up, modern imaging systems (FluorCam, PSI) were recently successfully used to monitor dynamically PSII parameters and electron flow dynamics at the whole plant level (Humplik et al., 2015b; Awlia et al., 2016; Tschiersch et al., 2017). Usage of automated photosynthetic phenotyping approaches helps us to screen and characterize PHs real time interaction throughout the grow regime. Water taken up by plants or plant water content is a key to understand the efficiency with which plants are able to regulate stomatal conductance and CO_2 fixation. Water content in plants is the result of the equilibrium between root water uptake and shoot transpiration (Berger et al., 2010). Thermoimaging has been used in high-throughput phenotyping platforms to monitor plant transpiration rate and transpiration use efficiency (Kaňa and Vass, 2008; Paul et al., 2016).

Besides in plant phenotyping, metabolomics offers unique opportunities to understand the mode of action of PHs on crops and to identify biomarkers of biostimulant action. For instance, Lucini et al. (2015) identified several differentially expressed key metabolites associated with osmotic adjustment, oxidative stress mitigation and hormone network in PH-treated lettuce plants exposed to salt stress. Considering that tomato is the most important crop grown in the world, an experimental trial was performed to evaluate the effect of a plant-derived PH applied through foliar spray or substrate drench on morpho-physiological traits and metabolic profile of tomato plants grown under limited water availability in controlled environment.

MATERIALS AND METHODS

Plant Material and Growing Conditions

Seeds of tomato (*Solanum lycopersicum* L. - Hybrid F1 Chicco Rosso) were sown in trays with size of pots of 100 ml each containing freshly sieved substrate (Substrate 2, Klasmann- Deilmann GmbH, Germany) which was already watered to water holding capacity. Trays with seeds were kept for two days at 4 °C in the dark. Trays with seeds were placed in the controlled growth chamber (FS-WI, PSI, Czech Republic) at 16 h day/8 h night regime, 22 °C Day/20 °C night, 60% relative humidity and with cool-white LED (250 µmol photons m^{-2} s^{-1}) and far-red LED (5.5 µmol photons $m^{-2}s^{-1}$) lighting.

Fertigation and Watering Protocol

Prior to plant transplanting into 3 L pots, trays were uniformly watered at 6, 7, 12 and 14 days after placement of trays in controlled growth chamber. On day 7 and day 14, plants were fertigated with a solution containing: 1.04 g L^{-1} calcium nitrate (15.5% N; 28% CaO), 0.04 g L^{-1} ammonium nitrate (34% N), 0.14 g L^{-1} monopotassium phosphate (52% P_2O_5, 34% K_2O), 0.18 g L^{-1} potassium sulphate (50% K_2O, 45%SO_3), 0.5 g L^{-1} magnesium sulphate (10%N, 16% MgO), and 0.5 ml L^{-1} FloraMicro (5% N, 1% K_2O, 5% Ca, 0.01% B, 0.001% Cu, 0.1% Fe, 0.05% Mn, 0.0008% Mo, 0.015% Zn).

Twenty-day-old plants were selected with uniform growth characteristics and transplanted into 3 L pots (mixture of Substrate 2 Klassman soil and river sand in 3:1 ratio was used). The pots were labelled with unique identification codes for each plant replicate and treatment. For determining the water content at container capacity, one set of substrate pots was dried for three days at 80 ^oC and another set was saturated with water and left to drain for one day before weighing 100% water holding capacity (Awlia et al., 2016). Water content at container capacity was calculated as the difference between substrate weight at water holding capacity and dried substrate. On the day before transplantation, soil was prepared, and moisture content was adjusted to 60% of container capacity. Twenty-one-day-old plants were transplanted into the prepared substrate mixture with 60% of container capacity. Following the transplantation plants were regularly watered to reference weight (40% of container capacity) defined as

low water availability condition by using automated watering and weighing unit of PlantScreen™ Modular System.

Plant Identification and Biostimulant Treatments

Plants were randomly distributed into three groups with six biological replicates per group. Three groups each containing six plants were identified as: no application, foliar application and drench application of PH. Each plant was labelled with a unique barcode identifier used for registration of the plants in the PlantScreen™ Modular System. Plant-derived protein hydrolysate (PH) biostimulant Trainer® was provided by Italpollina Company (Rivoli Veronese, Italy). The plant-derived protein hydrolysate Trainer® is a commercial PH obtained through enzymatic hydrolysis of proteins derived from legume seeds. It contains 50 g kg^{-1} of N as free amino acids, and soluble peptides (Rouphael et al., 2018a). The aminogram of the product in g kg^{-1} was: Ala (12), Arg (18), Asp (34), Cys (3), Glu (54), Gly (12), His (8), Ile (13), Leu (22), Lys (18), Met (4), Phe (15), Pro (15), Thr (11), Trp (3), Tyr (11), Val (14).

The PH was applied either as foliar spray or substrate drench (**Supplementary Figure 1B**) as water solution containing a non-ionic surfactant Triton X-100 at 0.1%. A control group (no application) was sprayed with distilled water containing 0.1% Triton X-100. PH application was performed twice: 5 days after transplanting (DAT) referred as Treatment 1 (T1) and 12 DAT referred to as Treatment 2 (T2). For 24 hours prior to and post spraying, humidity in the cultivation chamber was kept at 85% relative humidity. For foliar spray treatments, 2 ml of PH was diluted in 500 ml distilled water with 0.1% Triton X-100 and 60 ml of solution was applied by homogenous foliar spray over the entire plant surface per plant replica. Substrate of each pot was covered with aluminium foil during and upon spraying and was removed prior to the next phenotypical analysis in PlantScreen™ Modular System. For drenching treatment, 4 ml of biostimulant was diluted in 1000 ml of 0.1% triton and 60 ml per plant replicate was applied by drenching. At both PH application times (T1 and T2), plants in control treatment and those foliarly sprayed with PH were irrigated with 60 ml of water each to avoid changes of substrate water status in comparison with plants treated by drench application of PH. Right after PH treatment, plants were taken back to FytoScope FS-WI.

High-throughput Plant Phenotyping Protocol and Imaging Sensors

Plant phenotypic measurements were performed using PlantScreen™ Modular System (PSI, Drásov, Czech Republic) installed in semi-controlled greenhouse environment conditions in PSI Research Center (PSI, Drásov, Czech Republic). The platform was operated in closed imaging loop located in climatized environment with temperature ranging between 21-24 °C. The platform is equipped with four robotic-assisted imaging units, automatic height measuring light curtain unit, an acclimation tunnel, and a weighing and watering unit. Plants placed in individual transportation disks were transported by moving belt towards individual imaging units and watering and weighing station.

Twenty-two-day-old plants were randomly distributed into three batches, each batch containing 12 plants. Plant imaging started with 22-day-old plants (1 DAT, day 1 of phenotyping) and continued for 15 days (15 DAT, day 15 of phenotyping). Plants were imaged using the following protocol. Briefly, plants were manually transferred from the climate-controlled growth chamber to the manual loading station of the PlantScreen™ Modular System and were transported through the acclimation tunnel with automatic height measuring unit. Prior to the imaging, plants were dark adapted in acclimation tunnel for 15 minutes. Each batch of plants was automatically phenotyped for around 30 minutes by using kinetic chlorophyll fluorescence imaging measurement for photosynthetic performance analysis, top view and multiple angle side view Red Green Blue (RGB) imaging for morphological, growth and color analysis, and finally thermal imaging unit for plant surface temperature quantification (**Supplementary Figure 1A)**. Following the imaging, plants were automatically transported to watering and weighting unit for maintaining precise soil water holding capacity. After completion of the phenotyping protocol, plants were manually moved back to the climate-controlled growth chamber until the subsequent phenotyping day. We used the automatic timing function of PlantScreen™ Scheduler (PSI, Drásov, Czech Republic) to schedule the initiation of the phenotyping protocol at the same time of the diurnal cycle (after three hours of illumination in the climate-controlled growth chamber). The phenotyping data were acquired twice prior to biostimulant application in days 1 and 3 (pre-T measurements); three times post first biostimulant application in days 6, 8, 10 (post T1 application) and twice post second biostimulant application in days 13 and 15 (post T2 application). The acquired images were automatically processed using Plant Data Analyzer (PSI, Drásov, Czech Republic) and the raw data exported into CSV files were provided as input for further analysis.

Kinetic Chlorophyll Fluorescence Measurement

Kinetic chlorophyll fluorescence (ChlF) measurements were acquired using an enhanced version of the FluorCam FC-800MF pulse amplitude modulated (PAM) chlorophyll fluorometer (PSI, Czech Republic) with an imaging area in top view position of 800 × 800 mm, as described in Tschiers et al. (2017). We assessed the photosynthetic performance in the plants by quantifying the rate of photosynthesis at different photon irradiances using the light curve protocol (Henley, 1993; Rascher et al., 2000). The measuring protocol described previously (Awlia et al., 2016) was optimized for the tomato plants from early to later developmental stage. For the light curve characterization, three actinic light irradiances (Lss1- 170 µmol photons m^{-2} s^{-1}, Lss2 – 620 µmol photons m^{-2} s^{-1}, Lss3 - 1070 µmol photons m^{-2} s^{-1}) were used with a duration of 30 seconds in order to quantify the rate of photosynthesis.

From the fluorescence data, a range of parameters was extracted as described in detail by Awlia et al. (2016). Additionally, 1-qP was calculated that reflects proportion of PSII reaction centers that are closed (Maxwell and Johnson, 2000; Na et al., 2014).

Visible RGB Imaging

To assess digital biomass of the plants, RGB imaging was done from top view (RGB2) and side view from multiple angles (RGB1). RGB imaging unit is light isolated box equipped with turning table with precise angle positioning, two RGB cameras (top and side) mounted on robotic arms and each supplemented with LED-based lighting source to ensure homogenous illumination of the imaged object.

Projected shoot area parameter, together with regularly determined weight of the plants, was used to estimate transpiration use efficiency (TUE). TUE was defined by the ratio of aboveground biomass produced per unit of water transpired and depends on the characteristics of the plants and on the environment where the plants grow (Al-Tamimi et al., 2016). TUE was estimated from transpiration defined by measures of water loss and growth from PSA by plant-specific pixel counts quantification.

Thermal Imaging

To assess leaf surface temperature of the plants, thermal imaging unit based on side view imaging was used. Thermal imaging unit incorporated in the PlantScreen™ System consists of light isolated box with one side view camera mounted on robotic arm, precise plant positioning and background heated wall with integrated temperature sensor to increase contrast for image processing step. Imaged area is 1205 mm × 1005 mm (height × width). To assess spatio-temporal variations in temperature over plant surface we used FLIR A615 thermal camera with 45° lens and resolution 640 × 710 pixels, with high-speed infrared windowing option and <50 mK thermal sensitivity (FLIR Systems Inc., Boston, MA, USA). The thermal images were acquired in line scan mode with each image consisting of 710 pixels with scanning speed of 50 Hz (lines per second). Thermal images were acquired in darkness. Image acquisition conditions, plant positioning and camera settings were fixed throughout the experiment. Leaf surface temperature of each plant was automatically extracted with Plant Data Analyzer software (PSI, Drásov, Czech Republic) by mask application, background subtraction and pixel-by-pixel integration of values across the entire plant surface area. To minimize the influence of the environmental variability and the difference in the image acquisition timing among individual plants, the raw temperature of each plant (°C) was normalized by the actual background temperature and expressed as ΔT (°C).

Sample Harvest and Metabolomic Analysis

Plant material was harvested 19 DAT for metabolomic analysis by harvesting and combining the 3rd and 4th fully expanded leaves from the top of each plant. Additionally, final biomass of each plant was determined by measuring fresh weight and dry weight of remaining shoot.

Plant samples were homogenized in pestle and mortar using liquid nitrogen, and then an aliquot (1.0 g) was extracted in 10 mL of 0.1% HCOOH in 80% aqueous methanol using an Ultra-Turrax (Ika T-25, Staufen, Germany) (Borgognone et al., 2016). The extracts were centrifuged (12000 × *g*) and filtered into amber vials through a 0.22 μm cellulose membrane for analysis. Thereafter, metabolomic analysis was carried out through a UHPLC liquid chromatographic coupled to a quadrupole-time-of-flight mass spectrometer (UHPLC/QTOF-MS). The metabolomic facility included a 1290 ultra-high-performance liquid chromatograph, a G6550 iFunnel Q-TOF mass spectrometer and a JetStream Dual Electrospray ionization source (all from Agilent technologies, Santa Clara, CA, USA). The untargeted analysis was

carried out as previously described (Rouphael et al., 2016). Briefly, reverse phase chromatography was carried out on an Agilent Zorbax Eclipse-plus C18 column (100 × 2.1 mm, 1.8 µm) and using a 34 min linear elution gradient (5% to 95% methanol in water, with a flow of 220 µL min^{-1} at 35 °C). The mass spectrometric acquisition was done in SCAN (100–1000 *m/z*) and positive polarity.

Features deconvolution and post-acquisition processing were done in Agilent Profinder B.06. Mass and retention time alignment followed by a filter-by-frequency post-processing filter were done to retain only those compounds that were present in >75% of replications within at least one treatment. Compounds annotation was done using the 'find-by-formula' algorithm, i.e., using monoisotopic accurate mass, isotopes spacing and isotopes ratio, with a mass accuracy tolerance of < 5 ppm. The database PlantCyc 12.5 (Plant Metabolic Network, http://www.plantcyc.org; released April 2018) was used for annotation purposes. Based on the strategy adopted, identification was carried out according to Level 2 (putatively annotated compounds) of COSMOS Metabolomics Standards Initiative (http://cosmos-fp7.eu/msi). The classification of differential compounds into biochemical classes was carried following PubChem (NCBI, https://pubchem.ncbi.nlm.nih.gov/) and PlantCyc information.

Data Management and Statistical Analysis

For automatic image data processing, we used the data processing pipeline Plant Data Analyzer (PSI, Drásov, Czech Republic), which includes pre-processing, segmentation, feature extraction and post-processing of acquired images. Values for projected shoot area were calculated from images taken in the visible light spectrum and correspond to plant volume estimation. The plant volume was used as a proxy for the estimated biomass of the plants. Data were processed using MVApp application. Statistical differences between treatments and time points were determined by one-way analysis of variance (ANOVA) with *post hoc* Tukey's Honest Significant Difference (HSD) test (P-value < 0.05) performed using appropriate scripts in MVApp tool. Data are displayed as mean ± standard error of the six independent plants per treatment.

Elaboration of metabolomic data was carried out using Mass Profiler Professional B.12.06 as previously described (Salehi et al., 2018). Briefly, compounds' abundance was Log2 transformed and normalized at the 75th percentile, then baselined against the median. Unsupervised hierarchical cluster analysis was carried out using the fold-change based heatmap, setting similarity measure as 'Euclidean'

and 'Wards' linkage rule. Thereafter, the dataset was exported into SIMCA 13 (Umetrics, Malmo, Sweden), Pareto-scaled and elaborated for Orthogonal Projections to Latent Structures Discriminant Analysis (OPLS-DA). This latter supervised statistic allowed separating variance into predictive and orthogonal (*i.e.*, ascribable to technical and biological variation) components. Outliers were excluded using Hotelling's T2 and adopting 95% and 99% confidence limits, for suspect and strong outliers, respectively. Model cross validation was done through CV-ANOVA ($p < 0.01$) and permutation testing (N=300) was used to exclude overfitting. Model parameters (goodness-of-fit R^2Y and goodness-of-prediction Q^2Y) were also produced. Finally, Variable Importance in Projection (VIP) analysis was used to select the metabolites having the highest discrimination potential. A subsequent fold-change analysis, as well as two-way ANOVA, were finally performed from VIPs to identify extent and direction of the changes in accumulation related to the use of the biostimulants.

Chemical Similarity Enrichment Analysis (ChemRICH) was finally performed on VIP metabolites to critically highlight the chemical nature of the discriminant compounds, as previously described (Showalter et al., 2018). Such enrichment analysis is based on chemical similarities and used Tanimoto substructure chemical similarity coefficients to cluster metabolites into non-overlapping chemical groups. In our elaborations, OPLS-DA VIP scores were used instead of individual p values, and the regulation (up or down accumulation) of discriminant metabolites was compared across treatments following chemical enrichment. The online web-app tool (http://chemrich.fiehnlab.ucdavis.edu) was used for this analysis.

RESULTS

Advanced Integrative Simultaneous Analysis of Morpho-Physiological Traits

Integrative phenotyping facilities provide an opportunity to combine various methods of automated, simultaneous, non-destructive analyses for assessment of plant growth, morphology and physiology. Here we used the PlantScreen^{TM} Modular System (PSI, Czech Republic) available in PSI Research Center (Drásov, Czech Republic) for simultaneous analysis of multiple morpho-physiological traits in tomato plants treated with plant-derived protein hydrolysate (PH) biostimulant substances (**Supplementary Figure 1A**). Tomato plants were cultivated in control conditions and were phenotyped by using RGB imaging to capture plant growth dynamics, morphology and color, by chlorophyll

fluorescence (ChlF) imaging to quantify photosynthetic performance and by thermal imaging to analyze leaf surface temperature prior to and following the PH treatment (**Figure 1**). Finally, automated watering and weighing unit was used to maintain constant low water availability conditions in the tomato plants treated with PH by both drenching and spraying application (**Supplementary Figure 1B**).

Visible RGB Imaging to Assess the Effect of PH on Plant Growth Dynamics

Visible RGB digital color imaging was used for the assessment of range of visual traits in control plants (no application) and plants treated with PH by either drenching (drench application) or spraying application (foliar application) (**Figures 1A, B**). RGB imaging was used to quantify the effect of the PH on growth status, biomass accumulation and color of tomato plants cultivated under limited water availability condition (**Figure 2A**). Simple image stacks acquired from top view and two side view images were used to extract and calculate shoot volume as proxy of shoot digital biomass and quantify shoot color throughout the cultivation period. The morphological traits were assed dynamically and were used to calculate growth rates (**Figure 2B**).

The analysis of the above-mentioned traits revealed that tomato plants cultivated under low water availability conditions and treated with PH either by spraying or drenching grew better than control plants. The best performing plants treated with PH were those where PH was applied as substrate drench. At the end of the phenotyping period the digital shoot biomass was significantly increased (**Figure 2A; Supplementary Tables 1, 2 and 3**) as well as the height and width of the plants (**Supplementary Tables 4 and 5**). In addition, the growth rate calculated over the entire phenotyping period was also strongly enhanced in drench treated plants compared to foliarly sprayed ones under water limited availability (**Figure 2B**) suggesting that overall growth performance of the plants was improved following the drenching application of PH. The image-based data could be further confirmed by destructive plant biomass assessment as both fresh and dry weight of the PH-treated plants harvested at the end of the experiment was increased (**Supplementary Figure 2A**). Measurements of projected shoot area obtained using HTP imaging approach were strongly correlated with fresh and dry weights of the plants and there was no indication of any deviation from a linear relationship even at the highest biomasses measured in this experiment (**Supplementary Figures 2B and 2C**).

Results

The variation in shoot color of the tomato plants over the phenotyping period was assessed by quantification of greenness hue abundance from the color segmented RGB images (**Supplementary Figure 3**). The analysis algorithms were calibrated by using RGB images from all treatments and all measurements as described previously (Awlia et al., 2016). Some minor changes were observed in the analyzed green hues, but no clear trend could be observed except of slight increase in darker green hues at the end of phenotyping period for drench application variant (**Supplementary Table 6**).

Mining the Biostimulant Action on Photosynthetic Performance

To assess the effect of PH application on photosynthetic performance of tomato plants in water limiting conditions, chlorophyll fluorescence measurements were acquired using automated chlorophyll fluorescence imaging set-up (**Figure 1C**, **Supplementary Figure 1**). The rate of photosynthesis at different photon irradiances was quantified using the light curve protocol reported by Henley (1993) and Rascher et al. (2000). From the measured fluorescence transient states, the basic ChlF parameters were derived (i.e., F_o, F_m, F_t, F_v), which were used to calculate range of parameters characterizing plant photosynthetic performance (i.e., F_v/F_m, NPQ, qP, ΦPSII) (for overview refer to Paul et al., 2011; Awlia et al., 2016; Tschiersch et al., 2017). In addition, 1-qP and ETR parameters were calculated, which refer to proportion of closed PSII reaction centers (Maxwell and Johnson, 2000) and photosynthetic electron transport rate of photosystem II and indicates the efficiency of linear electron flow route in the photosynthetic machinery for producing energy-rich molecules ATP and NADPH, respectively.

Few of the parameters were selected to dynamically characterize the photosynthetic function of PSII in the tomato plants prior to and after the biostimulant treatment under limited water availability (**Figure 3**); the maximum quantum yield of PSII photochemistry in the dark-adapted state (F_v/F_m), the photochemical quenching coefficient that estimates the fraction of open PSII reaction centers (qP), steady-state non-photochemical quenching (NPQ) and electron transport rate (ETR) correlating to the quantum yield of the CO_2 assimilation mechanisms and to the overall photosynthetic capacity of the plants (Genty et al., 1989). No significant changes of those parameters between the control and PH-treated plants (**Figure 3, Supplementary Table 7**) were recorded during the phenotyping period. However, minor dynamic changes in lower actinic irradiance of the 1-qP parameter were observed at the end of the phenotyping period on day 15 (**Supplementary Figure 4**). 1-qP was used as indicator of closed PSII reaction center and as an estimate of the relative PSII excitation pressure to which an

organism is exposed (Maxwell and Johnson, 2000) suggesting that PH application induced a higher redox status than control treatment resulting in slightly lowered electron transport rates (ETR) (**Supplementary Figure 4**).

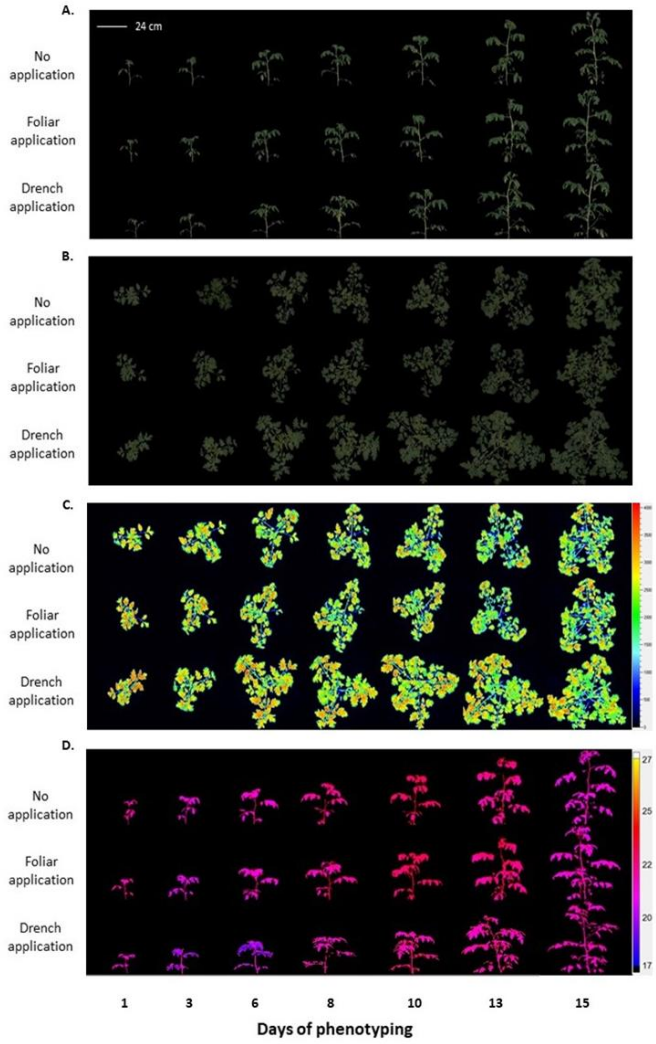

Figure 1| Non-invasive image-based phenotypical analysis of PHs treated and control tomato plants grown under water limiting conditions by using PlantScreen™ Modular System. *A) Color segmented side view RGB images of the tomato plants over the time of phenotyping period (D1-D15). B) Color segmented top view RGB images of the tomato plants. C) False-color images of maximum fluorescence value (Fm) of tomato plants captured by kinetic chlorophyll fluorescence imaging. D) False color side view images of plant leaf surface temperature captured by thermal camera.*

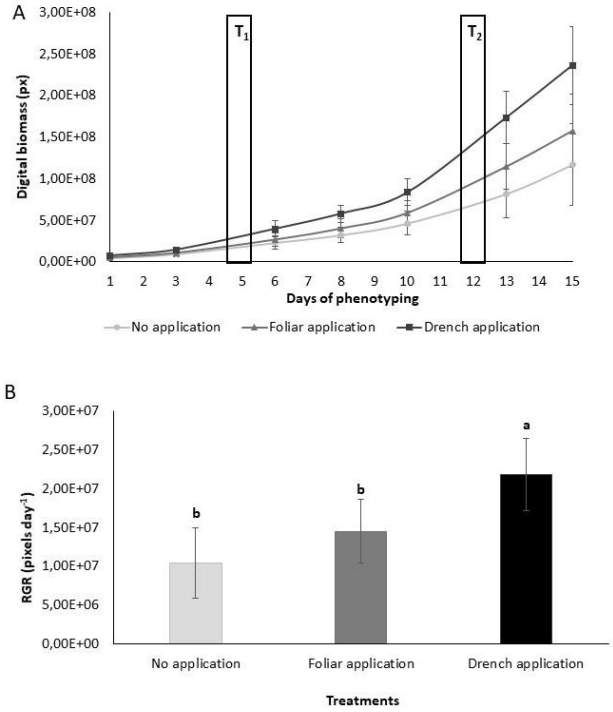

Figure 2| Growth performance of PHs treated and control tomato plants. A) Digital biomass quantified over time of phenotyping period. *Values represent the average of six biological replicates per treatment. Error bars represent standard deviation. T1 and T2 correspond to days of protein hydrolysate application by foliar spraying or substrate drench. B) Comparison of relative growth rate for the different treatments quantified over phenotyping period following the protein hydrolysate treatments. Values represent the average of six biological replicates per treatment. Error bars represent standard deviation. Different letters indicate significant difference according to one-way ANOVA post-hoc Tukey's test ($p<0.05$).*

Thermal Infrared Imaging for Monitoring Shoot Temperature and Leaf Transpiration

Plant water status is determined by the equilibrium between root water uptake and shoot transpiration (Berger et al., 2010). Under limited water availability in tomato seedlings, triggering of shoot transpiration and root respiration has been carried out by commercial PH provided to the plant by foliar and drenching application, respectively. Imaging thermography approach was used to measure the whole plant temperature in automated manner and the image data were utilized to assess the leaf transpiration of plants (**Figure 1D**).

To minimize the influence of the environmental variability and the difference in the image acquisition timing among individual plants, the raw temperature of each plant (°C) was normalized by the actual background temperature and expressed as ΔT (°C) (Paul et al., 2016). Experimental data showed that leaf surface temperature of the tomato plants was not influenced by PH treatment, and no difference compared to control plants was observed throughout entire phenotyping period (**Supplementary Figure 5A**). TUE increased in drenching PH-treated plants in comparison with foliar and control treatments (**Supplementary Figure 5B**).

A strong correlation was reported between plant transpiration rate and stomatal conductance (Berger et al., 2010). As stomatal conductance is the measure of the CO_2 entering or leaving the stomata of a leaf, higher TUE observed in PH-drench application suggests that more CO_2 might get fixed and generate more organic matter thereby increasing in biomass compared to other treatment methods.

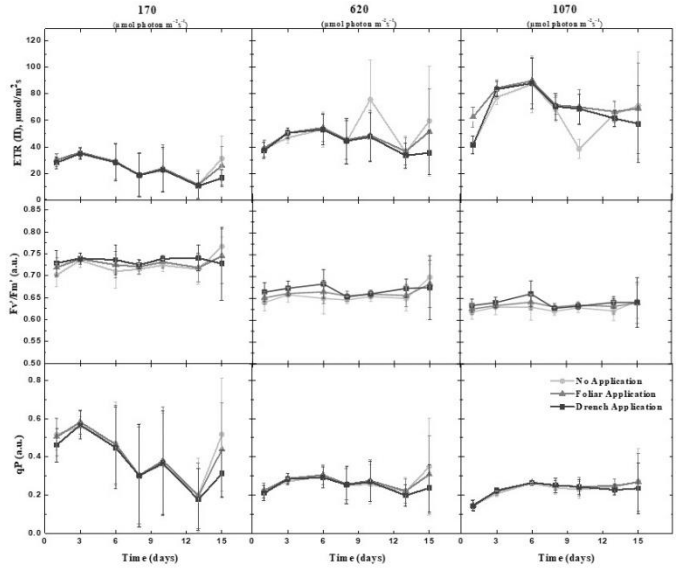

Figure 3| Photosynthetic performance of the tomato plants treated or untreated with protein hydrolysate*. Range of photosynthetic parameters were deduced from kinetic chlorophyll fluorescence imaging prior to and following the PH treatments. The photochemical quenching coefficient that estimates the fraction of open PSII reaction centers (qP), maximum quantum yield of PSII photochemistry for the dark-adapted state ($F_{V'}/F_{M'}$), and electron transport rate (ETR) were measured using the light curve protocol. Data are mean of six independent plants per treatment. Measurements at three actinic photon irradiance intensities were acquired. Measurements were taken at 170, 620, and 1,070 µmol photons m^{-2} s^{-1}, respectively.*

Metabolomic Profiles

An untargeted UHPLC/QTOF-MS metabolomic analysis was carried out to elucidate the molecular mechanisms underlying the effect of PH application on leaves of tomato plants grown under limited

water availability. Multivariate statistics from the metabolomic dataset pointed out similarities/dissimilarities among phytochemical profiles. The use of an untargeted profiling followed by annotation on the basis of a comprehensive database (namely PlantCyc) produced over 1900 compounds annotated, overall. These compounds exhibited a large chemical diversity and included metabolites from a wide range of biochemical classes and metabolic processes.

The first step of interpretation was a hierarchical clustering, produced from the fold change-based heatmap according to Euclidean distances. This unsupervised clustering approach allowed describing similarities/dissimilarities among treatments, as shown in **Figure 4**. As provided, two main clusters were generated-one comprising drench application and the other including foliar application and control. In this latter cluster, two distinct sub-clusters could be identified, thus indicating different metabolic profiles between foliar application of the biostimulant and control plants. Even though the application of PHs resulted in distinctive profiles in tomato under limited water availability, the naïve (unsupervised) hierarchical clustering of metabolomic signatures suggested that the application method of the PH was an additional and relevant factor determining the actual difference in such phytochemical profiles.

A consistent outcome could be produced through the supervised OPLS-DA multivariate modelling. This analysis allowed separating predictive and orthogonal components (i.e., those components ascribable to technical and biological variation) of variance. Therefore, OPLS-DA effectively discriminated among the three groups into the score plot hyperspace. The OPLS-DA score plot (**Figure 5**) indicated a complete separation among control, foliar and drench applications. The model parameters of the OPLS-DA regression were excellent, being R^2Y and Q^2Y 0.99 and 0.94, respectively. The model was validated (CV-ANOVA P = $2.47\ 10^{-10}$) and overfitting could be excluded through permutation testing (N = 100). Validation through misclassification table indicated a 100% model accuracy (Fisher's probability $3.5\ 10^{-7}$). Furthermore, the Hotelling's T2 allowed excluding suspect and strong outliers. Given the validated model outcomes, the variable selection method called VIP (Variable Importance in Projection) was used to identify compounds explaining the differences observed. The discriminating compounds having a VIP score > 1.25 were exported and subjected to fold change analysis to identify the trends of regulation altered by the treatments. Thereafter, one-way ANOVA (Tukey post hoc) was used to describe significance of the differences. The discriminant compounds, together with their VIP score, P and fold change values, were grouped into chemical classes to facilitate the discussion of results (**Table 1**).

Notably, relatively few biochemical classes included the most of discriminant metabolites. In more details, lipids (including membrane lipids, sterols, carotenoids and other terpenes) were the most represented class of compounds among VIP discriminants, followed by phytohormones, polyamine conjugates, prenyl quinones and chlorophyll-related compounds. Among hormones, brassinosteroids, indole-conjugates, salicylate, cytokinins and two gibberellins were identified among discriminant compounds among the treatments (**Table 1**). Furthermore, abietane diterpene resin acids, as well as pteridins and few other compounds could be outlined by VIP analysis. Interestingly, two osmolytes (trehalose and glycine betaine) were identified among VIP discriminants (**Table 1**).

The following chemical enrichment analysis carried out in chemRICH highlighted sterols (cholestanes, cholestadienols, and hydroxycholesterols), carotenoids, unsaturated fatty acids and phosphatidic acids, terpenes and coproporphyrins as the most represented chemical groups (**Supplementary Figure 6**). The analysis, carried out separately for each application method (foliar or drench as compared to control), represented differences in accumulation for the selected metabolites. Most of the classes reported exhibited a down accumulation following biostimulants treatment, as compared to control, except for terpenes (foliar application treatment) and unsaturated fatty acids (drench application treatment).

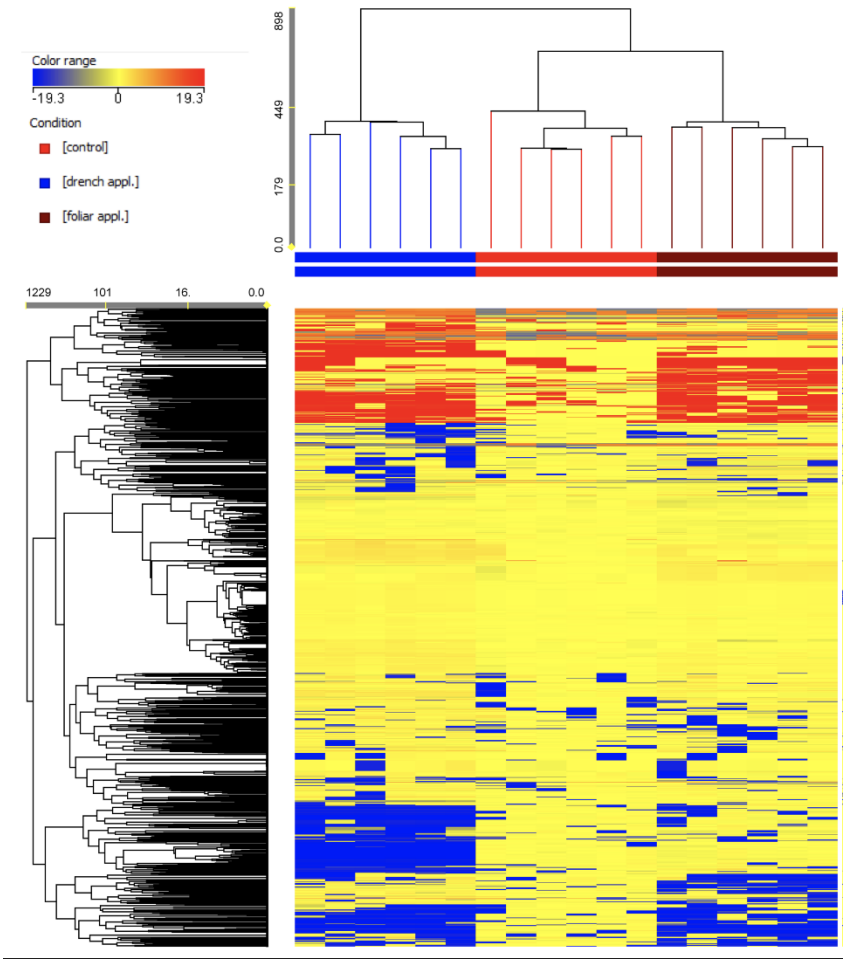

Figure 4*| Unsupervised hierarchical cluster analysis (Euclidean similarity; linkage rule: Ward's) carried out from metabolite profiles in tomato leaves, as gained from UHPLC/QTOF-MS untargeted metabolomics. Compounds intensity was used to produce fold change-based heat maps, based on which clustering was done.*

DISCUSSION

Biostimulant effect on sink and source organs is clearly visible in this study. PH biostimulant is directly entering sink areas like the roots through drenching application, while the same biostimulant, foliarly sprayed, directly enters the source region, the shoot and leaves. This may be reflected in photosynthetic and physiologic functions, differently. Regulation of stomatal function is an important mechanism in dealing with the adverse consequences of limited water availability. The typical response of plants to water limitation is stomatal closure through which the amount of water loss through transpiration can be decreased. On the other hand, water stress-induced closing of stomata also limits CO_2 uptake; therefore, it decreases the efficiency of net photosynthesis. Drenched PH application affected the physiological and

metabolic activity of plants. This could be due to enhanced stomatal conductance activity of drench application of PH through sink region. Moreover, tomato plants drenched with PH obtained a more favourable balance between carbon gain and water loss as shown by the increase of TUE (**Supplementary Figure 5B**). The reduced CO_2 uptake imposed by limited water availability causes an imbalance between PSII activity and the following carbon assimilation via the Calvin cycle, thus increasing the excitation energy on PSII and inducing photodamage (Baker and Rosenqvist, 2004).

Furthermore, it is known that the water-related osmotic stress generates a secondary oxidative stress. Reactive Oxygen Species (ROS) are produced via incomplete reduction of oxygen ($O_2^{\bullet-}$) and are known as signaling molecules integrated with hormone signaling networks (Foyer, 2018). As provided in **Table 1**, the specific application mode for the PH biostimulant imposed a wide variation of phytohormones profile. Two brassinosteroids (teasterone and cathasterone), a class of sterol-like hormones linked to several signaling networks including abiotic stress response, cell wall development and lignification, were detected. In more detail, brassinosteroids are reported to be involved in water stress resistance and osmotic stress-induced stomatal closure as well as to mediate ROS formation, jasmonate signaling and abscisic acid (ABA) response (Lee et al., 2018; Lucini et al., 2018). ABA and cytokinins antagonistically regulate environmental stress responses in plants, and their integrated and coordinated action modulates drought stress response (Huang et al., 2018). Indeed, cytokinins were down-accumulated, following both foliar and drench application. In plants, cytokinin signaling involves a canonical two-component system which comprises histidine kinases and histidine phosphotransfer proteins. Considering that cytokinin signaling components have been shown to act as negative regulators of plant tolerance to limited water availability (Huang et al., 2018), the trend observed following biostimulants application might represent a significant contribution in water stress resistance. Salicylic acid is another phytohormone playing a pivotal role in mediating water stress response via modulation of ROS production and redox state (La et al., 2019). Salicylic acid together with jasmonate have also been found to enhance water stress tolerance in plants (Li et al., 2018). The application of the PH biostimulant imposed a marked up-accumulation of salicylate, thus potentially modulating with ROS accumulation, ROS-mediated signaling and tolerance to low water availability. Indeed, salicylate mediates redox balance with an antagonistic depression of abscisic acid (La et al., 2019). Auxins are well-known phytohormones that promote root initiation and delay plant senescence (Li et al., 2018); interestingly, two conjugated forms (*i.e.*, storage forms) of indoleacetic acid were found down-accumulated following both PH treatments.

Besides affecting hormones profile, limited water availability conditions impair the consumption of reduction equivalents for CO_2 fixation, thus resulting in an oversupply of NADPH. Therefore, metabolic processes are expected to push toward the synthesis of highly reduced compounds (Radwan et al., 2017). With this regard, the increase in farnesyl diphosphate and triterpenes is not surprising. Consistently, Nasrollahi et al. (2014) reported a drought-induced accumulation of triterpenes.

Several other lipids, including membrane lipids and carotenoids, were modulated by biostimulant application under limited water availability conditions. Although a clear trend could not be outlined, membrane lipids are known to be altered under plant stress conditions and to play a role in plant adaptation to stress (Allakhverdiev et al., 2001; Lucini et al., 2015; Rouphael et al., 2016). These membrane components are involved in the production of signaling molecules and they are regulated by plant signaling under abiotic stress (Hou et al., 2016). Indeed, lipid-dependent signaling cascades contribute to trigger plant adaptation processes (Hou et al., 2016).

In the current study, hydroxycinnamic amides (two tyramine derivatives, a serotonin and a spermidine conjugates) were also induced by biostimulants application. This accumulation was observed for tyramine conjugates. It is interesting to note that biogenic amines and their hydroxycinnamic amides act in plants by interacting with phytohormone crosstalk together with mediating root growth and ROS signaling (Mukherjee, 2018). In particular, tyramine hydroxycinnamic amides are said to also stimulate wound healing and suberization processes (Voynikov et al., 2016). Nonetheless, exogenous polyamines are reported to alleviate the drought-induced detrimental effects as well as to alter auxins, zeatin, gibberellins, salicylic acid and jasmonate (Li et al., 2018). Abietane diterpene resin acids were also stimulated by the treatment, in particular concerning palustric acid intermediates. These diterpenes are reported to function as antioxidants to protect membranes from oxidative stress (Munné-Bosch et al., 1999) and to display antibacterial and antifungal activity (Helfenstein et al., 2017).

An osmolyte, namely the trehalose, was found to be up-accumulated following biostimulants treatment under water scarcity. Indeed, the accumulation of sugars, predominantly trehalose, is a known protection mechanism in plants experiencing abiotic stresses, since they contrast protein denaturation, scavenge free radicals, and stabilize biological membranes (Asaf et al., 2017; Farooq et al., 2018). Trehalose, in particular, is able to bind to the polar region of membranes to scavenge the ROS (Farooq et al., 2018).

The involvement of prenyl quinones, generally found up-accumulated, suggests the enrollment of both signaling and antioxidant functions under oxidative stress. The chloroplastic pool of these compounds is related to the oxidation by the cytochrome *b6f* complex as well as to other thylakoid electron transfer pathways. The modulation of such prenyl quinones has been related to their function as signaling molecules in chloroplast-to-nucleus signal transduction and is involved in plant acclimation to stress (Kruk et al., 2016). Finally, among others, intermediates (tetrapyrrole coproporphyrins) and catabolites (pheophorbide *a*) of chlorophyll biosynthetic pathway(s) were identified among VIP discriminants. The formers were down-accumulated in treated plants, whereas an opposite trend could be observed for pheophorbide *a*. Ghandchi et al. (2016) reported that the degradation of chlorophyll to non-fluorescent pigments is a transcriptionally regulated intricate process that varies during the plant life cycle. These authors also suggested that the activity of the degrading enzyme pheophorbide *a* oxygenase (PAO) is altered by drought. Nonetheless, it is important to consider that chlorophyll intermediates play a pivotal role also in ROS signaling and production. Photoreduction of oxygen to the superoxide radical is related to a reduced electron transport in PSI and to a reaction linked to the photorespiratory cycle occurring in the peroxisome. This second process is enhanced under drought because of the limited availability of CO_2. Unlike mammals (where ROS are mainly produced in mitochondria), plants produce singlet oxygen mainly in thylakoids by chlorophyll and its tetrapyrrole intermediates in the presence of light. These compounds are partially hydrophobic and are therefore associated with the thylakoid membranes which do not form pigment protein complexes. Considering that most carotenoids are located in the pigment-protein complexes, they are spatially far from tetrapyrroles and therefore they are poorly effective in quenching their triplet states (Tripathy and Oelmüller, 2012). Therefore, coproporphyrins act as photosensitizers and their accumulation leads to light-dependent necrosis in plant (Hu et al., 1998; Ishikawa et al., 2001). On this basis, it can be postulated that the biostimulants-related down-accumulation of coproporphyrins under limited water availability can represent a key factor to mitigate ROS imbalance and to improve drought tolerance. Moreover, photosynthetic organisms can dissipate excess energy *via* non-photochemical quenching to avoid singlet oxygen formation; carotenoids play a crucial role in such non-photochemical quenching (Tripathy and Oelmüller, 2012). These findings suggest a complex and coordinated regulation of ROS under limited water availability involving both isoprenoid quinones and tetrapyrrole intermediates. Consistently, several carotenoids, as well as their epoxy- and diol-derivatives were down-accumulated in biostimulant-treated tomato plants. These

findings support and strengthen our previous evidences related to an improved capability of PH-treated tomato plants to cope with ROS-mediated oxidative stress.

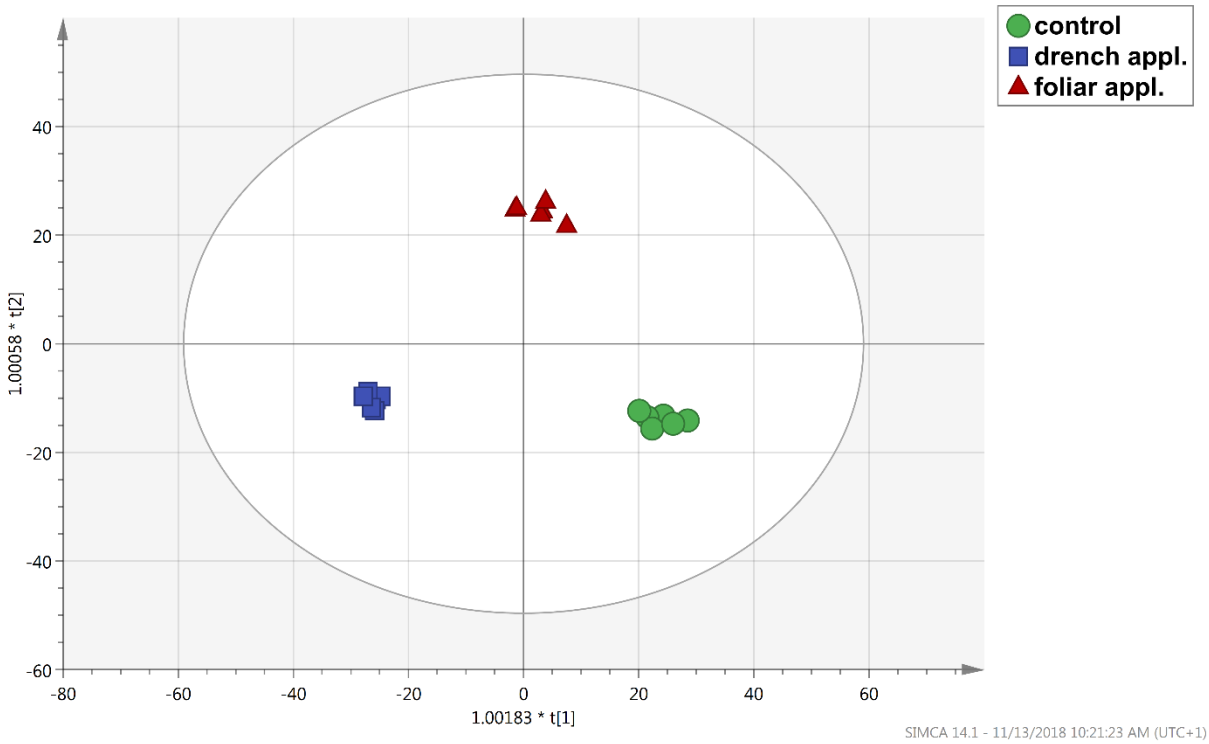

Figure 5| *Score plot of Orthogonal Projection to Latent Structures Discriminant Analysis (OPLS-DA) supervised analysis carried out from metabolite profiles in tomato leaves as gained from UHPLC/QTOF-MS untargeted metabolomics.*

CONCLUSIONS

Our findings indicate that protein hydrolysate (PH) application on tomato plants can be considered as a sustainable crop enhancement technology for agricultural productivity under water-limited conditions. Mining of variations in growth dynamics and physiological responses were clearly qualitatively and quantitatively phenotyped using high-throughput phenomic tools. Morpho-physiological data suggests that PH application, especially using substrate drench method, can be recommended as a highly sustainable approach under less water available conditions. PH application in drenching mode causes plants to transpire more and increase stomatal conductance leading to a better TUE; however light absorption parameters were unaffected by inducing higher redox status. The UHPLC-QTOF-MS metabolomic approach allowed identifying the molecular bases of the improved water stress tolerance following biostimulants treatment. Our approach identified a distinct metabolic signature imposed by

drench or foliar application of the PH under limited water availability in tomato, as highlighted by both unsupervised hierarchical clustering and supervised discriminant analysis. These outcomes supported and integrated phenomic outcomes, indicating the biochemical processes implicated in the enhanced tolerance to limited water availability following biostimulants application. In more detail, a wide and organized range of metabolic processes was involved in response of tomato plants to PH treatments. Phytohormone profile was significantly affected, even though the most represented among differential compounds were lipids (including membrane lipids, sterols and terpenes). As a general overview, PH-treated tomato plants exhibited an improved tolerance to ROS-mediated oxidative imbalance. Such tolerance involved a coordinated action of salicylic acid, hydroxycinnamic amides signaling, carotenoids and prenyl quinones radical scavenging, as well as reduced tetrapyrrole biosynthesis.

Conflict of Interest Statement

MTr is the owner and CEO of PSI (Photon Systems Instruments), Drasov, Czech Republic, and KP is an employee of his company. KP and MS are ex and actual PhD students that conducted the experiments at PSI. HR and RC are employees of Italpollina Company (Rivoli Veronese, Italy) and (Anderson, IN 46016, United States) who provided plant-derived protein hydrolysate. The other authors (LL, YR, MC, PB, MBMM and GC) declare that the research was conducted in the absence of any commercial or financial relationships that could be construed as a potential conflict of interest.

Acknowledgements

We thank Italpollina Company (Rivoli Veronese, Italy) for providing financial support for the trial. Further, we thank Jaromír Pytela for helping with the preparation of plant material for the phenotyping experiments at Photon Systems Instruments (PSI) Research Center (Drásov, Czech Republic), Zuzana Benedikty for useful discussions during optimization phase of the phenotyping experiments at PSI (Drásov, Czech Republic) and Petr Polach for helping with raw images re-processing at PSI (Drásov, Czech Republic). This work was supported by European Union's Horizon 2020 research and innovation program under the Marie Skłodowska-Curie grant agreement No 675006.

Table 1| Metabolites discriminating biostimulant-treated tomato plants (foliar and drench application) from control; results were gained from UHPLC/QTOF-MS untargeted metabolomics followed by OPLS-DA supervised statistics. Compounds are grouped in biochemical classes and are presented with their individual VIP score and standard error (SE), as well as p value (one-way ANOVA, Bonferroni multiple testing correction) and Log of fold change values. NS: not significant (p > 0.05). Missing values denote fold-change values < 1.5.

Compound		VIP score	VIP SE	p value	Log FC (foliar appl. *vs* control)		Log FC (drench appl. *vs* control)	
Lipids	a 1-acyl-sn-glycero-3-phosphoethanolamine (n-C14:1)	1.42	0.21	1.41E-24	-17.65	down	-17.38	down
	(5Z)-(15S)-11-alpha;-hydroxy-9,15-dioxoprostanoate	1.41	0.27	1.41E-24	-19.81	down	-19.55	down
	1-palmitoyl-2-vernoloyl-phosphatidylcholine	1.39	0.20	2.48E-02	0.18	up	-8.64	down
	1-18:1-2-trans-16:1-phosphatidylglycerol	1.39	0.44	2.07E-05	-1.38	down	0.05	up
	dipalmitoyl phosphatidate	1.36	0.37	9.07E-05	0.18	up	0.38	up
	phytosphingosine 1-phosphate	1.36	0.31	6.43E-23	-0.38	down	-21.52	down
	arachidoyl dodecanoate	1.36	0.28	NS	-	-	0.20	up
	14-oxolanosterol / 4-alpha-formyl,4-beta,14-alpha-dimethyl-9-beta,19-cyclo-5-alpha-cholest-24-en-3-beta-ol	1.35	0.31	1.19E-03	0.13	up	-15.58	down
	all-trans-heptaprenyl diphosphate	1.33	0.50	3.09E-21	0.34	up	18.12	up
	sphinganine 1-phosphate	1.33	0.36	9.11E-22	-0.37	down	-21.38	down
	4-alpha-formyl-stigmasta-7,24(24^1)-dien-3-beta-ol	1.35	0.31	1.19E-03	0.13	up	-15.58	down
	stearate	1.35	0.57	5.09E-03	13.73	up	-2.40	down
	9,10-epoxy-18-hydroxystearate	1.35	0.55	NS	11.39	up	10.34	up
	(9Z)-12,13-dihydroxyoctadeca-9-enoate	1.35	0.55	2.68E-02	11.39	up	10.34	up
	1-18:3-2-18:3-monogalactosyldiacylglycerol	1.34	0.38	NS	-1.73	down	-8.88	down
	1-18:2-2-18:2-monogalactosyldiacylglycerol	1.35	0.32	NS	-1.69	down	-4.66	down
	1-18:3-2-16:2-monogalactosyldiacylglycerol	1.28	0.34	3.23E-02	-14.89	down	-3.58	down
	1-18:2-2-16:1-phosphatidate	1.31	0.17	6.84E-05	-2.95	down	-18.17	down
	vernoleate	1.38	0.33	4.67E-03	13.71	up	12.14	up
	(9R,10S)-dihydroxystearate	1.34	0.15	NS	4.32	up	-0.16	down

	(9S,10S)-9,10-dihydroxyoctadecanoate	1.34	0.15	NS	4.32	up	-0.16	down
	4-hydroxybutanoate	1.37	0.32	1.01E-08	0.14	up	3.28	up
	9-cis-10'-apo-beta-carotenal	1.27	0.44	8.61E-04	-10.72	down	-19.94	down
	farnesyl diphosphate	1.27	0.47	4.12E-05	0.63	up	1.61	up
	epsilon, epsilon-carotene-3-diol / beta-carotene 15,15' epoxide	1.31	0.42	1.57E-03	-17.52	down	-17.62	down
	all-trans-4,4'-diapolycopene	1.33	0.36	3.24E-12	0.05	up	-7.17	down
	lutein	1.24	0.35	6.84E-05	3.42	up	-15.52	down
Resin acids	palustradienal	1.51	0.37	0.00E+00	23.29	up	4.07	up
	dehydroabietadiene	1.36	0.54	3.75E-04	1.31	up	0.57	up
	levopimaradiene / palustradiene / abieta-7,13-diene	1.39	0.35	1.57E-03	1.46	up	0.22	up
Triterpenes	glycyrrhetinate / gypsogenin	1.39	0.22	3.24E-12	0.20	up	-6.76	down
	betulinic aldehyde / ursolic aldehyde / 11-oxo-beta-amyrin	1.35	0.31	1.19E-03	0.13	up	-15.58	down
Hormones	gibberellin A98	1.36	0.24	9.07E-24	0.03	up	-18.86	down
	indole-3-acetyl-phenylalanine	1.34	0.34	1.04E-21	-0.42	down	-19.73	down
	indole-3-butyryl-glucose	1.34	0.35	3.97E-22	-0.28	down	-20.55	down
	a jasmonoyl-phenylalanine	1.33	0.32	1.59E-21	-0.42	down	-20.51	down
	salicylate	1.29	0.57	NS	13.26	up	18.76	up
	dihydrozeatin-7-N-glucose / dihydrozeatin-9-N-glucose	1.29	0.35	6.30E-05	-3.68	down	-21.15	down
	isopentenyladenine-9-N-glucoside / isopentenyladenine-9-N-glucoside	1.29	0.37	6.30E-05	-3.45	down	-19.71	down
	gibberellin A4 / gibberellin A20	1.25	0.62	1.80E-03	0.77	up	0.39	up
	7-oxateasterone	1.30	0.41	2.59E-21	-	-	-20.97	down
	cathasterone	1.25	0.66	8.05E-03	2.30	up	-12.73	down
Osmolytes	alpha,alpha-trehalose	1.40	0.37	3.68E-02	14.23	up	0.62	up
	glycine betaine	1.33	0.49	1.49E-02	-0.57	down	-0.23	down
Polyamines	triferuloyl spermidine	1.28	0.18	NS	-2.29	down	-9.75	down
	feruloylserotonin	1.34	0.35	1.96E-22	-0.15	down	-19.56	down

	serotonin	1.29	0.41	3.35E-20	-0.30	down	-18.65	down
	p-coumaroyltyramine	1.31	0.46	0.001	3.51	up	-11.96	down
	sinapoyltyramine	1.34	0.18	0.001	18.77	up	0.60	up
Pteridins	2-amino-6-carboxamido-7,8-dihydropteridin-4-one	1.31	0.47	1.97E-02	9.34	up	10.70	up
	5,10-methylenetetrahydropteroyl mono-L-glutamate	1.25	0.25	6.51E-04	-6.33	down	-18.05	down
	10-methyl-5,6,7,8-tetrahydropteroylglutamate	1.37	0.41	1.91E-22	-17.33	down	-17.06	down
Chlorophyll	red chlorophyll catabolite	1.33	0.28	NS	6.73	up	20.70	up
	coproporphyrinogen III	1.32	0.40	0.001	-0.66	down	-0.87	down
	coproporphyrin III	1.34	0.42	0.001	-0.84	down	-0.54	down
	pyropheophorbide *a*	1.31	0.32	NS	0.35	up	0.83	up
	coproporphyrin I	1.26	0.72	0.001	-1.11	down	-0.99	down
Quinones	phylloquinone	1.31	0.37	NS	-	-	-5.22	down
	demethylphylloquinol	1.35	0.31	1.19E-03	0.13	up	-15.58	down
	2-heptyl-3-hydroxy-4(1H)-quinolone	1.35	0.41	NS	16.38	up	22.27	up
	3"-hydroxy-geranylhydroquinone	1.34	0.66	1.17E-04	15.86	up	0.60	up
Others	(S)-coclaurine	1.43	0.41	6.24E-05	2.20	up	1.11	up
	coumarinic acid-beta-D-glucoside	1.46	0.17	3.36E-22	-19.86	down	-0.78	down
	3-methoxy-4-hydroxy-5-hexaprenylbenzoate	1.40	0.16	7.52E-12	0.17	up	-6.09	down
	a 6-hydroxy-5-isopropenyl-2-methylhexanoate	1.39	0.25	6.70E-05	8.10	up	7.56	up
	casbene	1.39	0.35	1.57E-03	1.46	up	0.22	up
	N,N-dihydroxy-L-isoleucine	1.36	0.21	6.93E-10	-0.17	down	-2.53	down
	secologanin	1.36	0.35	8.83E-04	-0.99	down	-0.38	down
	adenosine pentaphosphate	1.35	0.28	0.00E+00	16.57	up	16.17	up
	3-hydroxy-16-methoxy-2,3-dihydrotabersonine	1.34	0.33	3.57E-22	-0.45	down	-22.12	down
	thymidine	1.34	0.52	1.30E-19	-17.85	down	-17.59	down
	L-valine	1.33	0.49	NS	-0.57	down	-0.23	down

Supplementary Figures

Suppl. Fig. 1. Schematic overview of plant handling and phenotyping protocol. A) Plant phenotyping was carried out in PlantScreen^{TM} Modular System installed in semi-controlled greenhouse environment conditions in PSI research Center (PSI, Drásov, Czech Republic). Tomato plants were transferred from controlled environment to phenotyping system and automated phenotyping protocol was initiated. Plants were regularly screened using kinetic chlorophyll fluorescence imaging unit, calibrated RGB camera for top and multiple-angle side projections and thermal imaging unit. Low irrigation level watering regime was maintained by regular weighing and watering (WW) of the plants by automated WW unit. B) Protein hydrolysate biostimulant application protocol. Tomato plants were treated with PHs either by spraying (foliar application) or by drenching (drench application). Following the PHs application, plants were transferred back to control environment and were kept in high humidity conditions for the following 24 hours.

A. Phenotyping protocol

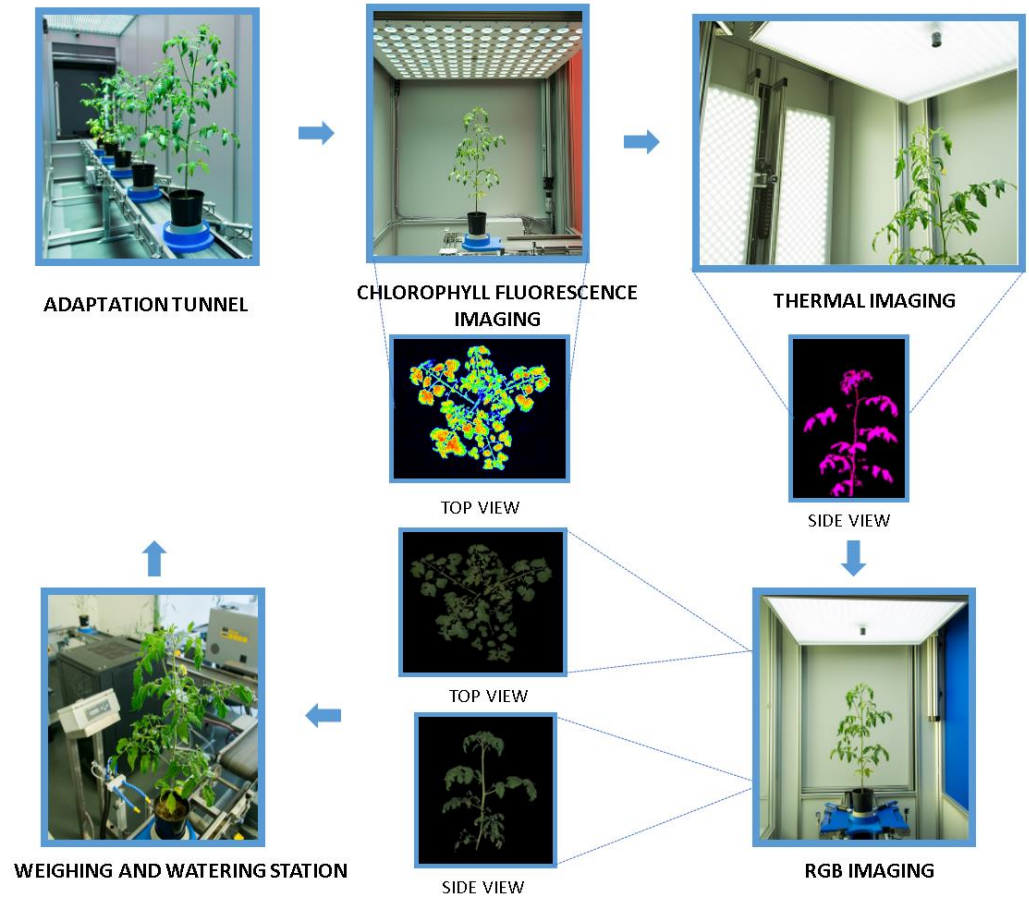

B. Biostimulant application

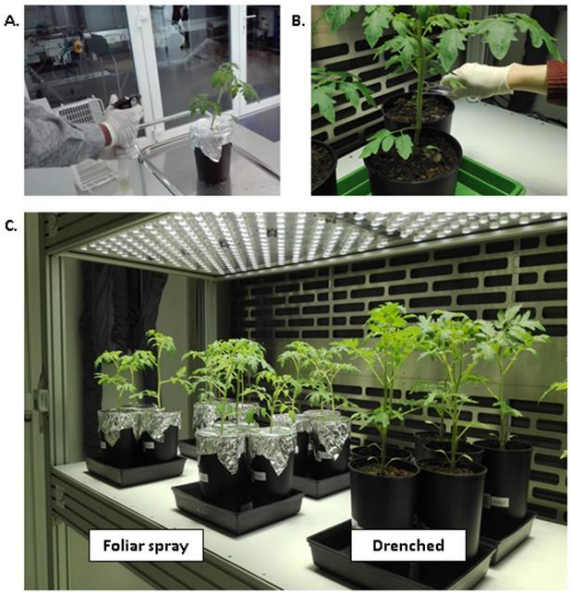

Suppl. Fig. 2. Destructive biomass quantification and correlation with digital biomass. A) Fresh and dry weight of tomato shoots harvested following the end of the phenotyping period (day 19). Values represent the average of six biological replicates per treatment. Error bars represent standard deviation. Different letters indicate significant difference according to one-way ANOVA post-hoc Tukey's test ($p<0.05$). B) Correlation of digital shoot biomass (px) acquired on day 15 with fresh weight (g) of tomato plants harvested on day 19 of phenotyping period. B**)** Correlation of digital shoot biomass (px) acquired on day 15 of phenotyping period with dry weight (g) of tomato plants harvested at the end of phenotyping period.

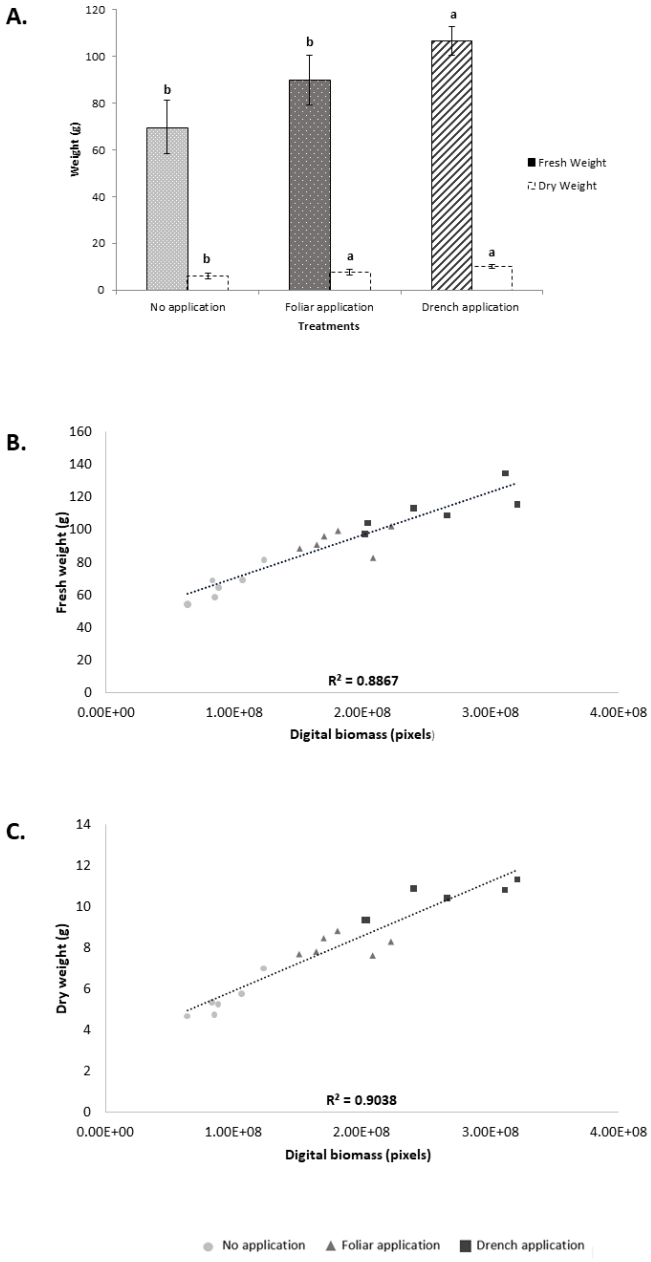

Suppl. Fig. 3. Variation in shoot colors of tomato plants prior to and following the biostimulant treatment. Dynamic relative changes in greenness hue abundance over the phenotyping period in control tomato plants and plants treated with PH either by spraying or drenching. The six most representative color hues are shown in RGB color scale as percentage of the shoot area (pixel counts) of six biological replicates per treatment.

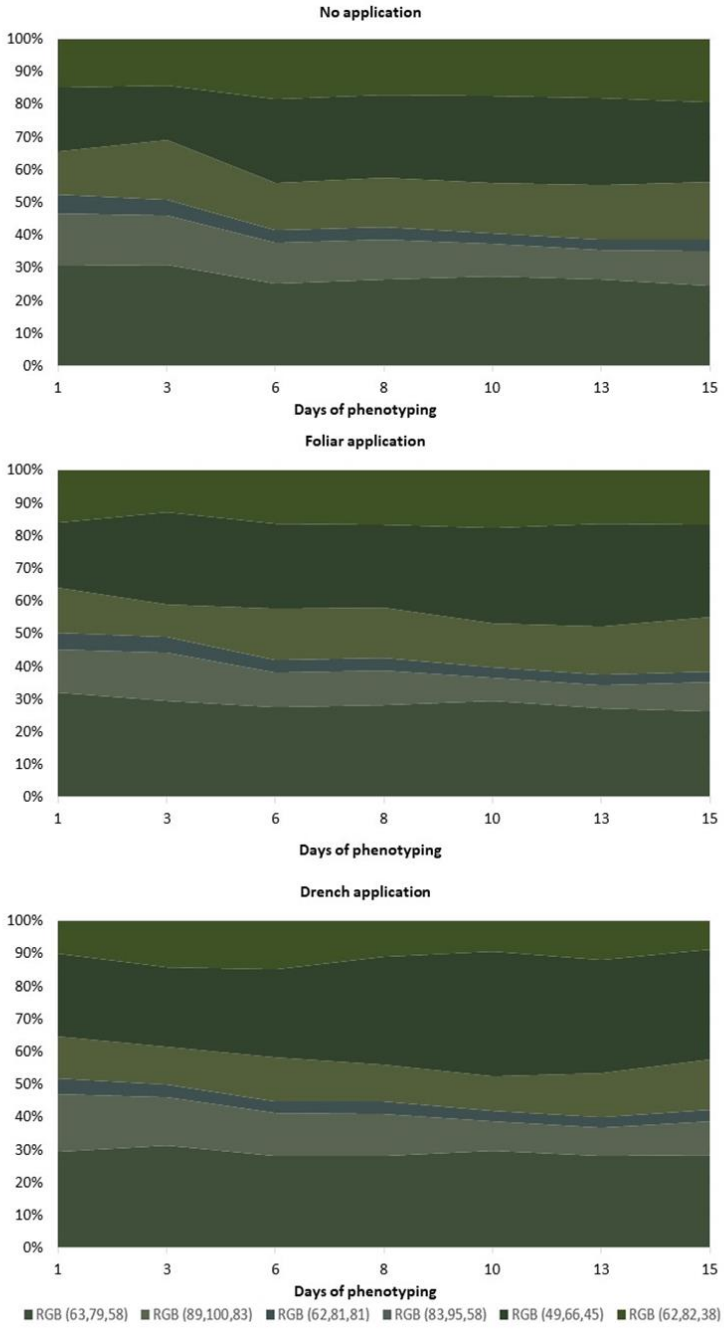

Suppl. Fig. 4. Photosynthetic performance of the tomato plants. The photochemical quenching coefficient that estimates the fraction of closed PSII reaction centers (1-qP), steady-state non- photochemical quenching (NPQ) and electron transport rate (ETR) were measured using the lightcurve protocol. Data are mean of six independent plants per treatment. Measurements at three actinic photon irradiance intensities were acquired. Measurements were taken at 170, 620 and 1070 µmol photons $m^{-2}s^{-1}$, respectively.

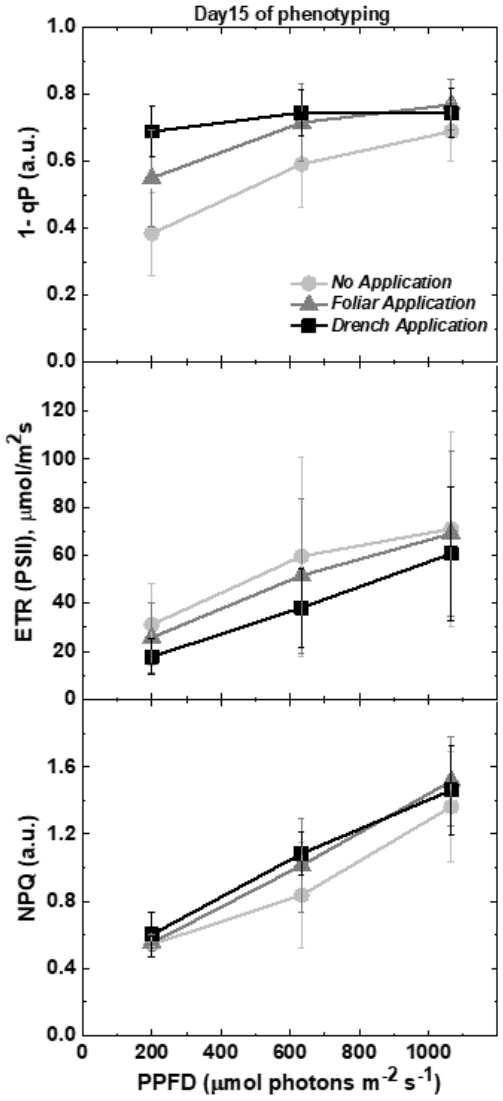

Suppl. Fig. 5. Leaf temperature quantification and estimation of transpiration use efficiency (TUE) in tomato plants prior to and following PH treatment. A) Leaf temperature was quantified by thermal imaging. To minimize the influence of the environmental variability and the difference in the image acquisition timing among individual plants raw temperature of each plant(°C) was normalized by the actual background temperature. Temperature of leaves of the plants was determined as difference relative to the surrounding air temperature and was expressed as ΔT (°C). Air temperature data were obtained from a reference surface, which is in thermal equilibrium with air in the background of the plant. B) TUE was estimated from transpiration and growth, measured by water loss and pixel counts over the whole experimental period, respectively. Values represent the average of six biological replicates per treatment. Error bars represent standard deviation. Different letters indicate significant difference according to one-way ANOVA post-hoc Tukey's test ($p<0.05$).

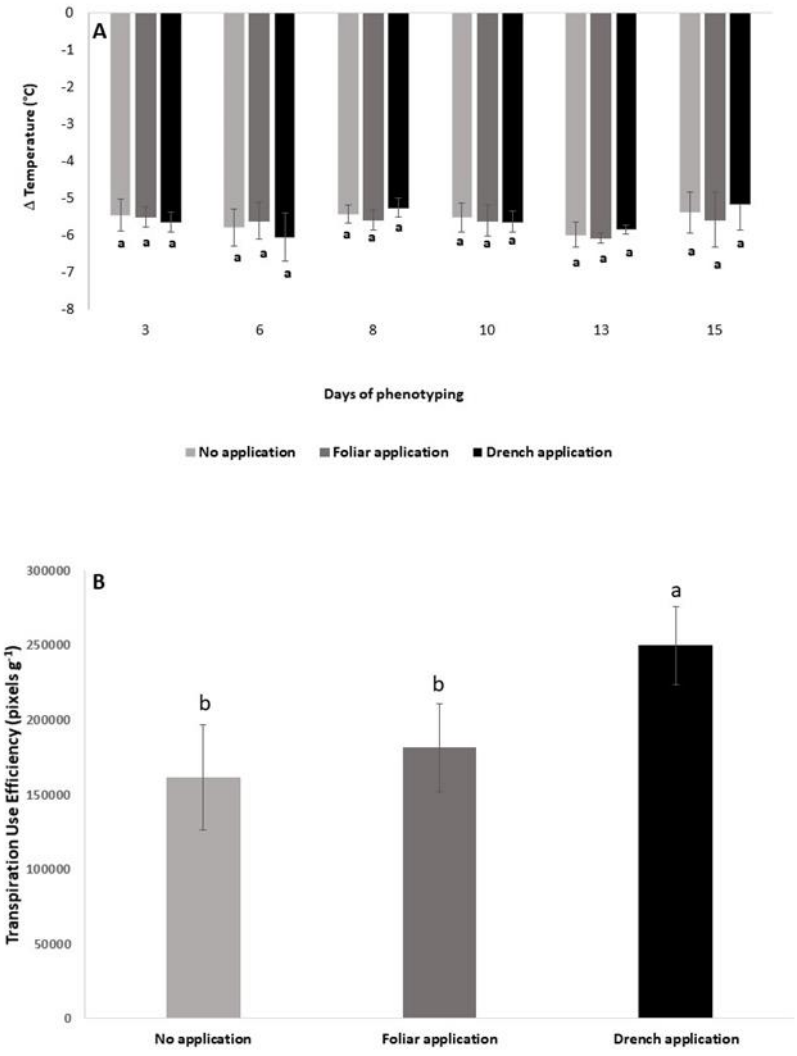

Suppl. Fig. 6. Chemical Similarity Enrichment Analysis (ChemRICH) carried out from discriminant metabolites in biostimulant-treated tomato plants. Enrichment analysis is based on chemical similarities and uses Tanimoto substructure chemical similarity coefficients to cluster metabolites into non-overlapping chemical groups. Distinct analyses were performed for foliar (A) and drench application (B).

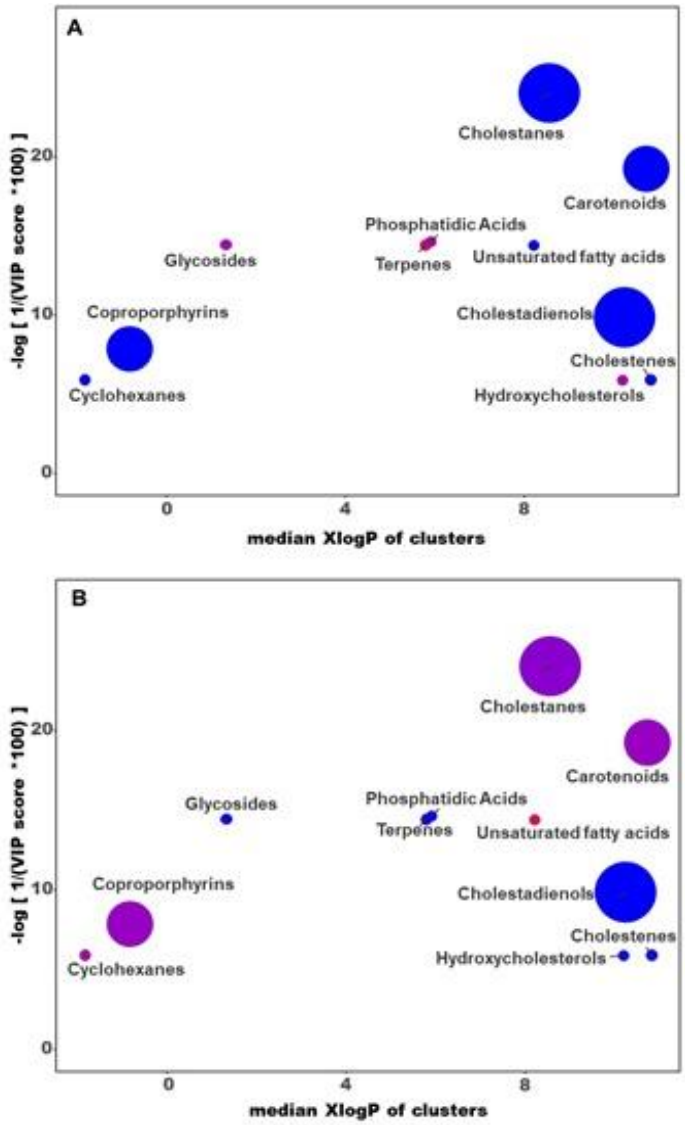

Results

Suppl. Table 1. Projected shoot area (PSA) of the tomato plants cultivated under limited irrigation and subjected to treatment by PH either by spraying or drenching. PSA values were extracted from multiple side view RGB images and are expressed as number of green pixels and represent the average of six biological replicates per treatment ± standard deviation. Within the same row and for the specified day different letters indicate significant difference according to one-way ANOVA post-hoc Tukey's test ($p<0.05$).

Treatment	Day 6		Day 8		Day 10		Day 13		Day 15	
No application	52746 ± 12318	*bc*	71389 ± 13402	*cd*	94289 ± 19056	*c*	158410 ± 35668	*d*	189604 ± 45074	*e*
Foliar application	58773 ± 13114	*abc*	82719 ± 15767	*bc*	114162 ± 21305	*bc*	186223 ± 35127	*cd*	237218 ± 41439	*cd*
Drench application	68336 ± 13632	*a*	90970 ± 10739	*b*	130816 ± 16357	*b*	224381 ± 33242	*b*	286059 ± 36138	*b*

Suppl. Table 2. Projected shoot area (PSA) of the tomato plants cultivated under limited irrigation and subjected to treatment by PH either by spraying or drenching. PSA values were extracted from top view RGB images and are expressed as number of green pixels and represent the average of six biological replicates per treatment ± standard deviation. Within the same row and for the specified day different letters indicate significant difference according to one-way ANOVA post-hoc Tukey's test ($p<0.05$).

Treatment	Day 6		Day 8		Day 10		Day 13		Day 15	
No application	23234863 ± 8513186	*b*	32552528 ± 10300538	*b*	46577667 ± 15866094	*b*	82032934 ± 32296685	*b*	117016673 ± 53533194	*b*
Foliar application	26600180 ± 8773383	*ab*	40048488 ± 12400100	*b*	58660490 ± 16185887	*ab*	114478104 ± 30378481	*b*	157341714 ± 48413891	*b*
Drench application	39638661 ± 10594869	*a*	58027767 ± 11330937	*a*	83371143 ± 17502021	*a*	173594850 ± 34176174	*a*	236193508 ± 51170025	*a*

Suppl. Table 3. Digital biomass of tomato plants cultivated under limited irrigation and subjected to treatment by PH either by spraying or drenching. Values are expressed as number of green pixels and represent the average of six biological replicates per treatment ± standard deviation. Within the same row and for the specified day different letters indicate significant difference in digital biomass, according to one-way ANOVA post-hoc Tukey's test ($p<0.05$).

Treatment	Day 6		Day 8		Day 10		Day 13		Day 15	
No application	23234863 ± 8513186	*b*	32552528 ± 10300538	*b*	46577667 ± 15866094	*b*	82032934 ± 32296685	*b*	117016673 ± 53533194	*b*
Foliar application	26600180 ± 8773383	*ab*	40048488 ± 12400100	*b*	58660490 ± 16185887	*ab*	114478104 ± 30378481	*b*	157341714 ± 48413891	*b*
Drench application	39638661 ± 10594869	*a*	58027767 ± 11330937	*a*	83371143 ± 17502021	*a*	173594850 ± 34176174	*a*	236193508 ± 51170025	*a*

Suppl. Table 4. Width of the tomato plants extracted from multiple side view RGB images of the tomato plants cultivated under limited irrigation and subjected to treatment by PH either by spraying or drenching. Values are expressed as number of green pixels and represent the average of six biological replicates per treatment ± standard deviation. Within the same row and for the specified day different letters indicate significant difference according to one-way ANOVA post-hoc Tukey's test ($p<0.05$).

Treatment	Day 6		Day 8		Day 10		Day 13		Day 15	
No application	582 ± 89	*b*	637 ± 69	*b*	672 ± 81	*b*	759 ± 86	*c*	851 ± 126	*c*
Foliar application	599 ± 85	*b*	674 ± 107	*b*	733 ± 100	*b*	861 ± 101	*b*	957 ± 116	*b*
Drench application	682 ± 105	*a*	813 ± 114	*a*	867 ± 144	*a*	1059 ± 141	*a*	1138 ± 149	*a*

Suppl. Table 5. Height of the tomato plants extracted from multiple side view RGB images of the tomato plants cultivated under limited irrigation and subjected to treatment by PH either by spraying or drenching. Values are expressed as number of green pixels and represent the average of six biological replicates per treatment ± standard deviation. Within the same row and for the specified day different letters indicate significant difference according to one-way ANOVA post-hoc Tukey's test ($p<0.05$).

Treatment	Day 6		Day 8		Day 10		Day 13		Day 15	
No application	514 ± 69	*b*	639 ± 100	*b*	739 ± 91	*b*	987 ± 120	*b*	1166 ± 145	*b*
Foliar application	508 ± 80	*b*	605 ± 92	*b*	715 ± 100	*b*	987 ± 142	*b*	1208 ± 156	*ab*
Drench application	615 ± 22	*a*	724 ± 28	*a*	850 ± 44	*a*	1090 ± 68	*a*	1281 ± 79	*a*

Suppl. Table 6. Variation in shoot colours of tomato plants cultivated under limited irrigation and subjected to treatment by PHs either by spraying or drenching. The values for 6 most representative colour hues are shown as percentage of the shoot area (pixel counts). Values represent the average of six biological replicates per treatment ± standard deviation. Within the same row and for the specified day different letters indicate significant difference according to one-way ANOVA post-hoc Tukey's test ($p<0,05$).

Day 6												
Treatment	RGB (63,79,58)		RGB (89,100,83)		RGB (83,95,58)		RGB (49,66,45)		RGB (62,81,81)		RGB (62,82,38)	
No application	24 ± 2	a	12 ± 1	ab	14 ± 6	a	24 ± 8	a	4 ± 1	a	17 ± 4	a
Foliar application	26 ± 5	a	10 ± 1	b	15 ± 4	a	25 ± 6	a	4 ± 1	a	16 ± 3	a
Drench application	29 ± 2	a	10 ± 3	a	14 ± 6	a	28 ± 5	a	3 ± 0.5	a	15 ± 5	a
Day 8												
Treatment	RGB (63,79,58)		RGB (89,100,83)		RGB (83,95,58)		RGB (49,66,45)		RGB (62,81,81)		RGB (62,82,38)	
No application	26 ± 5	a	12 ± 2	a	14 ± 7	a	25 ± 9	a	4 ± 0.4	a	17 ± 3	a
Foliar application	28 ± 3	a	11 ± 2	a	15 ± 4	a	25 ± 4	a	4 ± 0.5	a	16 ± 3	ab
Drench application	28 ± 4	a	13 ± 3	a	11 ± 4	a	33 ± 8	a	4 ± 0.6	a	11 ± 5	b
Day 10												
Treatment	RGB (63,79,58)		RGB (89,100,83)		RGB (83,95,58)		RGB (49,66,45)		RGB (62,81,81)		RGB (62,82,38)	
No application	27 ± 5	a	10 ± 2	a	15 ± 8	a	27 ± 9	b	3 ± 0.3	a	17 ± 3	a
Foliar application	29 ± 1	a	7 ± 1	b	13 ± 3	a	28 ± 4	ab	3 ± 0.3	a	17 ± 2	a
Drench application	31 ± 3	a	9 ± 1	a	11 ± 2	a	40 ± 6	a	3 ± 0.8	a	10 ± 5	b
Day 13												
Treatment	RGB (63,79,58)		RGB (89,100,83)		RGB (83,95,58)		RGB (49,66,45)		RGB (62,81,81)		RGB (62,82,38)	
No application	26 ± 5	a	9 ± 0.3	a	17 ± 5	a	26 ± 6	b	3 ± 0.3	a	18 ± 4	a
Foliar application	27 ± 1	a	7 ± 3	a	15 ± 2	a	31 ± 4	ab	3 ± 0.2	a	16 ± 2	ab
Drench application	28 ± 3	a	9 ± 2	a	13 ± 3	a	35 ± 5	a	3 ± 0.7	a	12 ± 3	b
Day 15												
Treatment	RGB (63,79,58)		RGB (89,100,83)		RGB (83,95,58)		RGB (49,66,45)		RGB (62,81,81)		RGB (62,82,38)	
No application	24 ± 4	a	11 ± 1	a	18 ± 5	a	25 ± 7	b	3 ± 0.4	a	19 ± 5	a
Foliar application	26 ± 2	a	9 ± 2	a	17 ± 3	a	28 ± 5	ab	3 ± 0.3	a	17 ± 2	a
Drench application	28 ± 4	a	10 ± 2	a	15 ± 1	a	34 ± 3	a	3 ± 0.4	a	9 ± 2	b

3.2 Salinity stress

3.2.1 Lettuce and tomato

Integration of Phenomics and Metabolomics Datasets Reveals Different Mode of Action of Biostimulants based on Protein Hydrolysates in Lettuce and Tomato under Salinity

Mirella Sorrentino[1], Klara Panzarova[2], Ioannis Spyroglou[3], Lukas Spichal[4], Valentina Buffagni[5], Paola Ganugi[5], Youssef Rouphael[6], Giuseppe Colla[7], Luigi Lucini[7*], Nuria De Diego[4*]

[1]University of Naples Federico II, Italy, [2]Photon Systems Instruments (Czech Republic), Czechia, [3]Masaryk University, Czechia, [4]Central Laboratories and Research Support, Centre of the Region Haná for Biotechnological and Agricultural Research, Czechia, [5]Catholic University of the Sacred Heart, Piacenza, Italy, [6]Agricultural Sciences, University of Naples Federico II, Italy, [7]Department of Agricultural and Forestry Sciences, University of Tuscia, Italy

Submitted to Journal:
Frontiers in Plant Science

Specialty Section:
Crop and Product Physiology

Article type:
Original Research Article

Manuscript ID:
808711

Received on:
03 Nov 2021

Journal website link:
www.frontiersin.org

Integration of Phenomics and Metabolomics Datasets Reveals Different Mode of Action of Biostimulants based on Protein Hydrolysates in *Lactuca sativa* L. and *Solanum lycopersicum* L. under Salinity

Mirella Sorrentino[1,2], Klára Panzarová[1], Ioannis Spyroglou[3], Lukáš Spíchal[4], Valentina Buffagni[5], Paola Ganugi[5], Youssef Rouphael[2], Giuseppe Colla[6], Luigi Lucini[5*] and Nuria De Diego[4*]

[1]*PSI (Photon Systems Instruments), spol. S.r.o., Drasov, Czech Republic*

[2]*Department of Agricultural Sciences, University of Naples Federico II, via Università 100, 80055 Portici (NA), Italy*

[3]*Plant Sciences Core Facility, Central European Institute of Technology, Masaryk University, Kamenice 5, 62500 Brno, Czech Republic*

[4]*Centre of the Region Haná for Biotechnological and Agricultural Research, Czech Advanced Technology and Research Institute, Palacký University, Šlechtitelů 27, 78371 Olomouc, Czech Republic*

[5]*Department for sustainable food process - DiSTAS, Università Cattolica del Sacro Cuore, via Emilia Parmense 84, 29122 Piacenza, Italy*

[6]*Department of Agriculture and Forest Sciences, University of Tuscia, via San Camillo De Lellis snc, 01100 Viterbo, Italy*

ABSTRACT

Plant phenomics is becoming a common tool employed to characterize the mode of action of biostimulants. A combination of this technique with other omics such as metabolomics can offer a deeper understanding of a biostimulant effect *in planta*. However, the most challenging part then is the data analysis and interpretation of the omics datasets. In this work, we present an example of how different tools based on multivariate statistical analysis can help to simplify the omics data and extract the relevant information. We demonstrate this by studying the effect of protein hydrolysate (PH)-based biostimulants derived from different natural sources in lettuce and tomato plants grown in controlled conditions and under salinity. The biostimulants induced different phenotypic and metabolomic responses in both crops. In general, they improved growth and photosynthesis performance under control and salt stress conditions, with better performance in lettuce. To identify the most significant traits for each treatment, a random forest classifier was used. Using this approach, we found out that in lettuce biomass-related parameters were the most relevant traits to evaluate the biostimulant mode of action, with a better response connected mainly to plant hormone regulation. However, in tomatoes, the relevant traits were related to chlorophyll fluorescence parameters in combination with certain antistress metabolites that benefit the electron transport chain such as 4-hydroxycoumarin and vitamin K1 (phylloquinone). Altogether, we show that to go further in the understanding of the use of biostimulants as plant growth promotors and/or stress alleviators, it is highly beneficial to integrate more advanced statistical tools to deal with the huge datasets obtained from the –omics to extract the relevant information.

Keywords: high-throughput phenotyping, *Lactuca sativa* L., metabolomics, multivariate salt stress, secondary metabolism, *Solanum lycopersicum* L., statistical analysis, vegetal-based protein hydrolysates

INTRODUCTION

Changes in climate patterns are dramatically influencing some agricultural areas, and with special impact in arid, semi-arid, and coastal agricultural areas (Corwing, 2021). Soil salinity already covers 20% of total cultivated, and 33% of the irrigated agricultural lands worldwide and is expected to increase at a faster rate than now by the year 2050 (Central Soil Salinity Research Institute (CSSRI), 2014) (Mukhopadhyay et al. 2021). The high salt concentration in the soil reduces plant growth and hence yield in two ways: increasing the osmotic potential of the soil solution, making it harder for the plant to extract water, and accumulating into the root and shoot tissue at a concentration that can be toxic for the plant (Munns and Tester, 2008). The extent of salinity damage to the fitness and final yield of the crop can change accordingly to the species. For example, lettuce (*Lactuca sativa* L.) reduces plant growth and yield under salt stress conditions (Moncada et al., 2020). However, whereas tomatoes (*Solanum lycopersicum* L.) can maintain the fruit yield and increase their quality under moderate stress (Meza et al. 2020), severe salt stress reduced tomato growth and provokes severe damages, especially in young seedlings (Ali et al. 2021).

To reduce the yield loss connected to salinity, scientists are moving towards the selection of more tolerant genotypes, through breeding, genetic engineering, and marker-assisted selection (MAS) (Munns and James, 2000; Yamaguchi and Blumwald, 2005). However, these methods are expensive, time-consuming, and, in the case of genetic engineering, received with suspicion by the general public (Yamaguchi and Blumwald, 2005; Halford and Shewry, 2000). A more sustainable alternative is represented by the use of protein hydrolysates (PHs), a class of non-microbial plant biostimulants obtained from the partial hydrolysis of protein sources of plant or animal origin (Colla and Rouphael, 2015). Many works from the last years have enlightened the effects of PHs as stress alleviators on different crops growing in saline conditions (Van Oosten et al., 2017; Dell'Aversana et al., 2020; Di Mola et al., 2021). Nonetheless, it is important to remember that the effects of the PHs on crops can vary with the plant species or varieties, the time of the application, and the dose (Lisiecka et al, 2011).

Before a new potential PH-based biostimulant is put on the market, it is, therefore, essential to test its effects in multiple conditions and on different crops. High-throughput automated platforms for plant phenotyping have proven to improve and speed up the biostimulant testing process (Rouphael et al., 2018). Different sensors can be implemented in high-throughput phenotyping platforms, allowing the user to monitor the effects of the PHs applications on many

morpho-physiological traits, throughout the entire crop life cycle (Paul et al, 2019a, 2019b). As a result, we can define in which crop, developmental stage, and dosage the application is recommended. Besides, a deeper physiological study allows the characterization of their mode of action; information that can be used for further possible applications.

The use of other -omic approaches such as metabolomics allows studying the biostimulant effect in a more complex manner, supporting and integrating the phenomics data to better understand the biochemical processes activated in the plants by the biostimulants application. However, the data analysis and interpretation of the complex omics datasets can become another challenging bottleneck. Here, we investigated the mechanism of action of a set of 7 PHs in lettuce and tomato subjected to early and late salinity stress. We hypothesise that salinity will reduce plant growth and change the physiology of the plant in tomato and lettuce. However, the PH application will ameliorate the salt negative effect in both plant species. Besides, a deep data analysis using advanced statistical tools will allow us i) to understand better the effect of the PHs on two species, lettuce and tomato, selected for their economic importance, their distinct architecture, and purpose, and their different sensitivity to salinity stress, ii) to evaluate the biological translation from the results obtained in PHs-primed Arabidopsis grown under salt stress (Sorrentino et al., 2021) to other crops under similar growing conditions, and iii) to demonstrate the necessity of the use of statistical approaches to simplify complex omic datasets allowing identification of the traits relevant for the understanding of a biostimulant mechanism of action.

MATERIALS AND METHODS

Plant Material and Growing Conditions

Seeds of *Lactuca sativa* L. var. capitata (Salanova® cv Aquino) and *Solanum lycopersicum* L. cv MicroTom were sown in 250 ml pots filled with 235 g of a mixture of sieved peat (Substrate 2, Klasmann-Deilmann GmbH, Geeste, Germany) and river sand in 1:1 proportion. All the pots were watered up to 55% of the soil relative water content (SRWC). The water holding capacity of the substrate was calculated as described by Junker et al. (2015). The covered pots were stratified at 4°C in the dark for two days. After that, the pots were moved to a climate-controlled growth chamber (FS-WI, Photon Systems Instruments, Czechia) under long day conditions (16 h light/8 h dark). The climate conditions in the growth chamber were set at 21/19 °C for day/night temperature with 60% relative humidity (RH) and 120 µmol m^{-2} s^{-1} cool-white LED (6500 K)

and 5.5 µmol m^{-2} s^{-1} far-red LED (735 nm) lighting. These conditions were kept constant throughout the entire experiment. The pots were kept covered with a plastic lid for the first 24 h to maintain the soil moisture, and then it was removed.

Selection of the Plants

Eight days after lettuce stratification and ten days after tomato stratification, when most of the germinated seedlings had reached the 2-true-leaf stage, a top view RGB picture of all plantlets was taken using the top view RGB2 camera in the PlantScreen™ Compact system (Photon Systems Instruments, Brno, Czech Republic). The plants with area between the 1st and the 4th quartile of the normal distribution of the population were used for the experiment. In tomato experiment, each variant counted 6 plantlets as biological replicates, with a total of 96 plants. For the lettuce experiment each variant counted 8 plantlets as biological replicates, with a total of 128 plants.

High-throughput Phenotyping

To investigate the effects of PHs application on the morpho-physiological parameters of lettuce and tomato grown under salt stress conditions, trays containing two pots with one plantlet each were automatically transported within PlantScreen™ Compact System on conveyor belts between the light-isolated imaging cabinets, weighing and watering station and the dark/light acclimation chamber. The trays were measured thrice a week, ending with 10 phenotyping rounds distributed in 21 days for lettuce and 24 days for tomato (**Figure 1**), with the starting point before the first salt application (Day of Phenotyping 1, henceforth defined as DoP 1). The phenotyping protocol used was the same for both crops. Physiological measurements [Chlorophyll Fluorescence (ChlF) and Thermal Imaging (IR)], being sensitive to circadian rhythm regulation mechanisms (Cano-Ramirez and Dodd, 2018) were always performed in the morning. A single round measuring protocol consisted of an initial 15 min light-adaptation period inside the acclimation chamber, followed by IR and red-green-blue (RGB) top view imaging (RGB2). Next 15 min dark-adaptation was applied, followed by chlorophyll fluorescence kinetic imaging, RGB side view imaging (RGB1) and weighing and watering (**Figure 1A**). Due to the limited capacity of the phenotyping system, for the lettuce experiment the trays were divided into 3 blocks with 16 trays each. Measuring round for one block lasted for 2 h and 45 min. The

PlantScreen™ Analyzer software (PSI, Czech Republic) was used to automatically process, re-analyse and export the data.

Biostimulants Selection and Application

Seven PHs obtained by enzymatic hydrolysis of vegetal-derived proteins were selected from a batch of eleven PHs, previously screened for their mode of action (Sorrentino et al., 2021), and used for the experiment. They included PHs from different plant sources belonging to the botanical families of Fabaceae (O), Malvaceae (C), Brassicaceae (F), Solanaceae (B), and Graminaceae (P) and two commercial products (Trainer® (D), and Vegamin® (H), commercialized by Hello Nature Inc. (former Italpollina) (Anderson, IN, United States) used as positive controls. The PH were obtained through enzymatic hydrolysis of the dry biomass and were then analysed for their total nitrogen and carbon content; for detailed description of the procedure, see Sorrentino et al. (2021) and Ceccarelli et al. (2021).

Biostimulants were applied to leaves through spraying once a week, using only distilled water for the controls or the given PH in a concentration of 3ml/l for the treated plants. A total of 4 foliar applications of PHs were done throughout the experiment (**Figure 1B**). The first spraying (priming) was performed one day before the first salt application. Two hours before and after the spraying of the plants, the Relative Humidity in the growing chamber (FS-WI) was increased up to 80%, in order to promote the stomata opening.

Due to the limited capacity of the phenotyping platform, the lettuce experiment was divided into two rounds, each consisting of 64 plants; the substances B, C and F were tested in the first round, while D, H, O and P in the second round.

Watering and Salt Treatment

All the pots were watered after each phenotyping round up to 55% SRWC with a modified Hoagland solution [0.36 g/l Ca $(NO_3)_2$, 0.1 g/l KH_2PO_4, 0,80 g/l KNO_3, 0,04 g/l NH_4NO_3, 0,13 g/l $MgSO_4$ and 0,01 mg/l of MIKROM fertilizer (Cifo Srl, S.Giorgio di Piano (BO), Italy)], using the Weighing and Watering station in the PlantScreen™ Compact. The solution was freshly prepared before each watering round and pH was adjusted to a value of 5.7.

Starting from 2 weeks after stratification, the plants belonging to the stress group were twice a week subjected to salt application, ending with 6 applications for both crops (**Figure 1B**). In the lettuce assay, our objective was to reach a concentration of 40 mM NaCl in the soil, corresponding to a moderate stress (Freitas et al., 2019). In order to avoid osmotic shock to the plants and NaCl accumulation in the soil, all the pots were first watered up to 55% of SRWC with plain nutrient solution. The plants belonging to the stress group were then given 40 ml each of an 80 mM NaCl (8,7 mS/cm) solution. In the end, after a couple of hours from the salt application, all the plants were watered again, up to 100% of their SRWC, in order to create drainage of the solution from the pot. The same setup was used with tomato, but in this case the salt solution increased to 120 mM NaCl (14 mS/cm) in order to reach a concentration of around 60 mM NaCl in the pot, corresponding to a moderate salt stress (Meza et al., 2020) (**Figure 1B**). The selection of the two used NaCl concentrations was the result of several preliminary tests conducted on both crops (data not shown).

Imaging Protocol and Data Analysis

RGB imaging

RGB imaging using high-resolution top-view and side-view RGB cameras and optimized image segmentation algorithm for automated analysis was used to calculate the number of plant-specific pixels throughout the whole experiment. The RGB images were processed as described by Awlia et al. (2015) and Paul et al. (2019a, 2019b).

Projected shoot area (PSA) from top (PSA_{top}) and side view (PSA_{side}) was used to calculate the Digital Biomass (DM) of each plant (Rahaman et al., 2017):

$$\sqrt{PSA_{side}^2 \times PSA_{top}}$$

Digital Biomass, corresponding to the approximate volume, was then used to calculate the Relative Growth Rate (RGR), where T_1 and T_2 indicates the time interval (days) and DM_1, DM_2 the corresponding digital biomass:

$$(\ln DM_2 - \ln DM_1)/(T_2 - T_1)$$

RGR was calculated twice during the experiment: from DoP 0 to DoP 12 (**Early Phase**) for both crops, and from DoP 12 to DoP 21 for lettuce plants or to DoP 24 for tomato plants (**Late Phase**).

ChlF imaging

To assess the effects of salt stress and biostimulants application on the photosynthetic performance of the plants, ChlF measurements were acquired using an enhanced version of the FluorCam FC-800MF pulse amplitude modulated (PAM) chlorophyll fluorometer incorporated into the PlantScreen™ Compact System (for more details, see Henley, 1993). After 15 min of dark adaptation, the light curve protocol as described in Awlia et al (2016) was used to quantify the rate of photosynthesis at different photon irradiances (Rascher et al., 2000). Four actinic light irradiances [Lss (Light steady state) 1: 180 µmol m^{-2} s^{-1}; Lss2: 480 µmol m^{-2} s^{-1}; Lss3; 780 µmol m^{-2} s^{-1} and Lss4: 1080 µmol m^{-2} s^{-1}] with a duration of 60 s were used to quantify the rate of photosynthesis. The raw data were automatically processed using the PlantScreen™ Analyser software (PSI, Brno, Czech Republic). From the measured fluorescence transient states, the basic ChlF parameters were derived (i.e., F0, Fm, Ft, and Fv), which were used to calculate a range of parameters characterizing plant photosynthetic performance (i.e., Fv/Fm, Fv'/Fm', NPQ and ΦPSII). We chose to evaluate the parameters obtained after the exposure of the plants to the light of intensity 480 µmol m^{-2} s^{-1} (Lss2), since they provide the highest discriminative power between control and stress plants.

Thermal imaging

To determine the leaf temperature of the plants, we used the thermal imaging unit implemented into the PlantScreen™ Compact system, that allows to assess the canopy temperature from top view. The thermal imaging unit incorporated in the PlantScreen™ Compact System consists of a light-isolated box with one top view camera mounted on a static frame and a temperature sensor to increase contrast for the image processing step. The imaged area is 440 x 340 mm (height × width). To assess spatio-temporal variations in temperature over plant surface, we used FLIR A615 thermal camera with 45◦ lens and resolution 640 ×480 pixels, with high-speed infrared windowing option and<50mK thermal sensitivity (FLIR Systems Inc., Boston, MA, United States). Canopy temperature of each plant was automatically extracted with PlantScreen™ Analyser software (PSI, Brno, Czech Republic) by mask application, background subtraction, and pixel-by-pixel integration of values across the entire plant surface area.

In order to minimize the influence of the differences in environmental conditions and in image acquisition timing among individual plants, the average canopy temperature of each plant (T_{avg}) was normalized with the actual temperature inside the Thermal Imaging box and expressed as canopy temperature depression, or ΔT (°C) (Hou et al., 2019).

Untargeted Metabolomic Analysis

At the end of the experiment, at DoP 21 and 24 in lettuce and in tomato, respectively, the third true leaf of each plant was harvested and freeze-dried. The material from control plants and from plants treated with the 7 PHs were used for the metabolomic analysis. Lyophilized plant material (50 mg for lettuce and 250 mg for tomato) was extracted in twenty volumes (w/v) of methanol/water solution (70:30, v/v) acidified with 0.1% formic acid by Ultra-Turrax (Polytron PT, city, Switzerland), centrifuged and then filtered through a 0.22 µm membrane as previously reported (Paul et al, 2019a, 2019b). Untargeted metabolomics was performed using a 6550 iFunnel quadrupole-time-of-flight mass spectrometer and a 1200 series ultra-high-pressure liquid chromatographic system (UHPLC-ESI/QTOF-MS) from Agilent Technologies (Santa Clara, CA, USA), as previously described (Miras-Moreno et al., 2021). Briefly, 6 µl were injected and reverse-phase chromatography applied under a water-acetonitrile gradient elution (6% to 94% acetonitrile in 33 min). The mass spectrometer worked in positive ionization (ESI+) and SCAN mode for the acquisition of accurate masses ranging from 100 to 1200 m/z. Four replicates were analyzed for each treatment and samples were randomly sequenced. Quality Controls (QCs) were prepared by pooling all the extracts and were analyzed throughout the chromatographic sequence using the same chromatographic conditions as samples but acquired in data dependent MS/MS mode (1 Hz, 50–1200 m/z, 12 precursors per cycle), at different collision energies (10, 20 and 40 eV).

Agilent Profinder B.07 (Agilent Technologies) software was used for mass (5-ppm tolerance) and retention time (0.05 min maximum shift) alignment, as well as to process all the mass features from UHPLC-ESI/QTOF-MS raw data. The combination of monoisotopic mass, isotopes accurate spacing and isotope ratio was used for annotation, using the PlantCyc 12.6 database (Plant Metabolic Network, http://www.plantcyc.org) as previously reported (Pretali et al., 2016; Schläpfer et al., 2017). Only those compounds identified in 75% of the replications

within at least one treatment were retained. Thereafter, MS/MS confirmations from QCs was carried out using the software MS-DIAL 4.24 (Tsugawa et al., 2015) formerly using MS/MS experimental spectra available in the software (Mass Bank of North America) and then using MS-Finder in-silico fragmentation (Tsugawa et al., 2016). The annotation process corresponded to level 2 of confidence as set out in COSMOS Metabolomics Standards Initiative (Salek et al., 2015).

Statistical Analysis

For the phenotyping data, statistical differences between treatments and time points were determined by Mixed model analysis (McCulloch and Searle, 2000; Boisgontier and Cheval, 2016) and multiple pairwise comparisons using post hoc Tukey's test (P-value < 0.05). The statistical analysis was implemented in R studio (R GUI 4.0.3) using the "lmer" and "emmeans" packages (R Core Team, 2014; Bates et al., 2015; Russell, 2020). Then, to define the specificities of each crop and their response to the foliar application with PHs, in order to go further in the mode of action, a hierarchical clustering was applied with the use of "Ward's" linkage method to find similarities between (crop, growth conditions and the best and worse performed biostimulant) and identify clusters (Saxena, 2017). Finally, random forest classification was applied also to identify significant variables for treatment classification (Qi, 2012).

Concerning metabolomics, the software Agilent Mass Profiler Professional B.12.06 (from Agilent Technologies, Santa Clara, CA, USA) was used for data normalization and baselining (Mimmo et al., 2017), and then unsupervised hierarchical cluster analysis (HCA) based on fold-change heatmaps (Squared Euclidean distance) used to naively describe patterns across treatments. Thereafter, supervised multivariate statistics were performed in SIMCA 13 (Umetrics, Malmo, Sweden), where orthogonal projection to latent structures discriminant analysis (OPLS-DA) was carried out. Each supervised model (separate models for tomato and lettuce, and then a comprehensive model for salt-stressed versus control plants) was validated by CV-ANOVA, checked for overfitting by permutation testing (N=200) and then inspected for goodness-of-fit (R2Y) and prediction ability (Q2Y). After that, variable importance in projection (VIP) ranking was used to identify the most discriminant compounds in each OPLS-DA model. Finally, ANOVA (P-value < 0.01, Bonferroni multiple testing correction) and fold-change (FC) analysis ($FC \geq 1.3$) were combined into Volcano Plots, and differential compounds

imported into the Omic Viewer Pathway Tool of PlantCyc (Stanford, CA, USA) software (Caspi et al., 2013) for biochemical interpretations.

RESULTS

Development of the Experimental Protocol for Salt and Biostimulants Applications

To characterise effectively the outcome of biostimulants applications on lettuce and tomato performance in the early vegetative growth phase, we first optimized the experimental protocol for plant cultivation, mild-salt stress application and the stress response quantification. This was done for each crop separately as they are very diverse in their tolerance to salinity, with lettuce being more sensitive than tomato (**Figure 1**). Therefore, two different concentrations of NaCl in the nutrient solution were used to water the plants as described in M&M. Lettuce and tomato plants were grown for 35 and 39 days, respectively, and this period corresponded to the complete head maturation in lettuce and the beginning of the flowering stage in tomato.

The PHs were given via foliar application to the plants, by uniformly spraying the leaves with solutions with concentration of 3 ml/l each (**Figure 1**) (Di Mola et al., 2019a, 2019b). The morpho-physiological traits of the plants were quantified dynamically throughout the trial, in order to monitor the growth performance and physiological status of the plants during the development and salt stress response. As a result, we could clearly distinguish two periods in the experiment, an early and late phase, in which the response of the plants to the salt stress and the interaction with the biostimulants applications were clearly diverse. It is well-known that plants response to salt stress in in two phases (Ugena et al., 2018): a rapid, osmotic phase, here described as early phase (DoP 0-12) and a slower, ionic phase due to the ion toxicity, referred to as late phase (DoP 12-21 in lettuce or DoP 12-24 in tomato) (**Figure 2**).

Lettuce and Tomato Plants Have Different Physiological Response to Mild Salinity

In lettuce, salt stress treatment resulted in obvious reduction of plant growth in the later phase of the experiment with obvious growth inhibition after 4 salt applications salt stress imposition resulted in a visible reduction of plant growth performance only in the late phase of the stress (after DoP 14), (**Figure 2 A1, A2**). In both rounds of the lettuce trial similar biomass reduction was observed with 35% and 29% digital biomass (DB) reduction, respectively (Supplementary **Figure S1 A1-B1**). We further assessed other morphological parameters such as roundness, compactness and slenderness of the leaves (SOL) showing that they do not differ between the rounds, but clearly differed between controls and salt stressed plants in the late phase with salt treated lettuce plant being less compact and round (**Figure 2 A1 and Supplementary Figure S1 A-B).**

The photosynthetic performance of the plants during the development and with the progression of the salt stress was also affected **(Figure 2 A3 and Supplementary Figure S1 C-D)**. In the two rounds analysed, the most significant differences were observed in the late phase between the controls and NaCl-treated lettuce plants. We show that the maximum quantum yield of PSII photochemistry for the light-adapted (Fv'/Fm') state and PSII operating efficiency (ΦPSII) was significantly reduced in the treated plants, whereas the non-photochemical quenching (NPQ) was increased compared to the controls (**Figure 2 A3 and Supplementary Figure S1 C-D)**. Altogether, our data demonstrate that in lettuce only late phase of salt stress imposition (after DoP12) was important to detect differences in growth and fluorescence related parameters between treatments.

In tomato plants, the growth of the plant was not affected by the mild salt stress (**Figure 2 B1-B2**). The remaining morphological parameters did not show differences between control and salt stress, except of higher slenderness of the leaves (SOL) in salt-stressed plants during the transition from the early to late phase (**Supplementary Figure S2 A1-A4**). Regarding the physiology, however, there were significant differences in several fluorescence related parameters at the end of the early phase and late phase of the salt stress (**Figure 2 B3 and Supplementary Figure S2 B)**. In salt stressed tomato plants we observed a significant reduction in Fv'/Fm' and ΦPSII and increased NPQ values compared to the controls.

Protein Hydrolysates Specifically Improve Growth Performance of Lettuce Plants

As following step, we analysed how the foliar application of selected PHs could modify the responses observed in salt stressed and non-stressed plants. In lettuce plants, the substance P increased the DB at the late phase of stress after 3 foliar applications under both growth conditions (DoP13) (**Figure 3 A1-2**, **Supplementary Figure S3 B1 and Supplementary Table S1 A-B).** The substances D and H also improved the DB, but only when plants were grown under salt stress conditions. Other morphological traits such as roundness, compactness or SOL did not change (**Supplementary Figure S3 A2-A4, B1-B4 and Supplementary Table S1 A-B)**. Similarly, the foliar application with substance P increased the relative growth rate (RGR) of the plants in the early phase under control conditions **(Figure 3 A and Supplementary Figure S6 A1-A2).** Other PHs did not modify the RGR of the plants compared to their respective controls (salt or control) in both early and late phase. Interestingly application of the PHs resulted in the increase of the final plant biomass **(Supplementary Figure S6 B-C)**, especially the dry weight of the aerial part of the plants, when the substances B, C, F and P were applied to plants grown under control and salt stress conditions, or when the substances O was applied under control conditions.

The application of biostimulants had mild impact on the photosynthetic performance of the lettuce plants both under control and salt stress conditions. We show that the plants treated with the substances P and H have increased Fv'/Fm' and □PSII values both under control and stress conditions, while we observed reduced NPQ levels along the experiment (**Figure 3 A, Supplementary Figure S3 C-D and S4 C-D and Supplementary Table S2 A).**

In tomato plants, the application of PHs did not have any effect on the morphological traits; the differences in DB, RGR, fresh and dry weight were only due to the growth conditions. DB, as well as fresh weights of the plants, were similar in PHs treated plants and control plants during both phases of the experiment (**Figure 3 B**, **Supplementary Figure S5 A-B, Supplementary Figure S7 and Supplementary Table S1 C)**. Similarly, no significant improvement of the photosynthetic efficiency of the plants was observed in tomato plants sprayed with PHs in any growth conditions (**Figure 3 B, Supplementary Figure S5 C-D and Supplementary Table S2 C).**

We have further analysed the impact of PHs applications on the leave surface temperature profile of both crops using thermal image analysis. The salt stress significantly increased the temperature of the leaf surface in lettuce but not in tomato plants **(Supplementary Figure S8)**. Similarly, the changes of the temperature by the application with biostimulants was more visible in lettuce than

tomato plants. We show that the lettuce plants treated with the substances C and F had significantly reduced surface temperature when grown both under control and stress conditions (**Figure 3 A, Supplementary Figure S8 A-B and Supplementary Table S3 A)**. In tomato, the biostimulants reduced the temperature of the leaf surface after the first application in plants under control and salt stress conditions. However, in the late phase they increased the temperature over the respective control in almost all the cases **(Supplementary Figure S8 C and Supplementary Table S3A)**.

Investigating the Mode of Action of the PHs Through the Plant Biostimulant Characterization Index

To simplify the results and to identify the specific mode of action of each of the 7 PHs, we used the Plant Biostimulant Characterization (PBC) index as described previously (Ugena et al., 2018; Sorrentino et al., 2021). For the calculation of the PBC indexes, we selected the five traits (DB, RGR, Fv'/Fm', ΦPSII and ΔT) that provided the highest discriminative power between the different treatments (**Supplementary Table S1, S2 and S3**). The PBC indexes for the Early Phase (from DoP 0 to 12) and the Late Phase (from DoP 12 to 21 in lettuce or from DoP 12 to 24 in tomato) were calculated independently since we could clearly observe different responses of the plants treated with the 7 PHs in the two phases. To determine the index value, the log2 of the ratio between the biostimulant treated plants and untreated ones was determined for each crop and growth conditions, and then represented in parallel plots **(Figure 3)**. Then, the five obtained values represented in each parallel plots were summed to end with a unique number that represents the PBC index (for further detail see Sorrentino et al. 2021), which was included in the **Table 1**. The calculated PBC index for each compound, growing condition and phase of the trial could be negative (red) or positive (blue), providing information about the mode of action of that specific combination **(Table 1)**. More in detail, the substances with positive PBC indexes (darker blue) in control conditions are characterized as plant growth promotor, whereas the negative (darker red) are plant growth inhibitors. Overall, our data clearly show that in lettuce plants, the substance P was both the best Growth Promotor and Stress Alleviator, improving the fitness of the plants in all growing conditions and in both stages of the trial. The second best was H, while the absolute worst was B (**Table 1 A**). Some of the other PHs proved to be beneficial to the crop only in a specific growing condition and/or phase of the trial. For example, F showed an effect as Growth Promotor, but only in the Late Phase of the experiment, while O acted as a Stress Alleviator in the Early Phase, but its effect fainted in the Later Phase (**Table 1 A**).

For tomato, the absolute best performer was the substance O, followed by D, F and H, all acting as a Growth Promotor and as a Stress Alleviator. Contrarily, the plants treated with the substance B showed the worst performances, especially in salt stress conditions (**Table 1 B**).

The results obtained from the PBC index were also corroborated by a cluster analysis performed with the complete phenotyping data set (**Figure 4**). In lettuce, the plants treated with H and P were located in an independent cluster divided in two subclusters due to the growth conditions (control or salt) but independent of the stress and unstressed control plants **(Figure 4 A**). Contrarily, the rest of substances were located with their respective controls that were only separated by the stress effect (**Figure 4 A and B**). In tomato plants, except for the substances B and C, all PHs were beneficial for the plant fitness, especially when they were grown under salt stress conditions (**Figure 4 C**). Altogether, we could conclude that H and P were the best Plant Growth Promotors and Stress alleviators, whereas B was more a plant growth inhibitor.

The Applications of PHs Activate Different Metabolic Pathways in Lettuce and Tomato Plants

An untargeted metabolomic analysis (UHPLC/QTOF-MS) was performed to understand the molecular mechanisms triggered by PH treatments in tomato and lettuce plants grown under either control or salinity conditions. The untargeted profiling allowed putatively annotating more than 2000 compounds; the whole list of metabolites, together with composite mass spectra and individual abundances are provided as supplementary material (**Supplementary Table S5A** for lettuce**, S5B** for tomato). The metabolomics dataset included a broad biochemical diversity, including metabolites from a large range of metabolic processes of primary and secondary metabolism. Multivariate statistics were applied on the metabolomic dataset highlighted similarities/dissimilarities among the metabolomic profiles across treatments. At first, unsupervised and supervised statistics were carried out separately considering metabolomics datasets from lettuce and tomato. These statistics served as a first step of interpretation to point out similarities/dissimilarities among all treatments.

When the lettuce plants were analyzed, the unsupervised fold-change based hierarchical clustering output **(Figure 5A)** naively evidenced that within each trial (first for PHs B, C, F and second for D, H, O, P) salinity application was the main clustering factor. Nevertheless, the score plot from the supervised OPLS-DA multivariate modeling **(Figure 5B)** allowed to efficiently

discriminate among the different groups of treatments whereas control samples from the two different trials merged into the score-plot. The model was validated (P-value <0.001), parameters of the OPLS-DA were excellent (R2Y = 0.983, Q2Y = 0.935), and overfitting was avoided through permutation testing. Therefore, discriminants compounds (VIP score > 1.2 - **Supplementary Table S6A**) were exported and considered. Overall, primary and secondary metabolites were equally represented among the VIP discriminants. In more detail, the most represented primary metabolites included carbohydrates, membrane lipids, hormones (mainly brassinosteroids, a cytokinin and two gibberellins) and electron-carriers (quinol and quinones). Among secondary metabolites, the most represented compounds were phenylpropanoids, alkaloids and isoprenoids. Exploring the OPLS-DA score plot **(Figure 5 B)**, the variants showed a clear distributed through all score space with a clear separation between stressed and non-stressed plants treated with the same PHs. Under non-saline conditions, the plants treated with B, C, and F presented metabolomic signatures similar to the untreated control, depicting a separated group of response. However, a second group formed by the plants treated with H, O and P, corresponding to the best performing biostimulants according to the phenotyping data, formed an independent group under control and salt stress conditions **(Figure 5 B).**

Different results were obtained in tomato plants. As a preliminary approach, unsupervised HCA **(Figure 6 A)** suggests that salinity did not have a primary effect on metabolic signatures. In fact, tomato samples clustered in two main groups, distinguishing PH treatments, with a cluster including O, P, F and H, and a second group composed by the plants treated with the substance B and C, more similar to untreated controls. These results were furtherly confirmed by the OPLS-DA supervised statistics, which allowed separating better the samples in the score space according to the combined treatments **(Figure 6 B)**. The model parameters of the OPLS-DA were excellent (R2Y = 0.981, Q2Y = 0.941), validation was adequate (P-value <0.001) and overfitting could be excluded by permutation testing. Discriminants compounds (VIP score > 1.1 - **Supplementary Table S6B**) mainly related to secondary metabolism (phenylpropanoids and to a lesser extent terpenoids and alkaloids), cofactors/electron carriers, and phytohormones (gibberellins, brassinosteroids, jasmonate, and IAA-conjugates). Primary metabolites range from carbohydrates, lipids, organic acids and nucleic acid components. OPLS-DA evidenced that some PHs (O, P, H, D) were better able to minimize the differences between stressed and non-stressed plants, so the plants were grouped together independently of the plant growth conditions. This feature might imply a hierarchically stronger effect of the biostimulant above the salt-stress, and thus the ability of these PHs to well-play as stress alleviator on plant metabolism **(Figure 6B).**

Biochemical Insights on the Metabolomic Reprogramming Triggered by the Best and the Worst Performers PHs

To understand further the differences between the mode of action of good and bad performing biostimulants, we analyzed the plants treated with the best substance, H as plant growth promotor and stress alleviator and with the worst, B as growth inhibitor (according to the PBC indexes and the cluster analysis (**Figure 3 and 4**, **Table 1**). The two corresponding sub-datasets were then considered, including 669 compounds for lettuce and 1090 for tomato. The HCA confirmed the strongest effect of salinity above PH-treatments in lettuce, whereas PHs had a hierarchically stronger effect on tomato **(Supplementary Figure S9A-B)**. Indeed, for lettuce, the two main clusters divided stressed from non-stressed plants, even though the metabolic profiles of control plants were more similar to B-treated plants. On the other hand, the metabolic signatures of tomato samples merged in two main clusters, one including H-treated plants and a second cluster grouped controls and B-treated. Consistent results were obtained by OPLS-DA where the separation of treatments could be observed in the score plot hyperspace (**Supplementary Figure S9A-B**). The OPLS-DA model was robust, being R2Y= 0.996 and Q2Y=0.987 in lettuce (P-value <0.001) and R2Y=0.996 and Q2Y=0.977 in tomato (P-value <0.001). Thereafter the Volcano plot analysis (P-value < 0.01, FC ≥ 1.3) was applied to identify differential compounds. Overall, we evidenced that 414 (in lettuce, **Supplementary Table S7A**) and 261 compounds (in tomato, **Supplementary Table S7B)** were significantly modulated by treatments, compared to control. The Pathway Tool analysis from PlantCyc was applied to simplify the interpretation in terms of plant metabolism. **Figure 7 A** and **figure 8 A** show the biosynthetic processes modulated by treatments, along with cumulate FC values. Overall, biosynthesis processes related to secondary metabolism were generally decreased in both crops (**Figure 7 B, Figure 8 B**), except for tomato plants treated with PH B under non-stress conditions. In both species, N-containing compounds (mostly alkaloids), phenylpropanoids and terpenes underwent the most evident modulation. In lettuce, several membrane lipids were impaired, such as long-chain fatty acid (also in the epoxy form) and sterols. Phytohormones were broadly affected by the treatments in lettuce, whereas in tomato we evidenced a weaker impact (**Figure 7 C, Figure 8 C**). The main modulations concerned gibberellins, which decreased in both crops. In treated lettuce, a reduction of brassinosteroids, auxin-conjugates (IAA-Ile, IAA-Leu, IAA-Asp) and N-glycosylated cytokinins were observed. The ethylene precursor (1-aminocyclopropane-1-carboxylate, ACC) down-accumulated only in control plants of lettuce treated with H-substance. In tomato, changes in cytokinin content with mainly accumulation of trans-zeatin-O-glucoside-

7-N-glucoside in response to PH B (either under control or salt stress) and in H-treated plants grown under control conditions were also detected.

Similar results were obtained when the effect of the two PHs (B and H) was investigated in respect of their ability as growth improver and stress alleviator by independently explore on non-stressed and stressed plants. Two different OPLS-DA models were validated regardless of the plant species, one considering metabolomics data from salt-stressed plants and the other including non-stressed plants (**Supplementary Figure S10 A-B**). Validation parameters were excellent in both models, showing a R2Y= 0.992 and Q2Y=0.964 (P-value =1.57 e-17) for non-stressed samples and R2Y= 0.996 and Q2Y=0.949 (P-value =6.41 e-15) for samples grown under salt stress. The strongest discriminant compounds were selected from each model by means of the VIP method (VIP score > 1.20). A total of 310 (salinity, **Supplementary Table S8-A**) and 333 (control, **Supplementary Table S8-B**) metabolites were considered and exported along with their FC values into the Omic Viewer Pathway Tool of PlantCyc for interpretations (**Supplementary Figure S11A-C, Supplementary Figure S12 A-C**). This analysis evidenced that about half of the total discriminant compounds are classified as secondary metabolites. However, whereas B substance downregulated the accumulation, H promoting the accumulation of secondary metabolites (phenylpropanoids, terpenes and N-containing compounds) and others such as fatty acid/lipids, cofactors and electron carriers.

Regarding phytohormones, several discriminant compounds were differentially modulated by the two PHs. Under non-stress conditions, brassinosteroids (3-dehydroteasterone and (22S,24R)-22-hydroxy-5α-ergostan-3-one) strongly down-accumulated in response to PH B but not to PH H, which on the other hand remarkably induced a strong accumulation of methyl (indol-3-yl) acetate (MeIAA), a storage form of IAA. Among cytokinins, two glycosylated forms of trans-zeatin accumulated by H applications, whereas only one (*trans*-zeatin-7-*N*-glucoside) in response to B. PH-treated plants caused a depletion in the ethylene precursor (1-aminocyclopropane-1-carboxylate) but PH H had the strongest effect. Under salinity conditions, MeIAA showed the same modulations recorded in control plants. The only cytokinin found as discriminant (cis-zeatin) accumulated in response of PH H.

Integrative Analysis of Phenomic and Metabolomics Datasets

The multivariate generalization of the squared Pearson correlation coefficient was investigated through co-inertia (CIA), in terms of global similarity between the integrated phenotyping and metabolomic datasets (**Supplementary Figure S13**). The overall correlation between the two datasets was expressed as RV coefficient. This is a measure of global similarity between the datasets and assumes values between 0 and 1. The closer to 1 the higher the similarity between the datasets (Robert & Escoufier, 1976). The overall similarity in structure between phenotyping and metabolomics data was higher in lettuce than in tomato, with a RV coefficient equal to 0.37 and 0.29, respectively. However, the obtained RV for both crops reflected the lack of joint structure in these two datasets (phenomics and metabolomics). Altogether, we could say that according to the low synchrony obtained between the phenotypical and metabolomics data after CIA analysis, the changes in the metabolic content doesn't define the phenotype of the plants.

To deal with this low concordance between the two datasets, we decided to work with the phenotypical and metabolomic data obtained from the plants treated with the substance H as plant growth promotor and stress alleviator, and with the substance B that worked as growth inhibitor in both lettuce and tomato plants. As first step, we used the random forest classification method to identify the most important phenotyping traits for each species. As result, in lettuce the importance was mainly focused in morphological traits, whereas in tomato the physiology was most relevant (**Supplementary Table S4 A and B).** Concretely, the volume represented as DB was the parameter with the highest discriminative power between treatments, followed by the physiological parameter WUE, related to water balance. However, in tomato, the most important parameters were related to the photosynthetic performance of the plant, with QY_max and QY_Lss4 as the main ones. Clearly, the two crops respond different way to the changes in the growth conditions, where is included not only the growth conditions but also whatever treatment applied. Once defined the main phenotypical traits, the correlated metabolites ($p < 0.05$) were identified performing correlation matrix (**Supplementary Table S9 A and B).** For lettuce, many secondary metabolites, including alkaloids, terpenoids and phenols or certain metabolites involved in amino acid metabolism (mainly degradation compounds) were negatively correlated with the volume of lettuce plants. However, this phenotyping trait was positively correlated with IAA, IAA-Asp and L-arginino-succinate among others. In tomato, however, QY_max was positively correlated to certain secondary metabolites such as the phenol 4-hydroxycoumarin, and the vitamin K1 (phylloquinone) among others, and the carbohydrate D-erythrose 4-phosphate.

DISCUSSION

Results

In the last years, the use of plant phenotyping approaches is becoming an efficient tool for characterizing the mode of action of biostimulants obtained from many different sources and in many plant species (Briglia et al., 2019; Danzi et al., 2019; Akhtar et al., 2020; Mutale-joan et al., 2020). Non-invasive approaches allow the simultaneous study of the crops grown under different growth conditions treated with biostimulant substances for better understanding of their mode of action. To this end, our study could be another example of this type of studies. We show that two distance crops such as lettuce and tomato differ in the response to salt stress alone or to the interaction between the stress and the application of PHs based biostimulants. The PH application modified the kinetics of the curves for the different phenotyping traits, including plant growth, fluorescence related parameters and thermal imaging, separated the plant response in early and late phase, being more evident for lettuce than for tomato plants (**Supplementary Figures S1-8**). However, the effect was different for both crops, and from the one obtained in previous studied performed in Arabidopsis (Sorrentino et al., 2021). Whereas in lettuce the biostimulant application induced changes during the early phase and after few applications, in the case of tomato the changes were mainly visible at late phase.

To go further in the understanding of the biostimulant mode of action we probed the combination of phenotyping experiments with other omics, especially metabolomics, which can give additional information. In this context, the most difficult part is the data management, as both –omics approaches are ending with a huge amount of data to process and interpret. Thanks to the fast evolution of the data analysis based on the multivariate statistical analysis, this is possible, and this aims to be a good example of such approach. For that, the first step done was the clustering of the variants analyzed independently for both lettuce and tomato using phenomic data (**Figure 4**). The high dimensionality of the data is a characteristic that creates many challenges in clustering and data analysis in general. The clustering tree is defined by the analysis of the L_K norm distances that depend on the value of K (Euclidean, Manhattan, Minkowski etc.). The most often L_k norm used is Euclidean distance. In this regard, Aggarwal and co-workers (2001) showed some interesting results comparing different L_K norm distances. More specifically, they stress that the meaningfulness of L_K norm (K=1 for Manhattan, K=2 for Euclidean etc.) is worse on high dimensions. This means that the Manhattan distance is preferred in situations where the number of traits (metabolomics or phenomics) is considerably large. That is the reason why Euclidean and Manhattan distances were both examined in this study. However, in this case, the results were not significantly different for both lettuce and tomato. One of the reasons for this result could be that there was a clear different response of the plant when the H or B substance was applied.

As second step after the performance of the metabolic analysis and data processing, the concordance between both datasets (phenomics + metabolomics) was performed using COI analysis. This tool is becoming a particularly attractive method for the identification of relationships between large datasets, but it is mainly used in ecology or genetics (Bady et al. 2004; Genitsaris et al., 2016; Devarajan et al., 2021). However, there are not any case studies using this tool for integrating phenotyping data with other omics. In our study, we observed low values of the RV coefficient between both datasets (phenomics + metabolomics). (**Supplementary Figure S13**). This would mean that the metabolic profiling cannot explain the phenotypes of the plants making the integration of both data more difficult One of the reasons for this could be that the most of modulated metabolites were secondary metabolites, including alkaloids, phenylpropanoids and terpenes (**Figure 7, Figure 8, Suppl. Table S7**). On the contrary, relevant molecules such as plant growth regulators are not so abundant and mainly appeared in lettuce. For example, in lettuce plants there was a clear reduction of the conjugated forms of IAA, most probably to maintain the pool of IAA and thus allow the plant growth (reviewed by Ludwig-Müller et al., 2011). Besides, the precursor the ethylene, ACC, was also reduced in lettuce plants treated with the H substance. It could mean that the H application is able to reduce the ethylene synthesis and with that, its negative effects, (e.i. growth inhibition). However, recent studies also showed that ACC itself is enough to reduce the plant growth (Vanderstraeten et al., 2019)

To solve the low concordance between the phenotyping and metabolomic data, we decided to identify the most significant traits for each treatment (or treatment + biostimulant) among the phenotyping traits identified. For that, we used a random forest classifier. Such tool is mainly used in plant science for machine learning approaches applied in the image analysis (Barradas et al., 2021; Singh et al., 2016), but it has never been used for characterizing the biostimulant mode of action. Apart from a powerful classification method, the random forest has the advantage of revealing the significance of the traits used for identifying (classifying) treatments. This is done by means of the decrease in classification accuracy if a specific variable – trait is removed. The random forest classifiers applied for lettuce and tomato have high accuracy percentages (>95%), which makes them valid for the interpretation of the significant traits. The significant traits found for lettuce were the volume (based on the DB) and WUE. The most relevant result was the volume positively correlating with the IAA levels (**Supplementary File S9**). Higher IAA levels in leaves can improve cell extensibility and consequently induce the leaf growth (Veselov et al., 2002). Additionally, under stress conditions, the IAA accumulation can be a stress tolerance mechanism that permit the plant to keep growing (De Diego et al., 2012). Besides, this result

could also explain the aforementioned reduction of the conjugated IAA metabolites observed in the plants treated with the H substance, and hence, their better growth under both control and stress conditions. The amide-linked IAA-amino acid conjugates are considered reversible storage forms with no or low biological activity (Mellor et al, 2016), with the Gretchen Hagen3 (GH3) family of auxin-inducible acyl amido synthetases as the enzymes converting IAA to IAA-amino acids. Thus, we could think that the application of the substance H in lettuce downregulated the activity of GH3 to reduce auxin-conjugates and maintain the IAA levels as a stress response strategy.

In tomato, the most important trait was the QY_max, which was positively correlated to D-erythrose 4-phosphate (**Supplementary File S9**), an intermediate in the pentose phosphate pathway and the Calvin cycle that serves as a precursor in the shikimate pathway (Billakurthi and Schreier, 2020). This result could also explain the positive correlation with other metabolites product of this pathway such as 4-hydroxycoumarin, and the vitamin K1 (phylloquinone). The hydroxycoumarins have been described as efficient antibacterial compounds that can improve plant stress resistance (Yang et al., 2018). The vitamin K1 has been detected inside thylakoid membranes as an electron carrier and key element within the photosystem I redox chain (reviewed by Lüthje et al., 2013) suggesting that it can serve as a mobile carrier transferring electrons across the plasma membrane and as contributing to maintenance of a suitable redox state of some important proteins embedded in the plasma membrane with protective functions against stress. The better performance in tomato plants can thus be related to the use of D-erythrose 4-phosphate as precursor for the synthesis of antistress compounds from the shikimate pathway.

CONCLUSIONS

We assume that PH-based biostimulants improve plant growth and salt stress response in crops such as lettuce and tomato through different mechanisms. For better understanding of the mode of action it was necessary to use powerful statistical tools, which helped to simplify the results and, hence, their interpretation. Thus, we observed that for lettuce the most interesting traits to study the PHs based biostimulants are those representing the aerial biomass (*i.e.*volume).

These were correlated with altered levels of certain phytohormones such as auxin and ethylene and consequently with plant growth. However, in tomato the chlorophyll fluorescence related

parameters were the most relevant defining the plant growth capacity and salt stress tolerance affecting also the stress related metabolites from the shikimate pathway. We believe that these results corroborated the relevant role of the multivariate statistical analysis as a further step to uncover relevant traits and metabolites for a deeper understanding of the biostimulant mode of action.

CONFLICT OF INTEREST

The authors declare no conflict of interest.

DATA AVAILABILITY STATEMENT

All datasets generated for this study are included in the article **Supplementary Material**.

AUTHORS CONTRIBUTIONS

YR, LL and GC prepared and selected the protein hydrolysates. MS and KP designed the phenotyping experiments, MS performed the experiments, the image processing, and image-based data analysis. LL, VB and PG carried out the untargeted metabolomics and performed the analysis of the metabolomic data. IS and NDD performed the multivariate statistical analysis. All authors discussed the results and contributed to write the manuscript.

FUNDING

This work was supported by European Union's Horizon 2020 Research and Innovation Program under the Marie Skłodowska- Curie grant agreement no. 675006, by Italian Ministry of Education, University and Research (MiUR) under the PRIN 'PHOBOS' (no. 2017FYBLPP), by European Regional Development Fund-Project "SINGING PLANT" (No. CZ.02.1.01/0.0/0.0/16_026/0008446) with financial contribution from the Ministry of Education, Youths and Sports of the Czech Republic through the National Programme for Sustainability II funds and by the ERDF project "Plants as a tool for sustainable global development" (No. CZ.02.1.01/0.0/0.0/16_019/0000827) from the Ministry of Education, Youth and Sports of the Czech Republic.

ACKNOWLEDGEMENTS

We thank Hello Nature Company (Rivoli Veronese, Italy) for helping in the development of tested protein hydrolysates and providing them. Plant Sciences Core Facility of CEITEC Masaryk University and Phenotyping and Cultivation facility of PSI Research Center is acknowledged for the technical support.

Table 1| Classification of the 7 PHs with PBC index. *PBC index values for each substance, in Early (0-12 Days of Phenotyping for both crops) and Late Phase of the experiment (21-21 Days of Phenotyping in lettuce, 12-24 Days of Phenotyping in tomato). PBC index of the 7 PHs in lettuce plants, in control and salinity conditions (A). PBC index of the 7 PHs in tomato plants, in control and salinity conditions (B). White corresponds to 0, positive values are highlighted in blue and negative values are highlighted in red; the farther the value from 0, the darker is the corresponding hue.*

	A. Lettuce				**B. Tomato**			
	Control		*NaCl*		*Control*		*NaCl*	
	Early Phase	**Late Phase**	**Early Phase**	**Late Phase**	**Early Phase**	**Late Phase**	**Early Phase**	**Late Phase**
B	-0.38	-0.21	-1.04	-0.78	0.35	0.18	0.09	0.10
C	-0.54	-0.07	-1.73	1.01	0.17	-0.32	0.84	1.00
D	0.12	-0.10	-1.18	-0.42	1.27	1.14	1.14	1.33
F	-0.73	1.23	-1.77	0.15	1.21	1.24	0.92	1.00
H	0.63	0.30	0.53	1.00	0.73	0.63	1.36	0.77
O	0.15	-0.02	0.38	0.19	1.96	1.45	1.49	1.23
P	1.37	1.32	0.84	1.29	0.60	0.64	0.34	0.36

Figure Captions

Figure 1|Scheme of plant cultivation and phenotyping protocol. *Plants were manually transferred from cultivation chamber to PlantScreenTM Compact System for imaging using four different sensors (thermal camera, chlorophyll fluorescence and top and side RGB). Resulting false–color and segmented images and list of extracted parameters obtained from the sensors are shown (A). Timeline of plant cultivation (yellow bar) and phenotyping protocol (blue bar). Green dots show four time points of the foliar application for the selected biostimulants and the orange dots show six timepoints for the salt treatment (B).*

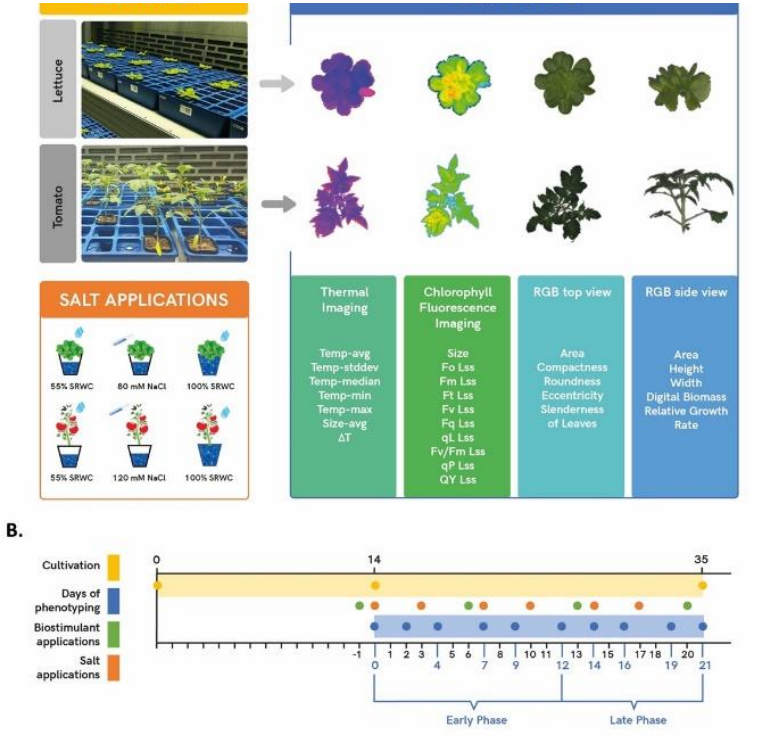

Figure 2| Salinity response in tomato and lettuce plants. *RGB top view colour-segmented images of lettuce (A1) and tomato (B1) control and salinity stressed plants over the time-course of the experiment. Digital biomass (DB) of the lettuce (A2) and tomato (B2) plants. Maximum quantum efficiency of photosystem II in the light-adapted state (Fl'/Fm') for lettuce (full line, A3) and tomato (dashed line, B3) plants. Values represent the average of 8 (lettuce) and 6 (tomato) biological replicates per treatment, error bars represent standard deviation. The significant differences between control and salt treatment are indicated with *, ** and *** for p-values below 0.05, 0.01 and 0.001, respectively. Data and images shown are from the 1st round of the lettuce experiment.*

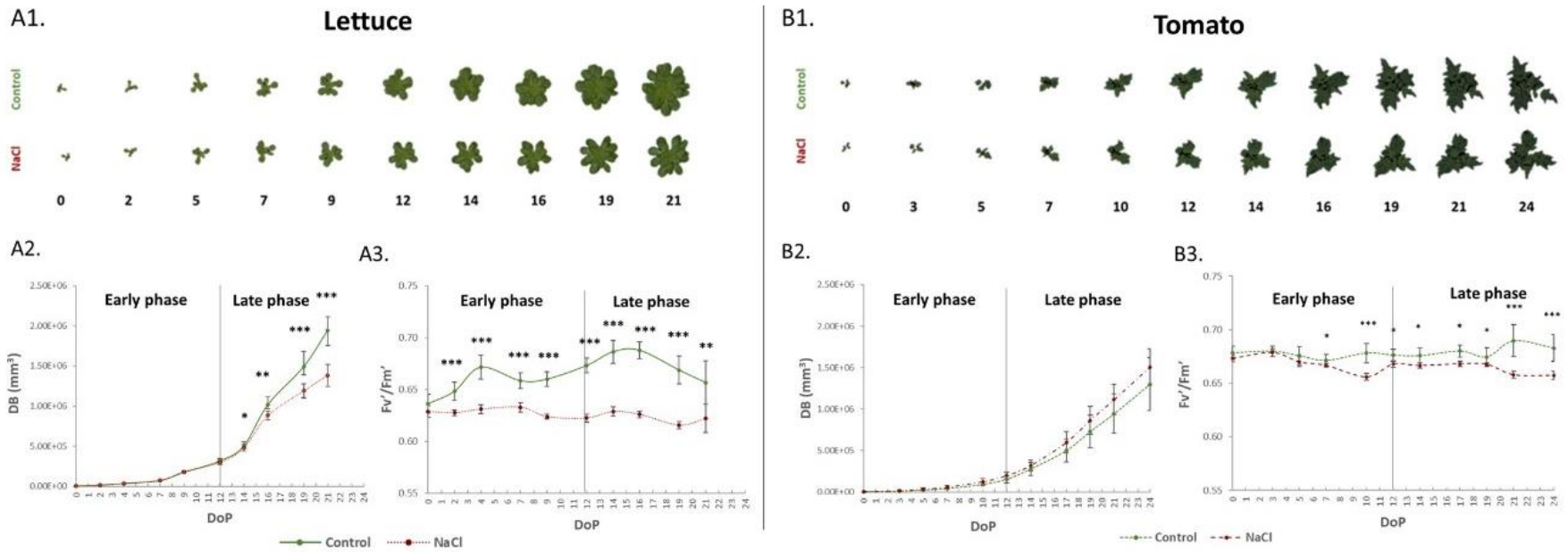

Figure 3| Characterization of the biostimulants effect on performance of tomato and lettuce plants grown in control and salinity conditions. *Parallel coordinate plots of the 5 main morpho-physiological parameters (Digital Biomass, RGR, Fv'/Fm', ΦPSII and ΔT) are shown for lettuce plants grown in control (full lines, A1) and salt stress conditions (dotted lines, A2) and for tomato plants grown in control (dashed lines, B1) and salt stress conditions (dotted and dashed lines, B2). The values represent the log2 of the ratio between the plants treated with the 7 PHs and their respective controls; the sum of the resulting 5 values corresponds to the PBC index, used for the characterization of the PHs. Data are shown for early (0-12 Days of Phenotyping) and late phase (12-21 Days of Phenotyping) of the plant growth.*

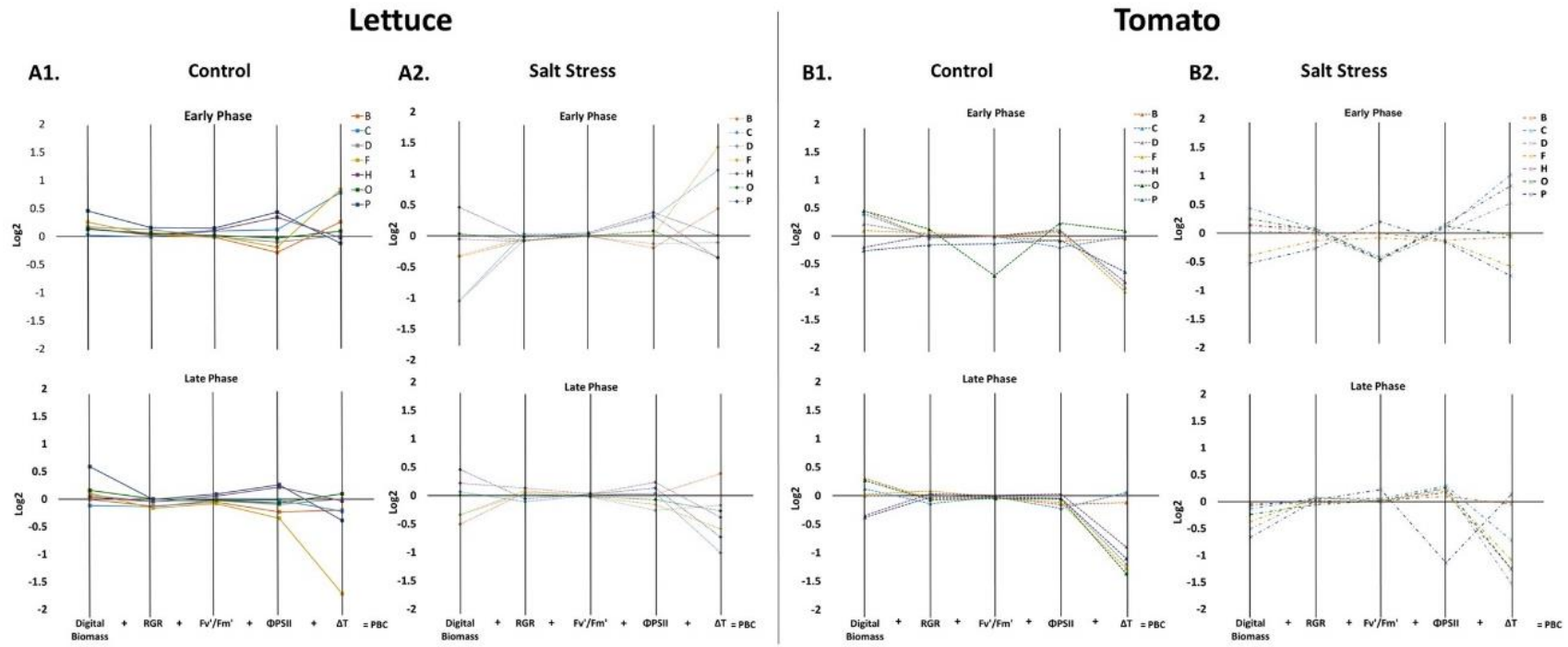

Figure 4| Cluster Dendrograms for all phenotypical data. *Cluster analysis of the lettuce plants treated with 7 different PHs and grown under control and salt stress conditions (A and B). Cluster analysis of the tomato plants treated with the 7 PHs under control and salt stress conditions (C).*

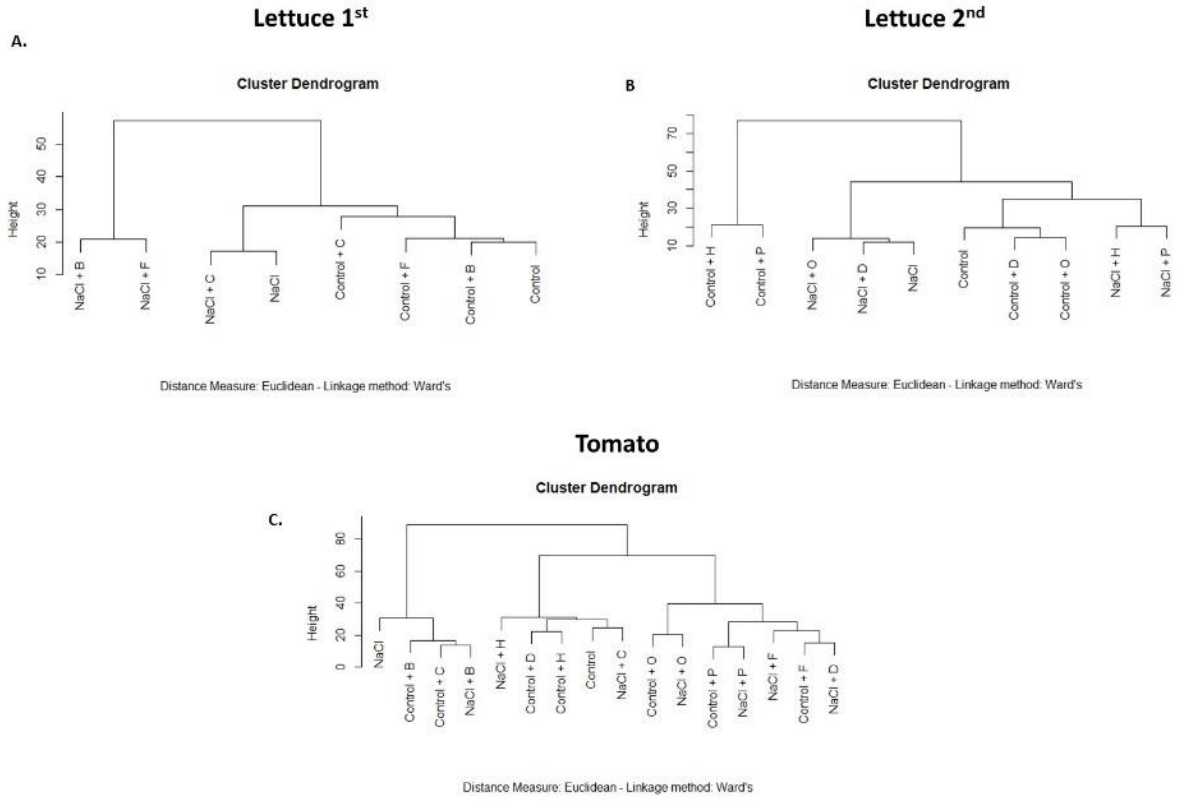

Figure 5| Metabolomic analysis of lettuce plants. *Unsupervised hierarchical cluster analysis carried out from UHPLC-ESI/QTOF-MS metabolomics analysis of lettuce plants after 7 PHs (i.e., biostimulant) applications, under control and salt stress (NaCl) conditions. The fold-change based heat map was used to build hierarchical clusters (linkage rule: Ward; distance: Euclidean) (A). Score plot of orthogonal projection to latent structures discriminant analysis (OPLS-DA) supervised modelling carried out on untargeted metabolomics profiles of lettuce plants after 7 PHs application, under control and salt stress (NaCl) conditions (R2Y = 0.98, Q2Y = 0.93) (B).*

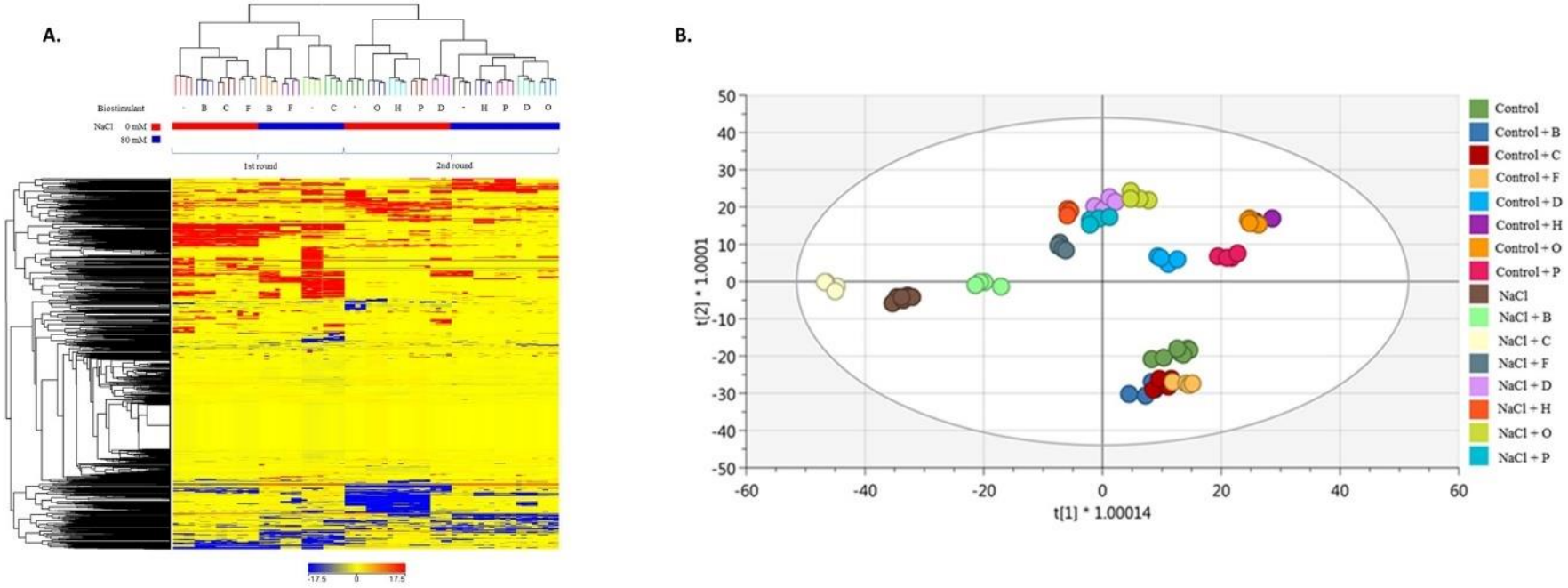

Figure 6| Metabolomic analysis of tomato plants. *Unsupervised hierarchical cluster analysis carried out from UHPLC-ESI/QTOF-MS metabolomics analysis of lettuce plants after 7 PHs (i.e., biostimulant) applications, under control and salt stress (NaCl) conditions. The fold-change based heat map was used to build hierarchical clusters (linkage rule: Ward; distance: Euclidean) (A). Score plot of orthogonal projection to latent structures discriminant analysis (OPLS-DA) supervised modelling carried out on untargeted metabolomics profiles of lettuce plants after 7 PHs application, under control and salt stress (NaCl) conditions (R2Y = 0.98, Q2Y = 0.94) (B).*

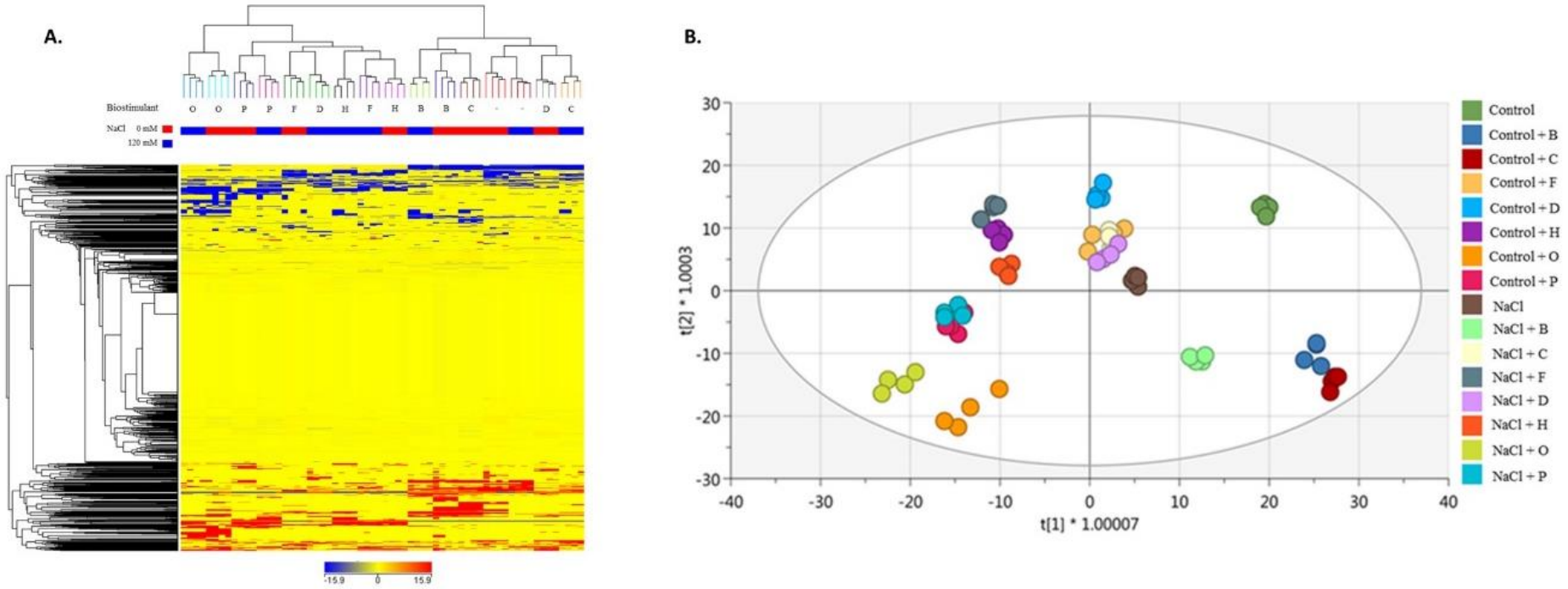

Figure 7| Metabolites in lettuce plants. *Metabolic processes (A), secondary metabolism (B) and (C) hormone biosynthesis impaired by treatments in lettuce plants compared to control samples. Differential metabolites from the Volcano analysis (P-value < 0.01, FC ≥ 1.3) were elaborated using the Omics Viewer Dashboard of the Plant Cyc pathway Tool software (www.pmn.plantcyc.com). The large dots represent the average (mean) of all log Fold-change (FC) for metabolites, and the small dots represent the individual log FC for each metabolite. The x-axis represents each set of subcategories, while the y-axis corresponds to the cumulative log FC. FA/Lipid: fatty acids and lipids; Amine: amines and polyamines; Cofactor: cofactors, prosthetic groups, electron carriers, and vitamins; FA Derives: fatty acid derivatives; N-containing: Nitrogen-containing secondary metabolites; S-containing: Sulfur-containing secondary metabolites; Sugar Derives: sugar derivatives.*

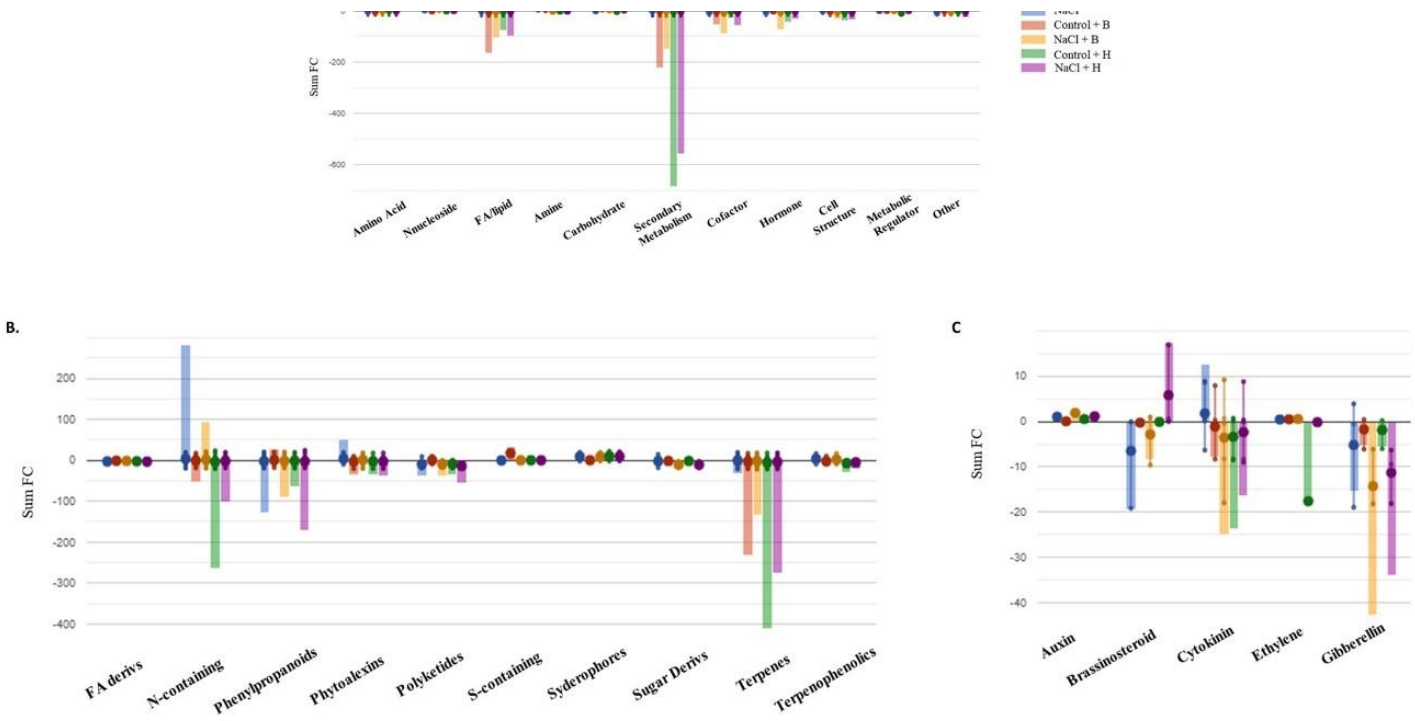

Figure 8| *Metabolic processes (A), secondary metabolism (B) and (C) hormone biosynthesis impaired by treatments in tomato plants compared to control samples. Differential metabolites from the Volcano analysis (P-value < 0.01, FC ≥ 1.3) were elaborated using the Omics Viewer Dashboard of the Plant Cyc pathway Tool software (www.pmn.plantcyc.com). The large dots represent the average (mean) of all log Fold-change (FC) for metabolites, and the small dots represent the individual log FC for each metabolite. The x-axis represents each set of subcategories, while the y-axis corresponds to the cumulative log FC. FA/Lipid: fatty acids and lipids; Amine: amines and polyamines; Cofactor: cofactors, prosthetic groups, electron carriers, and vitamins; FA Derives: fatty acid derivatives; N-containing: Nitrogen-containing secondary metabolites; S-containing: Sulfur-containing secondary metabolites; Sugar Derives: sugar derivatives.*

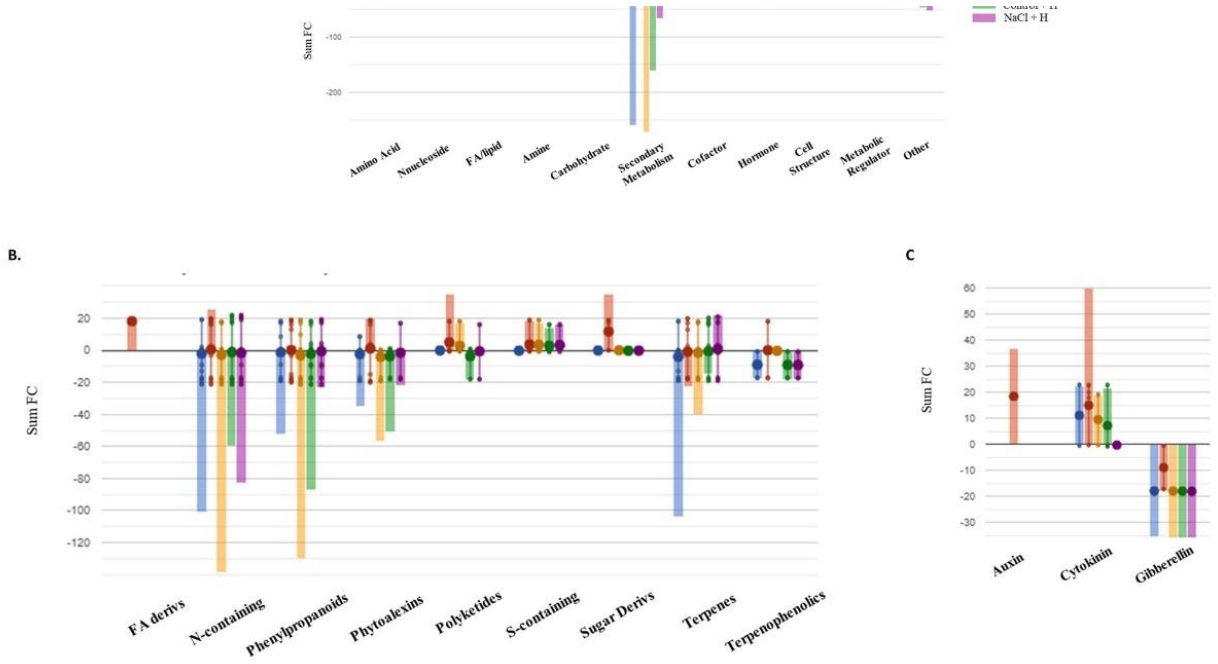

Supplementary Material

Supplementary Figure S1|Morphological and physiological parameters of lettuce plants in control and stress conditions. Variations throughout time of the digital biomass (DM, A1-B1), roundness (A2-B2), compactness (A3-B3) and slenderness of leaves (SOL, A4-B4) of lettuce plants grown under control or salt stress conditions for 21 days of phenotyping (DoP). Variations throughout time of maximum quantum yield of PSII photochemistry for the light-adapted state (Fv'/Fm', C1-D1), PSII operating efficiency (ΦPSII, C2-C3) and non-photochemical quenching (NPQ, C3-D3). Values shown were measured after the exposure of the plants to the light of intensity 480 µmol m-2 s-1 (Lss2). Morphological and physiological values shown represent the average of 8 biological replicates per variant. Error bars represent standard deviation. The significant differences between control and salt treatment are indicated with *, ** and *** for p-values below 0.05, 0.01 and 0.001, respectively.

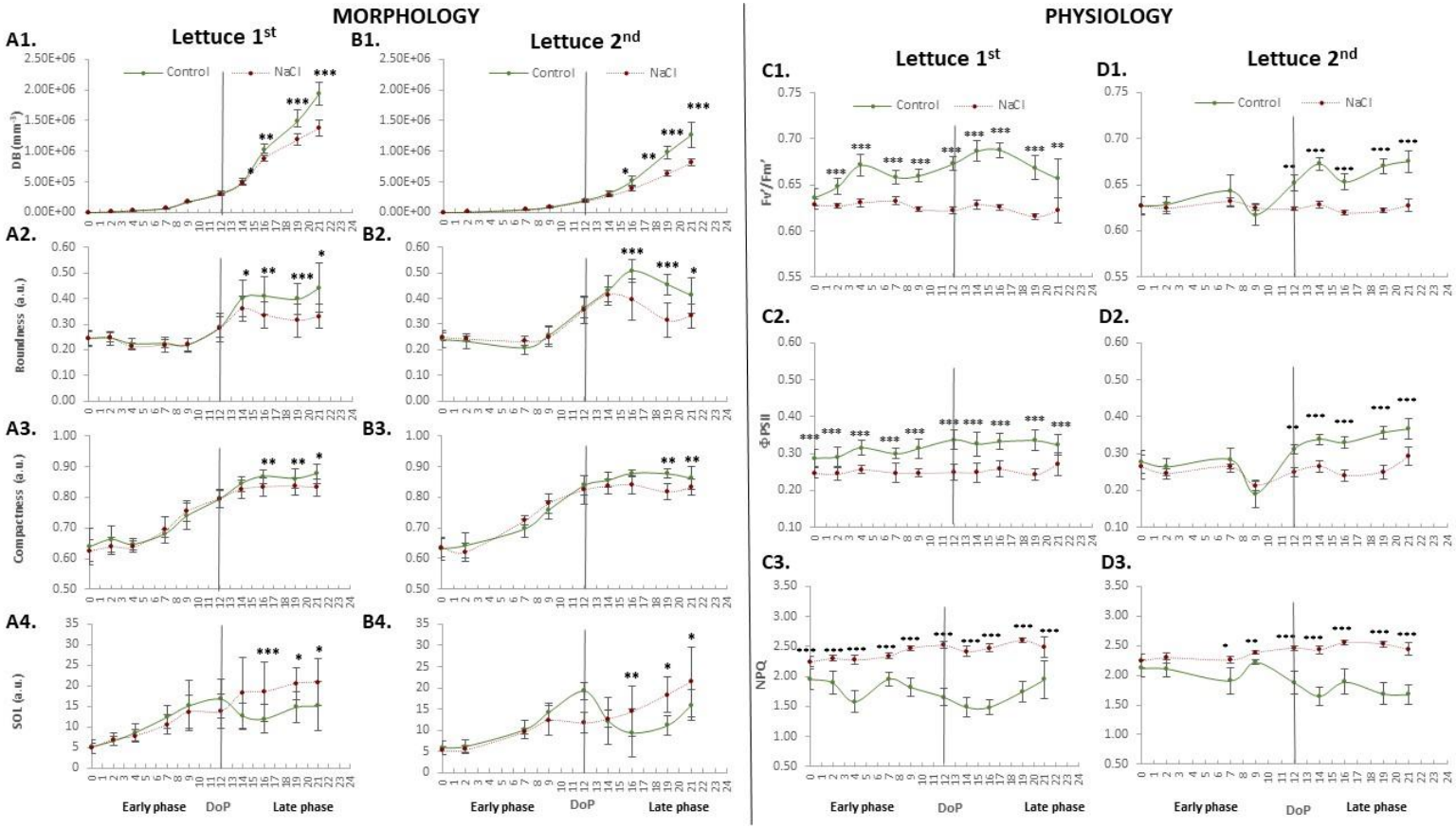

Results

Supplementary Figure S2|Morphological and physiological parameters of tomato plants under control and stress conditions. Digital biomass (DB, A1), roundness (A2), compactness (A3) and slenderness of leaves (SOL, A4) of tomato plants grown under control or salt stress conditions for 24 days of phenotyping (DoP). Maximum quantum yield of PSII photochemistry for the light-adapted state (Fv'/Fm', C1) , PSII operating efficiency (ΦPSII, C2) and non-photochemical quenching (NPQ, C3). Values shown were measured after the exposure of the plants to the light of intensity 480 µmol m-2 s-1 (Lss2). Morphological and physiological values shown represent the average of 6 biological replicates per variant. Error bars represent standard deviation. The significant differences between control and salt treatment are indicated with *, ** and *** for p-values below 0.05, 0.01 and 0.001, respectively.

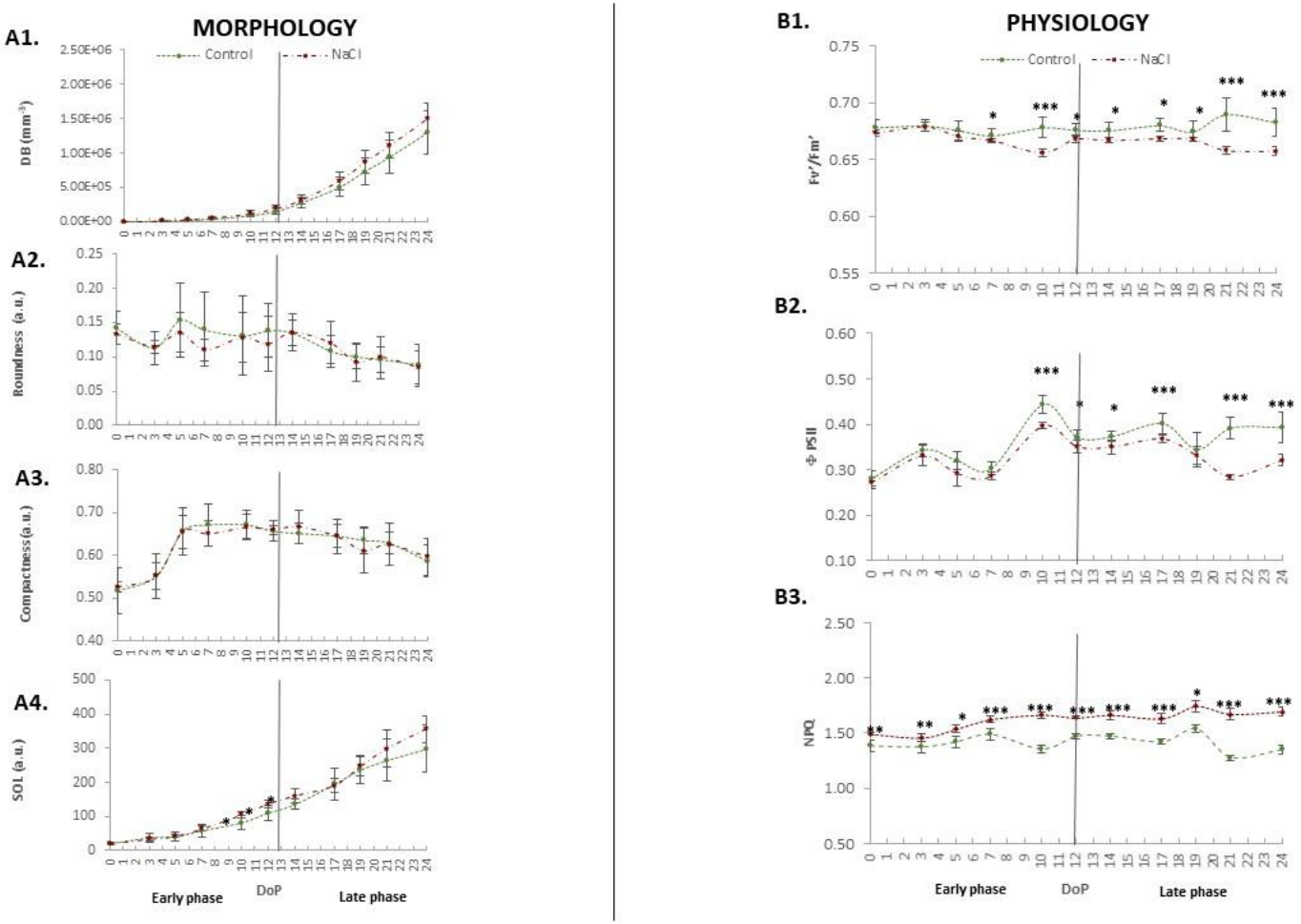

Results

Supplementary Figure S3|Morphological and physiological parameters of lettuce plants in control conditions: PHs treated and untreated lettuce plants. Variations throughout time of the digital biomass (DB, A1-B1), roundness (A2-B2), compactness (A3-B3) and slenderness of leaves (SOL, A4-B4) of lettuce plants sprayed with 7 PHs and grown under control conditions for 21 days of phenotyping (DoP). Maximum quantum yield of PSII photochemistry for the light-adapted state (Fv'/Fm', C1-D1) , PSII operating efficiency (ΦPSII, C2-C3) and non-photochemical quenching (NPQ, C3-D3). Values shown were measured after the exposure of the plants to the light of intensity 480 µmol m-2 s-1 (Lss2). Morphological and physiological values shown represent the average of 8 biological replicates per variant. Error bars represent standard deviation.

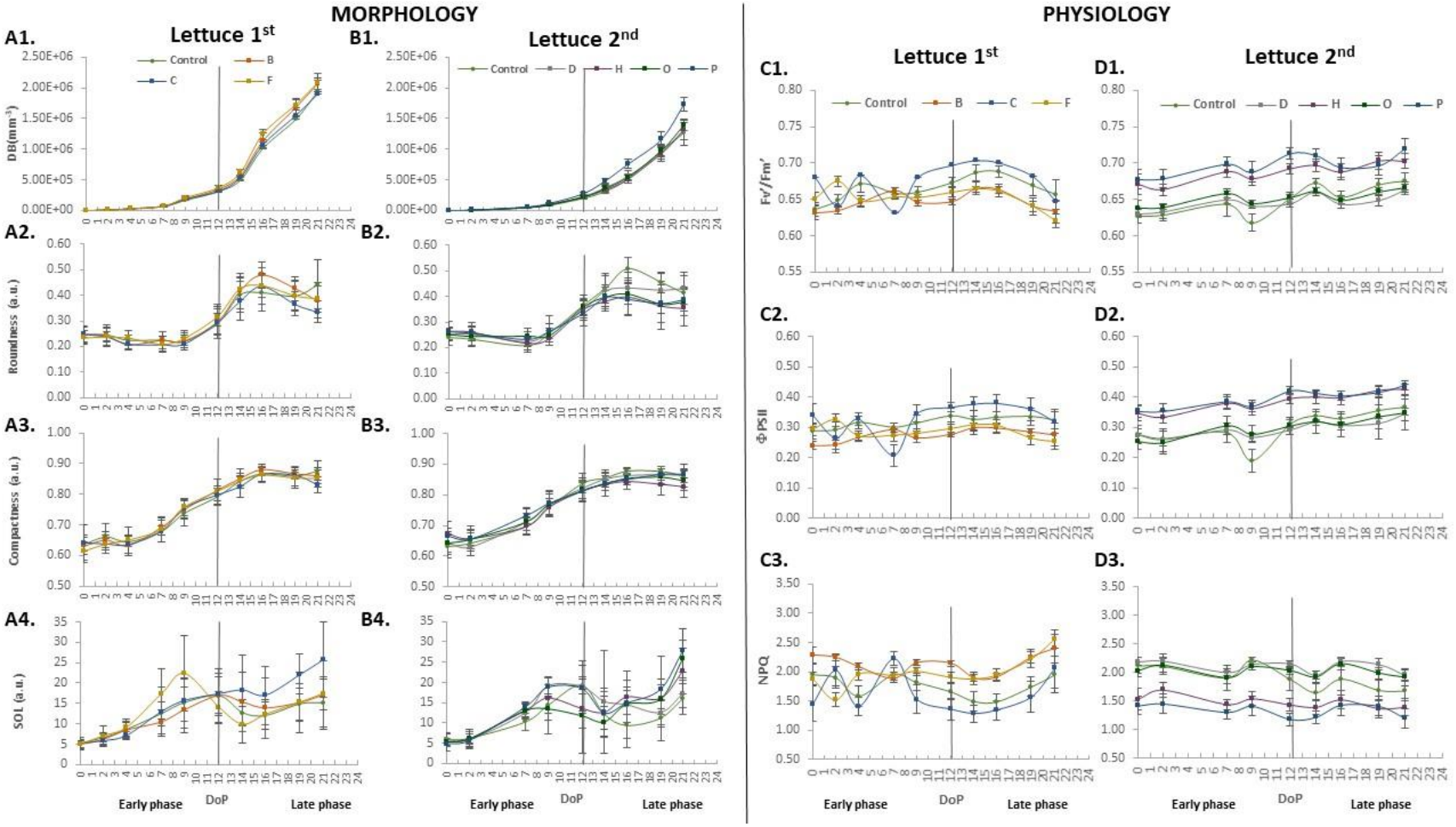

Results

Supplementary Figure S4|Morphological and physiological parameters of lettuce plants in salt stress conditions: PHs treated and untreated lettuce plants. Variations throughout time of the digital biomass (DM, A1-B1), roundness (A2-B2), compactness (A3-B3) and slenderness of leaves (SOL, A4-B4) of lettuce plants sprayed with 7 PHs and grown under salt stress conditions for 21 days of phenotyping (DoP). Maximum quantum yield of PSII photochemistry for the light-adapted state (Fv'/Fm', C1-D1) , PSII operating efficiency (ΦPSII, C2-C3) and non-photochemical quenching (NPQ, C3-D3). Values shown were measured after the exposure of the plants to the light of intensity 480 µmol m-2 s-1 (Lss2). Morphological and physiological values shown represent the average of 8 biological replicates per variant. Error bars represent standard deviation.

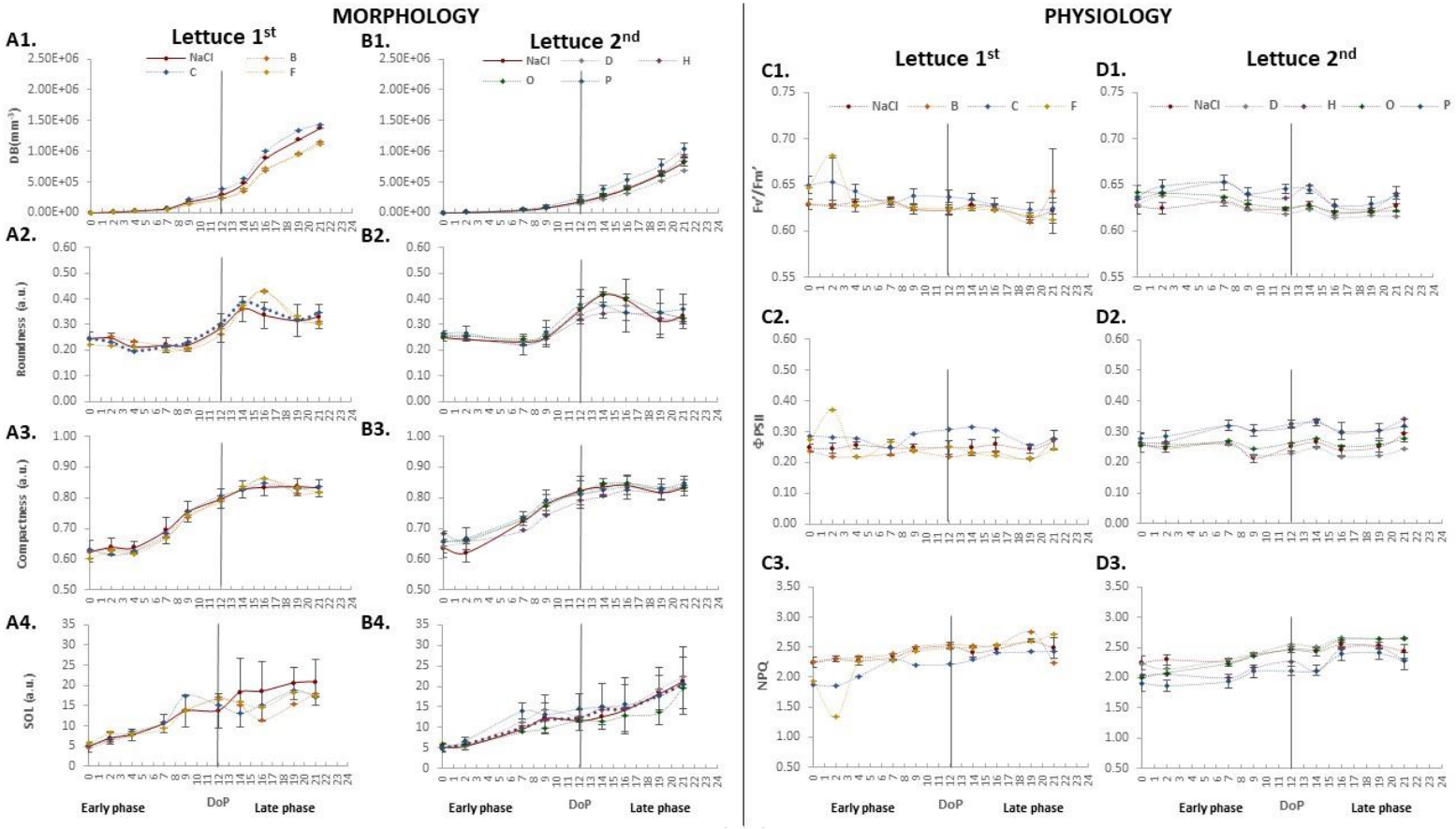

Results

Supplementary Figure S5|Morphological and physiological parameters of tomato plants grown in control and salt stress conditions: PHs treated and untreated lettuce plants. Variations throughout time of the digital biomass (DM, A1-B1), roundness (A2-B2), compactness (A3-B3) and slenderness of leaves (SOL, A4-B4) of tomato plants sprayed with 7 PHs and grown under control and salt stress conditions for 24 days of phenotyping (DoP). Maximum quantum yield of PSII photochemistry for the light-adapted state (Fv'/Fm', C1-D1) , PSII operating efficiency (ΦPSII, C2-C3) and non-photochemical quenching (NPQ, C3-D3). Values shown were measured after the exposure of the plants to the light of intensity 480 µmol m-2 s-1 (Lss2). Morphological and physiological values shown represent the average of 6 biological replicates per variant. Error bars represent standard deviation. The significant differences between control and salt treatment are indicated with *, ** and *** for p-values below 0.05, 0.01 and 0.001, respectively.

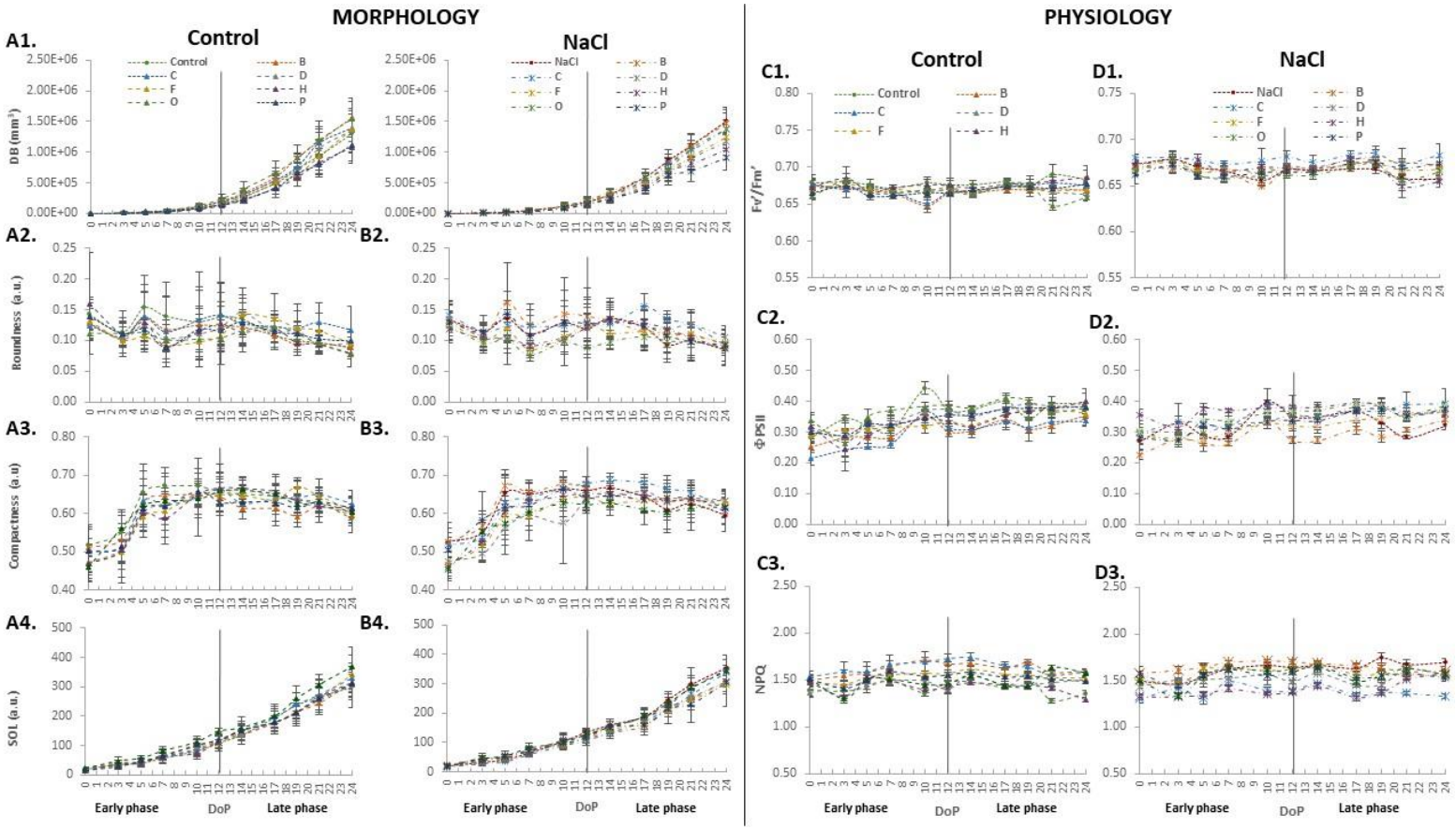

Results

Supplementary Figure S6|Relative Growth Rate and final biomass of lettuce plants treated with PHs. Relative Growth Rate (RGR, A1-A2) of the different treatments over time, calculated for the Early phase (from DoP 0 to DoP 12) and the Late Phase (from DoP 12 to DoP 21) in lettuce plants sprayed with 7 PHs grown under control conditions or salt stress. Total fresh (B1-B2) and dry (C1-C2) weight of the final aboveground biomass per variant. Values represent the average of the 8 biological replicates per variant. Error bars represent standard deviation. Different letters indicate significant difference according to one-way ANOVA post hoc Tukey's test ($p < 0.05$).

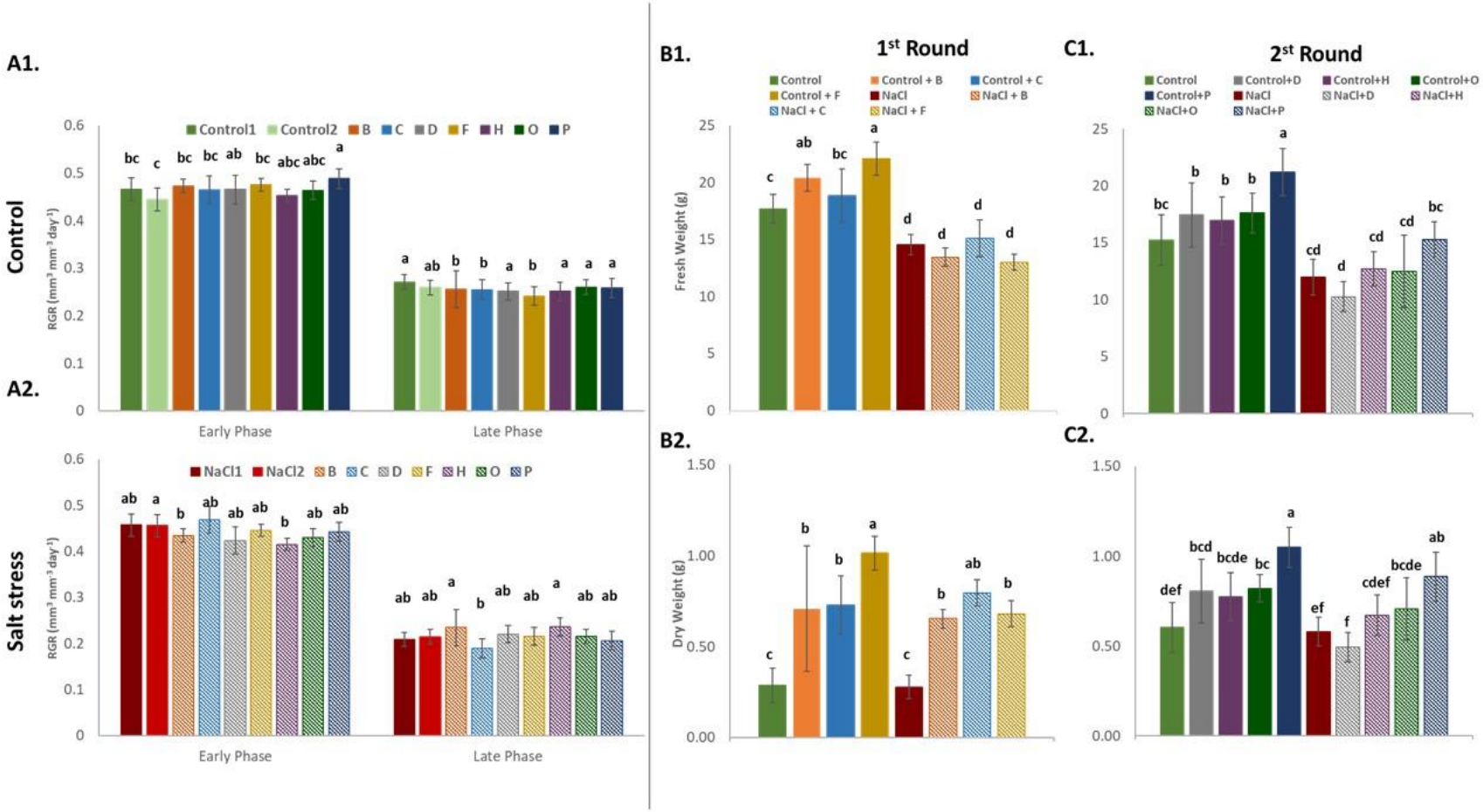

Results

Supplementary Figure S7|Relative Growth Rate and final biomass of tomato plants treated with PHs. Relative Growth Rate (RGR, A1-A2) of the different treatments over time, calculated for the Early phase (from DoP 0 to DoP 12) and the Late Phase (from DoP 12 to DoP 24) in tomato plants sprayed with 7 PHs, grown under control conditions or salt stress. Total fresh (B1-B2) and dry (C1-C2) weight of the final aboveground biomass per variant. Values represent the average of the 6 biological replicates per variant. Error bars represent standard deviation. Different letters indicate significant difference according to one-way ANOVA post hoc Tukey's test ($p < 0.05$).

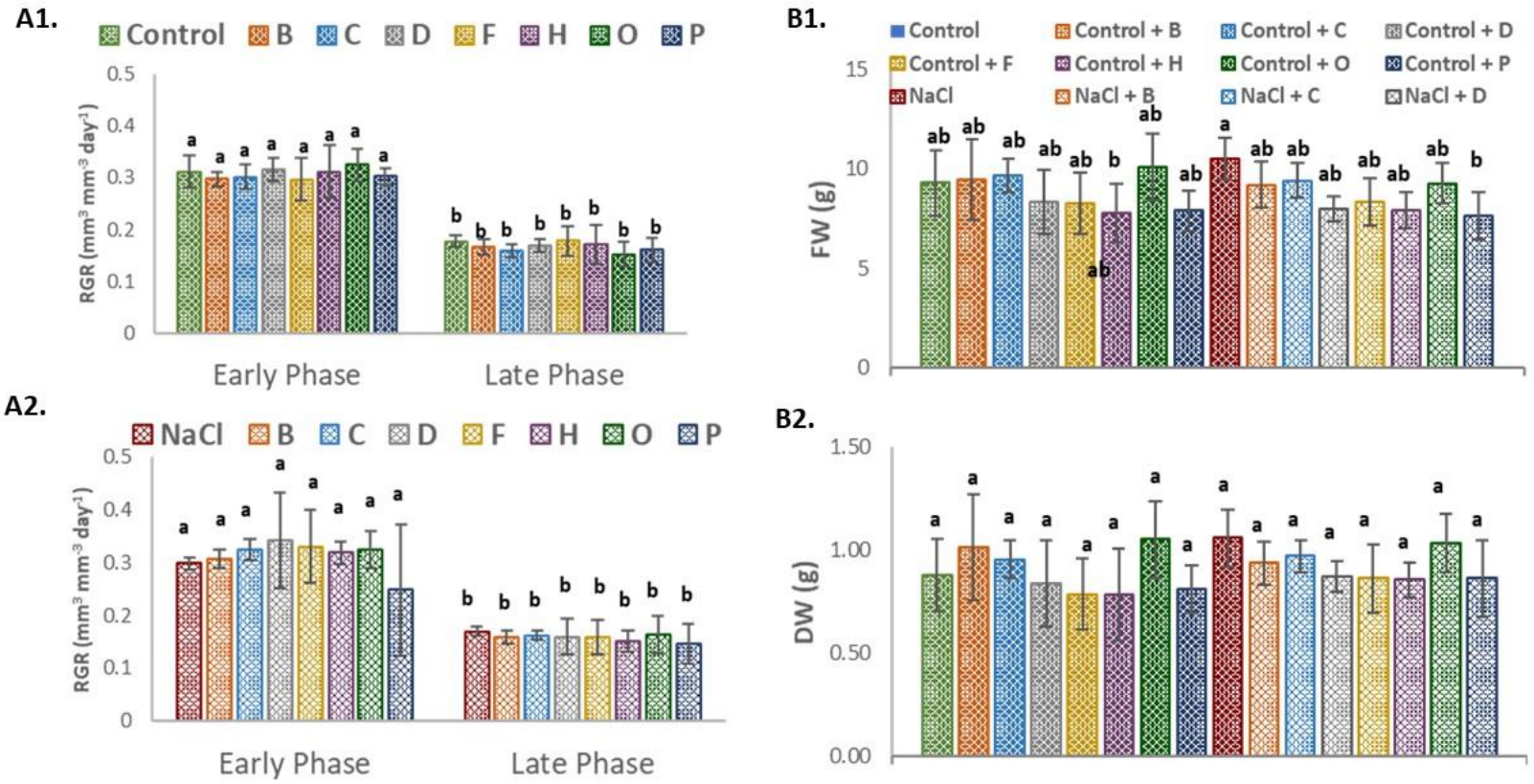

Results

Supplementary Figure S8|Temperature of the leaves for lettuce and tomato plants under control and salt stress conditions. Canopy temperature depression measured on lettuce (A1-3, B1-3, full and dotted lines) and tomato (C1-3, dashed and dotted + dashed lines) plants growing in control and salt stress conditions, treated or untreated with the biostimulant substances. Values represent the average of the 8 biological replicates per treatment in lettuce and 6 biological replicates in tomato; error bars represent standard deviation. The significant differences between control and salt treatment are indicated with *, ** and *** for p-values below 0.05, 0.01 and 0.001, respectively.

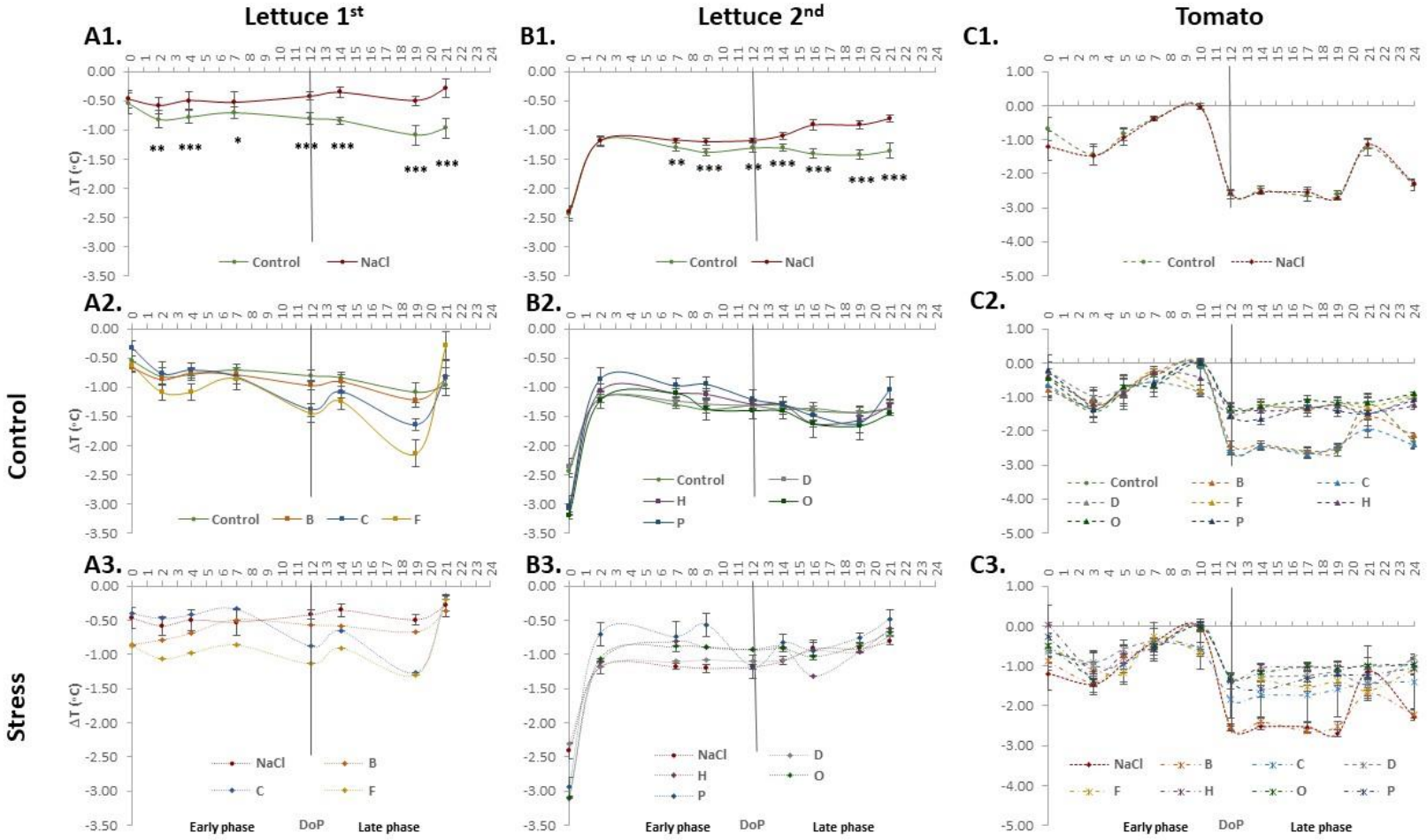

Results

Supplementary Figure S9| Metabolomic analysis for the best (H) and worst (B) performing biostimulants. Unsupervised hierarchical cluster analysis carried out from UHPLC-ESI/QTOF-MS metabolomics analysis of lettuce (A) and tomato (B) plants after B and H application, under control and salt stress (NaCl) conditions. The fold-change based heat map was used to build hierarchical clusters (linkage rule: Ward; distance: Euclidean). Score plot of orthogonal projection to latent structures discriminant analysis (OPLS-DA) supervised modelling carried out on untargeted metabolomics profiles of lettuce (C) and tomato (D) plants after B and H application, under control and salt stress (NaCl) condition.

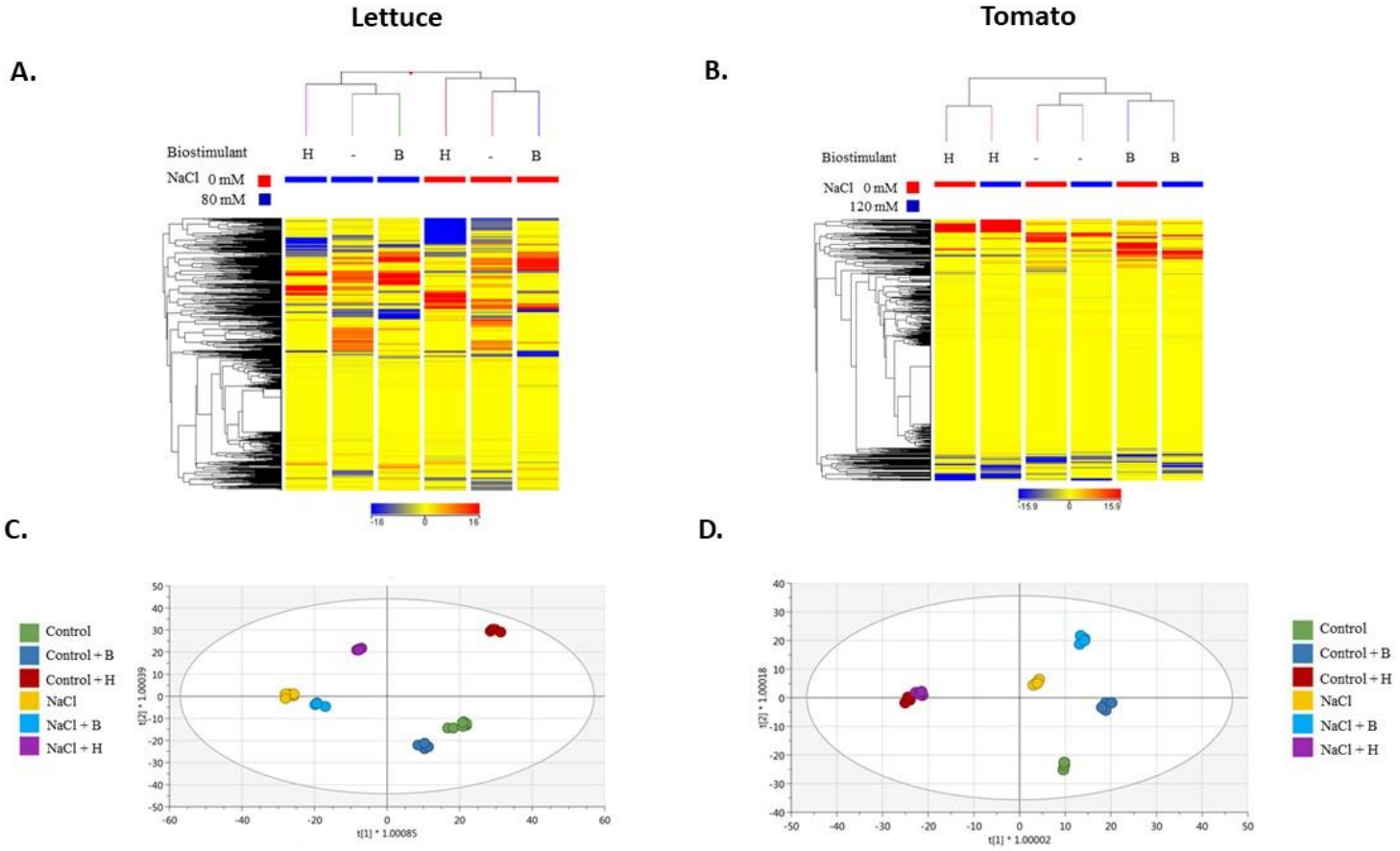

Supplementary Figure S10| Score plot of metabolomics profiles. Score plot orthogonal projection to latent structures discriminant analysis (OPLS-DA) supervised modelling carried out on untargeted metabolomics profiles of tomato and lettuce plants after B and H application, under control (A) and salt stress (B) conditions.

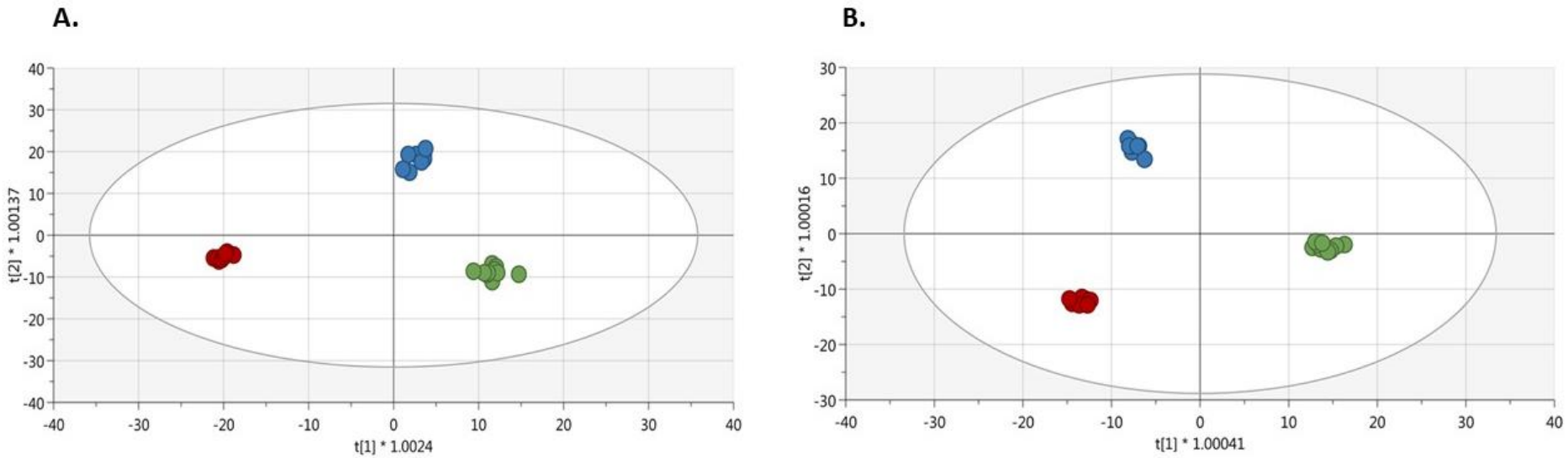

Supplementary Figure S11| Identified metabolites in control conditions. Metabolic processes (A), secondary metabolism (B) and hormone biosynthesis (C) impaired by treatments in plants (tomato and lettuce) grown under control conditions. Differential metabolites (VIP score > 1.20) along with their fold-change (FC) values were elaborated using the Omic Viewer Dashboard of the PlantCyc pathway Tool software (www.pmn.plantcyc.com). The large dots represent the average (mean) of all log FC for metabolites, and the small dots represent the individual log FC for each metabolite. The x-axis represents each set of subcategories, while the y-axis corresponds to the cumulative log FC. FA/Lipid: fatty acids and lipids; Amine: amines and polyamines; Cofactor: cofactors, prosthetic groups, electron carriers, and vitamins; N-containing: Nitrogen-containing secondary metabolites; S-containing: Sulphur-containing secondary metabolites; Sugar Derives: sugar derivatives.

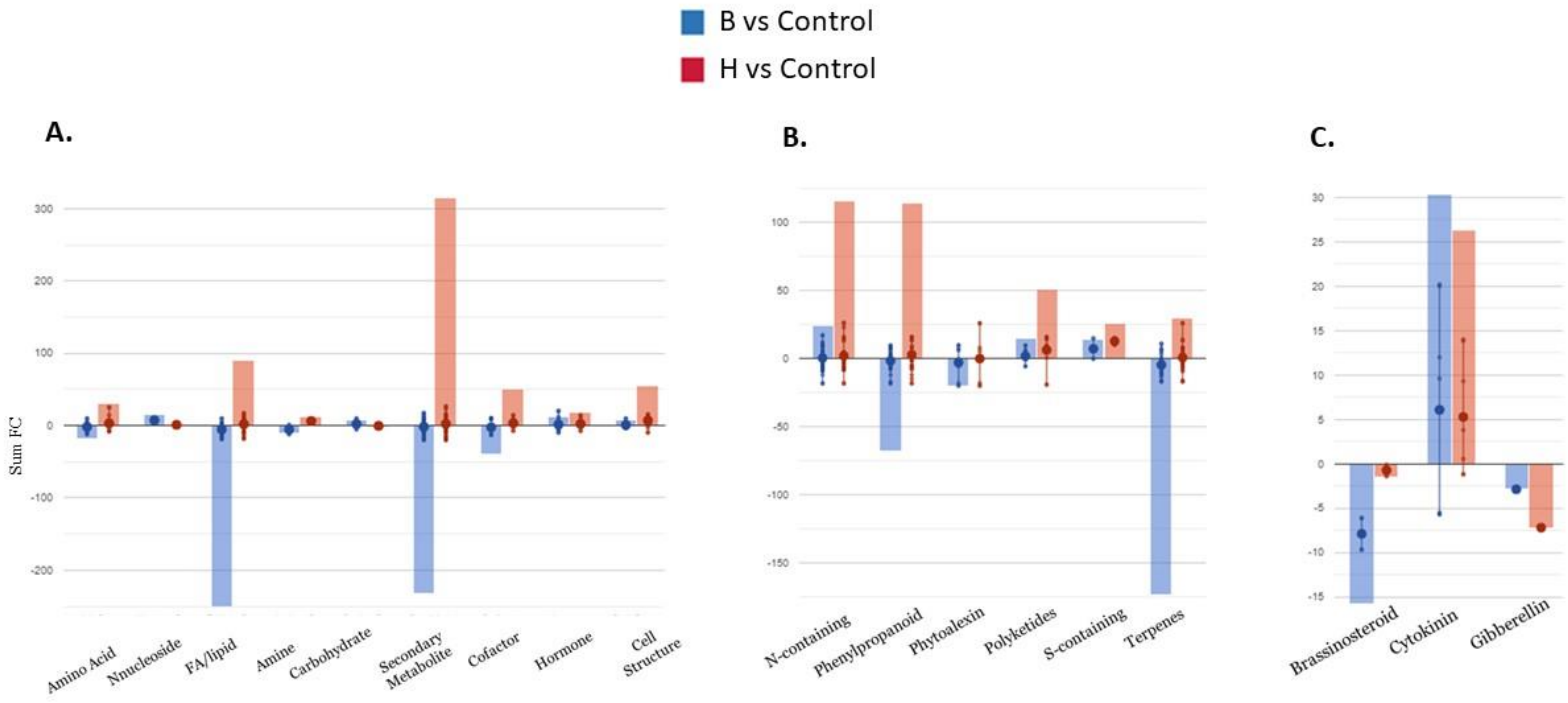

Supplementary Figure S12| Identified metabolites in NaCl conditions. Metabolic processes (A), secondary metabolism (B) and hormone biosynthesis (C) impaired by treatments in plants (tomato and lettuce) grown under salinity conditions. Differential metabolites (VIP score > 1.20) along with their fold-change (FC) values were elaborated using the Omic Viewer Dashboard of the PlantCyc pathway Tool software (www.pmn.plantcyc.com). The large dots represent the average (mean) of all log FC for metabolites, and the small dots represent the individual log FC for each metabolite. The x-axis represents each set of subcategories, while the y-axis corresponds to the cumulative log FC. FA/Lipid: fatty acids and lipids; Amine: amines and polyamines; Cofactor: cofactors, prosthetic groups, electron carriers, and vitamins; N-containing: Nitrogen-containing secondary metabolites; S-containing: Sulphur-containing secondary metabolites; Sugar Derivs: sugar derivatives.

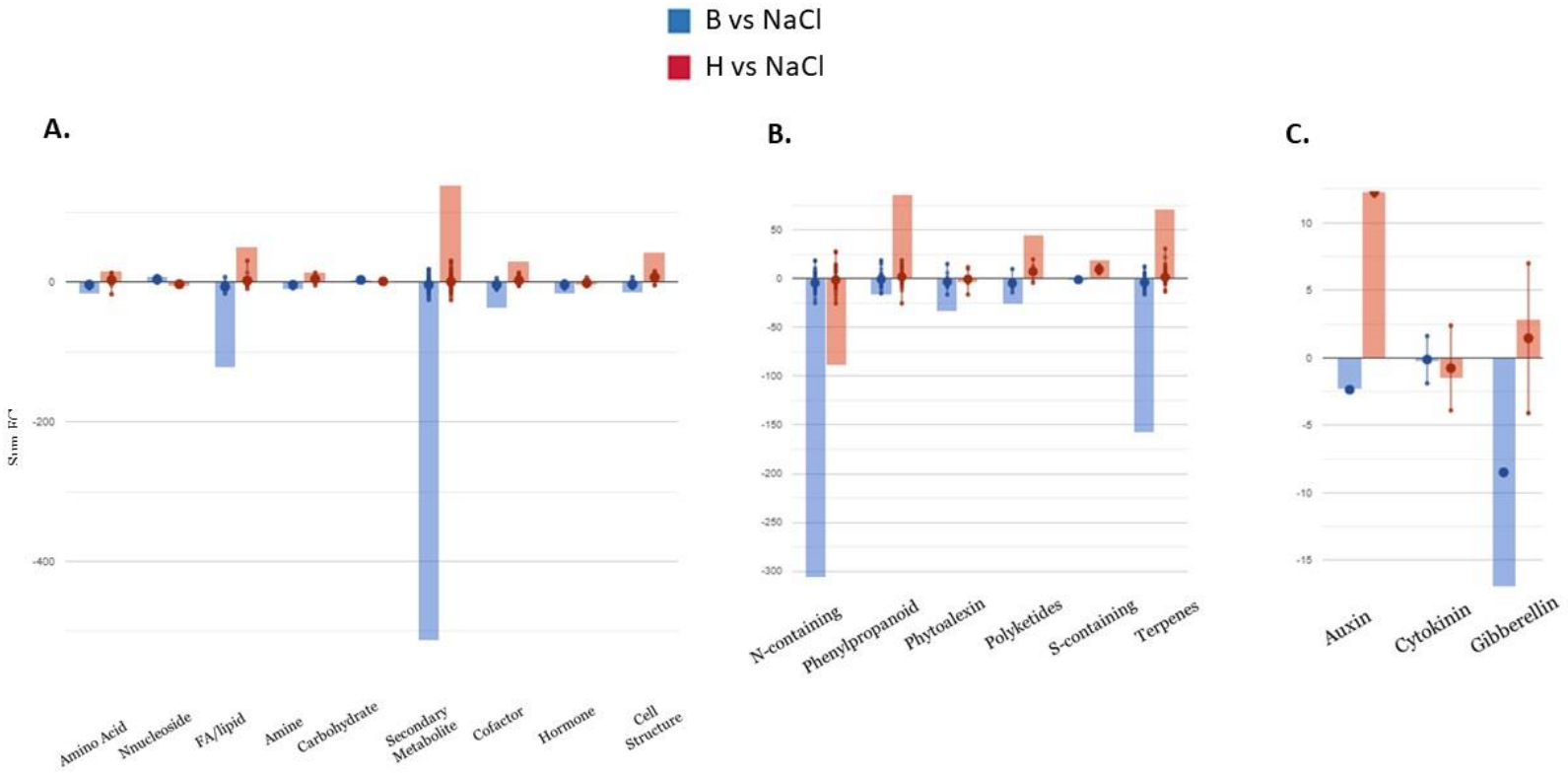

£Supplementary Figure S13| Graphical output of co-Inertia analysis (CIA). Scatter plot of tomato (A) and lettuce (B) samples. Each sample is represented by an arrow whose length is proportional to the divergence between the phenomic and the metabolomic datasets. Eigenvalues of the co-inertia analysis for tomato (C) and lettuce (D). Correlation circles (E and F) showing the projections of the PCA axes (from the phenomic datasets) onto the axes of the co-inertia analysis (x axes) and projections of the PCA axes (from the metabolomic datasets) onto the axes of the co-inertia analysis (y axes). These four circles represent a view of the rotations needed to associate the two datasets for tomato (E) and the two datasets for lettuce (F).

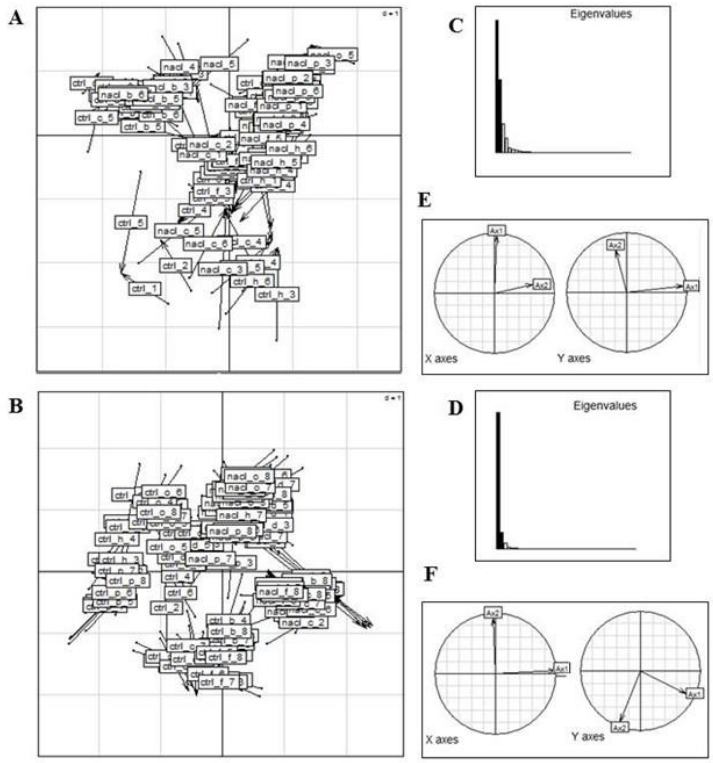

Results

Supplementary Table S1|Pairwise comparisons test using mixed models for determining the significant differences between the means of the morphological parameters in lettuce (1st round, A; 2nd round, B) and tomato plants (C) growing in control and NaCl stress conditions and treated with 7 PHs, at different time points. The p-values below 0.05 are highlighted in green.

Supplementary Table S2| Pairwise comparisons test using mixed models for determining the significant differences between the means of the photosynthetic parameters in lettuce (1st round, A; 2nd round, B) and tomato plants (C) growing in control and NaCl stress conditions and treated with 7 PHs, at different time points. The p-values below 0.05 are highlighted in green.

Supplementary Table S3| Pairwise comparisons test using mixed models for determining the significant differences between the means of the difference between canopy and air temperature in lettuce (1st round, A; 2nd round, B) and tomato plants (C) growing in control and NaCl stress conditions and treated with 7 PHs, at different time points. The p-values below 0.05 are highlighted in green.

Supplementary Table S4| Importance of variables for lettuce (A) and tomato plants (B) based on the random forest classifier used for treatment classification based on mean decrease in classification accuracy measure.

Supplementary Table S5| Whole dataset produced from untargeted metabolomics carried out in lettuce (A) and tomato plants (B) treated with 7 PHs either under stressed and non-stress conditions. Compounds are presented with individual intensities and composite mass spectra.

Supplementary Table S6| Discriminant metabolites identified by the variable importance in projection (VIP) analysis following OPLS-DA modelling of metabolome in lettuce (A) and tomato plants (B) treated with 7 PHs, either under non-stressed and stress conditions. Compounds were selected as discriminant by possessing a VIP score>1.20.

Supplementary Table S7| Differential metabolites derived from Volcano analysis ($p<0.01$; $FC \geq 1.3$) in lettuce (A) and tomato plants (B) treated with PH B and PH H under control and salinity conditions.

Supplementary Table S8| Discriminant metabolites identified by the variable importance in projection (VIP) analysis following OPLS-DA modelling of metabolome of plants of lettuce and tomato plants treated with PH H and PH B under control (A) and stress (B) conditions along with their LogFC values in comparison to control samples. Compounds were selected as discriminant by possessing a VIP score>1.20

Supplementary Table S9| Correlation matrix between the most important phenotyping traits (according to the random forest analysis) and the metabolites for lettuce (A) and for tomato plants (B).

Results

The Supplementary Tables for this article can be found online at:

https://drive.google.com/drive/folders/1V8rIQ-H2Tu90vWEl0_XUOZVsfnd1lfIw?usp=sharing

Overall conclusions

This PhD project focused on the development of a reliable and reproducible method for the screening of potential biostimulant substances on different plant species, in optimal or sub-optimal conditions, using platforms for automated plant phenotyping and in-depth metabolomic analysis. The attention was mainly focused on the biomass accumulation, morphological modifications, photosynthetic efficiency and primary and secondary metabolites production in response to the biostimulants application. The results obtained with the different omics techniques were then integrated with the help of multivariate statistical analysis.

We chose to investigate four plant species at diverse developmental stages:

- The first experiment focused on the development of a simple method to test the effects of biostimulant coating on the germination and the early establishment of wheat seeds in control or salt stress conditions. Wheat is the most extensively cultivated cereal and a worldwide staple food, whose germination is especially affected by the soil salinity. To estimate the mode of action of the 6 compounds in a clear-cut way, we used the Plant Biostimulant Characterization (PBC) index, developed by Ugena and co-workers (2018). By using PBC index it is possible to quantitatively investigate the effects of the biostimulants application on multiple parameters at once, comparing the effects of different doses in diverse growing conditions. As a matter of fact, the results of the first experiment highlighted a high dose-dependent and growth conditions-dependent response of the seeds to the biostimulant coating. The biostimulants that proved to be the best in control and in conditions of NaCl stress also showed a dose-dependent performance, with the lowest concentration having little to no effect on the germination of the coated seeds. The aforementioned biostimulant was a PH-based substance derived from pea seed extract.
- The second phase of this work focused on the seedling stage. Young Arabidopsis plantlets primed with 11 different biostimulants at 3 increasing concentrations were transplanted in plain or salt-enriched growing media and were screened for a week for their growth performance. The use of a model plant such as Arabidopsis allowed us to screen a bigger set of biostimulants, increasing at the same time the number of replicates. The results of this experiment highlighted once again the importance of screening a range of biostimulant concentrations; for most of the substances, in fact, the highest dose proved to be detrimental to the growth and survival of the plants. Different results were also observed for plantlets

growing in control, mild and severe stress conditions. The use of the Plant Biostimulant Characterization Index was again essential to identify the two substances that acted as the best growth improver and stress alleviator in all 3 doses applied: the commercial product Trainer® and an experimental compound derived by the biomass of plants belonging to the *Malvaceae* family.

- Therefore, a third stage of the work was focused on evaluating the effects of biostimulant applications on crops, from the early stage up to maturity. For this purpose, we chose lettuce and tomato, two economically relevant crop species that differ greatly in regard to their structure and final commercial scope. The use of an integrative phenotyping platform, combining data obtained from multiple imaging sensors, and the metabolomic analysis of the plant tissue, highlighted a completely different response of the two species, both to the stress application and to the treatment with the biostimulants. The monitoring of the plant growth for a longer period of time (if compared to the two previous trials) allowed us to observe the changing responses of the individuals to the application of the different substances in an early or later phase of the growth.

As an internal control, we used the commercial substance Trainer® in all the aforementioned trials. The beneficial effects of Trainer® have already been proven in multiple works (Colla et al., 2014; Lucini et al., 2015; Rouphael et al., 2017b; Di Mola et al., 2019a; Luziatelli et al., 2019). However, our results greatly differed according to the application method, the dose used, the stress applied and the plant species to which the biostimulant was provided:

- In the germination assay, the coating of the wheat seeds with Trainer® did not improve germination or early development of the seedlings in control conditions. On the other hand, Trainer® increased the tolerance to salinity of the seedlings when supplied in its lower concentration (80 g/100 kg).
- In the in-vitro assay on Arabidopsis seedlings, Trainer® acted as the best growth improver and stress alleviator in all 3 doses applied. These results also confirmed the biological translation of the trial made on Arabidopsis to profitable agronomic crops.
- In mature tomato plants subjected to drought stress, between the 6 biostimulants applied Trainer® was the one that increased the most the biomass accumulation and the stress tolerance of the plants, especially when applied using the substrate drench method.

- Finally, when applied to lettuce and tomato plants grown in salinity stress conditions, Trainer® only had a weak effect on the photosynthetic efficiency of tomato plants, while showing little to no improving effects on lettuce.

In summary, high throughput automated phenotyping technology proved to be an extremely useful tool for the screening of potential new biostimulant substances on multiple crop species, shortening the time needed and allowing to test the mode of action of the compounds on hundreds of plants at the same time, at different developmental stages and in different growing conditions. The integration of phenomics with metabolomics helped us to investigate the metabolomic pathways activated by the biostimulants applications, deepening our knowledge about their mode of action.

Future lines of research arising from this PhD work may possibly focus on:

- Investigation of the mode of action on biostimulants applied on crops growing in field conditions, with non-controlled environmental settings. Field conditions may also allow the choice of crops with a longer life cycle, to be monitored until their complete maturity (e.g., cereals).
- Integration of the phenotyping technology with multi-omics methods (transcriptomics, proteomics, metabolomics) to develop biostimulants that can effectively boost the crops yielding and stress resistance.
- Development of specialized algorithms based on deep learning technology for simplifying the process of extracting phenotypic features of biostimulant-treated crops subjected to high-throughput automated phenotyping.

Literature cited

Abdelhakim, L.O.A.; Rosenqvist, E.; Wollenweber, B.; Spyroglou, I.; Ottosen, C.-O.; Panzarová, K. (2021) Investigating Combined Drought- and Heat Stress Effects in Wheat under Controlled Conditions by Dynamic Image- Based Phenotyping. Agronomy, 11, 364. https://doi.org/10.3390/ agronomy11020364

Adhikari N.D., Simko I. and Mou B. (2019). Phenomic and Physiological Analysis of Salinity Effects on Lettuce. Sensors, 19, 4814; doi:10.3390/s19214814

Afzal I., Basra S.A.M. and Iqbal A. (2005). The effects of growth regulators on seedling vigour of wheat under salinity stress. Journal of Stress Physiology & Biochemistry 1: 6–14.

Agati, G., Azzarello, E., Pollastri, S., and Tattini, M. (2012). Flavonoids as antioxidants in plants: location and functional significance. Plant Sci. 196, 67–76. doi: 10.1016/j.plantsci.2012.07.014

Aggarwal, C. C., Hinneburg, A., & Keim, D. A. (2001). On the Surprising Behavior of Distance Metrics in High Dimensional Space. Lecture Notes in Computer Science, 420–434. doi:10.1007/3-540-44503-x_27

Agudelo-Romero, P., Erban, A., Sousa, L., Pais, M. S., Kopka, J., and Fortes, A. M. (2013). Search for transcriptional and metabolic markers of grape pre-ripening and ripening and insights into specific aroma development in three Portuguese cultivars. PLoS ONE. 8, e60422. doi: 10.1371/journal.pone.0060422

Ahammed, G. J., Li, X., Liu, A., and Chen, S. (2020). Brassinosteroids in plant tolerance to abiotic stress. *J. Plant Growth Reg.* doi:10.1007/s00344-020-10098-0

Aimar D., Calafat M., Andrade A.M., Carassay L., Abdala G.I. and Molas M.L. (2011). Drought Tolerance and Stress Hormones: From Model Organisms to Forage Crops, in: Plants and Environment. doi: 10.5772/24279

Aires, A. (2018). Hydroponic Production Systems: Impact on Nutritional Status and Bioactive Compounds of Fresh Vegetables. https://dx.doi.org/10.5772/intechopen.73011.

Literature cited

Akhtar S.S., Amby D.B., Hegelund J.N., Fimognari L., Großkinsky D.K., Westergaard J.C., Müller R., Moelbak L., Liu F. And Roitsch T. (2020) Bacillus licheniformis FMCH001 Increases Water Use Efficiency via Growth Stimulation in Both Normal and Drought Conditions. Front. Plant Sci. 11:297. doi: 10.3389/fpls.2020.00297

Ali, M., Kamran, M., Abbasi, G.H. et al. (2021). Melatonin-induced salinity tolerance by ameliorating osmotic and oxidative stress in the seedlings of two tomato (*Solanum lycopersicum* L.) cultivars. J. Plant Growth Regul. 40, 2236–2248. doi: 10.1007/s00344-020-10273-3

Allakhverdiev, S. I., Kinoshita, M., Inaba, M., Suzuki, I., and Murata, N. (2001). Unsaturated fatty acids in membrane lipids protect the photosynthetic machinery against salt-induced damage in *Synechococcus*. Plant Physiol. 125, 1842–1853. doi: 10.1104/pp.125.4.1842

Al-Tamimi, N., Brien, C., Oakey, H., Berger, B., Saade, S., Ho, Y. S., et al. (2016). Salinity tolerance loci revealed in rice using high-throughput non-invasive phenotyping. *Nat. Commun.*7, 13342. doi: 10.1038/ncomms13342

Amirkhani, M., Mayton, H. S., Netravali, A. N., & Taylor, A. G. (2019). A Seed Coating Delivery System for Bio-Based Biostimulants to Enhance Plant Growth. Sustainability, 11(19), 5304. doi:10.3390/su11195304

Amirkhani M., Netravali A.N., Huang W. and Taylor A.G. (2016) Investigation of soy protein based biostimulant seed coating for broccoli seedling and plant growth enhancement. HortScience 2016, 51, 1121–1126 doi: 10.21273/HORTSCI10913-16

Apone F., Tito A., Carola A., Arciello S., Tortora A., Filippini L., Monoli I., Cucchiara M., Gibertoni S., Chrispeels M.J. and Colucci G. (2010). A mixture of peptides and sugars derived from plant cell walls increases plant defense responses to stress and attenuates ageing associated molecular changes in cultured skin cells. J. Biotechnol. 145, 367–376 doi: 10.1016/j.jbiotec.2009.11.021

Ariana D. P. and R. Lu. (2008). Detection of internal defect in pickling cucumbers using hyperspectral transmittance imaging. Trans. ASABE 51(2): 705-713. doi: 10.13031/2013.24367

Literature cited

Arioli T., Mattner S.W. and Winberg P.C. (2015). Applications of seaweed extracts in Australian agriculture: past, present and future. Journal of Applied Phycology volume 27, pages2007–2015(2015) doi: 10.1007/s10811-015-0574-9

Asaf, S., Khan, A. L., Khan, M. A., Imran, Q. M., Yun, B. W., and Lee, I. J. (2017). Osmoprotective functions conferred to soybean plants via inoculation with *Sphingomonas* sp. LK11 and exogenous trehalose. Microbiol. Res. 205, 135–145. doi: 691 10.1016/j.micres.2017.08.009

Atieno, J., Li, Y., Langridge, P., Dowling, K., Brien, C., Berger, B., Varshney, R.K., Sutton, T. (2017). Exploring genetic variation for salinity tolerance in chickpea using image-based phenotyping. Scientific Reports, 7(1). doi:10.1038/s41598-017-01211-7

Awlia M., Nigro A., Fajkus J., Schmoeckel S.M., Negrão S., Santelia D., Trtílek M., Tester M., Julkowska M.M. and Panzarová K. (2016) High-Throughput Non-destructive Phenotyping of Traits that Contribute to Salinity Tolerance in Arabidopsis thaliana. Front. Plant Sci. 7:1414. doi: 10.3389/fpls.2016.01414

Bady, P., Dolédec, S., Dumont, B., & Fruget, J.-F. (2004). Multiple co-inertia analysis: a tool for assessing synchrony in the temporal variability of aquatic communities. Comptes Rendus Biologies, 327(1), 29–36. doi: 10.1016/j.crvi.2003.10.007

Baker, N. R. (2008). Chlorophyll Fluorescence: A Probe of Photosynthesis In Vivo. Annual Review of Plant Biology, 59(1), 89–113. doi:10.1146/annurev.arplant.59.032607.092759

Baker, N.R., and Rosenqvist, E. (2004). Applications of chlorophyll fluorescence can improve crop production strategies: an examination of future possibilities. *J. Exp. Bot.* 55, 1607–1621 doi: 10.1093/jxb/erh196

Banerjee, B. P., Joshi, S., Thoday-Kennedy, E., Pasam, R. K., Tibbits, J., Hayden, M. et al. (2020). High-throughput phenotyping using digital and hyperspectral imaging-derived biomarkers for genotypic nitrogen response. Journal of Experimental Botany, 71(15), 4604–4615. doi:10.1093/jxb/eraa143

Literature cited

Barbosa, G.L., Almeida Gadelha, F.D., Kublik, N., Proctor, A., Reichelm, L., Weissinger, E., Wohlleb, G.M., and Halden, R.H. (2015). Comparison of Land, Water, and Energy Requirements of Lettuce Grown Using Hydroponic vs. Conventional Agricultural Methods. Int. J. Environ. Res. Public Health 12, 6879-6891 https://doi.org/10.3390/ijerph120606879.

Barczak-Brzyzek A.K., Kiełkiewicz M., Gawronski P., Kot K., Filipecki M., Karpinska B. (2017). Cross-talk between high light stress and plant defence to the two-spotted spider mite in Arabidopsis thaliana. Exp Appl Acarol 73:177–189 doi:10.1007/s10493-017-0187-x

Barradas A., Correia P.M.P., Silva S., Mariano P., Pires M.C., Matos A.R., da Silva A.B., Marques da Silva J. (2021) Comparing Machine Learning Methods for Classifying Plant Drought Stress from Leaf Reflectance Spectra in Arabidopsis thaliana. Appl. Sci. 2021, 11, 6392. https://doi.org/10.3390/app11146392

Bates, D., Mächler, M., Bolker, B., Walker, S. (2015) Fitting linear mixed-effects models using lme4. J. Stat. Softw. 2015, 67, doi:10.18637/jss.v067.i01.

Beach C.B. and Morton McMurry F. (1914). The new student's reference work for teachers, students and families. F. E. Compton and Company (Chicago)

Behie S.W. and Bidochka M.J. (2014). Nutrient transfer in plant-fungal symbioses. Trends Plant Sci. 19, 734–740. doi: 10.1016/j.tplants.2014.06.007

Ben-Jabeur M., Gracia-Romero, A., López-Cristoffanini C., Vicente R., Kthiri Z., Carlisle Kefauver S., López-Carbonell M., Serret M.D., Araus J.L. and Hamada W. (2020) The promising MultispeQ device for tracing the effect of seed coating with biostimulants on growth promotion, photosynthetic state and water–nutrient stress tolerance in durum wheat. Euro-Mediterr J Environ Integr 6, 8. doi:10.1007/s41207-020-00213-8

Berger B., Parent B. and Tester M. (2010). High-throughput shoot imaging to study drought responses. Journal of Experimental Botany, Vol. 61, No. 13, pp. 3519–3528, 2010 doi:10.1093/jxb/erq201

Literature cited

Billakurthi, K., & Schreier, T. B. (2020). Insights into the control of metabolism and biomass accumulation in a staple C4 grass. Journal of Experimental Botany, 71(18), 5298–5301. doi:10.1093/jxb/eraa307

Biostimulant Market (2020). Biostimulants Market by Active Ingredient (Humic Substances, Amino Acids, Seaweed Extracts, Microbial Amendments), Crop Type (Fruits & Vegetables, Cereals, Turf & Ornamentals), Application Method, Form, and Region – Global Forecast to 2025. Available at: https://www.marketsandmarkets.com/Market-Reports/biostimulant-market-1081.html

Boisgontier, M.P.; Cheval, B. (2016) The anova to mixed model transition. Neurosci. Biobehav. Rev. 2016, 68, 1004–1005, doi: 10.1016/j.neubiorev.2016.05.034.

Bonfante P. and Genre A. (2010). Mechanisms underlying beneficial plant–fungus interactions in mycorrhizal symbiosis. Nat. Commun. 1, 1–11. doi: doi.org/10.1038/ncomms1046

Borgognone, D., Rouphael, Y., Cardarelli, M., Lucini, L., and Colla G. (2016). Changes in biomass, mineral composition, and quality of cardoon in response to NO3−:Cl−ratio and nitrate deprivation from the nutrient solution. Front. Plant Sci. 7: 978. doi: 10.3389/fpls.2016.00978

Botta A. (2013). Enhancing plant tolerance to temperature stress with amino acids: an approach to their mode of action. Acta Hortic. 1009, 29–35. doi: 10.17660/actahortic.2013.1009.1

Brestic, M., and Zivcak, M. (2013). PSII fluorescence techniques for measurement of drought and high temperature stress signal in crop plants: protocols and applications. Molecular stress physiology of plants. 87–131. doi: 0.1007/978-81-322-0807-5_4

Briglia N., Petrozza A., Hoeberichts F.A., Verhoef N. and Povero G. (2019). Investigating the Impact of Biostimulants on the Row Crops Corn and Soybean Using High-Efficiency Phenotyping and Next Generation Sequencing. Agronomy 2019, 9, 761; doi:10.3390/agronomy9110761

Brown, P., and Saa, S. (2015) Biostimulants in agriculture. *Front. Plant Sci.* 6, 671. doi: 10.3389/fpls.2015.00671

Literature cited

Brunetti, C., Di Ferdinando, M., Fini, A., Pollastri, S., & Tattini, M. (2013). Flavonoids as Antioxidants and Developmental Regulators: Relative Significance in Plants and Humans. International Journal of Molecular Sciences, 14(2), 3540–3555. doi:10.3390/ijms14023540

Bulgari R., Franzoni G. and Ferrante A. (2019). Biostimulants Application in Horticultural Crops under Abiotic Stress Conditions. Agronomy 2019, 9, 306; doi:10.3390/agronomy9060306

Bulgari, R., Morgutti, S., Cocetta, G., Negrini, N., Farris, S., Calcante, et al. (2017) Evaluation of borage extracts as potential biostimulant using a phenomic. Agronomic, physiological, and biochemical approach. *Front. Plant Sci.* 8, 935. doi: 10.3389/fpls.2017.00935

Burrell T., Fozard S., Holroyd G.H., French A.P., Pound M.P., Bigley C.J., Taylor C.J. and Forde B.G. (2017). The Microphenotron: a robotic miniaturized plant phenotyping platform with diverse applications in chemical biology. Plant Methods (2017) 13:10 doi:10.1186/s1007-017-0158-6

Busemeyer L, Mentrup D, Möller K, Wunder E, Alheit K, Hahn V, et al. (2013). BreedVision — A Multi-Sensor Platform for Non-Destructive Field-Based Phenotyping in Plant Breeding. Sensors 13(3):2830–47. doi:10.3390/s130302830

Calvo P., Nelson L. and Kloepper J. W. (2014). Agricultural use of plant biostimulants. Plant Soil (2014) 83:3–41 doi: 10.1007/s11104-014-2131-8

Campobenedetto C, Grange E, Mannino G, van Arkel J, Beekwilder J, Karlova R, Garabello C, Contartese V and Bertea CM (2020) A Biostimulant Seed Treatment Improved Heat Stress Tolerance During Cucumber Seed Germination by Acting on the Antioxidant System and Glyoxylate Cycle. Front. Plant Sci. 11:836. doi: 10.3389/fpls.2020.00836

Cano-Ramirez, D.L. & Dodd, A.N. (2018) New connections between circadian rhythms, photosynthesis, and environmental adaptation. Plant, Cell & Environment, 41(11), pp.2515–2517. doi:10.1111/pce.13346.

Care D.A., Nichols S.N., Woodfield D.R. (1998) Image analysis techniques to characterise white clover root morphology. Proceedings of the New Zealand Grassland Association 60: 187-191. doi: 10.33584/jnzg.1998.60.2296

Literature cited

Carillo, P., Ciarmiello, L. F., Woodrow, P., Corrado, G., Chiaiese, P., and Rouphael, Y. (2020). Enhancing sustainability by improving plant salt tolerance through macro- and micro-algal biostimulants. *Biol.* 9, 253. doi:10.3390/biology9090253.

Caspi, R., Dreher, K., & Karp, P. D. (2013). The challenge of constructing, classifying, and representingmetabolic pathways. In FEMS Microbiology Letters. doi:10.1111/1574-6968.12194

Cattivelli, L., Rizza, F., Badeck, F.W., Mazzucotelli, E., Mastrangelo, A.M., Francia, E., Marè, C., Tondelli, A., and Stanca, A.M. (2008). Drought tolerance improvement in crop plants: An integrated view from breeding to genomics. Field Crops Res. 105, 1-14 https://doi.org/10.1016/j.fcr.2007.07.004.

Cavani L. and Ciavatta, C. (2007). Attività biostimolante degli idrolizzati proteici. L'informatore Agrario 44, 46–52.

Caviglia, M., Mazorra Morales, L. M., Concellón, A., Gergoff Grozeff, G. E., Wilson, M., Foyer, C. H., et al. (2018). Ethylene signaling triggered by low concentrations of ascorbic acid regulates biomass accumulation in *Arabidopsis thaliana*. Free Rad. Biol. Med. 122, 130–136. doi: 10.1016/j.freeradbiomed.2018. 01.032

Ceccarelli, A.V.; Miras-Moreno, B.; Buffagni, V.; Senizza, B.; Pii, Y.; Cardarelli, M.; Rouphael, Y.; Colla, G.; Lucini, L. (2021) Foliar Application of Different Vegetal-Derived Protein Hydrolysates Distinctively Modulates Tomato Root Development and Metabolism. Plants 2021, 10, 326. doi: 10.3390/plants10020326

Cerdán, M., Sánchez-Sánchez, A., Oliver, M., Juárez, M., and Sánchez-Andreu J. J. (2009). Effect of foliar and root applications of amino acids on iron uptake by tomato plants. *Acta Hortic.* 830, 481–488. doi: 10.17660/actahortic.2009.830.68

Chaves M. M., Maroco J. P. and Pereira J. S. (2003) Understanding plant responses to drought - From genes to the whole plant. Functional Plant Biology 30(3), 239. doi:10.1071/FP02076

Chen T.H.H. and Murata N. (2008). Glycinebetaine: an effective protectant against abiotic stress in plants. Trends Plant Sci. 13, 499–505. doi: 10.1016/j.tplants.2008.06.007

Literature cited

Chen S, Wu F, Li Y, Qian Y, Pan X, Li F, Wang Y, Wu Z, Fu C, Lin H and Yang A (2019) NtMYB4 and NtCHS1 Are Critical Factors in the Regulation of Flavonoid Biosynthesis and Are Involved in Salinity Responsiveness. Front. Plant Sci. 10:178. doi: 10.3389/fpls.2019.00178

Colantoni, A., Recchia, L., Bernabei, G., Cardarelli, M., Rouphael, Y., and Colla, G. (2017). Analyzing the environmental impact of chemically-produced protein hydrolysate from leather waste vs. enzymatically-produced protein hydrolysate from legume grains. *Agric.* 7, 62. doi.org/10.3390/agriculture7080062

Colla, G., Cardarelli, M., Bonini, P., and Rouphael, Y. (2017a). Foliar applications of protein hydrolysate, plant and seaweed extracts increase yield but differentially modulate fruit quality of greenhouse tomato. HortScience 52(9), 1214–1220. doi: 10.21273/hortsci12200-17

Colla, G., Hoagland, L., Ruzzi, M., Cardarelli, M., Bonini, P., Canaguier, R., et al. (2017b). Biostimulant action of protein hydrolysates: unravelling their effects on plant physiology and microbiome. Front. Plant Sci. 8, 2202. doi: 10.3389/fpls. 2017.02202

Colla, G., Nardi, S., Cardarelli, M., Ertani, A., Lucini, L., Canaguier, R., et al. (2015a). Protein hydrolysates as biostimulants in horticulture. *Sci. Hortic.* 196, 28–38. doi:10.1016/j.scienta.2015.08.037

Colla, G., and Rouphael, Y. (2015). Biostimulants in agriculture. *Sci. Hortic.* 196, 1–2. doi: 10.1016/j.scienta.2015.10.044

Colla, G., Rouphael, Y., Bonini, P. & Cardarelli, M. (2015b). Coating seeds with endophytic fungi enhances growth, nutrient uptake, yield and grain quality of winter wheat. International Journal of Plant Production. 9. 171-189. doi:10.22069/IJPP.2015.2042

Colla, G., Rouphael, Y., Canaguier, R., Svecova, E., and Cardarelli, M. (2014). Biostimulant action of a plant-derived protein hydrolysate produced through enzymatic hydrolysis. *Front. Plant Sci.* 5. doi: 10.3389/fpls.2014.00448

Colla, G., Rouphael, Y., Leonardi, C., and Bie, Z. (2010). Role of grafting in vegetable crops grown under saline conditions. *Sci. Hortic.* 127, 147–155. doi: 10.1016/j.scienta.2010.08.004

Literature cited

Colla, G., Rouphael, Y., Lucini, L., Canaguier, R., Stefanoni, W., Fiorillo, A., et al. (2016). Protein hydrolysate-based biostimulants: Origin, biological activity and application methods. Acta Hortic. 1148, 27–34. doi: 10.17660/actahortic.2016.1148.3

Colla, G., Svecova, E., Rouphael, Y., Cardarelli, M., Reynaud, H., Canaguier, R., Planques, B. (2013). Effectiveness of a plant –derived protein hydrolysate to improve crop performances under different growing conditions. Acta Hortic. 1009, 175–179. doi:10.17660/actahortic.2013.1009.21

Conrath, U. (2011). Molecular aspects of defence priming. Trends Plant Sci. 16, 524–531. doi: 10.1016/j.tplants.2011.06.004

Corwin, D. L. (2020). Climate change impacts on soil salinity in agricultural areas. Eur. J. Soil Sci. 72(2), 842–862. doi:10.1111/ejss.13010

Craigie, J.S. (2011). Seaweed extract stimuli in plant science and agriculture. J. Appl. Phycol. 23, 371–393. doi: 10.1007/s10811-010-9560-4

Cramer G.R., Urano K., Delrot S., Pezzotti M. and Shinozaki K. (2011). Effects of abiotic stress on plants: a systems biology perspective. BMC Plant Biology 2011, 11:163 doi: 10.1186/1471-2229-11-163

Cuin, T. A., and Shabala, S. (2007). Amino acids regulate salinity-induced potassium efflux in barley root epidermis. *Planta* 25, 753–61. doi: doi.org/10.1007/s00425-006-0386-x

D'Amelia, V., Aversano, R., Chiaiese, P., and Carputo, D. (2018). The antioxidant properties of plant flavonoids: their exploitation by molecular plant breeding. *Phytochem. Rev.* 17, 611–625. doi: 10.1007/s11101-018-9568-y

Dalal, A., Bourstein, R., Haish, N., Shenhar, I., Wallach, R., and Moshelion, M. (2019). Dynamic physiological phenotyping of drought-stressed pepper plants treated with "productivity-enhancing" and "survivability-enhancing" biostimulants. *Front. Plant Sci*. 10, 905. doi: 10.3389/fpls.2019.00905

Literature cited

Danzi D., Briglia N., Petrozza A., Summerer S., Povero G., Stivaletta A., Cellini F., Pignone D., De Paola D. And Janni M. (2019) Can High Throughput Phenotyping Help Food Security in the Mediterranean Area? Front. Plant Sci. 10:15. doi: 10.3389/fpls.2019.00015

Davies, W. J., Bacon, M. A., Stuart Thompson, D., Sobeih, W., & González Rodríguez, L. (2000). Regulation of leaf and fruit growth in plants growing in drying soil: exploitation of the plants' chemical signalling system and hydraulic architecture to increase the efficiency of water use in agriculture. J Exp Bot, 51(350), 1617–1626. doi:10.1093/jexbot/51.350.1617

De Diego, N., Fürst, T., Humplík, J. F., Ugena L., Podlešáková, K., and Spíchal L. (2017). An automated method for high-throughput screening of *Arabidops*is rosette growth in multi-well plates and its validation in stress conditions. *Front. Plant Sci.* 8, 1702. doi: 10.3389/fpls.2017.01702

De Diego, N., Perez-Alfocea, F., Cantero, E., Lacuesta, M., & Moncalean, P. (2012). Physiological response to drought in radiata pine: phytohormone implication at leaf level. Tree Physiology, 32(4), 435–449. doi:10.1093/treephys/tps029

Dell'Aversana E., D'Amelia L., De Pascale S., Carillo P. (2020) Use of Biostimulants to Improve Salinity Tolerance in Agronomic Crops. In: Hasanuzzaman M. (eds) Agronomic Crops. Springer, Singapore. doi: 10.1007/978-981-15-0025-1_2

Devarajan, A.K.; Muthukrishanan, G.; Truu, J.; Truu, M.; Ostonen, I.; Kizhaeral S., S.; Panneerselvam, P.; Kuttalingam Gopalasubramanian, S. (2021) The Foliar Application of Rice Phyllosphere Bacteria induces Drought-Stress Tolerance in *Oryza sativa* (L.). Plants, 10, 387. https://doi.org/10.3390/plants10020387

Di Mola, I.; Conti, S.; Cozzolino, E.; Melchionna, G.; Ottaiano, L.; Testa, A.; Sabatino, L.; Rouphael, Y.; Mori, M. (2021) Plant-Based Protein Hydrolysate Improves Salinity Tolerance in Hemp: Agronomical and Physiological Aspects. Agronomy, 11, 342. doi: 10.3390/agronomy11020342

Di Mola, I., Ottaiano, L., Cozzolino, E., Senatore, M., Giordano, M., El-Nakhel, C. et al. (2019a). Plant-Based Biostimulants Influence the Agronomical, Physiological, and Qualitative

Responses of Baby Rocket Leaves under Diverse Nitrogen Conditions. Plants, 8(11), 522. doi:10.3390/plants8110522

Di Mola, I., Cozzolino, E., Ottaiano, L., Giordano, M., Rouphael, Y., Colla, G., & Mori, M. (2019b). Effect of Vegetal- and Seaweed Extract-Based Biostimulants on Agronomical and Leaf Quality Traits of Plastic Tunnel-Grown Baby Lettuce under Four Regimes of Nitrogen Fertilization. Agronomy, 9(10), 571. doi:10.3390/agronomy9100571

Digruber, T., Sass, L., Cseri, A., Paul, K., Nagy, A. V., Remenyik, J., et al. (2018). Stimulation of energy willow biomass with triacontanol and seaweed extract. Ind. Crops Products. 120, 104–112. doi: 10.1016/j.indcrop.2018.04.047

Du Jardin, P. (2012). The Science of Plant Biostimulants—A bibliographic analysis. Ad hoc Study Report to the European Commission DG ENTR. 2012; http://ec. europa.eu/enterprise/sectors/chemicals/files/fertilizers/final report bio 2012 en.pdf.

Du Jardin, P. (2015). Plant biostimulants: Definition, concept, main categories and regulation. *Sci. Hortic.* 196 3–14. doi: 10.1016/j.scienta.2015.09.021

Dubois, M., Van den Broeck, L., and Inzé, D. (2018). The pivotal role of ethylene in plant growth. Trends Plant Sci. 23, 311–323. doi: 10.1016/j.tplants.2018. 01.003

Dudits, D., Török, K., Cseri, A., Paul, K., Nagy, A. V., Nagy B., et al. (2016). Response of organ structure and physiology to autotetraploidization in early development of energy willow (*Salix viminalis*). *Plant Physiol.* 170, 1504–1523. doi: 10.1104/pp.15.01679

El-Hendawy S.E., Hassan W.M., Refay Y. and Schmidhalter U. (2017). On the use of spectral reflectance indices to assess agro- morphological traits of wheat plants grown under simulated saline field conditions. J Agro Crop Sci. 2017; 203:406–428 doi: 10.1111/jac.12205

Elmasry G., Kamruzzaman M., Sun D. and Allen P. (2012). Principles and Applications of Hyperspectral Imaging in Quality Evaluation of Agro-Food Products: A Review. Critical Reviews in Food Science and Nutrition, 52:11, 999-1023. doi: 10.1080/10408398.2010.543495

Literature cited

Eriksen, R., Knepper, C., Cahn, M.D., and Mou, B. (2016). Screening of lettuce germplasm for agronomic traits under low water conditions. HortScience 51(6), 669–679.

Ertani, A., Cavani, L., Pizzeghello, D., Brandellero, E., Altissimo, A., Ciavatta C., et al. (2009). Biostimulant activities of two protein hydrolysates on the growth and nitrogen metabolism in maize seedlings. *J. Plant. Nutr. Soil Sci.* 172, 237–244. doi: 10.1002/jpln.200800174

Ertani, A., Francioso, O., Tinti, A., Schiavon, M., Pizzeghello, D., and Nardi S. (2018). Evaluation of seaweed extracts from *Laminaria* and *Ascophyllum nodosum* spp. as biostimulants in *Zea mays* L. using a combination of chemical, biochemical and morphological approaches. *Front. Plant Sci.* 9, 428. doi: 0.3389/fpls.2018.00428

Ertani, A., Nardi, S., and Altissimo, A. (2012). Review: long-term research activity on the biostimulant properties of natural origin compounds. Acta Hortic. 1009, 181–188. doi: 10.17660/actahortic.2013.1009.22

Ertani A., Pizzeghello D., Francioso O., Sambo P., Sanchez-Cortes S. and Nardi S. (2014). *Capsicum chinensis* L. growth and nutraceutical properties are enhanced by biostimulants in a long-term period: chemical and metabolomic approaches. Front. Plant Sci. 5, 375. doi: 10.3389/fpls.2014. 00375 doi: 10.3389/fpls.2014.00375

Ertani A., Schiavon M., Muscolo A. and Nardi S. (2013). Alfalfa plant-derived biostimulant stimulate short-term growth of salt stressed Zea mays L. plants. Plant Soil 364, 145–158. doi: 10.1007/s11104-012-1335-z

Ertani, A., Schiavon, M., and Nardi, S. (2017). Transcriptome-wide identification of differentially expressed genes in *Solanum Lycopersicon* L. in response to an alfalfa-protein hydrolysate using microarrays. Front. Plant Sci. 8, 1159. doi: 10.3389/fpls.2017.01159

European Commission (2016). Proposal for a regulation laying down rules on the making available on the market of CE marked fertilizing products and amending Regulations (EC)1069/2009 and (EC)1107/2009.COM(2016) 157

Literature cited

Fahlgren, N., Gehan, M. A., & Baxter, I. (2015). Lights, camera, action: high-throughput plant phenotyping is ready for a close-up. Current Opinion in Plant Biology, 24, 93–99. doi:10.1016/j.pbi.2015.02.006

FAO and ITPS (2015). Status of the World's Soil Resources (SWSR) – Main Report. Food and Agriculture Organization of the United Nations and Intergovernmental Technical Panel on Soils, Rome, Italy

Farooq, M., Ullah, A., Lee, D. J., Alghamdi, S. S., and Siddique, K. H. M. (2018). *Desi* chickpea genotypes tolerate drought stress better than *kabuli* types by modulating germination metabolism, trehalose accumulation, and carbon assimilation. Plant Physiol. Biochem. 126, 47–54. doi: 10.1016/j.plaphy.2018.02.020

Fehér-Juhász, E., Majer, P., Sass, L., Lantos, C., Csiszár, J., Turóczy, Z., et al. (2014). Phenotyping shows improved physiological traits and seed yield of transgenic wheat plants expressing the alfalfa aldose reductase under permanent drought stress. Acta Physiol. Plant. 92, 663–673. doi: 10.1007/s11738-013- 1445-0

Fernández, V., and Eichert, T. (2009). Uptake of hydrophilic solutes through plant leaves: current state of knowledge and perspectives of foliar fertilization. Crit. Rev. Plant Sci. 28, 36-68. doi: 10.1080/07352680902743069

Ferrara A., Lovelli S., Di Tommaso T. and Perniola M. (2011). Flowering, growth and fruit setting in greenhouse bell pepper under water stress. J Agron 10: 12–19. doi: 10.3923/ja.2011.12.19

Feussner, I., and Polle, A. (2015). What the transcriptome does not tell - proteomics and metabolomics are closer to the plants' patho-phenotype. Current Opinion in Plant Biol. 26, 26-31. doi: 10.1016/j.pbi.2015.05.023

Fiorani F., Rascher U., Jahnke S. and Schurr U. (2012). Imaging plants dynamics in heterogenic environments. Current Opinion in Biotechnology 2012, 23:227–235 DOI 10.1016/j.copbio.2011.12.010

Fisher LHC, Han J, Corke FMK, Akinyemi A, Didion T, Nielsen KK, Doonan JH, Mur LAJ and Bosch M (2016) Linking Dynamic Phenotyping with Metabolite Analysis to Study Natural

Variation in Drought Responses of *Brachypodium distachyon*. Front. Plant Sci. 7:1751. doi: 10.3389/fpls.2016.01751

Fleming, T. R., Fleming, C. C., Levy, C. C. B., Repiso, C., Hennequart, F., Nolasco, J. B., & Liu, F. (2019). Biostimulants enhance growth and drought tolerance in *Arabidopsis thaliana* and exhibit chemical priming action. Annals of Applied Biology, 174(2), 153–165. doi:10.1111/aab.12482

Foolad M.R., Zhang L.P. and Subbiah P. (2003). Genetics of drought tolerance during seed germination in tomato: inheritance and QTL mapping. Genome, 46: 536-545. doi: 10.1139/g03-035

Foyer, C. H. (2018). Reactive oxygen species, oxidative signaling and the regulation of photosynthesis. Environ. Exp. Bot. 154, 134–142. doi: 10.1016/j.envexpbot. 2018.05.003

Foyer, C. H., Ruban, A. V., and Noctor, G. (2017). Viewing oxidative stress through the lens of oxidative signalling rather than damage. Biochem. J. 474, 877–883. doi: 10.1042/BCJ20160814

Freitas, W. E. de S., Oliveira, A. B. de, Mesquita, R. O., Carvalho, H. H. de, Prisco, J. T., & Gomes-Filho, E. (2019). Sulfur-induced salinity tolerance in lettuce is due to a better P and K uptake, lower Na/K ratio and an efficient antioxidative defense system. Scientia Horticulturae, 257, 108764. doi: 10.1016/j.scienta.2019.108764

Fricke W., Akhiyarova G., Veselov D. and Kudoyarova G. (2004). Rapid and tissue-specific changes in ABA and in growth rate response to salinity in barley leaves. J. Exp. Bot. 55:1115–23 doi: 10.1093/jxb/erh117

Furbank, R.T., and Tester, M. (2011). Phenomics - technologies to relieve the phenotyping bottleneck. Trends Plant Sci. 16, 12 doi:10.1016/j.tplants.2011.09.005

Gao G., Tester M.A, and Julkowska M.M. (2020). The Use of High-Throughput Phenotyping for Assessment of Heat Stress-Induced Changes in Arabidopsis, Plant Phenomics, vol. 2020, Article ID 3723916. doi: 10.34133/2020/3723916

Gémes, K., Kim, Y. J., Park, K. Y., Moschou, P. N., Andronis, E., Valassaki, C., et al. (2016). An NADPH-oxidase/polyamine oxidase feedback loop controls oxidative burst under salinity. Plant Physiol. 172, 1418–1431. doi: 10.1104/pp. 16.01118

Gémes, K., Mellidou, I, Karamanoli, K., Beris, D., Park, K. Y., Matsi, T., et al. (2017). Deregulation of apoplastic polyamine oxidase affects development and salt response of tobacco plants. J. Plant Physiol. 211, 1–12. doi: 10.1016/j.jplph. 2016.12.012

Genitsaris, S., Monchy, S., Breton, E., Lecuyer, E., & Christaki, U. (2016). Small-scale variability of protistan planktonic communities relative to environmental pressures and biotic interactions at two adjacent coastal stations. Marine Ecology Progress Series, 548, 61–75. doi:10.3354/meps11647

Genty, B., Briantais, J. M., and Baker, N. R. (1989). The relationship between the quantum yield of photosynthetic electron transport and quenching of chlorophyll fluorescence. Bioch. Biophy. Acta 990, 87-92. doi: 10.1016/s0304-4165(89)80016-9

Ghandchi, F. P., Caetano-Anolles, G., Clough, S. J., and Ort, D. R. (2016). Investigating the control of chlorophyll degradation by genomic correlation mining. PLoS One 11:e0162327. doi: 10.1371/journal.pone.0162327

Gill, S. S., and Tuteja, N. (2010). Polyamines and abiotic stress tolerance in plants. Plant Signal Behav. 7, 5(1). PMID: 20023386. doi: 10.4161/psb.5.1.10291

Goetz A.F.H., Vane G., Solomon J.E. and Rock B.N. (1985). Imaging Spectrometry for Earth Remote Sensing. Science Vol. 228, Issue 4704, pp. 1147-1153. doi: 10.1126/science.228.4704.1147

Gomiero, T. (2018). Food quality assessment in organic vs. conventional agricultural produce: findings and issues. Applied Soil Ecology 123, 714–728. doi:10.1016/j.apsoil.2017.10.014

Gonzalez, L., and Gonzalez-Vilar, M. (2003). Determination of relative water concentration. Handbook of plant ecophysiology techniques. Kluwer Academic Publishers, Netherlands 207–212 doi: 10.1007/0-306-48057-3_14.

Gorbe, E., and Calatayud, A. (2012). Applications of chlorophyll fluorescence imaging technique in horticultural research: A review. Sci.Hortic.138, 24–35. doi: 10.1016/j.scienta.2012.02.002

Gordon D.C., Hettiaratchi D. R. P., Bengough A.G. and Young I.M. (1992). Non-destructive analysis of root growth in porous media. Plant, Cell and Environment 15, 123-128 doi: 10.1111/j.1365-3040. 1992.tb01465.x

Grant O.L., Tronina L., Jones H.G. and Chaves M.M. (2007). Exploring thermal imaging variables for the detection of stress responses in grapevine under different irrigation regimes. Journal of Experimental Botany, Vol. 58, No. 4, pp. 815–825. doi:10.1093/jxb/erl153

Großkinsky, D. K., Svensgaard, J., Christensen, S., and Roitsch, T. (2015). Plant phenomics and the need for physiological phenotyping across scales to narrow the genotype-to-phenotype knowledge gap. J. Exper. Bot. 66, 5429–5440. doi: 10.1093/jxb/erv345

Guidi L. and Degl'Innocenti E. (2011). Imaging of Chlorophyll a Fluorescence: A Tool to Study Abiotic Stress in Plants. in: Abiotic Stress in Plants - Mechanisms and Adaptations. doi: 10.5772/22281

Habben, J. E., Bao, X., Bate, N. J., DeBruin, J. L., Dolan, D., Hasegawa, D., et al. (2014). Transgenic alteration of ethylene biosynthesis increases grain yield in maize under field drought-stress conditions. Plant Biotechnol. J. 12, 685–693. doi: 10.1111/pbi.12172

Halford NG, Shewry PR. (2000). Genetically modified crops: methodology, benefits, regulation and public concerns. Br Med Bull. 56(1):62-73. doi: 10.1258/0007142001902978.

Halpern, M., Bar-Tal, A., Ofek, M., Minz, D., Muller, T., and Yermiyahu, U. (2015). The use of biostimulants for enhancing nutrient uptake. Adv. Agron. 130, 141–174. doi: 10.1016/bs.agron.2014.10.001

Hamany Djande, C. Y., Pretorius, C., Tugizimana, F., Piater, L. A., & Dubery, I. A. (2020). Metabolomics: A Tool for Cultivar Phenotyping and Investigation of Grain Crops. Agronomy, 10(6), 831. doi:10.3390/agronomy10060831

Helfenstein, A., Vahermo, M., Nawrot, D. A., Demirci, F., İşcan, G., Krogerus, S., et al. (2017). Antibacterial profiling of abietane-type diterpenoids. Bioorg. Med. Chem. 25: 132–137. doi: 10.1016/j.bmc.2016.10.019

Henley, W. J. (1993). Measurement and interpretation of photosynthetic light-response curves in algae in the context of photoinhibition and diel changes. *J. Phycol*. 29, 729–739. doi: 10.1111/j.0022-3646.1993. 00729.x

Hichem, H., Mounir, D., and Naceur, E.A. (2009). Differential responses of two maize (*Zea mays* L.) varieties to salt stress: changes on polyphenols composition of foliage and oxidative damages. Ind. Crop Prod. 30, 144-51 doi: 10.1016/j.indcrop.2009.03.003.

Hou, Q., Ufer, G., and Bartels, D. (2016). Lipid signalling in plant responses to abiotic stress. Plant Cell Environ. 39, 1029–1048. doi: 10.1111/pce. 12666

Hou, Z.-H., Liu, G., Hua, Hou, L., Xia, Wang, L., et al. (2013). Regulatory Function of polyamine oxidase-generated hydrogen peroxide in ethylene- induced stomatal closure in *Arabidopsis thaliana*. J. Integr. Agric. 12, 251–262. doi: 10.1016/S2095-3119(13)60224-5

Houle, D., Govindaraju, D. R., and Omholt, S. (2010). Phenomics: the next challenge. Nat. Rev. Gen. 11, 855–866. doi: 10.1038/nrg2897.

Howell, C. R. (2003). Mechanisms Employed by *Trichoderma* Species in the Biological Control of Plant Diseases: The History and Evolution of Current Concepts. Plant Disease, 87(1), 4–10. doi:10.1094/pdis.2003.87.1.4

Hu, G., Yalpani, N., Briggs, S. P., and Johal, G. S. (1998). A porphyrin pathway impairment is responsible for the phenotype of a dominant disease lesion mimic mutant of maize. Plant Cell 10, 1095– 1105. doi: 10.1105/tpc.10.7.1095

Huang, X., Hou, L., Meng, J., You, H., Li, Z., Gong, Z., et al. (2018). The antagonistic actionof abscisic acid and cytokinin signaling mediates drought stress response in Arabidopsis. Mol. Plant. 11, 970–982. doi: 10.1016/j.molp.2018.05.001

Humplík, J. F., Lazár, D., Fürst, T., Husičková, A., Hýbl, M., & Spíchal, L. (2015a). Automated integrative high-throughput phenotyping of plant shoots: a case study of the cold-tolerance of pea (Pisum sativum L.). Plant Methods, 11(1), 20. doi:10.1186/s13007-015-0063-9

Humplík, J. F., Lazár, D., Husičková, A., & Spíchal, L. (2015b). Automated phenotyping of plant shoots using imaging methods for analysis of plant stress responses – a review. Plant Methods, 11(1). doi:10.1186/s13007-015-0072-8

Ibrahim, H.A. and Abdellatif, Y.M. (2016). Effect of maltose and trehalose on growth, yield and some biochemical components of wheat plant under water stress. Annals of Agricultural Sciences 61 (2), 267e274. doi: 10.1016/j.aoas.2016.05.002

Ishikawa, A., Okamoto, H., Iwasaki, Y., and Asahi, T. (2001). A deficiency of coproporphyrinogen III oxidase causes lesion formation in *Arabidopsis*. Plant J. 27, 89– 772 99. doi:10.1046/j.1365-313X.2001.01058.x

Ito, Y., Nakanomyo, I., Motose, H., Iwamoto, K., Sawa, S., Dohmae, N., et al. (2006). Dodeca-CLE peptides as suppressors of plant stem cell differentiation. *Science* 313, 842–845. doi: 10.1126/science.1128436

Jamil A., Riaz S., Ashraf M. and Foolad M.R. (2011). Gene expression profiling of plants under salt stress. Crit. Rev. Plant Sci. 30 (5), 435–458. doi: 10.1080/07352689.2011.605739

Janka E., Körner O., Rosenqvist E. and Ottosen C.A. (2013). High temperature stress monitoring and detection using chlorophyll a fluorescence and infrared thermography in chrysanthemum (Dendranthema grandiflora). Plant Physiol. Biochem. 2013, 67, 87–94. doi: 10.1016/j.plaphy.2013.02.025

Jisha, K. C., Vijayakumari, K., and Puthur, J. T. (2012). Seed priming for abiotic stress tolerance: an overview. *Acta Physiol. Plant* 35, 1381–1396. doi: 10.1007/s11738-012-1186-5

Jones, H. G. (2004). Application of Thermal Imaging and Infrared Sensing in Plant Physiology and Ecophysiology. Incorporating Advances in Plant Pathology, 107–163. doi:10.1016/s0065-2296(04)41003-9

Literature cited

Jones H.G., Serraj R., Loveys B.R., Xiong L., Wheaton A. and Price A.H. (2009). Thermal infrared imaging of crop canopies for the remote diagnosis and quantification of plant responses to water stress in the field. Functional Plant Biology, 2009, 36, 978–989. doi: 10.1071/FP09123

Julkowska, M. M., Saade, S., Agarwal, G., Gao, G., Pailles, Y., Morton, M., et al. (2019). MVApp—Multivariate analysis application for streamlined data analysis and curation. *Plant Physiol.* 180, 1261–1276. doi:10.1104/pp.19.00235

Junker, A., Muraya, M. M., Weigelt-Fischer, K., Arana-Ceballos, F., Klukas, C., Melchinger, A. E., et al. (2015). Optimizing experimental procedures for quantitative evaluation of crop plant performance in high throughput phenotyping systems. Front. Plant Sci. 5:770. doi: 10.3389/fpls.2014.00770

Kalaji M.H. and Rutkowska A. (2004) Reactions of photosynthetic apparatus of maize seedlings to salt stress. Zesz Probl Post NaukRol 496:545–558

Kaňa, R., and Vass, I. (2008). Thermoimaging as a tool for studying light-induced heating ofleaves: correlation of heat dissipation with the efficiency of photosystem II photochemistry and non-photochemical quenching. Environ. Exp. Bot. 64, 90-96. doi: 10.1016/j.envexpbot.2008.02.006

Kauffman G.L., Kneivel D.P. and Watschke, T.L. (2007). Effects of a biostimulant on the heat tolerance associated with photosynthetic capacity, membrane thermostability, and polyphenol production of perennial ryegrass. Crop Sci. 47, 261–267. doi: 10.2135/cropsci2006.03.0171

Khan W., Rayirath U.P., Subramanian S., Jithesh M.N., Rayorath P., Hodges D.M., Critchley A.T., Craigie J.S., Norrie J., Prithiviraj B. (2009). Seaweed extracts as biostimulants of plant growth and development. J. Plant Growth Regul. 28, 386–399. doi: 10.1007/s00344-009-9103-x

Khan S.H., Khan A., Litaf U., Shah A.S., Khan M.A., Bilal M. and Ali M.U. (2015). Effect of drought stress on tomato cv. Bombino. J. Food Process. Technol. 6 (07), 465 doi: 10.4172/2157-7110.1000465.

Literature cited

Klukas, C., Chen, D., and Pape, J. M. (2014). Integrated analysis platform: An open-source information system for high-throughput plant phenotyping. Plant Physiol. 165: 506–518. doi: 10.1104/pp.113.233932

Knepper C. and Mou, B. (2015) Semi-High Throughput Screening for Potential Drought-tolerance in Lettuce (*Lactuca sativa*) Germplasm Collections. J. Vis. Exp. (98), e52492, doi:10.3791/52492.

Kolhar, S., & Jagtap, J. (2021). Plant trait estimation and classification studies in plant phenotyping using machine vision – A review. Information Processing in Agriculture. doi:10.1016/j.inpa.2021.02.006

Kondo T., Sawa S., Kinoshita A., Mizuno S., Kakimoto T., Fukuda H. et al. (2006). A plant peptide encoded by CLV3 identified by in situ MALDI-TOF MS analysis. Science 313, 845–848. doi: 10.1126/science.1128439

Krauss S.W., Schnitzler H., Grassmann J. and Woitke M. (2006). The influence of different electrical conductivity values in a simplified recalculating soilless system on inner and outer fruit quality characteristics of tomato. Journal of Agricultural and Food Chemistry 54, 441–448. doi: 10.1021/jf051930a

Kruk, J., Szymańska, R., Nowicka, B., and Dłużewska, J. (2016). Function of isoprenoid quinones and chromanols during oxidative stress in plants. New Biotechnol. 33, 363–643. doi: 10.1016/j.nbt.2016.02.010

Kumar, A., Altabella, T., Taylor, M., and Tiburcio, A. F. (1997). Recent advances in polyamine research. Trends Plant Sci. 2, 124–130. doi: 10.1016/S1360-1385(97) 01013-3

Kumar, P., Lucini, L., Rouphael, Y., Cardarelli, M., Kalunke, R. M., and Colla, G. (2015). Insight into the role ofgrafting and arbuscular mycorrhiza on cadmium stress tolerance in tomato. Front. Plant Sci. 6:477. doi: 10.3389/fpls.2015. 00477

Kumar, P., Rouphael, Y., Cardarelli, M., and Colla, G. (2017). Vegetable grafting as a tool to improve drought resistance and water use efficiency. Fron. Plant Sci. 8, 1130. doi: 10.3389/fpls.2017.01130

Literature cited

Kumar, K., Manigundan, K., & Amaresan, N. (2016). Influence of salt tolerant *Trichoderma* spp. on growth of maize (Zea mays) under different salinity conditions. Journal of Basic Microbiology, 57(2), 141–150. doi:10.1002/jobm.201600369

Kunicki E., Grabowska A., Sekara A. and Wojciechowska R. (2010). The effect of cultivar type, time of cultivation, and biostimulant treatment on the yield of spinach (*Spinacia oleracea* L). Folia Hortic. 22, 9–13. doi: 10.2478/fhort-2013- 0153

La, V. H., Lee, B. R., Islam, M. T., Park, S. H., Jung, H. il, Bae, D. W., et al. (2019).Characterization of salicylic acid-mediated modulation of the drought stress responses: Reactive oxygen species, proline, and redox state in *Brassica napus*. Environ. Exp. Bot. 157, 1–10. doi: 10.1016/j.envexpbot.2018.09.013

Lamichhane, S., Sen, P., Dickens, A. M., Hyötyläinen, T., and Orešič, M. (2018). An overview of metabolomics data analysis: Current tools and future perspectives, comprehensive analytical chemistry, Elsevier, ISSN 0166-526X, Vol. 82, 387-413. doi: 10.1016/bs.coac.2018.07.001.

Lara M.A., Diezma B., Lleó L., Roger J.M., Garrido Y., Gil M.I. and Ruiz-Altisent M. (2016). Hyperspectral Imaging to Evaluate the Effect of Irrigation Water Salinity in Lettuce. Appl. Sci. 2016, 6, 412; doi:10.3390/app6120412

LeCun, Y., Bengio, Y., and Hinton, G. (2015). Deep learning. Nature 521, 436–444. doi: 10.1038/nature14539

Lee, AY., Kim, SY., Hong, SJ., Han, S.Y., Choi Y., Kim M., Yun S.K. and Kim G. (2019). Phenotypic analysis of fruit crops water stress using infrared thermal imaging. J. Biosyst. Eng. 44, 87–94. doi:10.1007/s42853-019-00020-2

Lee, J., Shim, D., Moon, S., Kim, H., Bae, W., Kim, K., et al. (2018). Genome-wide transcriptomic analysis of BR-deficient Micro-Tom reveals correlations between drought stress tolerance and brassinosteroid signaling in tomato. Plant Physiol. Biochem. 127, 553–560. doi: 10.1016/j.plaphy.2018.04.031

Levitt J. (1972). Responses of plants to environmental stresses. London, UK: Academic Press.

Literature cited

Li L., Zhang Q. and Huang D. (2014). A Review of Imaging Techniques for Plant Phenotyping. Sensors 2014, 14, 20078-20111; doi:10.3390/s141120078

Li, L., Gu, W., Li, J., Li, C., Xie, T., Qu, D., et al. (2018). Exogenously applied spermidine alleviates photosynthetic inhibition under drought stress in maize (*Zea mays* L.) seedlings associated with changes in endogenous polyamines and phytohormones. Plant Physiol. Biochem.129, 35–55. doi: 10.1016/j.plaphy.2018.05.017.

Lisiecka J., Knaflewski M., Spizewski T., Fraszczak B., Kaluzewicz A. and Krzesinski W. (2011). The effect of animal protein hydrolysate on quantity and quality of strawberry daughter plants cv. 'Elsanta'. Acta Sci. Pol. Hortic. 10, 31–40.

Liu, J., Li, J., Su, X., and Xia, Z. (2014). Grafting improves drought tolerance by regulating antioxidant enzyme activities and stress-responsive gene expression in tobacco. Environ. Exp. Bot. 107, 173–179. doi: 10.1016/j.envexpbot.2014.06.012

Llorach, R., Martínez-Sánchez, A., Tomás-Barberán, F. A., Gil, M.I., and Ferreres, F. (2008). Characterisation of polyphenols and antioxidant properties of five lettuce varieties and escarole. Food Chemistry 108(3), 1028- 1038. doi: 10.1016/j.foodchem.2007.11.032

Lucini, L., Borgognone, D., Rouphael, Y., Cardarelli, M., Bernardi, J., & Colla, G. (2016). Mild potassium chloride stress alters the mineral composition, hormone network, and phenolic profile in artichoke leaves. Front. Plant Sci. 7. doi:10.3389/fpls.2016.00948

Lucini, L., Rouphael, Y., Cardarelli, M., Bonini, P., Baffi, C., and Colla, G. (2018). A vegetal biopolymer-based biostimulant promoted root growth in melon while triggering brassinosteroids and stress-related compounds. *Front. Plant Sci*. 9, 472. doi: 10.3389/fpls.2018.00472

Lucini, L., Rouphael, Y., Cardarelli, M., Canaguier, R., Kumar, P., and Colla G. (2015). The effect of a plant-derived biostimulant on metabolic profiling and crop performance of lettuce grown under saline conditions. *Sci. Hortic.* (Amsterdam). 182, 124–133. doi: 10.1016/j.scienta.2014.11.022

Ludwig-Müller, J. (2011). Auxin conjugates: their role for plant development and in the evolution of land plants. Journal of Experimental Botany, 62(6), 1757–1773. doi:10.1093/jxb/erq412

Lüthje, S., Möller, B., Perrineau, F. C., and Wöltje, K. (2013). Plasma membrane electron pathways and oxidative stress. Antioxid. Redox Signal. 18, 2163–2183. doi: 10.1089/ars.2012.5130

Luziatelli, F., Ficca, A. G., Colla, G., Baldassarre Švecová, E., and Ruzzi, M. (2019). Foliar application of vegetal-derived bioactive compounds stimulates the growth of benefcial bacteria and enhances microbiome biodiversity in lettuce. *Front. Plant Sci.* 10, 60. doi: 10.3389/fpls.2019.00060

Ma, Y., Látr, A., Rocha, I., Freitas, H., Vosátka, M., & Oliveira, R. (2019). Delivery of Inoculum of *Rhizophagus irregularis* via Seed Coating in Combination with *Pseudomonas libanensis* for Cowpea Production. Agronomy, 9(1), 33. doi:10.3390/agronomy9010033

Maas E.V. (1986). Salt tolerance of plants. Appl. Agric. Res. 1, 12±26 doi: 10.1201/9780429286735-2

Maas E.V. (1990). Crop salt tolerance, p. 262–304. In: Tanji, K.K. (ed.). Agricultural salinity assessment and management. Amer. Soc. of Civil Engineers, ASCE Manuals and reports on engineering practice No. 71, New York, NY

Machado R. M. A. and Serralheiro R. P. (2017). Soil salinity: Effect on vegetable crop growth. Management practices to prevent and mitigate soil salinization. Horticulturae 3, 30 doi:10.3390/horticulturae3020030

Maes WH, Steppe K (2012) Estimating evapotranspiration and drought stress with ground-based thermal remote sensing in agriculture: a review. J Exp Bot 63:4671–4712 doi:10.1093/jxb/ers165

Mahajan S. and Tuteja N. (2005). Cold, salinity and drought stresses: An overview. Arch. Biochem. Biophys. 444, 139–158. doi: 10.1016/j.abb.2005.10.018

Literature cited

Mahdavi, B. (2013). Seed germination and growth responses of Isabgol (*Plantago ovata* Forsk) to chitosan and salinity. *Int. J. Agric. Crop Sci.* 5, 1084–1088. doi: IJACS/2013/5-10/1084-1088

Maini P. (2006). The experience of the first biostimulant, based on amino acids and peptides: a short retrospective review on the laboratory researches and practical results. Fertil. Agrorum 1, 29–43.

Marchetti C.F., Ugena L., Humplík J.F., Polák M., Cavar Zeljkovic S., Podlešáková K., Fürst T., De Diego N. and Spíchal L. (2019) A Novel Image-Based Screening Method to Study Water-Deficit Response and Recovery of Barley Populations Using Canopy Dynamics Phenotyping and Simple Metabolite Profiling. Front. Plant Sci. 10:1252. doi: 10.3389/fpls.2019.01252

Martynenko A., Shotton K., Astatkie T., Petrash G., Fowler C., Neily W. and Critchley A.T. (2016). Thermal imaging of soybean response to drought stress: the effect of *Ascophyllum nodosum* seaweed extract. SpringerPlus (2016) 5:1393 doi: 10.1186/s40064-016-3019-2

Matsumiya Y. and Kubo M. (2011). Soybean peptide: novel plant growth promoting peptide from soybean, in Soybean and Nutrition, ed. H. El-Shemy (Rijeka: In Tech Europe Publisher), 215–230

Maxwell, K., and Johnson, G. N. (2000). Chlorophyll fluorescence—a practical guide. J. Exp.Bot. 51, 345, 659–668. doi: 10.1093/jexbot/51.345.659

McArthur J. W. (2016). Agriculture in the COP21 Agenda, in: COP21 at Paris: What to expect. The issues, the actors, and the road ahead on climate change, Global Economy and Development, Brookings Institution, Washington, DC, pp. 37-42.

McCulloch, C.E.; Searle, S.R. (2001) Generalized, Linear and Mixed Models; John Wiley: New York, NY, USA, 2001.

Meier, R., Ruttkies, C., Treutler, H., and Neumann, S. (2017). Bioinformatics can boost metabolomics research. J. Biotec. doi: 10.1016/j.jbiotec.2017.05.018

Literature cited

Mellor, N., Band, L. R., Pěnčík, A., Novák, O., Rashed, A., Holman, T., et al. (2016). Dynamic regulation of auxin oxidase and conjugating enzymes AtDAO1 and GH3 modulates auxin homeostasis. Proc. Natl. Acad. Sci. 113(39), 11022–11027. doi:10.1073/pnas.1604458113

Meza SLR, Egea I, Massaretto IL, Morales B, Purgatto E, Egea-Fernández JM, Bolarin MC and Flores FB (2020) Traditional Tomato Varieties Improve Fruit Quality Without Affecting Fruit Yield Under Moderate Salt Stress. Front. Plant Sci. 11:587754. doi: 10.3389/fpls.2020.587754

Mercer, K. L., Alexander, H. M., & Snow, A. A. (2011). Selection on seedling emergence timing and size in an annual plant, *Helianthus annuus* (common sunflower, Asteraceae). American Journal of Botany, 98(6), 975–985. doi:10.3732/ajb.1000408

Mimmo, T., Tiziani, R., Valentinuzzi, F., Lucini, L., Nicoletto, C., Sambo, P., Scampicchio, M., Pii, Y., Cesco, S. (2017). Selenium Biofortification in Fragaria × ananassa: Implications on Strawberry Fruits Quality, Content of Bioactive Health Beneficial Compounds and Metabolomic Profile. Frontiers in Plant Science, 8. doi:10.3389/fpls.2017.01887

Miras-Moreno, B., Zhang, L., Senizza, B., & Lucini, L. (2021). A metabolomics insight into the Cyclic Nucleotide Monophosphate signaling cascade in tomato under non-stress and salinity conditions. doi:10.1101/2021.03.22.436432

Mochida, K., Koda, S., Inoue, K., Hirayama, T., Tanaka, S., Nishii, R., & Melgani, F. (2018). Computer vision-based phenotyping for improvement of plant productivity: a machine learning perspective. GigaScience, 8(1). doi:10.1093/gigascience/giy153

Monakhova O.F. and Chernyadèv I.I. (2002) Protective role of kartolin-4 in wheat plants exposed to soil drought, Appl. Biochem. Micro+ 38, 373–380

Moreira FF, Oliveira HR, Volenec JJ, Rainey KM and Brito LF (2020) Integrating High-Throughput Phenotyping and Statistical Genomic Methods to Genetically Improve Longitudinal Traits in Crops. Front. Plant Sci. 11:681. doi: 10.3389/fpls.2020.00681

Motooka S., Hayashi T., Mima Y. and Konishi K. (1991) Measurement of in vitro plant growth by image processing. Journal of Japan Soc. Hortic Sci. 60:677-684. doi: 10.2503/jjshs.60.677

Mukherjee, S. (2018). Novel perspectives on the molecular crosstalk mechanisms of serotoninand melatonin in plants. Plant Physiol.Biochem. 132, 33–45. doi: 10.1016/j.plaphy.2018.08.031

Mukhopadhyay, R., Sarkar, B., Jat, H. S., Sharma, P. C., and Bolan, N. S. (2021). Soil salinity under climate change: Challenges for sustainable agriculture and food security. J. Environ. Manage. 280:111736. doi:10.1016/j.jenvman.2020.111736

Munné-Bosch, S., Schwarz, K., and Alegre, L. (1999). Response of abietane diterpenes to stress in *Rosmarinus officinalis* L.: New insights into the function of diterpenes in plants. Free Rad. Res. 31 Suppl:S107-12. doi: 10.1080/10715769900301391

Munns R. (2002). Comparative physiology of salt and water stress. Plant Cell Environ. 25, 239–250. doi: 10.1046/j.0016-8025.2001.00808.x

Munns R. (2005). Genes and salt tolerance: bringing them together. New Phytol. 167:645– 63. doi: 10.1111/j.1469-8137.2005. 01487.x

Munns, R. & James, R.A. (2000). Screening methods for salinity tolerance: a case study with tetraploid wheat. Plant and Soil 253: 201–218 doi: 10.1023/a:1024553303144

Munns R., James R.A., Sirault X. R. R., Furbank R.T. and Jones H.G. (2010). New phenotyping methods for screening wheat and barley for beneficial responses to water deficit. Journal of Experimental Botany, Vol. 61, No. 13, pp. 3499–3507 doi:10.1093/jxb/erq199

Munns R. and Tester M. (2008). Mechanisms of Salinity Tolerance. Annu. Rev. Plant Biol. 59:651–81 doi: 10.1146/annurev.arplant.59.032607.092911

Murashige, T., and Skoog, F. (1962). A revised medium for rapid growth and bio assays with tobacco tissue cultures. *Physiol. Plant.* 15, 473–497. doi: 10.1111/j. 1399-3054.1962.tb08052.x

Murchie, E., & Lawson, T. (2013). Chlorophyll fluorescence analysis: a guide to good practice and understanding some new applications. Journal of experimental botany, 64 13, 3983-98 .

Muscolo, A., Sidari, M., and da Silva, J. A. T. (2013). Biological effects of water- soluble soil phenol and soil humic extracts on plant systems. *Acta Physiol. Plant* 35, 309–320. doi: 10.1007/s11738-012-1065-0

Mutale-joan C., Redouane B., Najib E, Yassine K., Lyamlouli K., Sbabou L., Zeroual Y. and El-Aroussi H. (2020) Screening of microalgae liquid extracts for their bio stimulant properties on plant growth, nutrient uptake and metabolite profile of *Solanum lycopersicum* L. Sci Rep 10, 2820 (2020). https://doi.org/10.1038/s41598-020-59840-4

Mwando E, Han Y, Angessa TT, Zhou G, Hill CB, Zhang X-Q and Li C (2020) Genome-Wide Association Study of Salinity Tolerance During Germination in Barley (*Hordeum vulgare* L.). Front. Plant Sci. 11:118. doi: 10.3389/fpls.2020.00118

Na, Y. W., Jeong, H. J., Lee, S. Y., Choi, H. G., Kim, S. H., and Rho, I. R. (2014). Chlorophyll fluorescence as a diagnostic tool for abiotic stress tolerance in wild and cultivated strawberry species. Hort. Environ. Biotechnol. 55, 280–286. doi: 10.1007/s13580-014-0006-9

Naik H. S., Zhang J., Lofquist A., Assefa T., Sarkar S., Ackerman D., Singh A., Singh A.K., Ganapathysubramanian B. (2017). A real-time phenotyping framework using machine learning for plant stress severity rating in soybean. Plant Methods, 13(1). doi:10.1186/s13007-017-0173-7

Nardi, S., Pizzeghello, D., Schiavon, M., and Ertani, A. (2016). Plant biostimulants: physiological responses induced by protein hydrolyzed-based products and humic substances in plant metabolism. Sci. Agric. 73, 18–23. doi: 10.1590/0103- 9016-2015-0006

Nasrollahi, V., Mirzaie-Asl, A., Piri, K., Nazeri, S., and Mehrabi, R. (2014). The effect of drought stress on the expression of key genes involved in the biosynthesis of triterpenoid saponins in liquorice (*Glycyrrhiza glabra*). Phytochem. 103, 32–37. doi: 10.1016/j.phytochem.2014.03.004

Nedbal L., Soukupová J., Kaftan D., Whitmarsh J. and Trtílek M. (2000). Kinetic imaging of chlorophyll fluorescence using modulated light. Photosynthesis Research 66: 3–12. doi: 10.1023/A:1010729821876.

Literature cited

Neilson, E. H., Edwards, A. M., Blomstedt, C. K., Berger, B., Møller, B. L., & Gleadow, R. M. (2015). Utilization of a high-throughput shoot imaging system to examine the dynamic phenotypic responses of a C4 cereal crop plant to nitrogen and water deficiency over time. Journal of Experimental Botany, 66(7), 1817–1832. doi:10.1093/jxb/eru526

Ng, J. L. P., Hassan, S., Truong, T.T., Hocart, C. H., Laffont, C., Frugier, F., et al. (2015). Flavonoids and auxin transport inhibitors rescue symbiotic nodulation in the *Medicago truncatula* cytokinin perception mutant cre1. *Plant Cell* 27, 2210–2226. doi: 10.1105/tpc.15.00231

Niculescu, M., Bajenaru, S., Gaidau, C., Simion, D., and Felipescu, L. (2009). Extraction of the protein components as amino-acids hydrolysates from chrome leather wastes through hydrolytic processes. Rev. Chim. 60, 1070–1078.

Novák, J., Černý, M., Roignant, J., Skalák, J., Saiz-Fernández, I., Luklová, M., et al. (2021). Limited light intensity and low temperature: Can plants survive freezing in light conditions that more accurately replicate the cold season in temperate regions? Environmental and Experimental Botany, 190, 104581. doi:10.1016/j.envexpbot.2021.104581

Oljira, A.M.; Hussain, T.; Waghmode, T.R.; Zhao, H.; Sun, H.; Liu, X.; Wang, X.; Liu, B. (2020) Trichoderma Enhances Net Photosynthesis, Water Use Efficiency, and Growth of Wheat (*Triticum aestivum* L.) under Salt Stress. Microorganisms, 8, 1565. doi:0.3390/microorganisms8101565

Omari MK, Lee J, Faqeerzada MA, Joshi R, Park E, Cho BK. (2020). Digital image-based plant phenotyping: a review. Korean Journal of Agricultural Science 47:119-130. doi:10.7744/ kjoas.20200004

Osakabe, Y., Osakabe, K., Shinozaki, K., and Tran, L.S.P. (2014). Response of plants to water stress. Front. Plant Sci. 5, 86 https://doi.org/10.3389/fpls.2014.00086.

Paine, C.E.T., Marthews, T.R., Vogt, D.R., Purves, D., Rees, M., Hector, A. & Turnbull, L.A. (2012) How to fit nonlinear plant growth models and calculate growth rates: An update for ecologists Methods Ecol. Evol. 3 245 256 doi: 10.1111/j.2041-210x.2011.00155.x

Pandey P., Ge Y., Stoerger V. and Schnable J.C. (2017) High Throughput In vivo Analysis of Plant Leaf Chemical Properties Using Hyperspectral Imaging. Front. Plant Sci. 8:1348. doi: 10.3389/fpls.2017.01348

Paparella, S., Araújo, S., Rossi, G., Wijayasinghe, M., Carbonera, D., and Balestrazzi A. (2015). Seed priming: state of the art and new perspectives. *Plant Cell Rep.* 34. 1–13. doi: 10.1007/s00299-015-1784-y.

Paradikovic N., Vinkovic T., Vrcek I. V., Zuntar I., Bojic M. and Medic-Saric M. (2011). Effect of natural biostimulants on yield and nutritional quality: an example of sweet yellow pepper (*Capsicum annuum* L.) plants. J. Sci. Food Agric. 91, 2146–2152. doi: 10.1002/jsfa.4431

Paul, K., Deák, Z., Csôsz, M., Purnhauser, L., and Vass, I. (2011). Characterization and early detection of tan spot disease in wheat in vivo with chlorophyll fluorescence imaging. Acta Biol. Szeged. 55, 87–90. doi: 10.13140/2.1.3021.6320

Paul, K., Pauk, J., Deák, Z., Sass, L., and Vass, I. (2016). Contrasting response of biomass and grain yield to severe drought in cappelle desprez and plainsman V wheat cultivars. PeerJ 4:e1708. doi: 10.7717/peerj.1708

Pennisi E. (2008). Plant genetics: the blue revolution, drop by drop, gene by gene. Science 320, 171–173. doi: 10.1126/science.320.5873.171

Petrozza A., Santaniello A., Summerer S., Di Tommaso G., Di Tommaso D., Paparelli E., Piaggesi A., Perata P. and Cellini F. (2014) Physiological responses to Megafol®treatments in tomato plants under drought stress: A phenomic and molecular approach. Sci. Hortic. (Amsterdam). doi: 10.1016/j.scienta.2014.05.023

Pfeffer W. (1907). Untersuchungen über die Entstehung der Schlafbewegungen der Blattorgane. Leipzig,B. G. Teubner,1907. doi: 10.5962/bhl.title.13150

Pichyangkura, R., and Chadchawan, S. (2015). Biostimulant activity of chitosan in horticulture. *Sci. Hortic.* 196, 49–65. doi: 10.1016/j.scienta.2015.09.031

Pilon-Smits E.A.H., Quinn C.F., Tapken W., Malagoli M. and Schiavon M. (2009). Physiological functions of beneficial elements. Curr. Opin. Plant Biol. 12, 267–274. doi.org/10.1016/j.pbi.2009.04.009

Posmyk M.M. and Szafranska K. (2016) Biostimulators: A New Trend towards Solving an Old Problem. Front. Plant Sci. 7:748 doi: 10.3389/fpls.2016.00748

Povero, G., Mejia, J. F., Di Tommaso, D., Piaggesi, A., and Warrior, P. (2016). A Systematic approach to discover and characterize natural plant biostimulants. *Front. Plant Sci.* 7, 435. doi: 10.3389/fpls.2016.00435

Pratap, A., Gupta, S., Nair, R., Gupta, S., Schafleitner, R., Basu, P. et al. (2019). Using Plant Phenomics to Exploit the Gains of Genomics. Agronomy, 9(3), 126. doi:10.3390/agronomy9030126

Prerostova, S., Dobrev P. I., Gaudinova, A., Knirsch, V., Körber, N., Pieruschka, R., et al. (2018). Cytokinins: Their impact on molecular and growth responses to drought stress and recovery in *Arabidopsis*. *Front. Plant Sci.* 9, 655. doi: 10.3389/fpls.2018.00655

Pretali, L., Bernardo, L., Butterfield, T. S., Trevisan, M., and Lucini, L. (2016). Botanical and biological pesticides elicit a similar induced systemic response in tomato (*Solanum lycopersicum*) secondary metabolism. Phytochemistry 130, 56–63. doi: 10.1016/j.phytochem.2016.04.002

Qiu,Y., Amirkhani, M., Mayton, H., Chen, Z., and Taylor, A.G. (2020). Biostimulant Seed Coating Treatments to Improve Cover Crop Germination and Seedling Growth. Agronomy, 10(2), 154. doi:10.3390/agronomy10020154

Qi, Y. (2012). Random forest for bioinformatics. In Ensemble machine learning (pp. 307-323). Springer, Boston, MA.

Radwan, A., Kleinwächter, M., and Selmar, D. (2017). Impact of drought stress on specialised metabolism: biosynthesis and the expression of monoterpene synthases in sage (*Salvia officinalis*). Phytochemistry 141, 20–26. doi: 10.1016/ j.phytochem.2017.05.005

Literature cited

Rady, M. M., Kuşvuran, A., Alharby, H. F., Alzahrani, Y., & Kuşvuran, S. (2018). Pretreatment with Proline or an Organic Bio-stimulant Induces Salt Tolerance in Wheat Plants by Improving Antioxidant Redox State and Enzymatic Activities and Reducing the Oxidative Stress. Journal of Plant Growth Regulation, 38(2), 449–462. doi:10.1007/s00344-018-9860-5

Rahaman, M. M., Chen, D., Gillani, Z., Klukas, C., and Chen, M. (2015). Advanced phenotyping and phenotype data analysis for the study of plant growth and development. *Front. Plant Sci.* 6, 619. doi: 10.3389/fpls.2015.00619

Rahaman, M. M., Ahsan, M. A., Gillani, Z., and Chen, M. (2017). Digital biomass accumulation using high-throughput plant phenotype data analysis. J. Integr. Bioinform. 20170028. doi: 10.1515/jib-2017-0028

Rascher, U., Liebig, M., and Luttge, U. (2000). Evaluation of instant light- response curves of chlorophyll fluorescence parameters obtained with a portable chlorophyll fluorometer on site in the field. *Plant Cell Environ.* 23, 1397–1405. doi: 10.1046/j.1365-3040.2000.00650.x.

R Core Team (2014). R: A Language and Environment for Statistical Computing; R Foundation for Statistical Computing: Vienna, Austria, 2014. Available online: http://www.R-project.org/ (accessed on 20 November 2020).

Rentsch, D., Schmidt, S., Tegeder, M. (2007). Transporters for uptake and allocation of organic nitrogen compounds in plants. FEBS Lett. 581, 2281–2289 doi: 10.1016/j.febslet.2007.04.013

Ritchie G.A. (2008). Chlorophyll Fluorescence: What Is It and What Do the Numbers Mean? In: Riley, L . E.; Dumroese, R. K.; Landis, T. D., tech. coords. 2006. National Proceedings: Forest and Conservation Nursery Associations—2005. Proc. RMRS-P-43. Fort Collins, CO: U.S. Department of Agriculture, Forest Service, Rocky Mountain Research Station. 160 p. Available at: http:/ /www.rngr.net/nurseries/publications/proceedings

Robert, P., & Escoufier, Y. (1976). A Unifying Tool for Linear Multivariate Statistical Methods: The RV- Coefficient. Applied Statistics, 25(3), 257. doi:10.2307/2347233

Literature cited

Rouphael, Y., Cardarelli, M., Bonini, P., and Colla G. (2017a). Synergistic action of a microbial-based biostimulant and a plant derived-protein hydrolysate enhances lettuce tolerance to alkalinity and salinity. *Front. Plant Sci.* 8, 131. doi: 10.3389/fpls.2017.00131

Rouphael, Y., Cardarelli, M., Schwarz, D., Franken, P., and Colla, G. (2012). "Effects of drought on nutrient uptake and assimilation in vegetable crops," in Plant Responses to Drought Stress: From Morphological to Molecular Features, ed. R. Aroca (Berlin: Springer-Verlag).

Rouphael,Y., and Colla, G. (2018). Synergistic biostimulatory action: designing the next generation of plant biostimulants for sustainable agriculture. *Front. Plant Sci.* 9, 1655. doi: 10.3389/fpls.2018.01655

Rouphael, Y., Colla, G., Bernardo, L., Kane, D., Trevisan, M., and Lucini, L. (2016). Zinc excess triggered polyamines accumulation in lettuce root metabolome, as compared to osmotic stress under high salinity. *Front Plant Sci.* 2016, 7, 842. doi: 10.3389/fpls.2016.00842.

Rouphael, Y., Colla, G., Giordano, M., El-Nakhel, C., Kyriacou, M. C., and De Pascale, S. (2017b). Foliar applications of a legume-derived protein hydrolysate elicit dose dependent increases of growth, leaf mineral composition, yield and fruit quality in two greenhouse tomato cultivars. Sci. Hort. 226, 353–360. doi: 10.1016/j.scienta.2017.09.007

Rouphael, Y., Colla, G., Graziani, G., Ritieni, A., Cardarelli, M., and De Pascale, S. (2017c). Phenolic composition, antioxidant activity and mineral profile in two seed-propagated artichoke cultivars as affected by microbial inoculants and planting time. Food Chem. 234, 10–19. doi: 10.1016/j.foodchem.2017.04.175

Rouphael, Y., Giordano, M., Cardarelli, M., Cozzolino, E., Mori, M., Kyriacou, M. C., et al. (2018a). Plant- and seaweed-based extracts increase yield but differentially modulate nutritional quality of greenhouse spinach through biostimulant action. Agronomy 8:126. doi: 10.3390/agronomy8070126

Rouphael, Y., Kyriacou, M., Vitaglione, P., Giordano, M., Pannico, A., Colantuono, A., et al. (2017d). Genotypic variation in nutritional and antioxidant profile among iceberg lettuce cultivars. Acta Sci. Pol. Hortorum Cultus 16, 37–45. doi: 10.24326/asphc.2017.3.4

Rouphael Y., Spíchal L., Panzarová K., Casa R. and Colla G. (2018b) High-Throughput Plant Phenotyping for Developing Novel Biostimulants: From Lab to Field or From Field to Lab? Front. Plant Sci. 9:1197. doi: 10.3389/fpls.2018.01197

Rousseau, C., Belin, E., Bove, E., Rousseau, D., Fabre, F., Berruyer, R., et al. (2013). High throughput quantitative phenotyping of plant resistance using chlorophyll fluorescence image analysis. *Plant Methods* 9, 17. doi:10.1186/1746-4811-9-17

Ruban, A. V. (2016). Nonphotochemical Chlorophyll Fluorescence Quenching: Mechanism and Effectiveness in Protecting Plants from Photodamage. Plant Physiology, 170(4), 1903–1916. doi:10.1104/pp.15.01935

Russell, L. (2020) Emmeans: Estimated Marginal Means, Aka Least-Squares Means, R package version 1.4.5. Available online: https://cran.r-project.org/web/packages/emmeans/index.html (accessed on 22 December 2020).

Saito T. and Matsukura C. (2015) Effect of Salt Stress on the Growth and Fruit Quality of Tomato Plants. In: Abiotic Stress Biology in Horticultural Plants, Springer, 3-16 doi: 10.1007/978-4-431-55251-2_1

Saito T., Matsukura C., Ban Y., Shoji K., Sugiyama M., Fukuda N. and Nishimura S. (2008). Salinity stress affects assimilate metabolism at the gene-expression level during fruit development and improves fruit quality in tomato (Solanum lycopersicum L.). Journal of the Japanese Society for Horticultural Science 77, 61–68. doi: 10.2503/jjshs1.77.61

Salehi, H., Chehregani, A., Lucini, L, Majd, A., and Gholami, M. (2018). Morphological, proteomic and metabolomic insight into the effect of cerium dioxide nanoparticles to Phaseolus vulgaris L. under soil or foliar application. Sci. Tot. Envion. 616, 1540-1551. doi: 10.1016/j.scitotenv.2017.10.159

Salek, R. M., Neumann, S., Schober, D., Hummel, J., Billiau, K., Kopka, J., et al. (2015). COordination of Standards in MetabOlomicS (COSMOS): facilitating integrated metabolomics data access. Metabolomics, 11(6), 1598–1599. doi:10.1007/s11306-015-0822-7

Sánchez-Rodríguez, E., Rubio-Wilhelmi, Mªm., Cervilla, L. M., Blasco, B., Rios, J. J., Rosales, M. A. et al. (2010). Genotypic differences in some physiological parameters symptomatic for oxidative stress under moderate drought in tomato plants. Plant Science, 178(1), 30–40. doi:10.1016/j.plantsci.2009.10.001

Saxena, Amit, et al. (2017) A review of clustering techniques and developments. Neurocomputing 267 (2017): 664-681.

Schaepman M.E. (2007). Spectrodirectional Remote Sensing: From Pixels to Processes. International Journal of Applied Earth Observation and Geoinformation 9: 204–223. doi:10.1016/j.jag.2006.09.003

Schaller, G. E. (2012). Ethylene and the regulation of plant development. BMCBiol. 10:9. doi: 10.1186/1741-7007-10-9

Schiavon M., Ertani A. and Nardi S. (2008). Effects of an alfalfa protein hydrolysate on the gene expression and activity of enzymes of the tricarboxylic acid (TCA) cycle and nitrogen metabolism in Zea mays L. J. Agric. Food Chem. 56, 11800–11808. doi: 10.1021/jf802362g

Schläpfer, P., Zhang, P., Wang, C., Kim, T., Banf, M., Chae, L., Dreher, K., Chavali, A. K., Nilo-Poyanco, R., Bernard, T., Kahn, D., Rhee, S.Y. (2017) Genome-Wide Prediction of Metabolic Enzymes, Pathways, and Gene Clusters in Plants. Plant Physiology. 173(4):2041-2059. doi: 10.1104/pp.16.01942

Schreiber, U., Schliwa, U., & Bilger, W. (1986). Continuous recording of photochemical and non-photochemical chlorophyll fluorescence quenching with a new type of modulation fluorometer. Photosynthesis Research, 10(1-2), 51–62. doi:10.1007/bf00024185

Senizza, B., Zhang, L., Miras-Moreno, B., Righetti, L., Zengin, G., Ak, G., et al. (2020). The strength of the nutrient solution modulates the functional profile of hydroponically grown lettuce in a genotype-dependent manner. *Foods* 9, 1156. doi:10.3390/foods9091156

Serena, M., Leinauer, B., Sallenave, R., Schiavon, M., & Maier, B. (2012). Media Selection and Seed Coating Influence Germination of Turfgrasses under Salinity, HortScience, 47(1), 116-120. doi: 10.21273/HORTSCI.47.1.116

Serôdio J., Schmidt W. and Frankenbach S. (2017). A chlorophyll fluorescence-based method for the integrated characterization of the photo-physiological response to light stress. Journal of Experimental Botany, Vol. 68, No. 5 pp. 1123–1135. doi:10.1093/jxb/erw492

Sestili, F., Rouphael, Y., Cardarelli, M., Pucci, A., Bonini, P., Canaguier, R. et al. (2018). Protein hydrolysate stimulates growth in tomato coupled with N-dependent gene expression involved in N assimilation. Front. Plant Sci. 9, 1233. doi: 10.3389/fpls.2018.01233

Shah, A., & Smith, D. L. (2020). Flavonoids in Agriculture: Chemistry and Roles in Biotic and Abiotic Stress Responses, and Microbial Associations. Agronomy, 10(8), 1209. doi:10.3390/agronomy10081209

Shahbaz, M., and Ashraf, M. (2013) Improving salinity tolerance in cereals. *Critical Rev. Plant Sci.* 32, 237–249. doi: 10.1080/07352689.2013.758544

Shalaby, S., and Horwitz, B. A. (2015). Plant phenolic compounds and oxidative stress: integrated signals in fungal–plant interactions. Curr. Gen. 61, 347–357. doi: 10.1007/s00294-014-0458-6

Shannon, M. C., and Grieve, C. M. (1999). Tolerance of vegetable crops to salinity. *Sci. Hortic.* (Amsterdam) 78, 5–38. doi: 10.1016/s0304-4238(98)00189-7

Sharma, H. S. S., Fleming, C., Selby, C., Rao, J. R., and Martin, T. (2014). Plant biostimulants: a review on the processing of macroalgae and use of extracts for crop management to reduce abiotic and biotic stresses. *J. Appl. Phycol.* 26, 465–490. doi: 10.1007/s10811-013-0101-9

Sharma, A., Shahzad, B., Rehman, A., Bhardwaj, R., Landi, M., and Zheng, B. (2019a). Response of phenylpropanoid pathway and the role of polyphenols in Pplants under abiotic stress. *Molecules* 24, 2452. doi: 10.3390/molecules24132452

Sharma, A., Yuan, H., Kumar, V., Ramarakrishnan, M., Kohli, S. K., Kaur, R., et al. (2019b). Castasterone attenuates insecticide induced phytotoxicity in mustard. *Ecotoxicology Environ. Saf.* 179, 50–61. doi: 10.1016/j.ecoenv.2019.03.120

Literature cited

Shi G, Ranjan R, Khot LR. (2020). Robust image processing algorithm for computational resource limited smart apple sunburn sensing system. Inform Process Agric 2020;7 (2):212–22.

Shin SY, Park J-S, Park H-B, Moon K-B, Kim H-S, Jeon J-H, Cho HS and Lee H-J (2021) FERONIA Confers Resistance to Photooxidative Stress in Arabidopsis. Front. Plant Sci. 12:714938. doi: 10.3389/fpls.2021.714938

Shirley B.W. (1998). Flavonoids in seeds and grains: physiological function, agronomic importance and the genetics of biosynthesis. Seed Science Research, 8, pp 415422 doi:10.1017/S0960258500004372

Showalter, M. R., Nonnecke, E. B., Linderholm, A. L., Cajka, T., Sa, M. R., Lönnerdal, B., et al. (2018). Obesogenic diets alter metabolism in mice. PLoS One 13:e0190632. doi: 10.1371/journal.pone.0190632

Shrivastava P. and Kumar R. (2015) Soil salinity: A serious environmental issue and plant growth promoting bacteria as one of the tools for its alleviation. Saudi J. Biol. Sci., 22, 123–131. doi: 10.1016/j.sjbs.2014.12.001

Siddiqui, Z. S., Cho, J.-I., Park, S.-H., Kwon, T.-R., Lee, G.-S., Jeong, M.-J., Kim, K.-W., Lee, S.-K. and Park, S.-C. (2014). Phenotyping of rice in salt stress environment using high-throughput infrared imaging. Acta Botanica Croatica, 73(1), 312–321. doi:10.2478/botcro-2013-0027

Simko, I., Hayes, R. J., and Furbank, R. T. (2016). Non-destructive phenotyping of lettuce pants in early stages of development with optical sensors. *Front. Plant Sci.* 7, 1985. doi: 10.3389/fpls.2016.01985

Singh, A., Ganapathysubramanian, B., Singh, A. K., & Sarkar, S. (2016). Machine Learning for High-Throughput Stress Phenotyping in Plants. Trends in Plant Science, 21(2), 110–124. doi: 10.1016/j.tplants.2015.10.015

Sirault X. R. R., James R.A. and Furbank R.T. (2009). A new screening method for osmotic component of salinity tolerance in cereals using infrared thermography. Functional Plant Biology, 2009, 36, 970–977 doi: 10.1071/FP09182

Skirycz A. and Inze D. (2010) More from less: plant growth under limited water. Curr Opin Biotechnol, 21(2):197-203. doi: 10.1016/j.copbio.2010.03.002

Small, C. C., and Degenhardt, D. (2018). Plant growth regulators for enhancing revegetation success in reclamation: a review. Ecol. Engin. 118, 43–51. doi: 10.1016/j.ecoleng.2018.04.010

Smith M.A. and Spomer L.A. (1987). Direct quantification of in vitro cell growth through image analysis. In Vitro Cell Dev Biol, 23(1):67-74. doi: 10.1007/BF02623496.

Soldal T. and Nissen P. (1978). Multiphasic uptake of amino acids by barley roots. Physiol. Plant. 43, 181–188 doi: 10.1111/j.1399-3054. 1978.tb02561.x

Subbarao, S. B., Aftab Hussain, I. S., and Ganesh, P. T. (2015). Biostimulant activity of protein hydrolysate: Influence on plant growth and yield. J. Plant Sci. Res. 2, 125.

Sytar O., Brestic M., Zivcak M., Oslovska K., Kovar M., Shao H. and He X. (2017). Applying hyperspectral imaging to explore natural plant diversity towards improving salt stress tolerance. Science of the Total Environment 578 (2017) 90–99 doi: 10.1016/j.scitotenv.2016.08.014

Sytar, O., Zivcak, M., Olsovska, K., & Brestic, M. (2018). Perspectives in High-Throughput Phenotyping of Qualitative Traits at the Whole-Plant Level. Eco-Friendly Agro-Biological Techniques for Enhancing Crop Productivity, 213–243. doi:10.1007/978-981-10-6934-5_10

Tardieu, F., Cabrera-Bosquet, L., Pridmore, T., and Bennett, M. (2017). Plant Phenomics, From Sensors to Knowledge. Current Biol. 27, R770–R783 doi:10.1016/j.cub.2017.05.055.

Tattersall E.A., Grimplet J., Deluc L., Wheatley M.D., Vincent D., Osborne C., Ergul A., Lomen E., Blank R.R., Schlauch K.A., Cushman J.C. and Cramer G.R. (2007). Transcript abundance profiles reveal larger and more complex responses of grapevine to chilling compared to osmotic and salinity stress. Funct Integr Genomics 7(4):317-333. doi: 10.1007/s10142-007-0051-x

Thalmann, M., and Santelia, D. (2017). Starch as a determinant of plant fitness under abiotic stress. *New Phytol.* 214, 943–951. doi: 10.1111/nph.14491

Thorp, K. R., Wang, G., Bronson, K. F., Badaruddin, M., & Mon, J. (2017). Hyperspectral data mining to identify relevant canopy spectral features for estimating durum wheat growth, nitrogen status, and grain yield. Computers and Electronics in Agriculture, 136, 1–12. doi:10.1016/j.compag.2017.02.024

Tiwari, G.N. (2003). Greenhouse Technology for Controlled Environment. Narosa Publishing House, New Delhi, pp: 67-77.

Tjørve K.M.C. and Tjørve E. (2017) The use of Gompertz models in growth analyses, and new Gompertz-model approach: An addition to the Unified-Richards family. PLoS ONE 12(6): e0178691. doi: 10.1371/journal.pone.0178691

Troszyńska, A., Estrella, I., López-Amóres, M. L., & Hernández, T. (2002). Antioxidant Activity of Pea (Pisum sativum L.) Seed Coat Acetone Extract. LWT - Food Science and Technology, 35(2), 158–164. doi:10.1006/fstl.2001.0831

Tripathy, B. C., and Oelmüller, R. (2012). Reactive oxygen species generation and signaling in plants. Plant Signal. Behav. 7, 1621–1633. doi: 10.4161/psb. 22455

Tsaftaris, S. A., Minervini, M., and Scharr, H. (2016). Machine learning for plant phenotyping needs image processing. Trends Plant Sci. 21, 989–991. doi: 10.1016/j.tplants.2016.10.002

Tschiersch, H., Junker, A., Meyer, R. C., and Altmann T. (2017). Establishment of integrated protocols for automated high throughput kinetic chlorophyll fluorescence analyses. *Plant Methods* 13. doi:10.1186/s13007-017-0204-4

Tsugawa, H. (2018). Advances in computational metabolomics and databases deepen the understanding of metabolisms. Curr. Opin. Biotechnol. 54, 10-17. doi: 10.1016/j.copbio.2018.01.008

Tsugawa, H., Cajka, T., Kind, T., Ma, Y., Higgins, B., Ikeda, K., Kanazawa, M., Vandergheynst, J., Fiehn, O., & Arita, M. (2015). MS-DIAL: Data-independent MS/MS deconvolution for comprehensive metabolome analysis, Nature Methods, 12, 523-526. doi:10.1038/nmeth.3393

Literature cited

Tsugawa, H., Kind, T., Nakabayashi, R., Yukihira, D., Tanaka, W., Cajka, T., et al. (2016). Hydrogen Rearrangement Rules: Computational MS/MS Fragmentation and Structure Elucidation Using MS-FINDER Software. Analytical Chemistry, 88(16), 7946–7958. doi: 10.1021/acs.analchem.6b00770

Turner N. (1986). Crop Water Deficits: A Decade of Progress. Advances in Agronomy. 39. 1-51. 10.1016/S0065-2113(08)60464-2.

Ubbens JR and Stavness I (2017) Deep Plant Phenomics: A DeepLearning Platform for Complex Plant Phenotyping Tasks. Front. Plant Sci. 8:1190. doi: 10.3389/fpls.2017.01190

Ugena, L., Hýlová, A., Podlešáková, K., Humplík, J. F., Doležal, K., De Diego, N., et al. (2018). Characterization of biostimulant mode of action using novel multi-trait high-throughput screening of *Arabidopsis* germination and rosette growth. *Front. Plant Sci*. 9. doi:10.3389/fpls.2018.01327

USDA-ARS. 2008. Research Databases. Bibliography on Salt Tolerance. George E. Brown, Jr. Salinity Lab. US Dep. Agric., Agric. Res. Serv. Riverside, CA. http://www. ars.usda.gov/Services/docs.htm?docid=8908

Vanderstraeten L, Depaepe T, Bertrand S and Van Der Straeten D (2019) The Ethylene Precursor ACC Affects Early Vegetative Development Independently of Ethylene Signaling. Front. Plant Sci. 10:1591. doi: 10.3389/fpls.2019.01591

Van Oosten, M. J., Pepe, O., De Pascale, S., Silletti, S., and Maggio A. (2017). The role of biostimulants and bioeffectors as alleviators of abiotic stress in crop plants. *Chem. Biol. Technol. Agric.* 4, 5 doi: 10.1186/s40538-017-0089-5

Vergauwen D. and De Smet I. (2017). From early farmers to Norman Borlaug: the making of modern wheat. Current Biology. 27(17). p.R858-R862 doi: 10.1016/j.cub.2017.06.061

Vernieri P., Ferrante A., Mugnai S. and Pardossi A. (2006). Abiotic stresses and hormonal balance in crops. Italus Hortus 13 (1), 2006: 19-31

Verpoorte R, Choi YH, Kim HK (2005) Ethnopharmacology and systems biology: a perfect holistic match. J Ethnopharmacol 100(1–2):53–56 doi:10.1016/j.jep.2005.05.033

Veselov, D., Mustafina, A., Sabirjanova, I., Akhiyarova G.R., Dedov A.V., Veselov S.U. & Kudoyarova G.R. (2002). Effect of PEG-treatment on the leaf growth response and auxin content in shoots of wheat seedlings. Plant Growth Regulation 38, 191–194. doi: 10.1023/A:1021254702134

Vidya Vardhini, B. (2017). Modifications of morphological and anatomical characteristics ofplants by application ofbrassinosteroids under various abiotic stress conditions—A review. Plant. Gene. 11, 70–89. doi: 10.1016/j.plgene.2017. 06.005

Viégas, R. A., Silveira, A. R. L., Junior, J. E., Queiroz, M. J., and Fausto, M. (2001). Effect of NaCl salinity on growth and inorganic solute accumulation in young cashew plants. *Braz. J. Agric. Eng.* 5, 216–222. doi: 10.1590/s1415-43662001000200007

Virtanen, O., Constantinidou, E., & Tyystjärvi, E. (2020). Chlorophyll does not reflect green light – how to correct a misconception. Journal of Biological Education, 1–8. doi:10.1080/00219266.2020.1858930

Visconti F., de Paz J.M., Bonet L., Jordà M., Quinones A. and Intrigliolo D.S. (2015). Effects of a commercial calcium protein hydrolysate on the salt tolerance of *Diospyros kaki* L. cv. Rojo Brillante grafted on *Diospyros lotus* L. Sci. Hortic. 185, 129–138 doi: 10.1016/j.scienta.2015.01.028

Vojta, P., Kokáš, F., Husičková, A., Gruz, J., Bergougnoux, V., Marchetti, C. F., et al. (2016). Whole transcriptome analysis of transgenic barley with altered cytokinin homeostasis and increased tolerance to drought stress. *New Biotechnol.* 33, 676-691. doi: 10.1016/j.nbt.2016.01.010

Voynikov, Y., Zheleva-Dimitrova, D., Gevrenova, R., Lozanov, V., Zaharieva, M. M., Tsvetkova, I., et al. (2016). Hydroxycinnamic acid amide profile of *Solanum schimperianum* hochst by UPLC-HRMS. Int. J. Mass Spectr. 408, 42–50. doi: 10.1016/j.ijms.2016.08.008

Literature cited

Walter A., Liebisch F. and Hund A. (2015). Plant phenotyping: from bean weighing to image analysis. Plant Methods 11:14. doi: 10.1186/s13007-015-0056-8

Wang X., Wang L., Shangguan Z. (2016) Leaf Gas Exchange and Fluorescence of Two Winter Wheat Varieties in Response to Drought Stress and Nitrogen Supply. PLoS ONE 11(11): e0165733. doi:10.1371/journal.pone.0165733

Watson R. and Fowden L. (1975). The uptake of phenylalanine and tyrosine by seedling root tips. Phytochemistry 14, 1181–1186. doi: 10.1016/s0031-9422(00)98591-1

Weiner, J., and Thomas, S. C. (1986). Size variability and competition in plant monocultures. *Oikos* 47, 211-222. doi: 10.2307/3566048

Wery J., Silim S.N., Knights E.J., Malhotra R.S. and Cousin R. (1994) Screening techniques and sources and tolerance to extremes of moisture and air temperature in cool season food legumes. Euphytica 73, 73–83. doi: 10.1007/978-94-011-0798-3_26

Wilson HT, Amirkhani M and Taylor AG (2018) Evaluation of Gelatin as a Biostimulant Seed Treatment to Improve Plant Performance. Front. Plant Sci. 9:1006. doi: 10.3389/fpls.2018.01006

Wu Y., Li Q., Jin R., Chen W., Liu X., Kong F., Ke Y., Shi H. and Yuan J.(2018). Effect of low-nitrogen stress on photosynthesis and chlorophyll fluorescence characteristics of maize cultivars with different low- nitrogen tolerances. Journal of Integrative Agriculture 2018, 17(0): 60345-7. doi: 10.1016/S2095-3119(18)62030-1

Xu, L., and Geelen, D. (2018). Developing biostimulants from agro-food and industrial by-products. *Front. Plant Sci.* 9, 1567. doi: 10.3389/fpls.2018.01567

Xu, C., and Mou, B. (2017). Drench application of fish-derived protein hydrolysates affects lettuce growth, chlorophyll content, and gas exchange. HortTechnology 27, 539–543. doi: 10.21273/horttech03 723-17

Yakhin, O. I., Lubyanov, A. A., Yakhin, I. A., and Brown, P. H. (2017). Biostimulants in plant science: A global perspective. *Front. Plant Sci.* 7, 2049. doi: 10.3389/fpls.2016.02049

Yamaguchi, T., and Blumwald, E. (2005). Developing salt-tolerant crop plants: Challenges and opportunities. Trends Plant Sci. 10, 615–620. doi: 10.1016/j.tplants.2005.10.002

Yang Y, Saand MA, Huang L, Abdelaal WB, Zhang J, Wu Y, Li J, Sirohi MH and Wang F (2021). Applications of Multi-Omics Technologies for Crop Improvement. Front. Plant Sci. 12:563953. doi: 10.3389/fpls.2021.563953

Yang, L., Wu, L., Yao, X., Zhao, S., Wang, J., Li, S., & Ding, W. (2018). Hydroxycoumarins: New, effective plant-derived compounds reduce *Ralstonia pseudosolanacearum* populations and control tobacco bacterial wilt. Microbiological Research, 215, 15–21. doi: 10.1016/j.micres.2018.05.011

Yao J., Sun D., Cen H., Xu H., Weng H., Yuan F. and He Y. (2018) Phenotyping of Arabidopsis Drought Stress Response Using Kinetic Chlorophyll Fluorescence and Multicolor Fluorescence Imaging. Front. Plant Sci. 9:603. doi: 10.3389/fpls.2018.00603

Ye, X., Abe, S., & Zhang, S. (2019). Estimation and mapping of nitrogen content in apple trees at leaf and canopy levels using hyperspectral imaging. Precision Agriculture, 21(1), 198–225. doi:10.1007/s11119-019-09661-x

Yordanov I., Velikova V. and Tsone V. (2000). Plant response to drought, acclimation and stress tolerance. Photosynthetica. 30: 171-186. doi: 10.1023/a:1007201411474

Zhang, H., Irving, L. J., McGill, C., Matthew, C., Zhou, D., & Kemp, P. (2010). The effects of salinity and osmotic stress on barley germination rate: sodium as an osmotic regulator. Annals of Botany, 106(6), 1027–1035. doi:10.1093/aob/mcq204

Zhang P., Senge M. and Dai Y. (2016). Effects of salinity stress on growth, yield, fruit quality and water use efficiency of tomato under hydroponics system. Reviews in Agricultural Science 4: 46–55 doi: 10.7831/ras.4.46

Zhao D., Reddy K.R., Kakani V.G. and Reddy V.R. (2005). Nitrogen deficiency effects on plant growth, leaf photosynthesis, and hyperspectral reflectance properties of sorghum. Europ. J. Agronomy 22 (2005) 391–403. doi: 10.1016/j.eja.2004.06.005

Appendix

List of publications

Complete list of articles published during the Ph.D. period:

1. Cirillo, C., Rouphael, Y., El-Nakhel, C., Pannico, A., **Sorrentino, M.,** Cirillo, V., Caputo, R., and De Pascale, S. (2018). Valorisation of biorefinery by-products in potted ornamental shrub cultivation: effects on growth, water relations and leaf gas exchanges. Acta Horticulturae, (1215), 439–442. doi:10.17660/actahortic.2018.1215.79
2. Paul K, **Sorrentino M**, Lucini L, Rouphael Y, Cardarelli M, Bonini P, Reynaud H, Canaguier R, Trtílek M, Panzarová K and Colla G (2019) Understanding the Biostimulant Action of Vegetal-Derived Protein Hydrolysates by High-Throughput

Plant Phenotyping and Metabolomics: A Case Study on Tomato. Front. Plant Sci. 10:47. doi: 10.3389/fpls.2019.00047

3. Paul K, **Sorrentino M**, Lucini L, Rouphael Y, Cardarelli M, Bonini P, Miras Moreno MB, Reynaud H, Canaguier R, Trtílek M, Panzarová K and Colla G (2019) A Combined Phenotypic and Metabolomic Approach for Elucidating the Biostimulant Action of a
Plant-Derived Protein Hydrolysate on Tomato Grown Under Limited Water Availability. Front. Plant Sci. 10:493. doi: 10.3389/fpls.2019.00493
4. **Sorrentino, M.,** Colla, G., Rouphael, Y., Panzarová, K., & Trtílek, M. (2020). Lettuce reaction to drought stress: automated high-throughput phenotyping of plant growth and photosynthetic performance. Acta Horticulturae, (1268), 133–142. doi:10.17660/actahortic.2020.1268.17
5. **Sorrentino M**, De Diego N, Ugena L, Spíchal L, Lucini L, Miras-Moreno B, Zhang L, Rouphael Y, Colla G and Panzarová K (2021) Seed Priming with Protein Hydrolysates Improves Arabidopsis Growth and Stress Tolerance to Abiotic Stresses. Front. Plant Sci. 12:626301. doi: 10.3389/fpls.2021.626301

Conferences

Poster presentations

1. 2nd Austrian Plant Phenotyping Network Meeting (APPN), 17-18 April 2018, Vienna, Austria
2. Integrated Plant and Algal Meeting (IPAP) 2018, 26-29 August 2018, Prague, Czech Republic
3. 3rd Austrian Plant Phenotyping Network (APPN) Meeting - Field phenotyping and remote sensing, 13 June 2019, Vienna, Austria
4. 2019 Eucarpia Leafy Vegetables International Conference, 24-28 June 2019, Olomouc, Czech Republic
5. International Congress on Biophysics of Photosynthesis: from molecules to the field, 2-4 October 2019, Rome, Italy

Appendix

Oral presentations

1. XI International Symposium on Protected Cultivation in Mild Winter Climates & I International Symposium on Nettings and Screens in Horticulture - *27-31 January 2019, Tenerife, Canary Islands*
2. 4th Biostimulants World Congress - *18-21 November 2019, Barcelona, Spain*
3. SE2B Solar Energy to Biomass – Optimisation of light energy conversion in plants and microalgae Conference - *11-14 February 2020, Porto, Portugal*
4. Fast and effective screening of biostimulants using high-throughput automated plant phenotyping - Biostimulant.com*, 28 May 2020*
5. Biostimolanti Conference 2021 Digital - *23-25 February 2021*
6. 1st International Electronic Conference on Agronomy, 10-11 May 2021
7. "State-of-art tools and approaches in plant phenotyping" Advanced phenotyping online training - *ECOBREED project, 24-25 May 2021*

Courses and seminars

1. Scientific career beyond academia, EuroSTEMpeers 2018 - *Ceitec, Brno, Czech Republic*
2. PREFEKT 2018: Transferable skills, Financing Research and Training in Grant Applications - *Ceitec, Brno, Czech Republic*
3. Microalgal industrial production – from theory to practice and from mass culture to product - *AlgaTech, Trebon, Czech Republic*
4. Spectroscopy course - *Wageningen University, The Netherlands*
5. Science and Society - *Vrije Universiteit Amsterdam, The Netherlands*
6. Introduction to Biostatistics - doc. RNDr. Jakub Těšitel, *Masaryk University, Brno, Czech Republic*
7. Setting up a start-up company: from science to industry - *Vrije Universiteit Amsterdam, The Netherlands*

Appendix